Université de Lille

Ecole Doctorale Biologie- Santé (ED446)

THESE

Présentée et soutenue publiquement par

Orgeta ZEJNELI

Pour l'obtention du grade de :

DOCTEUR DE L'UNIVERSITE DE LILLE

Discipline : Sciences médicales

Spécialité : Neurosciences

NANOBODIES DIRIGÉS CONTRE TAU EN TANT QU'OUTILS MOLÉCULAIRES POUR ÉTUDIER L'IMMUNOTHÉRAPIE DANS LA MALADIE D'ALZHEIMER ET LES TROUBLES CONNEXES

Le 29 Septembre 2021

JURY

Dr. Marc DHENAIN	**Rapporteur**
Prof. Efthimios SKOULAKIS	**Rapporteur**
Assoc. Prof. Caroline SMET-NOCCA	**Examinateur**
Dr. Kunie ANDO	**Examinateur**
Dr. Isabelle LANDRIEU	**Co- DIRECTEUR**
Dr. Luc BUEE	**DIRECTEUR**

Université de Lille

Ecole Doctorale Biologie- Santé (ED446)

THESE

Présentée et soutenue publiquement par

Orgeta ZEJNELI

Pour l'obtention du grade de :

DOCTEUR DE L'UNIVERSITE DE LILLE

Discipline : Sciences médicales

Spécialité : Neurosciences

NANOBODIES DIRECTED AGAINST TAU AS MOLECULAR TOOLS TO INVESTIGATE IMMUNOTHERAPY IN ALZHEIMER'S DISEASE AND RELATED DISORDERS

Le 29 Septembre 2021

JURY

Dr. Marc DHENAIN	**Rapporteur**
Prof. Efthimios SKOULAKIS	**Rapporteur**
Assoc. Prof. Caroline SMET-NOCCA	**Examinateur**
Dr. Kunie ANDO	**Examinateur**
Dr. Isabelle LANDRIEU	**Co- DIRECTEUR**
Dr. Luc BUEE	**DIRECTEUR**

Acknowledgments

I consider these words of acknowledgement, appreciation, and thanksgiving of similar importance as the following chapters of the three-year study contained in this dissertation. For those who know me well, I believe this is already clear, and for those who do not know me, I hope you receive this as an honest expression of gratitude. Truly believing that it takes more than one to reach the goals set in such a demanding course of study as a PhD, I have been blessed to have met and exchanged work with some of the most special people in the world along the way.

First of all, I wish to thank the members of the doctoral committee, who accepted the invitation and will evaluate the work which has been completed during my three-year scholarship. Among these include **Dr. Marc Dhenain**, **Prof. Efthimios Skoulakis, Assoc. Prof. Caroline Smet Nocca** and **Dr. Kunie Ando**, who each supported this committee with their well-established scholastic backgrounds.

It has also been a great pleasure and honor that my co directors **Dr. Isabelle Landrieu** and **Dr. Luc Buée** accepted to assist me in my PhD, supervising me all along the way. Through their guidance, engaged concern, and suggestions, I must admit that my straight path would not have been possible. Thanks is due also especially to **Assoc. Prof. Morvane Colin** for her assistance and direction in the project, and for keeping an active eye on the results of cellular and *in vivo* data.

Céline Brand is the first person I met in France, and I am grateful to her who clarified to me the importance to love and care the work we are doing.

As a member of two scientific groups, I was called upon to approach my project through two different perspectives and sought to find the right balance to navigate it to the final product. This would not have been possible without the scholastic exchange I shared with the Post Doc. Researcher **Elian Dupre** (RID AGE lab), who first started the project together with **Clément Danis**, a PhD student at the time of my earlier research. He helped me answer difficult questions during study, leading me to better structure my thoughts in the world of biochemistry and structural biology. Moreover, the technical support and enormous assistance I received from **Raphaelle Caillierez, Sabiha Eddarkaoui**, and **Severine Bégard** cannot be expressed in words. We worked together to achieve the goals for which a successful PhD calls. Their love for what they do was our common ground for setting and achieving the goals of the project. To them I will always be grateful.

I spent most of my three years in France on the Alzheimer and Tauopathies team, where I enjoyed working along its members, and thank them for exchanging memorable moments together in the lab. Getting to know the French culture and language through them was a new experience to me. For this I thank Dr. Colin's team, **Elodie, Thomas B., Corentin** and **Assoc. Prof. Sophie Halliez** for their inclusive spirit, and the nice environment they offered in the office for me, and for their kindness "to adopt" me as part of their group. I also thank **Romain Perbet**, for his willingness to help me with the human samples needed for the project. Elodie had been challenged by me who needed a lot of translation of the mails I got from the Doctoral School, but her answer was always affirmative, and for this I am very grateful. I also need to mention **Sarrah** and **Mo**, with whom I passed through the lab for only a short time together, although in my heart they will remain not any less longer.

Over these past three years, I have never forgot joking with **Sarrita**, learning my first French with the help of **Florian**, exchange memories and hopes with **Thomas R.**, questions of wonder with **Marine** and **Sarrah G**., enjoying the presence of a real team-player with **Sarrah Lieger**, and my first and everyday pleasure of saying good morning to **Kevin** in French in a "screamy" way. Dr. David Blum's team also offered me a friendship with the most wonderful Spanish lady, **Victoria Gomez**. Furthermore, following a common effort with **Emilie Faivre** to organize the PhD and Post-Doc lectures in the institution, I understand how beautiful it is to know people who are open to advice and suggestions.

I would also like to thank **Sebastian** and **Thomas C.** for their technical support when needed, **Natalie** and **Sophie** in the office, the FRET ladies, **Emilie** and **Nathalie**, and, of course, **Antonino Bogiovanni**, for his endless help. I should not forget my beautiful **Esperance**, who from the very beginning approached me and sought to learn about me in the kindest way. I am proud to say that at the time of writing this acknowledgement our conversation turned to be entirely in French.

The brief time which I spent in the RID-AGE lab allowed me to get to know kind people like **Joao Neves**, **Hamida, Alessia** and **Assoc. Prof. Robert Schneider**. The latter did not feel tired of translating for me in the common lunch when I could not follow even a single word. Also, **Danai and Justine,** who recently joined the team, has always been a joy each time we met.

By getting to this line, I realize what a journey I have had, but there are many and much more.

For all of us, COVID-19 created unusual conditions, with the first lock down isolating us at home. I must admit that being in a foreign country in such conditions was not an easy situation. That time taught me how important it is to be surrounded by people who share the same needs. This is when my relationships with members of the Dr. Vincent Prevot and Dr. Paulo Giacobini teams began. I am so thankful to know so many people from all over the world and eat, laugh, share, and joke with each of them as life brought us closer in these moments for a reason. Thank you, **Eleonora, Virginia, Adrian, Monica, Nour, Ludovica, Nantia,** of course **Valerie, Daniela, Caio, Mauro, Marion** for allowing me to get to know you. My stay in Lille would not have been the same without you. I keep **Sreekala** separately as she was my trouble-shooter in Lille, for reasons we both know and for whom I can say that I have a beautiful Indian friend.

In the context of my stay in Lille, I need to thank **Fr. Aimilianos Bogiannos** for his support as I continued to encounter such a different cultural environment from my own, afraid and full of wonder, along with others from the Greek community of Lille who opened their houses to me.

At first Lille, as strange as it seemed, ended up being very generous with special people like **Aggeliki, Joa, Julie, Ilda and Elis,** who each became long life friends.

The PhD life, and my engagement with totally new situations in a whole new environment, called me to seek strength and courage from the example of those incredible hearts God blessed me with the opportunity to meet along my path and call family. Without them, surely at points my life would have felt poor and unreasonable. At this point, I need to mention that I would have been not even close to who I am today as a human being without the prayers, the love, and the care of my spiritual father, **Fr. Spyridon, the Family of Acheiropoietos, and the Monastery of Dormitory of Mother of God** back to Thessaloniki. They are silently present all these three years along my side, and I miss them every day. Furthermore, I owe a lot to my close and beloved friends **Isaac** and **Sophia,** as well as to **Melody, Akis, Eleni, Ioanna, Victoria, Despoina and Mbampis** for their positivity and encouragement in this decision I made to complete my PhD.

As an international person whose life brought her to be in multiple places all the time in search of her destination and dreams being in a revolutionary statement with herself, I need to thank my so-called Greek mother **Theodora,** and my American mother **Kathy**, who stood and continue to stand by me.

Last but not least, I thank my beloved family who trusted me when I first left home in pursuit of my dreams, and whose unconditional love and support made me not to hesitate even in the face of my biggest fears.

Definitely, this project would have not been possible without the support of the **Tunable (TaU Nanobodies in aLzheimer) scholarship,** which I am thankful to.

« ΔΟΞΑ ΤΩ ΘΕΩ ΠΑΝΤΩΝ ΕΝΕΚΕΝ »

Abstract

Tau is a microtubule-associated protein, best known to regulate cytoskeletal dynamics of neurons in the brain. Although the mechanisms leading to Tau aggregation in tauopathies are still ill-defined, the peptide PHF6 is described as a nucleus of Tau aggregation. Immunotherapy is proposed as a therapeutic approach in tauopathies. This strategy is indeed effective in attenuating Tau pathology in animal models, improving also cognitive and motor functions. However, it remains important to better define several parameters to design the best strategy in Tau-specific immunotherapy. For example, even-though the intracellular accumulation of Tau aggregates into paired helical filaments (PHFs) are the major events connected to neuropathological lesions, extracellular tau is lately considered as the key driver in the spread and seeding of the pathology. In view of the challenges to design the most effective Tau-specific immunotherapy, we have used antibody fragments called VHHs (Variable domain of the Heavy- chain of the Heavy-chain-only-antibodies, or nanobodies) because they are easier to generate, select and engineered compared to conventional antibodies. Of interest, VHHs can be used for intracellular applications, by engineering their ability to penetrate the cells or by direct intracellular expression. A VHH named Z70, binding the PHF6 peptide, was previously selected, characterized and optimized in the laboratory. VHH Z70 has the ability to block Tau seeding in *in vitro* assays. Based on these results, VHH Z70 capacity of blocking Tau seeding was investigated in THY-tau30 transgenic mouse model. For this, LVVs expressing VHH Z70, VHH Z70 fused to mCherry, VHH Z70 fused to a Fc fragment of mouse immunoglobulin (Minibody) and VHH anti-GFP for negative control, were produced and injected to one-month old mice in the hippocampus area. Exogenous human Alzheimer's disease brain lysates were subsequently injected to induce the endogenous aggregation process. AT-8 immunostaining was chosen to define the level of the pathology in the brain. Animals injected with LVVs (lentiviral vectors) expressing VHH Z70 showed a decreases tendency of the seeded Tau pathology, but this tendency became only significant in the case of VHH Z70 fused to mCherry. For the mice treated with VHHs expressing the Minibody, the immunohistochemistry analysis did not reveal any change in the treated mice, compared to the negative control (Minibody VHH anti-GFP). Given these promising results, optimizations of VHH Z70 activity in the intracellular compartment were performed. The strategy for optimization involved random mutagenesis coupled with yeast two-hybrid for selection, in partnership with Hybrigenics company. Eight functional variants were selected from this screen with conserved epitope recognition. Determination of the affinity by surface plasmon resonance suggested that the binding of the epitope can be improved by mutations located in both the complementary determining regions and the framework regions. These variants were further tested in comparison with VHH Z70 for their ability to inhibit Tau aggregation in fluorescence-based seeding reporter cells. Three of these mutants have an *in vitro* inhibitory activity that matched VHH Z70 and could be used in future *in vivo* assays. To conclude, the results of this three-year project have established that VHH Z70 has potential in mitigating Tau accumulation, at least in a mouse model of seeding. In addition, these studies demonstrated that the Tau-specific VHHs are useful molecular tools to decipher the best target in Tau immunotherapies.

Résumé

Tau est une protéine associée aux microtubules, bien connue pour réguler la dynamique du cytosquelette des neurones dans le cerveau. Bien que les mécanismes conduisant à l'agrégation de Tau dans les tauopathies sont encore mal définis, le peptide PHF6 est décrit comme un noyau d'agrégation de Tau. L'immunothérapie est proposée comme une approche thérapeutique dans les tauopathies. Cette stratégie est en effet efficace pour atténuer la pathologie Tau dans les modèles animaux. Cependant, il reste important de mieux définir plusieurs paramètres pour concevoir la meilleure stratégie en immunothérapie spécifique de Tau. Par exemple, même si l'accumulation intracellulaire d'agrégats de Tau en filaments hélicoïdaux appariés (PHF) sont les événements majeurs liés aux lésions neuropathologiques, la protéine Tau extracellulaire est considérée comme le facteur clé de la propagation et du “seeding” de la pathologie. Compte tenu des défis pour concevoir une immunothérapie spécifique de Tau efficace, nous avons utilisé des fragments d'anticorps appelés VHH (Variable domain of the Heavy-chain of the Heavy-chain-only-antibodies) car ils sont plus faciles à générer, sélectionner et modifier que les anticorps conventionnels. Il est intéressant de noter que les VHHs peuvent être utilisés pour des applications intracellulaires, en modifiant leur capacité à pénétrer dans les cellules ou par expression intracellulaire. Un VHH nommé Z70, liant le peptide PHF6, a été préalablement sélectionné, caractérisé et optimisé dans le laboratoire. VHH Z70 a la capacité de bloquer l’agrégation de Tau dans les tests *in vitro*. Sur cette base, la capacité de VHH Z70 à bloquer le “seeding” de Tau a été étudiée dans le modèle de souris transgénique THY-tau30. Pour cela, des LVVs (vecteurs lentiviraux) exprimant VHH Z70, VHH Z70 fusionné à mCherry, VHH Z70 fusionné à un fragment Fc d'immunoglobuline de souris (Minibody) et VHH anti-GFP pour contrôle négatif, ont été produits et injectés à des souris âgées d'un mois, dans la zone de l'hippocampe. Afin d'induire le processus d'agrégation endogène, des lysats de cerveaux humains atteints de la maladie d’Alzheimer ont ensuite été injectés. L'immunomarquage AT-8 a été choisi pour définir le niveau de la pathologie dans le cerveau. Les animaux injectés avec des LVVs exprimant VHH Z70 ont montré une tendance à la diminution de la pathologie Tau, mais cette tendance n'est devenue significative que dans le cas de VHH Z70 fusionné à mCherry. Pour les souris traitées avec des VHH exprimant le Minibody, l'analyse n'a révélé aucun changement chez les souris traitées, par rapport au contrôle négatif (Minibody VHH anti-GFP). Compte tenu de ces résultats prometteurs, des optimisations de l'activité VHH Z70 dans le compartiment intracellulaire ont été réalisées. La stratégie d'optimisation impliquait une mutagenèse aléatoire couplée à une sélection par double hybride de levure, réalisés par la société Hybrigenics, Paris. Huit variants fonctionnels ont été sélectionnés à partir de ce criblage avec une reconnaissance d'épitope conservée. La détermination de l'affinité par résonance plasmonique de surface suggère que la liaison de l'épitope peut être améliorée par des mutations situées à la fois dans les régions déterminantes complémentaires et dans les régions charpentes. Ces variantes ont été testées en comparaison avec VHH Z70 pour leur capacité à inhiber l'agrégation de Tau dans des cellules où l’agrégation est détectée sur base d’une fluorescence. Trois de ces mutants ont une activité inhibitrice *in vitro* qui correspond à VHH Z70 et pourraient être utilisés dans de futurs tests *in vivo*. Pour conclure, les résultats de ce projet de trois ans ont établi que VHH Z70 a le potentiel d'atténuer l'accumulation de Tau, au moins dans un modèle de souris. De plus, ces études ont démontré que les VHH spécifiques à Tau sont des outils moléculaires utiles pour déchiffrer les meilleures cibles dans les immunothérapies Tau.

Acknowledgments 2

Abstract 7

Résumé 8

Introduction 15

Chapter 1: Tau protein – general aspects 15

1.1 Gene organization 15

1.2 The structural basis and functions of Tau 15

1.3 Role of tau as Microtubule Associated Protein 16

Chapter 2: Tauopathies- Alzheimer's disease case 17

2.1 Description of Alzheimer's Disease 17

2.1.1 The Aβ peptide and the senile plaque formation 18

2.1.2 Tau phosphorylation in Alzheimer's disease 19

Chapter 3: Tau aggregation 21

3.1 Structural analysis of tau filaments in Alzheimer Disease 21

3.1.2 Local structure of inert and seed-competent tau monomers 23

Chapter 4: Post Translational Modifications 25

4.1 Protein Phosphorylation 25

4.1.1 Physiological Phosphorylation 25

4.1.2 Pathological Phosphorylation 25

4.1.3 Tau Kinases 27

4.1.3.1 GSK-3β 27

4.1.3.2 Cdk5 27

4.1.4 Tau phosphatases 28

4.1.5 Is the phosphorylation the one to blame? 28

4.2 Tau glycosylation 29

4.3 Tau truncation 30

4.4 Tau clearance by the ubiquitin-proteasome system and autophagic-lysosomal degradation 30

Chapter 5: Tau seeding and propagation 32

5.1 Modelling of the prion-like propagation 32

5.1.1 Tau secretion 32

5.1.2 Tau uptake/transfer 33

5.1.3 Tau seeding 34

Chapter 6: Tau- targeted therapies in clinical trials 36

6.1 Therapeutic approaches to toxic gain of function *37*
6.1.1 Reducing tau expression 37
6.1.2 Modulate post-translational modifications 38
6.1.2.1 Phosphorylation inhibitors 38
6.1.2.1a Kinase Inhibitors 38
6.1.2.1b Inhibiting tau de-O-GlcNAcylation (OGA) 39
6.1.2.2 PP2a activators 39
6.1.3 Inhibiting tau aggregation (TAI) 39
6.1.4 Immunotherapy approach 40
6.1.4.1 Active immunization 41
6.1.4.2 Passive immunization 42
6.1.5 Targeting extracellular tau 48

6.2 Therapeutic approaches for tau loss of function *49*
6.2.1 Replace tau physiologic function- Microtubule stabilizers 49

6.3 Clinical anti-tau antibodies and the BBB *49*

6.4 Fc receptors and their role *50*

6.5 Importance of affinity of therapeutic anti-tau antibodies *52*

6.6 Mechanism of action of Immunotherapies *54*
6.6.1 Peripheral Sink 54
6.6.2 Neutralization 54
6.6.3 Clearance by Microglia 55
6.6.4 Intracellular sequestration or Clearance 55

Chapter 7: Models used for studying tau aggregation in tauopathies 57

7.1 Advantages of use of animal models in research *57*
7.1.1 Tau transgenic mouse model 57
7.1.2 Non-transgenic mouse model 58
7.1.3 Transgenic mouse models used in the current PhD project 59
7.1.4 Drosophila models of tauopathy 59

7.2 Cellular model of tau seeding *60*

Chapter 8: Variable Heavy Chain of the Heavy Chain only Antibodies 62

8.1 Origin-General description *62*

8.2 Structure and biochemical properties of VHH *63*
8.2.1 Three-dimensional structure of VHH 63
8.2.2 Biochemical properties 64
8.2.2.1 VHH are easy to generate, select and produce 64
8.2.2.2 VHH are stable 65
8.2.2.3 Antigen specificity and affinity of the VHHs 65
8.2.2.4 VHHs lack immunogenicity 65
8.2.2.5 VHHs properties can be improved through protein engineering 65

8.3 Applications of VHHs *66*
8.3.1 Application as a research tool 66
8.3.2 Diagnostic application 67

8.3.3 Therapeutic applications of VHHs 68
8.3.4 Use of antibody fragments in neurodegenerative diseases 68
8.3.4.1 Development of bifunctional intrabodies 68
8.3.4.2 Use of VHHs as a research tool in understanding the intracellular fibril formation 70

8.4 VHH against tau protein *72*

8.5 Nanobodies can cross membranes and the BBB and function intracellularly *73*

II. Objectives 75

III. Materials and Methods 76

1. Cellular experiments *76*

1.1 Seeding assay in HEK293 reporter cell-line *76*

1.2 FRET Flow Cytometry *76*

1.3 MTBD seeds *76*

2. In vivo experiments *77*

2.1 Mouse model THY-tau30 *77*

2.2 Human brain lysate *77*

2.3 Stereotaxic injection and sacrifice procedures *77*

3. AT-8 immunohistochemical labeling, quantification, and statistical analysis *78*

3.1 Immunohistochemistry *78*

3.2 Quantifications *79*

4. Cellular assay- infected with LVV *79*

5. Western Blotting *79*

6. Immunohistofluorescence *79*

7. Cloning of VHH Z70 Minibody *80*

8. Production and purification of the VHHs *80*

9. ELISA *80*

10. Immunocytochemistry *80*

11. Statistical Analysis *81*

IV. Results 82

1.1 Preliminaries *82*

1.2 Optimization of VHH Z70 to improve the affinity for its target *82*

1.3 Inhibition of tau seeding in HEK293 tau repeat domain, P301S FRET Biosensor aggregation reporter cells84
1.3.1 Test of the inhibition efficacy of VHH Z70 and Mutants towards tau seeding 84

2.1 Inhibition of tau seeding in vivo *88*
2.1.1 The efficacy of VHH Z70 expressed intracellularly (intrabody) in THY-tau30 Tg model 89
2.1.2 Testing the ability of non-AD brain as negative control in *in vivo* experiments 94

2.2 Use of the VHH Z70 to prevent propagation- Minibody Case *96*

2.3 Testing the long-term effect of VHH Z70 in vivo *98*

2.4 Generation of a monoclonal antibody *99*
2.4.1 Testing the monoclonal antibody generated for Minibody detection- Standardizing the conditions of expression of Minibody 102

V. Discussion **104**

VI. Perspectives **109**

VII. References **111**

VIII. Publications **137**

IX. Congress Attendancies **226**

List of Figures

Figure 1 : Schematic presentation of the MAPT gene. 15
Figure 2 : Tau structure. 16
Figure 3. Amyloid precursor protein (APP) cleavage in normal (non-amyloidogenic) and AD (amyloidogenic) pathways. 18
Figure 4 : Spatio- temporal evolution of Thal stages describing the progression of Aβ aggregates...19
Figure 5 : Typical electrophoretic profiles of pathological tau proteins....20
Figure 6 : Spatio- temporal evolution of tau pathology in AD as described by the Braak staging scheme 20
Figure 7. Cross-sections of the PHF (a) and SF (b) cryo-EM structures 22
Figure 8: The common protofilament core. 23
Figure 9 : Phosphorylated epitopes of tau protein in physiological (above the tau structure) and pathological case (below the tau structure) in AD brain....26
Figure 10. Prion-Like propagation of tau pathology in Alzheimer's disease 35
Figure 11. Tau related therapeutic targets. Based on (Congdon & Sigurdsson, 2018) 37
Figure 12 : Clinical anti-tau passive immunotherapies binding epitope on the full length of tau. 48
Figure 13 : Proposed mechanism of action of anti-tau antibodies....56
Figure 14. FRET flow cytometry detecting tau seeding. 61
Figure 15 : Structure of antibody fragments....62
Figure 16: The structure of VHH. 64
Figure 17 : Immunohistochemical characterization of VHH A2 as a specific probe for labeling neurofibrillary tangles 68
Figure 18 : Schematic representation of the S- shaped curve kinetics of fibril formation of an amyloidogenic protein.. 71
Figure 19 : Nanobodies use in understanding the fibrillary formation. 72
Figure 20 : VHH Z70 and Mutants effect on intracellular seeding of Tau MTBD in HEK293 TAU RD P301S FRET Biosensor cells....85
Figure 21 : VHH Z70 and Mutants block intracellular seeding of Tau MTBD in HEK293 TAU RD P301S FRET Biosensor cells.....86
Figure 22 : Percentage of total FRET positive cells, determined from FACS data for cells transfected with pcDNA 3.1- VHH (F8-2, Z70 and Mutants) followed by MTBD seeds 87
Figure 23 : Percentage of total FRET positive cells (A) and percentage of mCherry gated FRET positive cells (B), determined from FACS data for cells co-transfected with pcDNA 3.1- VHH and empty pmCherry followed by MTBD seeds. 88
Figure 24 : Intracellular expression of VHH Z70: HEK293 cells were infected with LVVs encoding VHH Z70-mCherry or non- infected (NI)....89
Figure 25 : Testing the pathological pattern of different human derived AD brains. 90
Figure 26 : Protocol of injection and the injection site in THY-tau30 Tg mouse hippocampus. 91
Figure 27 : Expression of the VHH Z70- fused to mCherry. 92
Figure 28 : Effect of VHH Z70 on seeding induced by h-AD brain in THY-tau30 Tg mouse model....93
Figure 29 : VHH Z70 effect on human tau seeding induced by extracellular human pathological tau seeds…… 94
Figure 30 : Presentation of the tau pattern of three different human non- AD brains……95
Figure 31 : Effect of different extracellular injected non-AD brain homogenates on inducing Tau seeding in THY-tau30 Tg mouse model 96
Figure 32 : Minibody sturcture. 97
Figure 33 : Effect of the Minibody VHH Z70 on extracellular tau aggregates in THY-tau30 Tg mouse model. 97
Figure 34 : Effect of the VHH Z70 on aged developed intracellular tau aggregates in THY-tau22 Tg mouse model 98
Figure 35 : Testing the ability of serum of immunized Balb/c mice, labeled as 975; 976; 977 and 993, to detect VHH Z70 and VHH anti-GFP 99
Figure 36 : Testing the ability of the serum of Balb/c mice 993 (S2), to detect VHH Z70 and VHH anti-GFP 100
Figure 37 : Testing the detection of expressed VHH Z70 in HEK293 cell line with different subclones generated from hybridoma cell line 101
Figure 38 : Testing the ability of the serums of Balb/c mice, to detect Minibody-VHH Z70....103

List of Tables

Table 1 : Active and passive tau-immunotherapies that are currently in clinical trials.....47
Table 2 : Human Fc Receptor.....51
Table 3 : Mouse Fc receptor 51
Table 4 : Anti-tau immunotherapies currently in the clinical phase.....53
Table 5 : The amino acid sequence of the VHH Z70. 83
Table 6 : Affinity determination for the series of VHHs binding tau, by surface plasmon resonance (SPR).. 83
Table 7 : The scheme of the bilateral injected Tg30tau mice. 89

Introduction

Chapter 1: Tau protein – general aspects

1.1 Gene organization

Tau is a microtubule associated protein (MAP) and in humans is encoded by MAPT gene located on chromosome 17 (17q21). The MAPT gene contains 16 exons. Through the alternative splicing of three exons (2, 3 and 10), six different isoforms (352 to 441 amino acids) occur in the brain. These isoforms differ depending on the absence or the presence of one or two 29 amino acids inserts encoded in the amino-terminal part (0N, 1N or 2N, respectively), in combination with either three (R1, R3 and R4) or four (R1-R4) repeat regions in the carboxy-terminal part (Buée et al., 2000; Guo et al., 2017). Shown in Figure 1.

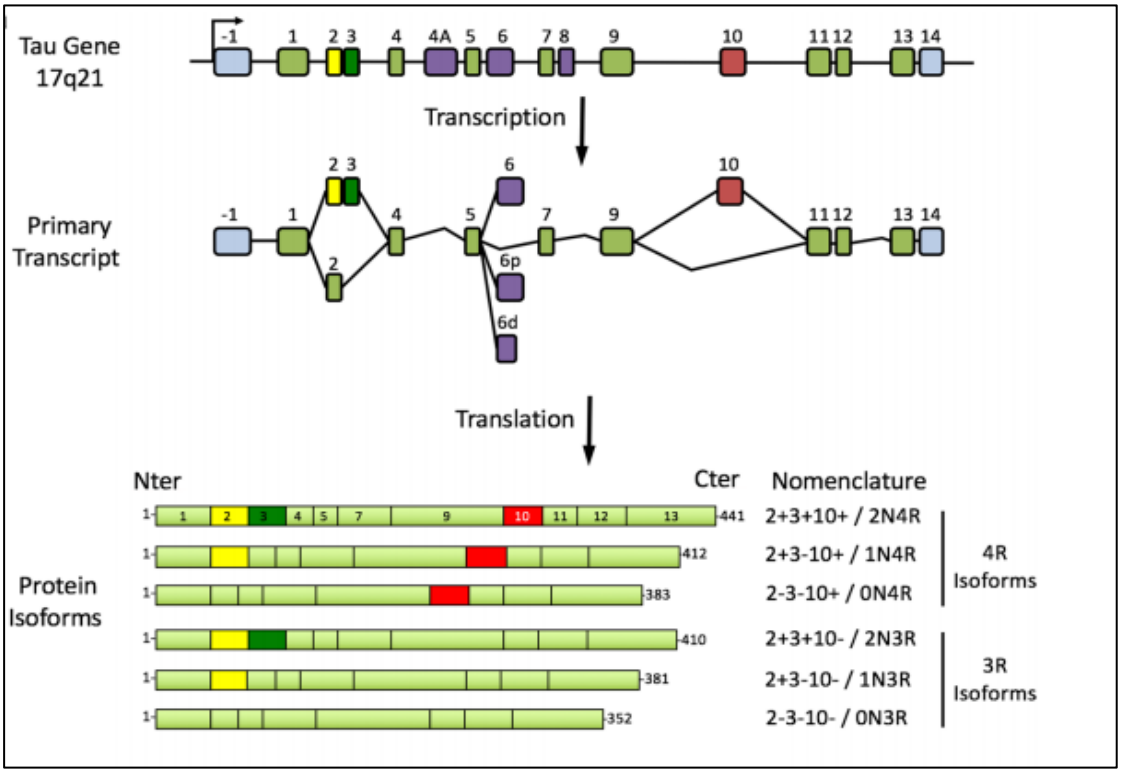

Figure 1 : Schematic presentation of the MAPT gene. The MAPT gene is composed of 16 exons. In the brain, exons 4A and 8 are excluded from the primary transcript. Exons 1, 4, 5, 7, 9, 11, 12 and 13 are constitutive, whereas exons 2, 3, 6 and 10 are alternative. Exon 3 never appears independently of exon 2. Exons 1 and 14 are present in the mRNA, but are never translated. Six main transcripts are present in the adult brain: 2 – 3 – 10 − or 0N3R; 2+3 − 10 − or 1N3R; 2+3+10 − or 2N3R; 2 – 3 − 10+or 0N4R; 2+3 − 10+or 1N4R; 2+3+10+or 2N4R. Adapted from (Colin et al., 2020).

1.2 The structural basis and functions of Tau

Tau protein is subdivided into four major domains, which are distinguished by their biochemical properties. The N-terminal domain (1-150aa), counting based on the longest isoform, including the two peptide inserts encoded by exons 2 and 3, is acidic. This domain does not bind directly to microtubule but is involved in microtubule dynamics and function. Furthermore, it is involved on the interaction of tau with molecules from the neural plasma membrane and on a signaling cascade that influences axon transport in neurons (Fuhrman, Jed; McCallum, Kirk; Davis, 1992). Interestingly, this domain

also influences the protein interaction partners of tau (Fuhrman, Jed; McCallum, Kirk; Davis, 1992). Although while not yet well established, the inserts appear to affect the distribution of tau (C. Liu & Götz, 2013). The region of 151-243aa encompasses a basic proline-rich region. The proline-rich domain of tau contains seven Pro-X-X-Pro motifs that are related with the interaction of tau with Src homology-3 (SH3) domain containing proteins. It has also been reported that this domain is a binding site for nucleic acids and that it is implicated in the regulation of microtubule assembly (Guo et al., 2017). The microtubule binding domain contains the microtubule binding repeats and the flanking sequences, which together provide the primary structures by which tau binds and stabilizes microtubules (Bibow, Mukrasch, et al., 2011). Considering the C-terminal region (370-441aa), a neutral domain (Mandelkow & Mandelkow, 2012), its function is poorly known. It has been reported that changes in this domain may affect tau proteins interaction with other proteins as well as its accessibility to phosphorylation (Guo et al., 2017). The protein's primary structure is presented in Figure 2.

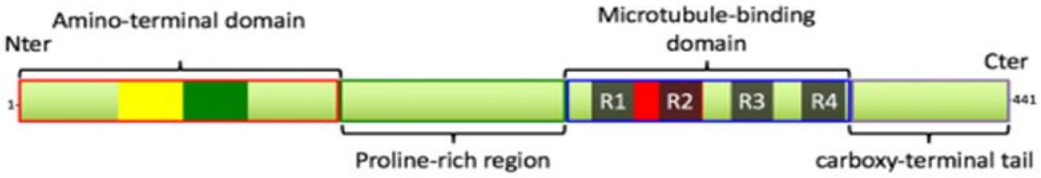

Figure 2 : Tau structure. Consist of four domains with different biochemical properties: an amino terminal region, a proline-rich domain, the MTBD with four repeated sequences (R1–R4), and a carboxy-terminal. Adapted from (Colin et al., 2020).

1.3 Role of tau as Microtubule Associated Protein

Tau is one of the major proteins of MAPs family present in the central nervous system. The expression of one or the other isoform is developmentally regulated. Furthermore, tau is mainly found in axons, while MAP2 (the second protein) is expressed in cell bodies and dendrites (Melková et al., 2019). By far the most predominant interaction of tau is tau association with microtubules (MTs). This interaction leads to the stability of the microtubules, transport along the axons and axonal differentiation. The repetitive regions of the C-terminal part of tau protein (R1-R4), represent the binding region with the microtubules, acting as promotor of tubulin polymerization and inhibitor of de-polymerization. This results in an increased growth rate and decreased catastrophe frequency (Murphy et al., 1977; Trinczek et al., 1995). However, due to inherent dynamics of the system and the disordered nature of tau the exact mechanism of assembly and stabilization of MTs remain challenging to characterize (Barbier et al., 2019). The binding capacity of tau to MTs depends partially upon the phosphorylation state since phosphorylated tau proteins are less effective than non-phosphorylated tau proteins on microtubule polymerization.

Chapter 2: Tauopathies- Alzheimer's disease case

Tauopathies are defined as neurodegenerative disorders characterized by neuronal loss and intraneuronal accumulations of neurofibrillary tangles (NFT) (Buée et al., 2000) the major constituent of which is the tau protein aggregated into straight or paired helical filaments (SFs or PHFs, respectively) (Guo et al., 2017). It is important to mention that certain *MAPT* mutations result in abnormalities in tau protein causing neurodegenerative disease, such as frontemporal dementia (FTDL-tau), proving that tau inclusions can form in the brain in the absence of Aβ deposits (Poorkaj et al., 1998; Spillantini et al., 1998). This can correlate tau with cognitive dysfunction and neurodegeneration. However, tau neuropathology never exists in isolation because as a cytosolic protein it easily interacts with other amyloidogenic proteins showing the relationship of tau with the other developed pathologies (like for example Parkinson and Pick's disease). Between tauopathies there is a strong heterogeneity, with over- lapping but distinct pathologies (Alicea et al., 2021). The most well characterized among tauopathies is Alzheimer's Disease (AD), which characteristic pathological features will be developed in this chapter.

2.1 Description of Alzheimer's Disease

The relevance of tau for neurodegeneration became apparent between 1985 and 1991, when it was found to be the major component of the filaments that make up the neurofibrillary lesions of AD (Michel Goedert et al., 2017). In 1907, Alois Alzheimer had identified these lesions by light microscopy (Morris & Salmon, 2007) and Michael Kidd later used electron microscopy of sections to show their agreement. Alzheimer's disease is a progressive neurodegenerative disorder that leads to dementia and affects approximately 10% of the population older than 65 years. The first clinical sign of AD patients is cognitive impairment related to memory loss. These symptoms are associated as the disease progress by aphasia, agnosia, apraxia and behavioral disturbances. The two hallmarks of the disease are: the extracellular accumulation of Aβ peptides and/or the intracellular aggregation of tau protein. In the first case there is creation of senile plaques (SPs), while in the second case the accumulation occurs in form of neurofibrillary tangles (NFTs). The relationship between tau and Aβ in progression of AD pathology is still controversial with most data supporting Aβ being the primary event in AD pathogenesis with secondary triggering of pathologic tau production (Braak & Del Tredici, 2013; Carare et al., 2013). Nonetheless, accumulation of pathologic tau in the brains correlates well with dementia in AD patients (Braak and Braak et al.,1991). Thus, by the time AD clinical signs appear, there is already substantial tau pathology in the brain (Cairns et al., 2013).

2.1.1 The Aβ peptide and the senile plaque formation

The senile plaque formation is one of the two major hallmarks of the AD (Hardy & Higgins, 1992). The proteolysis of transmembrane protein APP by two secretases, named as β and γ secretases, forms single units of Aβ, which further undergo certain structural modifications and accumulation of those lead to formation of the amyloid plaques. The Aβ protein proteolysis generate two peptides, Aβ40 and the Aβ42, where the latter is soluble. The APP is normally cleaved by an enzyme called alpha secretase, yielding sAPP-α (Karlawish et al., 2017; Soto, 2003), which is responsible for memory and learning activities of the brain (Agarwal et al., 2021). In the diseased condition, the APP is cleaved by β-secretase into sAPP-β and C99 fraction, which is membrane bound. The γ-secretase activity upon the C99 fraction produce either Aβ40 or Aβ42, which cause the plaques to deposit (Saito et al., 2005; Wei Qiang1 et al., 2017). Thus, the normal activity of the sAPP is disrupted, leading to metabolic changes, decreased neuronal excitability, conditions favoring oxidative stress and dysregulated calcium homeostasis. Aβ plays a role in memory and synaptic plasticity, although its proper function in the brain remains unknown yet (Puzzo & Arancio, 2013). Amyloid precursor protein (APP) cleavage in normal (non-amyloidogenic) and AD (amyloidogenic) pathways is shown in Figure *3*.

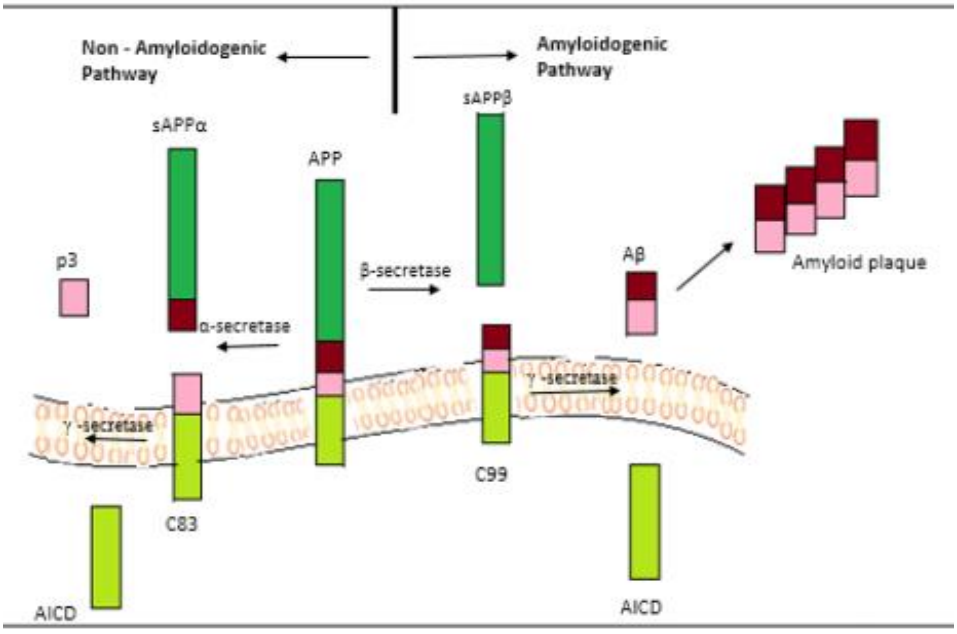

Figure 3. Amyloid precursor protein (APP) cleavage in normal (non-amyloidogenic) and AD (amyloidogenic) pathways. Adapted from (Agarwal et al., 2021)

Senile plaques are diffusely and variably distributed throughout the cerebral cortex and in subcortical structures. The progress of Aβ peptide deposits' is described by Thal stage (Thal et al., 2002), and it consists of five distinct phases. The spread starts from the neocortex to the entorhinal area and the hippocampus, reaching the subcortical structures, the brain stem and finally the cerebellum, as shown in Figure *4*.

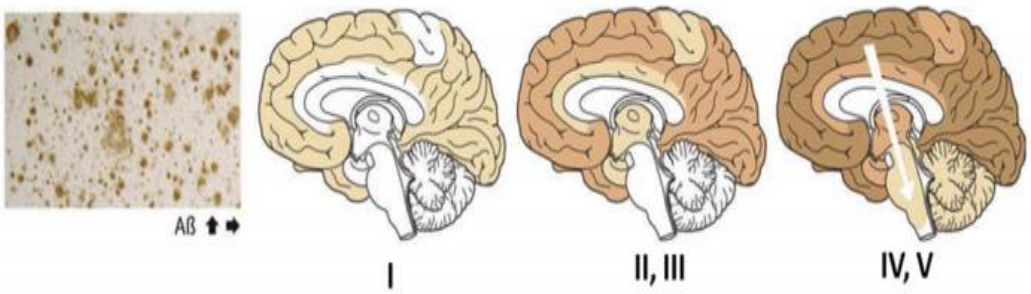

Figure 4 : Spatio- temporal evolution of Thal stages describing the progression of Aβ aggregates. On the left is shown amyloid plaques in human AD brain. In the right has been given the five stages of progression of β-amyloidosis through spatio-temporal way in the brain, described by Thal. The first phase displays only neocortical Aβ deposits. The second phase is characterized by the additional involvement of allocortical brain regions. In phase 3, diencephalic nuclei, the putamen, the caudate nucleus, the substantia innominata, and the magnocellular cholinergic nuclei of the basal forebrain exhibit Aβ deposits as well, whereas several brainstem nuclei first become involved in phase 4. The fifth and final phase is characterized by Aβ-deposition in the cerebellum and in additional brainstem nuclei. The five phases give a more precise description of the evolution of -amyloidosis in the entire brain. Adapted from (Jouanne et al., 2017).

2.1.2 Tau phosphorylation in Alzheimer's disease

The major antigenic components of NFT are PHFs, which are characterized by high phosphorylation state of tau protein. Their biochemical characterization by immunoblotting reveals the presence of a triplet of proteins, found at 55, 64 and 69 kDa. However, it is also found one band at a higher molecular weight, between 74 kDa, which is related to the longest tau isoform, as shown in Figure 5. The forms of tau detected in the triplet refers to different phosphorylation states of different tau isoforms. It is established that: the 55kDa results from the phosphorylation of the fetal isoform (tau 0N3R), the 64kDa from the phosphorylation of tau variants of one exon (1N3R and oN4R), the 69kDa from the phosphorylation of tau variants with two cassette exons (2N3R and/or 2N4R), inducing the formation of the additional hyperphosphorylated variant, the one found with low signal at the molecular weight of 74kDa (Buée et al., 2000). Both the size of tau isoforms and the phosphorylation state influence the electrophoretic mobility of the protein. Thus, immunological probes specific of tau hyperphosphorylation sites are used to identify of NFT in human brain samples. Figure *5* summarizes the link between the typical pattern of phosphorylated tau isoforms separated by electrophoresis to particular tauopathies. Besides Alzheimer's disease, tauopathies include tangle-only dementia, chronic traumatic encephalopathy, argyrophilic grain disease, progressive supranuclear palsy, corticobasal degeneration, globular glial tauopathy and Pick's disease. Unlike Alzheimer's disease, these other diseases lack amyloid-β plaques. In Alzheimer's disease, tangle-only dementia and chronic traumatic encephalopathy, all six tau isoforms (3R and 4R) are present in the disease filaments. In argyrophilic grain disease (AGD), progressive supranuclear palsy (PSP), corticobasal degeneration (CBD) and globular glial tauopathy , only 4R tau isoforms are found, whereas in Pick's disease (PiD) only 3R tau inclusions are present (Fitzpatrick et al., 2017).

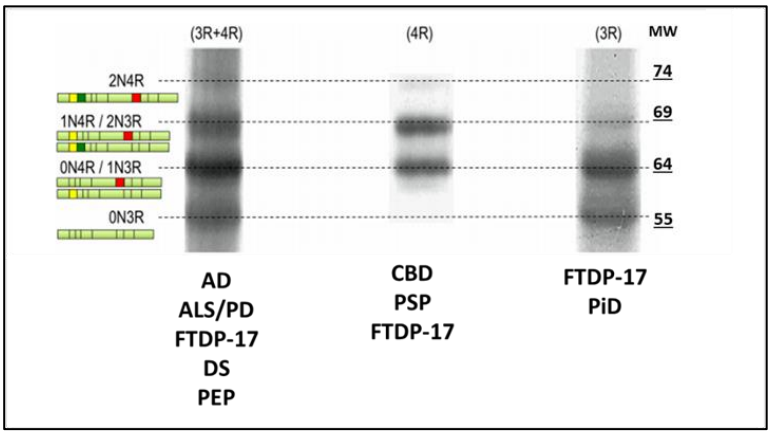

Figure 5 : Typical electrophoretic profiles of pathological tau proteins. Schematic representation of isoforms composition (left of each frame). The six tau isoforms are involved in the formation of the typical AD-triplet (55, 64 and 69kDa) and minor detection of the longest isoform at 74kDa. This pattern is also described in amyotrophic lateral sclerosis with Parkinson disease (ALS/PD), front temporal dementia with the mutation FTDP-17, Down syndrome (DS), and post-encephalitic parkinsonism (PEP). The doublet tau 64, 69 is related to the aggregation of hyperphosphorylated tau isoforms with exon 10 in Progressive supranuclear palsy (PSP) and corticobasal degeneration (CBD). The FTDP-17 families with mutations in exon 10 or intron 10 exhibit the same profile (middle panel). Hyperphosphorylated tau proteins without exon 10 aggregated in Pick's disease (PiD) and are detected as a tau 55, 64 doublets (right frame). Adapted by (Colin et al., 2020), based on (Sergeant et al., 2008).

Thus, Immunoblotting has been of value in the investigation of the progress of the tau pathology through the brain, as it has been a positive marker in detection of tau pathology once developed, demonstrating that AD is a disease involving the long cortico-cortical connections. Neuropathological Braak staging of AD brain characterizes six progressive stages of disease propagation (Braak and Braak., 1991). The NFTs are first detected at the entorhinal region (Braak's stages I and II) extending progressively to the hippocampus area (stages III and IV) and the neocortical region (stages V and VI), as shown in Figure 6.

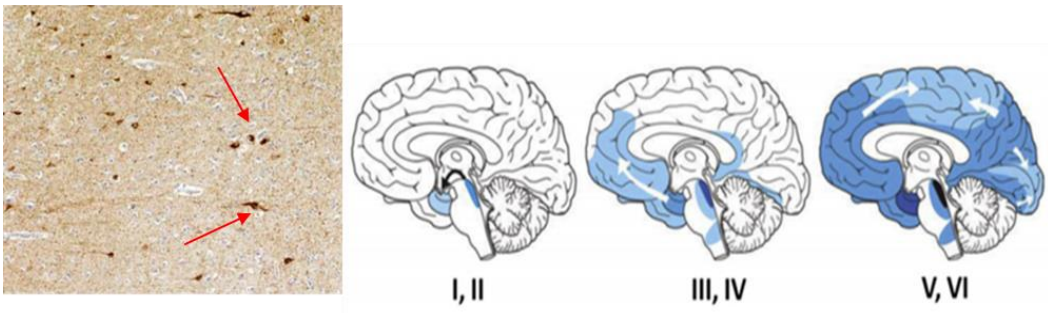

Figure 6 : Spatio- temporal evolution of tau pathology in AD as described by the Braak staging scheme. In the left it is shown the NFT detected, red arrows, in human brain slice from a postmortem histology in neocortex by using the AT-8 antibody. In the right it is presented the distribution of tau pathology at different Braak stages. Tau pathology begins in the locus coeruleus. Stages I and II, tau lesions invade entorhinal and transentorhinal regions. Stages III and IV: lesions involve the associative areas of the neocortex, and during stages V and VI, tau lesions invade all the primary and secondary neocortical areas. Adapted from (Jouanne et al., 2017).

Chapter 3: Tau aggregation

The amino acid composition of the longest tau isoform (2N4R) suggests an overall hydrophilic and soluble protein. Tau is also an intrinsically disordered protein and this is reflected in its amino acid composition with only five different amino acid residue types constituting 50% of the sequence, associated to a poor content in aromatic residues (Smet et al., 2004). However, in tauopathies, under the conjunction of a number of factors - mutations, isoform proportion modifications, post-translational modifications (PTMs), truncations - tau undergoes misfolding and oligomerization into insoluble tau deposits. Short hexapeptide motifs in the beginning of R2 (residues 274-281, named as PHF6*, VQIINK) and R3 (residues 306-311, named as PHF6, VQIVYK) (Pérez et al., 2002; Martin Von Bergen et al., 2001), were defined as nuclei of Tau aggregation and tend to adopt transient β-sheet structure in solution (Mukrasch et al., 2009). Furthermore, the analysis of the composition of NFT has revealed the presence of PHF and SF, mostly described in AD. Both types of filament are predominantly composed of abnormally phosphorylated tau protein (Guo et al., 2017), leading to the proposition that phosphorylation is the major post-translational modification that induces tau aggregation.

3.1 Structural analysis of tau filaments in Alzheimer Disease

To better understand the atomic structures of tau filaments is of importance to understand the molecular mechanisms underlying tauopathies. As already mentioned, tau inclusions are made of paired helical filaments (PHFs) and straight filaments (SFs) (Terry et al., 1963), which each consists of two protofilaments. Each protofilament, consists of a core region and a fuzzy coat. The core in both cases is a double helical stack of eight β-sheets (β1–8) (Figure *8*a) that adopt a C-shaped subunits (Crowther, 1991), as shown in Figure *7*a and b, whereas the amino- and carboxy-terminal regions of tau are disordered and project away from the core to form the fuzzy coat (C M Wischik et al., 1988). In Alzheimer's disease though, tau filaments form from full-length tau in cells, have lost most of their fuzzy coat in extracellular ghost tangles. Furthermore, cryo-electron microscopy on fibers extracted from human AD brain (Fitzpatrick et al., 2017), has revealed that the core of both PHFs and SFs is composed of the residues V306-F378, including hexapeptide $_{306}$VQIVYK$_{311}$ (PHF6), which is essential for the oligomerisation of recombinant tau and its assembly into filaments (M. Von Bergen et al., 2000). This part corresponds to the R3 and R4, plus 10aa at the C-terminus of these repeats. The N- and C- terminal of the protofilaments, have weaker electron densities, indicated by light pink color, shown Figure *7*a. Importantly, the N-terminus of R3 hosts 16 residues in a β-sheet-like conformation (indicated with grey dashed underlines, Figure *8*a), corresponding to the C-terminus of R1 and R2 domains. Further, the PHF protofilament interface is stabilized by extensive hydrogen bonding across the

extended β-spiral formed by residues $_{332}$PGGGQ$_{336}$, as well as salt- bridge interactions between K331 from one protofilament and Q336 and E338 of the other protofilament, as shown in the right of Figure *7*a. While in SFs case, the two similar protofilaments pack asymmetrically and appear to be stabilized by an additional density between the side chains of K317 and K321 from both protofilaments, as shown in the right of Figure *7*b. These data support the hypothesis of ultrastructural polymorphism, as both fiber types of SF and PHF consist of identical protofilaments, but they differ in the interfilament packing.

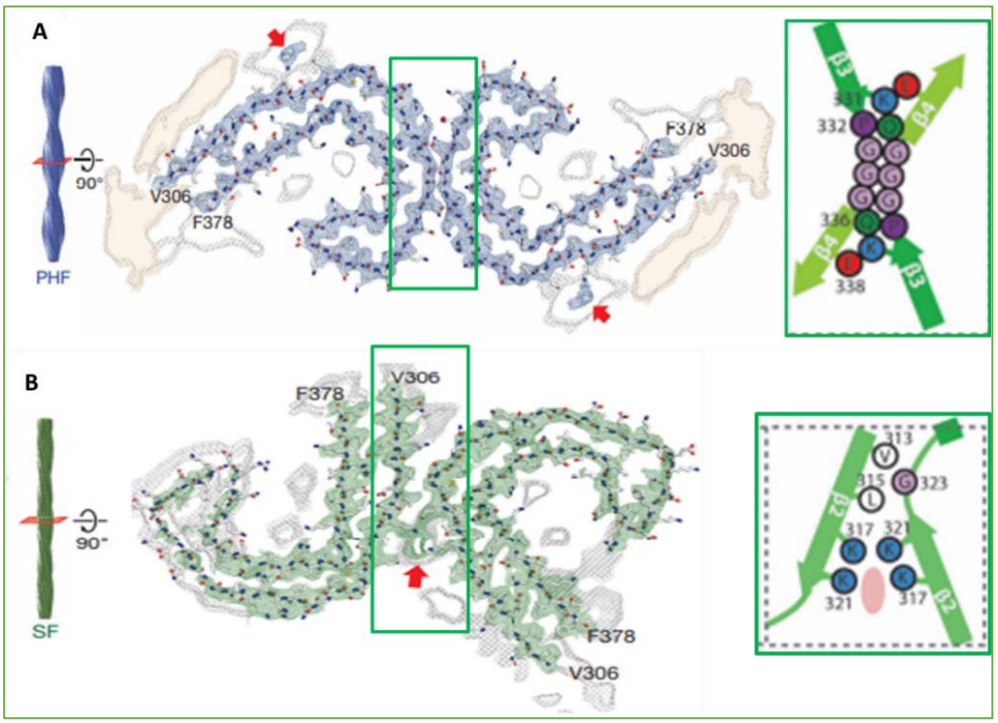

Figure 7. Cross-sections of the PHF (a) and SF (b) cryo-EM structures. Overviews of the helical reconstructions (left) show the orientation of the cross-sectional densities (right). Sharpened, high-resolution maps are shown in blue (PHFs) and green (SFs). Red arrows indicate additional densities in contact with K317 and K321. Unsharpened, 4.5Å low pass filtered density is shown in grey. Weaker density is highlighted with an orange background is reminiscent of a less-ordered β-sheet and could host an additional 16 amino acids, including the residues 259–274 (R1) from 3R tau and the residues 290–305 (R2) from 4R tau. Adapted from (Fitzpatrick et al., 2017) and (Scheres et al., 2020).

Each C-shape consists of a β-helix region, where three β-sheets are arranged in a triangular fashion, and two regions with a cross-β architecture, where pairs of β-sheets pack anti-parallel to each other (Figure *8*b and c). This continuous β-strand architecture along the chain of an individual tau molecule is achieved by interspersing the β-strand regions with β-breaking prolines (P312, P332, P364), β-turn glycines (G323, G355) or β-arc residues (E342, D348), Figure *8*a. The strain of having many twisted β-strand regions is relieved by changes in the height of the chain along the helical axis, resulting in differences of up to 10Å between the highest point in β1 and the lowest point in the tip of the β-helix (Figure *8*c).

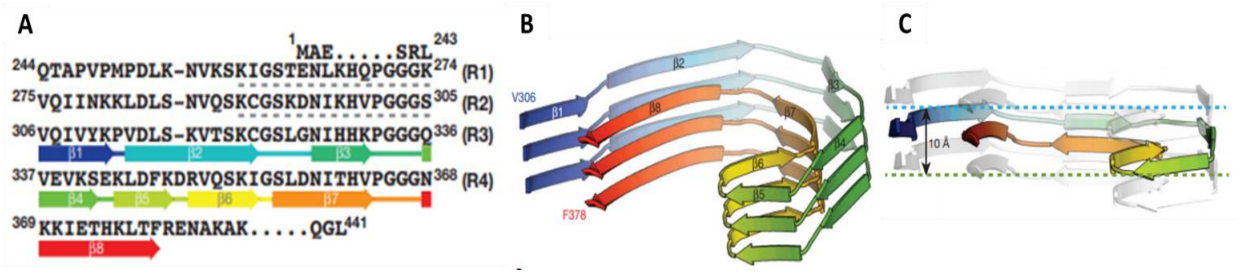

Figure 8: The common protofilament core. **A.** Sequence alignment of the four microtubule-binding repeats (R1–R4) with the observed eight β-strand regions colored from blue to red. The sixteen residues from R1 or R2 that may form an additional, less-ordered β-sheet are indicated with grey dashed underlines. **B.** Rendered view of the secondary structure elements in three successive rungs. **C.** As in b, but in a view perpendicular to the helical axis, revealing the differences in height within a single molecule. Adjusted from (Fitzpatrick et al., 2017).

In general, the relevance of distinct filament types between diseases remains unknown. It is possible that the different nature of their protofilament interfaces affects formation and disassembly of these filament types. In addition, the size of the ordered core, the polarity of the filaments, how many monomers are exposed laterally at the ends of filaments, which amino acid side chains are solvent-exposed, and the incorporation of additional, non-proteinaceous molecules may play a role. All these factors may affect the spreading of filaments throughout the brain.

3.1.2 Local structure of inert and seed-competent tau monomers

The amyloid motif $_{306}$VQIVYK$_{311}$ in R3 has been described to be one of those that have critical role , on conversion between the soluble and insoluble states, driving self-assembly *in vitro* (Sawaya et al.,2007), and promoting pathology *in vivo* (Martin Von Bergen et al., 2001), mediating important connections (Fitzpatrick et al., 2017). In line to this outcomes are NMR data, which indicate that in solution the $_{306}$VQIVYK$_{311}$ motif adopts a β-strand (Eliezer et al., 2005; Mukrasch et al., 2005), which remains the same between different strains of tau, that could indicate also an independent-folding behavior as part of the total MTBD region (Mukrasch et al., 2005). However, how or why a relatively inert form transits to one that efficiently self-assembles into ordered structures *in vivo* is unknown. This structural transition could be a critical event in the pathogenesis of neurodegeneration. Under defined conditions and relatively high concentrations (typically micromolar), recombinant tau monomer will form amyloid fibrils *in vitro*. The conversion of a protein from a monomer to a large, ordered multimer could occur by several mechanisms, but the first step involves the formation of a seed by a nucleation process. This event, and indeed the actual conformation or assembly state of the protein that constitutes the 'minimal' seed, has remained obscure. This has led to the idea that a seed is potentially transitory, arising from an equilibrium between two states: one relatively aggregation-resistant, and another that is short-lived. A seed could be a single molecule, or several. Based on extrapolation from kinetic aggregation studies, it has been suggested that a critical seed for tau and polyglutamine peptide amyloid

formation is a single molecule (Chirita et al., 2005; Bhattacharyya et al., 2005; Kar et al., 2011), Cryo-EM structures also suggested an extended conformation of tau when bound to tubulin. Other work mapping the recruitment of molecular chaperones to tau indicated that many chaperones, including Hsp40, Hsp70, and Hsp90, localize around $_{306}$VQIVYK$_{311}$. Furthermore, unfolding of tau repeated domain appeared to promote chaperone binding to the amyloid motif, suggesting that local conformational changes may help recruit factors to limit aggregation.

Chapter 4: Post Translational Modifications

The physiological functions of tau are highly regulated by a wide range of post-translational modifications (PTM), including phosphorylation, methylation, acetylation, glycation, isomerization, nitration, SUMOylation, and ubiquitination (Buée et al., 2000; Morris & Salmon, 2007). The alteration of these modifications can affect tau functions and potentially lead to pathological conditions. Further, the natively unfolded structure of tau protein in the cytosolic environment, make tau sequence highly accessible to a number of regulatory components of PTMs, such as protein kinases and phosphatases (Buée et al., 2000; Mandelkow & Mandelkow, 2012).

4.1 Protein Phosphorylation

Based on the longest isoform of tau (441aa) there are 45 serine (Ser), 35 threonine (Thr) and 5 tyrosine (Tyr) candidate sites for phosphorylation (Arendt et al., 2016; Guo et al., 2017; Noble et al., 2013). The phosphorylation sites, being described so far, have come through phosphorylation-dependent monoclonal antibodies raised against tau, mass spectrometry and sequencing (Figure 9). Most of the identified phosphorylated sites are on Ser-Pro and Thr-Pro motifs, localized outside the microtubule binding domain, with important exceptions of Ser262, Ser285, Ser305, Ser324, Ser352 and Ser356 located inside MTBD (Hasegawa et al., 1998; Roder et al., 1997; Seubert et al., 1995). The phosphorylation state of tau comes as result of specific kinases and phosphatases activity towards these 85 sites, with observed changing pattern during brain development (physiological phosphorylation) and disease progression (pathological phosphorylation).

4.1.1 Physiological Phosphorylation

Among 85 sites “eligible” for phosphorylation on tau protein, 30 are related to physiological phosphorylation (Hanger et al., 2009; Morishima-Kawashima et al., 1995). Phosphorylation changes the shape of tau molecule and regulates its biological activity (Johnson & Stoothoff, 2004). This is obvious during embryogenesis and early developmental process, when Tau contains 3–4 fold phosphates over the normal adult tau (Iqbal et al., 2016)(Mawal-Dewan et al., 1994) as there is an important neuronal plasticity (Brion et al., 1993; Hanger et al., 2009). Thus, in immature brain, tau is phosphorylated at a large number of sites (Morishima-Kawashima et al., 1995), while later on, in adult brain, the phosphorylation is more limited (Figure 9).

4.1.2 Pathological Phosphorylation

The state when other sites than the physiological ones are phosphorylated is referred as “abnormal”, “pathological” or “hyper-phosphorylated” (Figure 9). In this case, the balance between kinase and phosphatases changes, leading to increased number of the pathological phosphorylation sites. Phosphorylation found in PHF were proposed to be pathological sites of

tau phosphorylation, and were suggested to promote the aggregation and contribute to formation of neurofibrillary tangles (NFTs) found in AD (Grundke-Iqbal et al., 1986). This hypothesis relates the hyper-phosphorylation detected in the aggregates to the mechanism of tau aggregation and neuronal toxicity (Kosik & Shimura, 2005; Noble et al., 2013). The early stage of pathological phosphorylation induces the detachment from tubulin (Barbier et al., 2019), leading to cytoskeletal destabilization, also combined with the relocation of tau from the axons to somato-dendritic, where it is prone to further phosphorylation. Then, the detached tau allows tau-tau interactions and promoting self-aggregation, forming oligomers and higher order tau aggregates (Kopke et al., 1993a; M. Von Bergen et al., 2000). The latest progress of tau aggregate formation is related to increased levels of somatic tau (Augustinack et al., 2002; Harley et al., 2021). The AD brain tissue examined with phosphorylated dependent tau antibodies showed that NFT could be classified as pre-tangle, intra-neuronal and extra-neuronal tangles, indicating that the pathological phosphorylation is correlated with the disease progression. Epitopes correlated with pre-tangle are situated at: S199, S202, T231, S262, T153 and S409; with intra-neuronal tangle at: pS46, pT175/pT181, pT231, pS262/S356 (12E8), pS396, pS422 and pS214; with extracellular: pS202/pT205/pS08 (AT-8), pT212/pS214 (AT-100) and pS396/pS404 (PHF-1) (Augustinack et al., 2002; Morishima-Kawashima et al., 1995); while in later stage is also detected pT231/pS235 (AT180) (summarized in Figure 9). In the majority of the studies AT-8 (pS202, pT205 and pS208) and PHF1 (pS396 and S404) are used to perform time-course dependent analysis of tau hyper-phosphorylation (Alafuzoff et al., 2008; Braak et al., 2006, 2011; Picci, 2019), while for the aggregated forms AT100 (pT212 and pS214) is preferred.

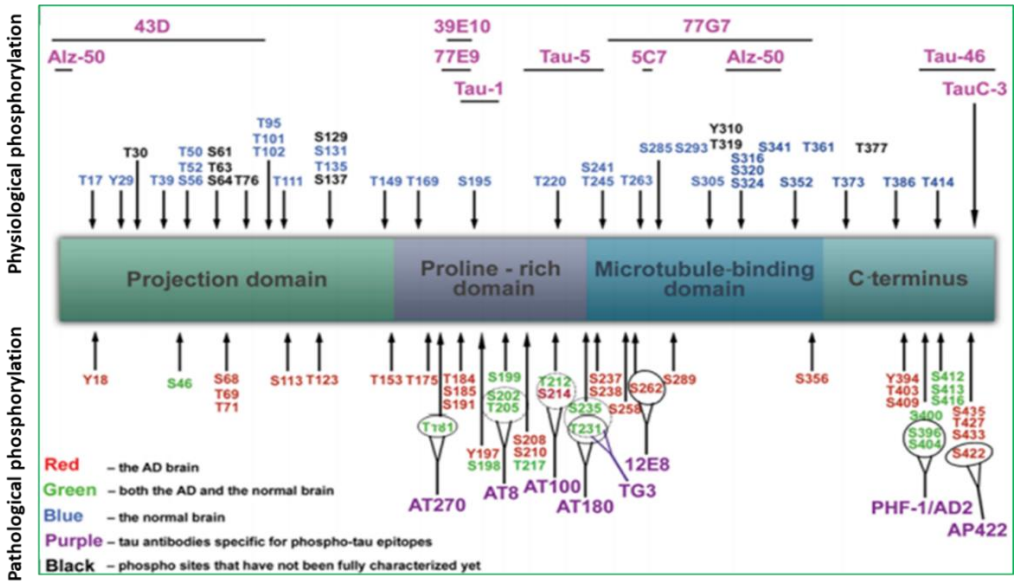

Figure 9 : Phosphorylated epitopes of tau protein in physiological (above the tau structure) and pathological case (below the tau structure) in AD brain. Red color denotes amino acids phosphorylated in AD brain, green in both AD and normal brain, blue in normal brain, while black color refers to the sites that have not been fully characterized yet. Also, in purple are given the tau antibodies specific

for phospho- tau epitopes are given in purple and in pink color denotes antibodies specific for non-phosphorylated tau epitopes. Adapted from (Šimić et al., 2016).

There are several evidence of the effect of site-specific phosphorylation without determining though the relation with the tau pathology. For example: the phosphorylation of the proline reach domain is related to the disruption of the microtubule assembly (Eidenmüller et al., 2001), while the phosphorylation of the C-terminal domain remarkably promotes tau self-aggregation (F. Liu et al., 2007).

4.1.3 Tau Kinases

There is a number of kinases (around 30) related to tau phosphorylation *in vitro* (Kopke et al., 1993a). Most of them phosphorylate several residues of tau while one single residue can be the target of more than one kinase. In order to better distinguish, they are classified in three groups a) proline directed serine/threonine- protein kinases (PDPK) b) non- proline-directed serine/threonine-protein kinases (non-PDPK) c) protein kinases specific for tyrosine residues (Guo et al., 2017). However, it is unclear how many kinases actually phosphorylate Tau *in vivo*. Currently, only glycogen synthase kinase (GSK3β), cyclin-dependent kinase 5 (Cdk5), cAMP-dependent protein kinase A (PKA) and microtubule affinity-regulating kinase (MARK) are known to modulate tau phosphorylation *in vivo* at some level, either directly or indirectly (Johnson & Stoothoff, 2004). The physiological phosphorylation of tau regulated by these kinases effect the neurite extension and retraction, while the hyper- phosphorylation by PDPKs, GSK-3β and Cdk5, have been long implicated in AD pathogenesis (Wilkaniec et al., 2016).

4.1.3.1 GSK-3β

GSK-3β is targeting multiple SP/TP epitopes, an more than 40 sites in total, (Hanger et al., 2009), including the pathological related ones of PHF-1, AT8, AT180, AT100. Different studies associated these phosphorylation sites of GSK3β with the formation of PHFs and NFT and further implication in the pathogenesis of AD, while GSK3β inhibition showed to reduce tau phosphorylation and pathology (Leroy et al., 2010). However, observing the multiple roles this kinase has, including pro-apoptotic (Jackson et al., 2016) may position GSK3β as a prominent player in the AD pathology beyond its phosphorylating role on tau protein.

4.1.3.2 Cdk5

Cdk5 is proline- serine/threonine related kinase mostly related to tau pathology in AD with the pre-tangle and early NFT stages, with the sites of its activity found to be co-localized with AT-8 positive tau (Augustinack et al., 2002). The activation of Cdk5 is dependent on the conversion of p35 to p25 by proteolysis (Ahlijanian et al., 2000). In the same study, it was observed that mice overexpressing p25 had higher Cdk5 activity, suggesting further that the pathological phosphorylation

of tau at AT-8 and PHF-1 epitopes, found in APP mice, (Otth et al., 2002) is related to Cdk5 due to increased levels of p25. These findings have related Cdk5 predominantly as modulator of Aβ pathology rather than tau phosphorylation.

4.1.4 Tau phosphatases

Compared to the large number of tau kinases, only few phosphatases have been identified with protein phosphatase 2A (PP2A) being responsible for over 70% of the total tau phosphatase activity (F. Liu et al., 2005). Expression of PP2A and its activators is significantly reduced in the brains of individuals with AD compared with age-matched controls, whereas PP2A inhibitors are upregulated (Sontag & Sontag, 2014). For instance, hyper-phosphorylation of tau Ser202/Thr205 is regulated negatively by PP2A activity (Kins et al., 2003). Interestingly, PP2A also regulates GSK3β and CDK5 providing an additional route to influence tau phosphorylation (Sontag & Sontag, 2014).

4.1.5 Is the phosphorylation the one to blame?

The first belief of highly relating the aggregation to the hyper-phosphorylation, triggered an extended search for kinases and phosphatases responsible for tau's pathological state (Hoffman et al., 2017; L. Martin et al., 2013), searches for specific p-tau in tau (Hanger et al., 2009) and treatments based on these results. However, it is still controversial whether or not tau phosphorylation is the cause of the aggregation process (*Mendelkow Phosp.Pdf*, n.d.; Tenreiro et al., 2014). It is shown in *in vitro* experiments that recombinant un-phosphorylated tau induced aggregate formation similar, but not the same, to PHFs derived from AD, questioning the need of phosphorylation for the aggregation process (Morozova et al., 2013; Terwel et al., 2008)(W. Zhang et al., 2019). The same was observed using an *in vivo* mouse model, PS19 mice (tauP301S mutation), where NFT pathology was induced by synthetic tau aggregates in the absence of tau hyperphosphorylation (Iba et al., 2013). The high rate of phosphorylation sites (~20%), being accessible to multiple kinases and phosphatases gives the thought that the degree of phosphorylation therefore depends on phosphorylation "tone" rather than on specific functional modifications. Further, the balance between kinases and phosphatases is affected by experimental conditions of tau purification from brains, which may influence tau pathology and thus produce artifactual results that are not related to the disease itself. In detail, a rapid isolation of brain tissue reveals a high phosphorylation state of AD-tau, explained by existence of tau aggregates being protected by PPase activity. Conversely, in a post-mortem delay, ATP is depleted (inactivating kinases) and PP2A category is activated, which makes adult human tau in low phosphorylation state. Further, in experimental mouse model processing's like anesthesia, where hypothermia conditions faced, activity of PPase decreases and the level of kinases is elevated, which may cause the impression of hyper-phosphorylation (Whitten., 2011; Matsuo et al., 1994; Planel et al., 2007). Consistent with the aforementioned observations, it is not found that any of the

phosphorylation states observed from post-mortem purified tau led to a pronounced increase in tau aggregation (Y. Wang et al., 2015). However, based on the extent of phosphorylation may lead to the change of the overall charge from positive to negative effecting the interactions with other proteins in the cytosolic environment (Mandelkow & Mandelkow, 2012) as well as to a possible conformation changes (Wegmann et al., 2018). Regarding the conformational changes, it is known that specific phosphorylation's like the one on the epitopes AT8, PHF-1 and AT-100 can affect the global conformation, where the compaction defined as a paperclip can become tighter or looser, (Bibow, Ozenne, et al., 2011; Jeganathan et al., 2008), or correlated to some structural changes localized in the proximity of phosphorylation sites (Schwalbe et al., 2013). Altogether, in all tauopathies, increased phosphorylation and aggregation of protein tau is evident, although it remains disputed what is cause, consequence and correlation.

4.2 Tau glycosylation

The non-canonical form of glycosylation is O-linked-N-acetylglucosaminylation (O-GlcNAcylation), which is added to protein residues by enzyme O-GlcNAc transferase (OGT), and removed by O-GlcNAcase (OGA) (Bourré et al., 2018). O-GlcNAcylation is another important PTM involved in regulation of tau pathophysiology. It is based on addition of a single sugar, the β-D-N-acetylglucosamine, on serine and threonine residues of nuclear and cytoplasmic proteins (Hart, 1997). O-GlcNAc modification has been implicated in numerous neurodegenerative disorders (Gong et al., 2016; Ma et al., 2017; Robert Cronin Yung Peng, Rose Khavari, 2017; Zhu et al., 2014), while variations in its levels in AD brain are still a matter of debate. Due to decreased glucose uptake/metabolism that is one of the main metabolic changes in aging brain (Heiss et al., 1991), including AD, O-GlcNAcylation of proteins is lowered (Gong et al., 2016; Heiss et al., 1991). Pharmacological increase of O-GlcNAcylation has shown that leads to neuroprotective effects and constitutes a potential strategy of treatment of neurodegenerative diseases, involving tau pathology (Yuzwa et al., 2012, 2014). Furthermore, O-GlcNAc has been described in the regulation of tau phosphorylation and reciprocally, competing at the same site or alternatively (Robertson et al., 2004). Additionally, the crosstalk between both PTMs may extend to the reciprocal modification of enzymes implicated in phosphorylation and O-GlcNAcylation dynamics (Z. Wang et al., 2008). It is found that O-GlcNAc negatively regulates tau phosphorylation in a site- specific manner in cultured cells, *in vivo* and in metabolically active brain slices (F. Liu et al., 2009). Conversely, inducing hyperphosphorylation of tau with the phosphatase inhibitor okadaic acid leads to a reduction of tau O-GlcNAcylation in human neuroblastoma cells together with a reduced transfer into the nucleus (Lefebvre et al., 2003). Interestingly, hyperphosphorylated tau is less O-GlcNAcylated than forms of tau that are less phosphorylated (Lefebvre et al., 2003; F. Liu et al., 2009). More recent data suggest that hyperphosphorylation of tau is not antagonistic of glycosylation

and may rather indirectly contribute to an increase of tau O-GlcNAcylation which could be a salvage mechanism to protect cells from tau toxicity and fibrillar aggregation, two processes which seems to have their origins in tau hyperphosphorylation (Bourré et al., 2018). This protective mechanism could be impaired in AD brain where the O-GlcNAc dynamics is strongly perturbed due to lower glucose metabolism/uptake.

4.3 Tau truncation

As a natively unfolded/poorly-folded protein, tau is very sensitive to protease digestion, which is found in a wide variety of human neurodegenerative diseases, including AD (Gamblin et al., 2003; Horowitz et al., 2004; C M Wischik et al., 1988) and PSP (Arai et al., 2004). Numerous studies have shown that tau is a substrate for calpain (Johnson et al., 1989), caspase (Gamblin et al., 2003), thrombin (Arai et al., 2005), cathepsin (Bednarski et al., 1996), Puromycin-specific aminopeptidase (Karsten et al., 2006), and asparagine endopeptidase (Zhang et al., 2014) *in vitro* and *in vivo*. These studies have shown that tau truncation plays an important role in both tau aggregation and neurodegeneration (Kovacech and Novak, 2010). As it may be the mechanism that modifies tau such that it becomes prone to misfolding, adopting an abnormal conformation and self-assembling into filaments more readily than does full-length tau. In AD brain, several specific truncations of tau have been identified (Wang et al., 2010). Truncation of tau at Asp421 (D421) and Glu391 (E391) has been shown to make tau prone to aggregation (Kovacech and Novak, 2010).

4.4 Tau clearance by the ubiquitin-proteasome system and autophagic-lysosomal degradation

Incomplete clearance from the brain of pathological tau could also result from its inefficient degradation through the ubiquitin- proteasome system (UPS) and/or autophagic-lysosomal system. The UPS mediates the selective degradation of nuclear and cytosolic proteins, whereas the autophagy-lysosomal system is primarily involved in the clearance of long-lived proteins and organelles through non-selective bulk degradation (Rubinsztein et al.). Several studies have demonstrated that tau can be degraded through the UPS and by the autophagic-lysosomal system. Identification of ubiquitination sites on both soluble and insoluble highly phosphorylated tau has provided a strong evidence for the role of the UPS in tau clearance (Lee et al.). Moreover, unfolded tau is proposed to be processed independent of ubiquitination (D. C. David et al., 2002). The significance of the UPS in tau clearance is further supported by the identification of UPS components, such as heat shock protein 27 and CHIP as tau binding partners (Lee et al.). Thus, it is not surprising that dysfunction of the UPS is observed in a number of tauopathy models and in AD (Deger et al., 2015). Whereas soluble tau is preferentially degraded by the proteasome, pathological forms of phosphorylated tau appear to be directed towards to the autophagic-lysosomal system for disposal. Indeed, direct evidence for autophagy as the primary route for clearing phosphorylated, but not endogenous,

tau has been obtained from monitoring the differential degradation rates of phosphomimic tau mutants, wild-type tau and endogenous tau in neurons (Rodríguez-martín et al., 2013).

Chapter 5: Tau seeding and propagation

The finding of tau secretion and the cell-cell transfer of pathological species of tau in stereotyped manner (Hyman et al., 1984), is described in a number of tauopathies, including Alzheimer's disease (Braak and Braak 1991, Cho et al., 2016). Thus, the deposits of aggregates inside neurons can contribute to the spreading of tau pathology through synaptically connected neurons (Clavaguera et al., 2009). In this model, tau aggregates or aggregate-prone seeds escape the cell of origin and gain access to neighboring-naïve cells (Dujardin, Lécolle, et al., 2014; Holmes et al., 2013) to nucleate intracellular aggregation (Clavaguera et al., 2009; Guo et al., 2017) through conformational templating. Newly transduced cells can then proceed to propagate misfolded tau to other naive cells (Lewis & Dickson, 2016). This molecular behavior it is reported as "prion-like" propagation hypothesis as the first templated propagation was first conceived from experiments in human and animal models of prion diseases (Prusiner, 1998). There are two distinct steps involved in the progression of the prion disease: 1) seeding, referring to the misfolding induction and 2) propagation, referring to the diffusion of the misfolded protein through extracellular space and axonal paths and further contact with normal proteins, such as tau in our case. The most striking evidence of transmission of pathology through connection is found in AD among tauopathies (Colin et al., 2020; Braak and Braak, 1991), even-though the active cell to cell transmission has not yet been visualized in the human brain by current available imaging methods (Joie et al., 2020). Better understanding of the molecular basis of tau propagation is key to preventing progression from early mild memory impairment to full cognitive deterioration and dementia.

5.1 Modelling of the prion-like propagation

To better understand the "prion-like" propagation hypothesis, several experimental models are developed with data received from humans. This will also help to determine whether tauopathies are reflecting this propagation hypothesis and will improve knowledge regarding the passage of tau in the extracellular space.

5.1.1 Tau secretion

There a number of evidence that tau is secreted in the extracellular space (Yanamandra et al., 2013, 2015), and thus found in the extracellular fluids (Mudher et al., 2017), referring to the interstitial fluid (ISF), cerebrospinal fluid (CSF) and lately findings in the plasma. Tau levels in plasma are low and might be connected to brain changes, while the mechanism of transfer is unknown (Banks et al., 2016). Of note, 20% of the CSF comes from the ISF (Santos et al., 2017), thus any changes to CSF reflects changes to ISF. CSF is of advantage on studying the pathophysiological processes in neurodegenerative diseases as it is the fluid closest to the brain and relatively easy to access for analysis. Thus, an increased level of tau over disease progression in CSF of AD patients, as well as the successful use of these CSFs in order to induce seeding in mouse

model (Clavaguera et al., 2013), could be of strong evidence of the prion –like hypothesis (Skachokova et al., 2019). Tau as soon as translated into the cytosol, is a prey of a number of mechanisms modulating its secretion including: oligomerization, mutations (Karch et al., 2012), phosphorylation, truncation, as well as a number of active interactions with other proteins including those of cell membrane (Buée et al., 2000; Pernègre et al., 2019). Further, an increased level of secreted tau has also been related with an increased neuronal activity (Pooler et al., 2013; Wu et al., 2016). However, the molecular mechanisms of tau secretion remain unknown. One of the main mechanisms supported in the latest years, is the protein release through the unconventional protein secretion (UPS), which is classified in four pathways and could dominate in tau due to lack of conventional signal sequences (Katsinelos et al., 2018; Rabouille, 2017). Furthermore, two of these pathways are dedicated to the cytosolic proteins, like tau, which are secreted either by direct translocation across plasma membrane (type I) or through vesicular intermediates derived from endosomal compartments (type III) (Duran et al., 2010). The latest may explain why tau protein in the extracellular space is found associated with extracellular vesicles (EVs) (Leroux et al., 2021; Mudher et al., 2017), in addition to either free (Dujardin, Bégard, et al., 2014; Katsinelos et al., 2018) or inside nanotubes form (Tardivel et al., 2016) as shown in Figure 10. Katsinelos et al. (Katsinelos et al., 2018) investigated the unconventional secretion of the full- length tau protein, identifying that tau interacts with components at the inner plasma membrane and directly translocate to the extracellular space. This was further triggered in the hyper -phosphorylated state of tau, as due to lower binding to MTs, the increased free tau becomes ready for translocation. An important finding was that the secretion of tau was mediated by sulfated proteoglycans. An important subtype of the latest are heparan sulfate proteoglycans (HSPGs) found to co-localize with NFTs (Goedert et al., 1996) and implicated also in tau uptake (Holmes et al., 2013), as it will be seen next. Furthermore, the non-conventional release of protein tau could explain 1) its presence in CSF, even in the absence of neuronal damage (Yamada et al., 2011), 2) its eventual contribution to the regional propagation of tauopathy (Clavaguera et al., 2009; Frost et al., 2009), and 3) the beneficial effects of tau-directed therapy, which then acts not on an intracellular, but on an extracellular target (developed in Chapter 6).

5.1.2 Tau uptake/transfer

The second step after the secretion of tau in the propagation hypothesis is the uptake. Again, many *in vivo* systems are developed to investigate the uptake of the extracellular tau. In most of the cases are based on the intracranial delivery of pathological material (oligomeric, fibrillary, human or mouse brain derived etc.) (Albert et al., 2019; C. ling Dai et al., 2017; Mudher et al., 2017; Sankaranarayanan et al., 2015), or even peripheral (Clavaguera et al., 2014). This is of further advantage, as it focuses on how tau is captured rather than how it is secreted, avoiding previous cell-autonomous models,

where there are imperfect pathological cellular mechanisms associated with progression of tau pathology. Thus, the uptake of tau protein can be investigated over time through detection of tau pathology in distant, synaptically connected areas, proving the propagation hypothesis (De Calignon et al., 2012; Takeda et al., 2015). The precise molecular nature of the MTBD-containing seed that transmits from cell to cell is unknown, with a predominant hypothesis that seeds should be oligomers or short fibrils rather than higher-order assemblies (Jackson et al., 2016). However, recent work has shown that monomeric seed-competent tau can be isolated from AD brain (Mirbaha et al., 2017). This seed-competent tau differs in intramolecular interactions when compared to inert, soluble monomeric tau. It is proposed that the two PHF6 motifs are exposed in the seed-competent tau that are otherwise buried in the soluble tau (Mirbaha et al., 2017). Conversely, the PHF6 motifs in inert tau are predicted to be shielded by a preferential hairpin conformation around this region making them less prone to aggregation (Mirbaha et al., 2017). Of note, the presence of monomers in CSF in healthy people remains enigmatic, where the most common speculations of their existence are either accidental leakage, or on purpose to serve a physiological function in signal transmission (Theunis et al., 2013). A number of pathways have been suggested for the spread of the seed competent tau including synaptic transfer, interstitial diffusion and even glial (astrocytes) (Kovacs et al., 2018), oligodendrocytes (Narasimhan et al., 2017) and microglia (Asai et al., 2015) transfers. Microglia is related to clearance of pathological tau (explained in Chapter 6), but lately found to transfer pathological species to new areas of the brain (Maphis et al., 2015). The uptake of aggregated tau appears to rely on mechanisms of micropinocytosis (Abulrob et al., 2005) and depends on the presence of cell-surface heparan sulphate proteoglycans (HSPGs) (Holmes & Diamond, 2017; Kfoury et al., 2012; Rauch et al., 2020). Recent studies of tau uptake through specific motifs of HSPGs (Rauch et al., 2018) are performed showing that low-density lipoprotein receptors (LDLRs), known to work in conjunction with HSPGs, have an important role in internalization of different forms of tau by binding to the MTBD (244-372) (Mah et al., 2021; Rauch et al., 2020).

5.1.3 Tau seeding

Both monomeric and aggregated tau are taken up by cells, but only aggregated tau is able to seed the aggregation of soluble, monomeric tau (Falcon et al., 2015). Thus, seeding represents the conversion of normal protein by abnormal one, into a pathological form. This was first shown in tauopathies by Clavaguera et al., where were injection of brain extracts from mice overexpressing P301S, into mice overexpressing human wild type, was sufficient to induce tau pathology (Clavaguera et al., 2009). the fact that when abnormal tau (referring to seed competent) in injected material is missing, no pathology can be detected is a proof of concept of the dependence of the process on tau (Nobuhara et al., 2017; Vandermeeren et al., 2018; Yanamandra et al., 2013). Further, the injection of different human brain lysates of different tauopathies developed

different lesions in animal models, suggesting the existence of different tau strains (Clavaguera et al., 2013). Despite this evidence, it remains unclear whether the development of proteopathic tau seeding represents a causal process of tauopathy, a downstream consequence of tau fibril accumulation, a coincident trait of neurodegeneration, or even an epiphenomenon. If proteopathic seeds are indeed a causal agent of disease, then their activity should exist in the brains of tauopathy precede other forms of pathology, and correlate with disease progression (Holmes et al., 2014). In *in vitro* studies, the internalization of seed competent tau by endocytosis is observed (Evans et al., 2018; Frost et al., 2009). However, it is still controversial whether the free form or membrane associated (like EVs) seed competent tau induces the seeding, as both are found in the CSF.

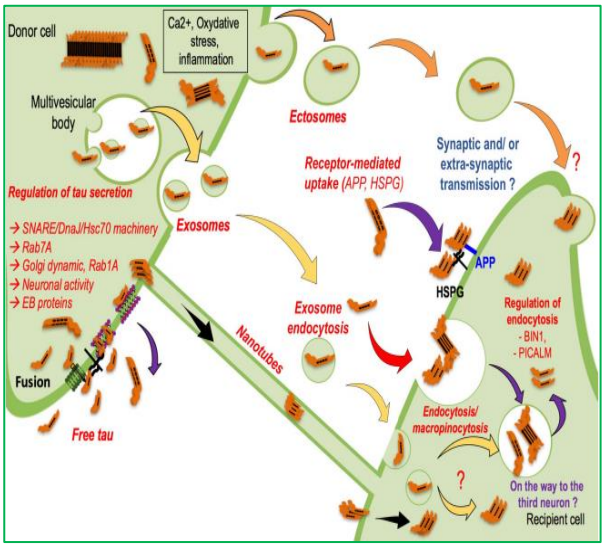

Figure 10. Prion-Like propagation of tau pathology in Alzheimer's disease. Mechanisms of tau spreading. 1) Release of tau into the extracellular space can occur via (from top to bottom) synaptic vesicles (ectosomes, 150–1000 nm), extracellular vesicles (exosomes, 50– 150 nm), direct translocation across the membrane. 2) Tau seeds can be taken up by healthy neurons via (from top to bottom) direct translocation across the membrane, macropinocytosis via heparan sulfate proteoglycans, bulk endocytosis, clathrin-mediated endocytosis, or fusion of extracellular vesicles with the plasma membrane. 3) Tau seeds can then seed physiological tau, leading to the growth of the fibrils and propagation of the aggregation process, or are targeted by intracellular degradative compartments. The way that tau is secreted depends on the models used, leading to be identified in many forms in the extracellular compartment. Further, the percentage of tau to be secreted that are transferred or probably cleared remain unknown. Adjusted by (Colin et al., 2020).

Chapter 6: Tau- targeted therapies in clinical trials

As mentioned above (Chapter 2) the most prevalent disease among tauopathies is Alzheimer Disease (AD), which is characterized by the presence of both extracellular accumulation of β-amyloid (as senile plaques, SP) and intracellular tau aggregates (in form of NFT) (Hyman, 1997; Scheltens et al., 2016; Serrano-Pozo et al., 2011). However, there is no efficient treatment for this group of diseases other than modification of neurotransmitter disturbance in order to ease the symptoms. A number of drugs targeting β-amyloid in AD case have failed in the last decades (Cummings et al., 2018), raising up the need for new therapeutic approaches. Tau has been recently linked to several pathophysiological processes (Jadhav et al., 2019a), besides its main function in axonal microtubule assembly, which suggest the opportunity for innovative therapeutic approaches targeting tau. Further, there was an increased attention on tau targeted therapy as the NFTs are better correlated with the onset and progression of cognitive decline than amyloid deposition (Duyckaerts & Hauw, 1997; Jellinger, 2000; Richards et al., 2018a). The multiple pathways that lead to tau pathology represent at the same time the multiple points of potential therapeutic intervention. So far, the therapeutic approaches targeting tau were mostly focused towards intra-neuronal tau, by modulating PTMs, by breaking down tau aggregates or by acting on stabilization of microtubules (Jadhav et al., 2019a). However, many of these approaches have been discontinued because of toxicity and/or lack of efficacy. Here, therapeutic approaches towards AD and related tauopathies will be presented, which are currently on clinical trials. The focus is on two directions: 1) either by considering that tauopathies are caused by a toxic gain of function of tau (post-translational modifications, misfolding, aggregation and or altered expression), which would require prevention, disruption and/or clearance; or 2) by considering that neurodegeneration comes as a consequence of loss of normal tau function, e.g. binding to and stabilizing microtubules or other cellular functions, which would require agents to supplement this functions (Summarized in Figure 11).

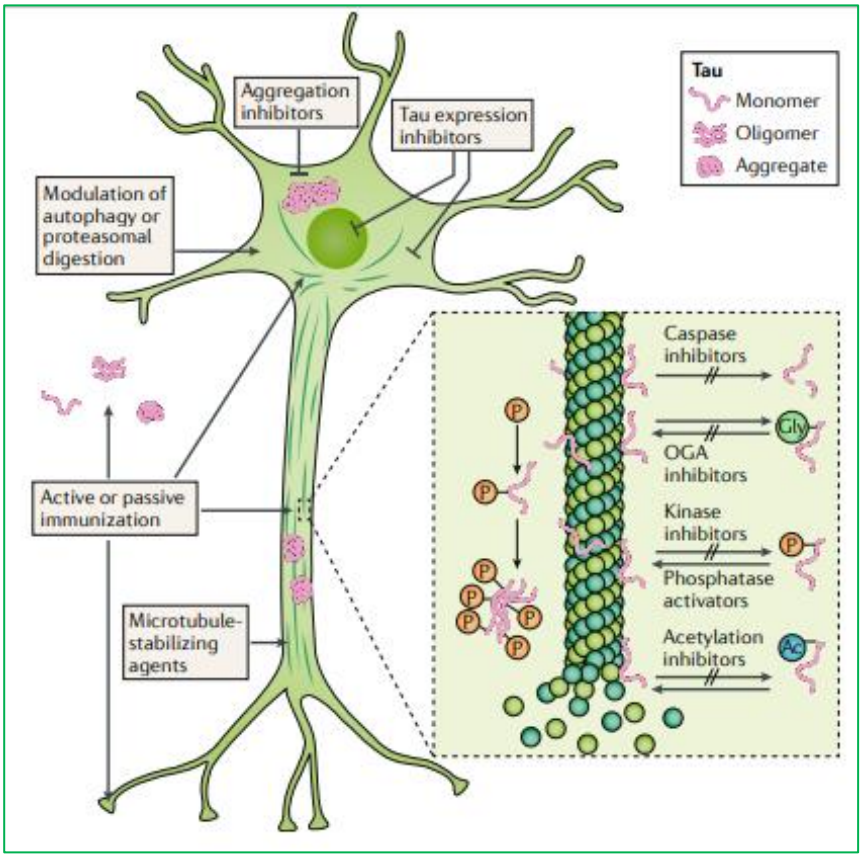

Figure 11. Tau related therapeutic targets. Based on (Congdon & Sigurdsson, 2018)

6.1 Therapeutic approaches to toxic gain of function

6.1.1 Reducing tau expression

One of the approaches suggested for tau therapy is decreasing the level of tau expression, by silencing MAPT gene for total tau or selectively, the most fibrillogenic 4R-tau. Thus, if the level of tau monomers in cells decreases, the equilibrium that governs aggregate formation dictates that the tau assemblies will decrease, leading to reductions in oligomeric tau and larger aggregates. In tau knock out mice few adverse effects are observed as the other microtubule-associated proteins can compensate the loss of activity of tau protein (Ke et al., 2012)(C. L. Dai et al., 2015), such as MAP1B (Hansen et al., 2018)(Takei, 2000). Tau expression can be reduced with small interfering RNA (siRNA) or antisense oligonucleotides (ASOs). ASOs are 8-50 nucleotides long that bind with complete specificity to complementary sense pre-messenger RNA (mRNA) or mature mRNA sequences. This “interaction” could mediate degradation of the target mRNA or prevent translation and thus, interfere with protein production. In cell and animal models, siRNA was found to reduce tau pathology and its associated functional impairments (Guo et al., 2017). These technologies have been applied in cancer cases (Richards et al., 2018b; Zuckerman & Davis, 2015) and seemed to have a positive impact in spinal muscular atrophy (Corey, 2017; Finkel et al., 2017) as well as in Hungtington’s disease (Tabrizi et al., 2019). Based on these positive and safety profile data, investigation on

tauopathies followed, resulting at the moment with **BIIB080 (IONIS MAPT Rx)** in clinical trial, an ASO that reduces total tau gene expression. In preclinical stage, it was delivered in P301S transgenic mice (via intrathecal way), and a 50% reduction in tau mRNA was observed. This resulted in reversing tau aggregation, and a decrease in the rate of hippocampal atrophy and neuronal loss (Devos et al., 2018). These led to an ongoing Phase 1/2 in 46 mild AD patients, who will be treated with BIIB080 for 36 weeks (NCT03186989). Another use of ASO in tauopathies, which is currently in preclinical stage, is the selective knockdown of 4R-tau, as the latest has higher potential to form pathological species (Norrbom et al., 2016).

6.1.2 Modulate post-translational modifications

As mentioned above (Chapter 4) there are several PTMs affecting tau-microtubule binding, promoting tau misfolding and aggregation. Thus, the inhibition of these events may lead to prevention of tau aggregation, and to restore the normal function of the protein.

6.1.2.1 Phosphorylation inhibitors

Among the PTMs of tau protein leading to tau aggregation, phosphorylation is the most well characterized (Kopke et al., 1993b). Briefly, the analysis of the composition of NFT has revealed the presence of PHFs and SFs, which are predominantly composed of abnormally phosphorylated tau protein (Guo et al., 2017; Kopke et al., 1993b). This observation lead to the proposition that this PTM may be directly related to induction of tau misfolding and its oligomerization into insoluble aggregates (Augustinack et al., 2002; Mirbaha et al., 2017; Tepper et al., 2014). The degree of tau phosphorylation results from the activity of both kinases and phosphatases (Hoffman et al., 2017; L. Martin et al., 2013). Thus, understanding the phosphorylation pattern of tau in AD is important to decipher its role in the progression of neuropathology and may facilitate development of therapeutics.

6.1.2.1a Kinase Inhibitors

First approaches target kinases, which were considered as a traditional drug target in the oncology field. However, the identification of the right kinase to inhibit as well as the prospect of long-term treatment that may be needed in tauopathies is challenging. Furthermore, given the great number of substrates that kinases have, their inhibition may lead to side effects. The inhibition of GSK3β has been shown to reduce tau phosphorylation, tau pathology development and axonal degeneration (Caccamo et al., 2013; Leroy et al., 2010) in transgenic mouse model. Among several small molecules tested as GSK3β inhibitors, such as Lithium and Valproic acid (G. Chen et al., 2000; Noble et al., 2005; Qing et al., 2008; Tariot et al., 2011), **Tideglusib (NP031112, NP-12),** an irreversible inhibitor**,** reduced tau hyper-phosphorylation, aggregation, protected against neuronal loss, prevented memory deficits and astrocytosis in preclinical studies (Del Ser et al., 2013;

Serenó et al., 2009). While it has reached clinical trials, no significant improvement were obtained during phase II, enrolling 306 patients, leaving unclear whether targeting specific mediators of tau phosphorylation will provide an effective tau therapy (Noble et al., 2013).

6.1.2.1b Inhibiting tau de-O-GlcNAcylation (OGA)

As developed in Chapter 4, tau phosphorylation is also regulated by O-GlcNAcylation. **Thiamet-G** (**LY3372689),** an OGA inhibitor, reduced tau phosphorylation in the brain after intraventricular delivery (Yu et al., 2012). While, in additional study in Tg4510 mouse model, Thiamet-G prevented the progression of hyperactivity, slowed brain atrophy, and reduced brain hyper-phosphorylated tau (X. Wang et al., 2018). Until August 2020, four independent Phase 1 clinical trial have been through, testing the dose of the drug, the binding of the molecule in the brain (PET scans), and safety, tolerability, pharmacokinetics of the drug in healthy adults, with no adverse outcomes so far.

6.1.2.2 PP2a activators

One of the molecules found as an enhancer of the activity on the PP2A, is Memantine (Chohan et al., 2006). In early clinical trials, in patients with moderate to severe AD, memantine resulted in small short-term improvements in cognition (Jiang & Jiang, 2015)(Matsunaga et al., 2015). However, its use in combination in patients with mild to moderate AD with cholinesterase inhibitors (Tsoi et al., 2016) or sodium selenate (Corcoran et al., 2010; Richards et al., 2018c; Van Eersel et al., 2010) showed to be of more advantages. The latest combination, in phase IIa clinical trial showed only benefits on diffusion MRI, while other clinical biomarkers were un-affected (CSF, PET) (Malpas et al., 2016).

6.1.3 Inhibiting tau aggregation (TAI)

Methylene blue (MB) is used for malaria treatment, and lately was found to block the polymerization of tau, by disrupting tau-tau bonds, and thus preventing aggregation (C. M. Wischik et al., 1996). The preclinical studies performed in P301S and TauΔK transgenic mice showed a decrease of phosphorylated tau aggregates and improved cognitive phenotypes, when MB was given prior to symptoms onset (Hochgräfe et al., 2015; Stack et al., 2014). After Phase 1 successfully safety testing in healthy individuals, Phase II followed, involving 321 mild to moderate Alzheimer's patients, where positive results were seen on a measure of cognition (ADAS-Cog) on the middle dose (138 mg/day) (Claude M. Wischik et al., 2014). Due to undesirable side effects, including diarrhea, urgency, painful urination, dizziness and others, in Phase III a reduced and stable formulation of MB called LMTM was used (leuco-methylthioninum, LMT-X, TRx0237). LMTM pharmacokinetic are different, compared to MB, but the permeability through BBB into brain tissue remains (Baddeley et al., 2015). Treatment with high dose of LMTM (200mg) in nearly 1700 mild AD cases did not have any effect compared to placebo controls (Gauthier et al.,

2016) (Wilcock et al., 2018). However, the placebo in this study was a low dose of LMTM at 8mg/day. Given the possibility that low dose may still be effective, an alternative active placebo was developed, and a Phase III trial (LUCIDITY) is ongoing to test the low dose of LMTM in 450 patients with early AD (NCT03446001).

6.1.4 Immunotherapy approach

Immunotherapy approach has been of great advantage in drug discovery lately, as the immune system itself is induced to clean up aggregates, preventing or slowing down the course of the disease. This approach started to be applied also in tauopathies, reviewed in (Congdon & Sigurdsson, 2018; Jadhav et al., 2019a; Katsinelos et al., 2019; Plotkin & Cashman, 2020; VandeVrede et al., 2020). In the beginning, many studies were using immunotherapies against Aβ, which ended up to have been unsuccessful, relating the result also with the fact of late targeting as the symptoms have already shown up (Abushouk et al., 2017; Lobello et al., 2012; Panza et al., 2014; Valera et al., 2016). Further, there were few studies approaching tau pathology through Aβ immunotherapy, with modest differences on pathological tau. These studies did not extend to phase III trials (Blennow et al., 2012; Boche, Denham, et al., 2010; Boche, Donald, et al., 2010; Serrano-Pozo et al., 2010). These disappointing results emphasize the need to focus on direct targeting of tau protein. However, the AD brain likely contains a heterogeneous pool of pathological forms of tau; thus, identification of appropriate epitopes in a specific tau species is essential to optimize a tau immunotherapy strategy. Ideally, the immunotherapy would target pathological tau protein derivatives, and select them from physiological tau molecules. This discrimination would be of great potential not only to the therapy of the disease but also to preventive strategy (Panza et al., 2016). Up to now, they have been several independent studies, which show that active and passive immunization approaches were effective in attenuating tau pathology in animals. The positive effect were mostly related to reduced pathology, improved behavioral phenotype, or delaying the onset of motor function decline and weight loss in mouse models of tau tangle pathology (Asuni et al., 2007; Bi et al., 2011; Boutajangout et al., 2010; Chai et al., 2011a; Theunis et al., 2013). An important advantage that needs to be emphasized at this point, by using tau immunotherapy, is the absence of pathological tau protein deposits in the walls of brain blood vessels (Braak and Braak et al., 1991). This feature is favorable because the treatments are unlikely to have the kind of dose-limiting toxic effects (amyloid-related imaging abnormalities such as oedema and micro-hemorrhages) that were seen with anti-amyloid monoclonal antibodies. Below will be described in detail the different immunotherapeutic strategies (active and passive), which are currently in the clinical stage (summarized Table 1) (Sperling et al., 2014).

6.1.4.1 Active immunization

In the active immunization cases used in tau (Kontsekova et al., 2014; Theunis et al., 2013), it has been paid attention to the characterization of the antibody response through vaccination, as an important issue correlated with the efficacy of the vaccine. There is still no agreement on the optimal methods of measurement of antibody response titer or the way these data should be reported. Thus, the preclinical data are referring to this information in descriptive manner (high, low, good or robust) rather than the concentration detected (Asuni et al., 2007; Boutajangout et al., 2011; Theunis et al., 2013), with few exceptions (Kontsekova et al., 2014; Richter et al., 2014). Maybe this will come at a later stage when a common strategy of measurement of antibody response as well as when the factors that determine the vaccines efficacy (affinity, avidity, isotype, target epitope etc.) will be applied.

AADvac1: This vaccine represents the first of its kind to be tested in man. It was prepared based on the cysteinated tau peptide $C\text{-}_{294}KDNIKHVPGGGS_{305}$ (non-phosphorylated tau, on the MTBD part), which contains the $_{299}HVPGGG_{304}$ peptide. The peptide was conjugated via its N-terminus to a carrier Keyhole limpet hemocyanin (KLH) (Kontsekova et al., 2014). The coupling to the KLH carrier molecule was done to outsource T-cell epitopes to the foreign KLH protein, which has no sequence homology in human beings, and, as such, avoid cell-mediated responses against self-antigens (Novak et al., 2017). Further, it is very important to be assessed the safety and immunogenicity of AADvac1 in the six-dose regiment provided (1 vaccination/month) in patients with mild-to-moderate Alzheimer's disease. Despite high antibody titers, higher than normally detected in elderly people (Assaf-Casals & Dbaibo, 2016), there was no meningoencephalitis and oedematous brain changes for none of the 30 patients involved in the study (Phase 1), often reported with anti-amyloid-β immunotherapies (Ferrer et al., n.d.; Masliah et al., 2005; Nicolll et al., 2003; Orgogozo et al., 2003; Patton et al., 2006). There was only one patient, who developed new micro- hemorrhages, but he already had a medical record in the past. The antibodies detected in the serum of the patients involved in the study had the ability to detect pathological tau and preferentially recognize pathological tau151-391/4R fragment with affinity six times higher than physiological tau 2N4R, confirming the selective, pathological tau-specific antibody response in elderly patients. Further, the progression of Alzheimer's disease to the people involved in the trial (mid age ~68 years old) was slowed down, with also cognitive related data positive outcome, enhancing the need for long term and larger sample size (Novak et al., 2017). Thus, the results of the Phase 2, applied to 208 people with same demographic (age, disease stage) characteristics as the Phase 1, are awaited.

ACI-35: The scope of this study (Novak et al., 2017) was to target through immunization pathological protein conformers of tau protein. Thus, a 16aa phosphorylated peptide, related to a pathological epitope of tau, was embodied into liposome

as adjuvant. The epitope corresponds to 393-408aa (pS396/pS404), residue numbering corresponding to the longest isoform tau2N4R isoform, and is an epitope resulting from GSK3β activity at S396/S400/S404 (Hanger et al., 1992). These residues are also epitopes for AD2 and PHF1 monoclonal antibodies that are used to define tau pathology (Buée-Scherrer et al., 1996; Torreilles et al., 2000). The ability of liposome-based vaccines to induce robust and specific antibody responses was assessed in wild-type and in transgenic tauopathy mouse model (Terwel et al., 2005, 2008). The data coming from animals showed safety as demonstrated by the absence of adverse effects, the lower clasping score, the attenuated loss of bodyweight, the prolonged survival and no neuroinflammation recorded. The titer of antibody response is referred as high, while the data coming from 24 patients tested are not yet published.

6.1.4.2 Passive immunization

The mechanism of passive immunization is likely mediated by humoral immunity, as passive transfer of anti-tau antibodies is sufficient to confer a protective effect (Collin et al., 2014; Congdon et al., 2013; Ittner et al., 2015; Sankaranarayanan et al., 2015; Yanamandra et al., 2013, 2015). The AD brain likely contains a heterogeneous pool of pathological forms of tau. Thus, there are several passive vaccines for tau immunotherapy (9 in clinical trials and many more in preclinical development) raised against various epitopes or conformation/s, considering this strategy as the largest area of active intervention. Tau therapeutic antibodies target, neutralize and/or eliminate either monomeric (Boutajangout et al., 2010; Yanamandra et al., 2013, 2015), phospho- specific (Boutajangout et al., 2011; Chai et al., 2011b; Collin et al., 2014; D'Abramo et al., 2015; Sankaranarayanan et al., 2015; Umeda et al., 2015) or conformationally altered forms of tau protein (Castillo-Carranza et al., 2014; Walls et al., 2014), and thus prevent formation of neurofibrillary lesions. The binding site of these antibodies could be either N-terminus, the proline rich domain, the microtubule, or the C-terminal domain. Targeting the N-terminal species could block tau uptake and its transfer between neurons (Nobuhara et al., 2017) and could reduce the accumulation of tau in the brain of mouse model of tauopathy (Spencer et al, 2019). On the other hand, the majority of tau in the AD brain is truncated, mostly at the N-terminus, resulting in disability of these antibodies to recognize pathological tau protein. Antibodies recognizing the mid region of tau have shown to be effective in the reduction of tau up-take and neutralization of tau seeding activity (Albert et al., 2019; Nobuhara et al., 2017). The third category are antibodies that recognize the MTBD region, which plays a crucial role in polymerization and stability of microtubules as well as being responsible for the pathological tau-tau interaction. The fourth region, the C-terminal region enhances the microtubule binding capacity of tau protein, hosting some of the phosphorylation sites identified in early and late stages of AD

progression. Thus, the investigation of these sites in terms of therapy has raised high interest (Boutajangout et al., 2011; Chai et al., 2011b).

Current immunotherapies in clinical trials directed against tau are listed in Table 1, along with the epitopes recognized by the therapeutic antibodies, mode of action and the improvement recorded. Figure 11 further shows the locations of their corresponding epitopes on the tau primary sequence.

E2814: is a humanized, high affinity antibody specifically binding the HVPGG sequences, present twice in tau isoforms within the four microtubule binding repeats (4R-tau; within R2 and R4) and once in three-repeat (3R-tau) isoforms (within R4 only). The antibody is a humanized form of mouse IgG, 7G6, originally raised against $_{296}$NIKHVPGGGSVQIVYKPVD$_{314}$, with high affinity towards full-length tau (KD= 63,6pM). E2814 may exert an effect by binding to and stabilizing the accessible HVPGG motifs in the β-hairpin pairings that mask the PHF6 motifs in soluble tau, thus preventing conformational conversion to seed-competent tau and further prevent the intermolecular seeding. Although the R4 HVPGG motif is predicted to be inaccessible in the structurally mature AD proto-fibril, it is possible that binding by E2814 at earlier stages of conformational conversion and misfolding could prevent formation and compaction of the protofibril and subsequent fibril assembly.

BIIB076 (originally named as 6C5, h-IgG1) is a human recombinant, monoclonal anti-tau IgG1 derived by recombinant cloning from human B cells of healthy elderly with no signs of cognitive impairment, targeting residues 125 to 131 (Nobuhara et al., 2017). In this strategy, by selection of monoclonal antibodies isolated from peripheral blood of healthy subjects with no signs of a neurodegenerative tauopathy, it is expected that the antibodies lack auto-immunogenicity and are already evolutionarily optimized, and affinity matured by the human immune system. The supernatants were screened for the ability to bind recombinant tau and human AD derived paired helical filament tau. In the case of human AD brain PHFs, High Molecular Weight (HMW) species which have been shown to have a high propensity for neuronal uptake, were purified (Takeda et al., 2015). To test tau uptake, a sensitive FRET-based assay of primary neuron culture was used, while to test the effect of tau antibody treatment on neuron-to-neuron propagation a unique microfluidic device was set. The 6C5 antibody, among several tested epitopes, resulted in capture and neutralization of extracellular pathological tau, preventing it from being taken up by neurons. Further, it inhibited neuronal tau aggregations even after the uptake process had been initiated. The latest is of great importance as the tau pathology develops years before the onset of clinical symptoms. A Phase I clinical trial with 56 participants, healthy and mid AD is under way.

BEPRANEMAB (UCB107, IgG4): Antibody D came from a rat immunization with recombinant tau fibrils, and it is binding the mid domain of tau protein, 234-246aa, which is the end of tau's second proline-rich region and just before the first repeat of MTBD part. Compared to other antibodies tested *in vitro*, it was the most efficacious in decreasing tau pathology. One possible explanation regarding the better effect from targeting the mid-region is related to the fact that N-terminal tails are thought to be exposed outside the core of tau fibrils where they may be cleaved by proteases (Courade et al., 2018). Similarly, for antibodies targeting the C-terminal end, it is suggested that the tau species involved in neuronal uptake and present in brain extract lack an accessible C-terminal end, because of folding, post-translational modifications, or cleavage (Nobuhara et al., 2017). With the *in vitro* data published at (Courade et al., 2018), the antibody found was further tested *in vivo*, in Tg30tau, by (Albert et al., 2019). In the *in vivo* testing (Albert et al., 2019), Tg30tau mice were injected intracranially with AD brain homogenate and antibody D was delivered intraperitoneally in high doses (30 mg/kg). Antibody D was able to block the progression of tau seeding pathology to distal brain regions. UCB0107 is the humanized version of antibody D, an IgG4. Results from two phase I clinical trials have not yet been reported and a phase I trial for PSP was initiated in December 2019 under Hoffmann- La Roche.

Lu AF87908 (originally known as C10.2, h-IgG1): The epitope defined by phosphorylation of S396 in tau has been heavily implicated in AD-associated tau pathology (Bramblett et al., 1993) and provides a valuable target for the development of therapeutic antibodies to capture tau and prevent spreading of tau pathology. C10.2 is a monoclonal antibody generated by immunization with P30-pS396/pS404-tau peptide in mouse model (Rosenqvist et al., 2018). Except of the specific binding towards tau peptide - pS396, it was identified to be able to bind full-length *in vitro* phosphorylated tau and tau from AD tissue. For the *in vivo* studies, the rTg4510 model was used to explore anti-seeding properties of the antibody. The results demonstrated that C10.2 antibody effectively prevents the development of the tau pathology induced by injection of crude rTg4510 or AD brain extracts into the hippocampus, by targeting tau seeds and neutralizing these when present in the extracellular space. Further, this study emphasizes well the fact that the optimal antibody for therapeutic intervention should access and recognize the more exposed MTBD flanking regions in case of seeds in order to be effective. Phase I started on September 2019 and it is still ongoing.

PNT001: is a monoclonal antibody to the *cis* isomer of tau phosphorylated at threonine 231 (pThr231), as modulated by the peptidyl-prolyl cis/trans isomerase Pin1. *Cis* isomer of pThr231 is a form of pathological tau suspected to play a role in traumatic brain injury, chronic traumatic encephalopathy, and early stages of AD (Hamdane et al., 2006). *In vitro* experiments showed that Pin1 binds to pThr231 and promotes tau dephosphorylation via PP2A (Wintjens et al., 2001; Zhou

et al., 2000). Furthermore, Pin1 could also be considered as a specific regulator between phosphorylation and dephosphorylation since the loss of function in AD promotes tau aggregation (Butterfield et al., 2006; Segat et al., 2007), whereas the abnormal phosphorylation at Thr231 by p25/Cdk5 kinase did not (Hamdane et al., 2003). The latter is likely an early marker of neurofibrillary degeneration (Augustinack et al., 2002; De Saint-Vis et al., 1998; Ramakrishnan et al., 2003). In preclinical models of brain injury, a mouse monoclonal antibody to *cis* pThr231 prevented axonal pathology, astrogliosis, tau oligomerization and tangle formation, brain atrophy and behavioral deficits (Albayram et al., 2017, 2019; Kondo et al., 2015). Primary outcomes from Phase I safety and tolerability, which started in September 2019 in 49 healthy adults, were adverse. Later measurements of the same study detecting antibody concentration in serum and CSF as well as measures of total tau, pThr231 and cis pThr231 showed dose-linear and CSF concentrations that stayed constant for 28 days. In December 2020, a Phase I study of multiple doses in 64 hospitalized patients with acute traumatic brain injury began.

Gosuranemab (BIIB092): Skin cells from patients with sporadic or presenilin-1-mutant AD were reprogrammed to induce pluripotent stem cells (iPSCs) that were differentiated into cortical neurons (Bright et al., 2015a)Bright et al., 2015a). The AD-derived cells secreted into the extracellular space N-terminal fragments of tau, which run between 20 and 35 kDa by SDS-PAGE (C. ling Dai et al., 2017). Mouse monoclonal antibodies, derived from immunization of *in vitro* aggregated full-length (2N4R) tau, were screened towards these N-terminal fragments and full length-tau. The selected ones were tested for their ability to suppress induced neuronal hyperactivity in primary human cortical neuron cultures and in P301L mouse model. The humanized version of the selected mouse monoclonal antibody is an IgG4 monoclonal that recognizes a linear, non-phosphorylated epitope in the N-terminal region of tau consisting of 17-28 amino acid residues (Griswold-prenner et al., 2015; Qureshi et al., 2018). The antibody binds the N-terminus of tau and neutralizes the effect of pathological extracellular tau. In Phase I, it was found to be safe and well tolerated, while now it is being evaluated in Phase II trials in PSP and early AD patient populations. However, after treatment with the antibody, the analysis of AD biomarkers such as total-tau and p-tau (181) did not show any improvement upon treatment (Yang et al., 2019), even if the N-terminal tau in CSF was reduced up to 97% (Boxer et al., 2019).

Semorinemab (RO7105705, h-IgG4): is a humanized IgG4 antibody, which aims at the clearance of the extracellular tau species, by minimizing Fcγ receptor activation, and consequently microglial and inflammatory responses. This is achieved by applying two single mutations in the Fc region of the antibody, which when combined, prevent binding to microglial Fcγ receptors (Couch et al., 2013). The preclinical studies showed that this approach can remove aggregates in mouse models and protect neurons from toxicity better than the unmodified version (Lee et al., 2016a). The antibody was obtained

following vaccination of mice with recombinant, phosphorylated, and oligomerized human tau (Adolfsson et al., 2012). To keep the afore-mentioned characteristics, the antibodies collected were screened towards the six tau isoforms, oligomerized and phosphorylated one, avoiding from the last case the ones that were binding to a high density of phosphorylated residues. Thus, semorinemab binds within $_{2}$AEPRQEFEVMEDHAGTYGLGDRK$_{24}$ (Adolfsson et al., 2012), of all 6 isoforms of human and primate tau but not mouse. In neuronal cell-based assays the antibody protected from tau-mediated toxicity, while in P301L mice it reduced pathological tau in the brain in a dose-dependent manner. Phase I studies have shown that the antibody is safe and tolerable in healthy volunteers, even at extraordinarily high single doses. Two current phase II trials, one for prodromal/probable AD participants, and one for moderate AD participants are ongoing.

Tilavonemab (ABBV- 8E12, originally known as HJ9.3, h-IgG4): ABBV-8E12 is the humanized IgG4 antibody version of HJ8.5 (IgG2b), which has been raised by conventional immunization using recombinant full-length human tau. The antibody is selective to human tau, specifically $_{25}$DQGGYT$_{30}$, and does not bind to mouse tau (Yanamandra et al., 2013). The antibody binds both tau monomer and stains neurofibrillary tangles, but not oligomeric or other species. In *in vitro* assays the antibody blocked uptake and inhibited seeded tau aggregation, where neuronal cells were exposed to tau-P301S mouse brain lysates containing tau aggregates (Yanamandra et al., 2013). Further, the *in vivo* testing in Tg-P301S mice showed a decreased tau aggregation and rescue of cognitive deficits (Yanamandra et al., 2015). A Phase I study in PSP patients showed that the antibody was well- tolerated, but the study was discontinued in Phase II, after futility analysis. ABBV-8E12 is also in a phase 2 trial for early AD, which is continuing without changes. One rationale for continuing is that the stage of tauopathy of patients in the AD trial may be relatively -early compared to those in the PSP trial.

Zagotenemb (LY3303560,h-IgG4): is the humanized version of MC-1 (IgG1) antibody, which came from the Alz-50 antibody (Wolozin et al., 1986), which was used to purify PHFs from AD brain homogenates by immune-affinity, and these purified PHFs were then used as immunogens in mice to raise the MC-1 (Jicha et al., 1997). They share the same epitope of binding, which is a discontinuous epitope on tau, requiring N-terminal amino acids 7–9, and amino acids 313–322 in the third microtubule binding repeat (Alam et al., 2017; Jicha et al., 1997). Removing either component of the epitope abolishes the binding. Reactivity to the antibody appears to be dependent based on the severity and progression of AD (Vitale et al., 2020). *In vivo* data coming after injections in the forebrain of transgenic P301L tau mice have shown that MC-1 could reduce tau pathology (Chai et al., 2011b; d'Abramo et al., 2013). Zagotenemab is selective for tau aggregates over monomer (Alam et al., 2017). Two phase I trials have completed, with mild to moderate AD volunteers involved, but results have not yet been reported. A phase II trial is currently ongoing for patients with early AD.

Table 1 : Active and passive tau-immunotherapies that are currently in clinical trials. Along with their epitopes, mode of action and the improvement recorded. The mode of action is based on the outcomes of the in vivo testing in animal models, while improvement is related to the patients Phasel/ Phase II outcomes, when reported. The immunotherapies presented are based on the FDA current status based on the AlzForum.com, Aprile 2021 given status. Ongoing refers to upcoming data.

Therapy	Name	Target disease	FDA status	Epitope of binding	Mode of action	Improvement	Reference
Active	AADvac1	• Mild Alzheimer's Disease • Progressive Nonfluent Aphasia	**Phase 2** **Phase 1**	$_{294}$KDNIKHVPGGGS$_{305}$	Block tau aggregation, remove extracellular tau and stop tau from spreading	Disease modifying effect on AD patients, especially of younger age	Novak et al. Kontsekova et al
	ACI-35	Alzheimer's Disease	**Phase 1**	$_{393}$VYKpSPVVSGDTpSPRHL$_{408}$	Anti phospho tau (pS396/pS404)	Not reported	Novak et al.
Passive	BIIB076	Alzheimer's Disease		aa125-131,2N4R	Reduce tau uptake and interneuronal propagation	Ongoing	Nobohura et al.
	Bepranemab	• Alzheimer's Disease • Progressive Supranuclear Palsy		$_{235}$PSSAKSRLQTA $_{246}$	Monomers, oligomers, PHFs, prevents spreading	Not reported	Albert et al.
	E2814	Alzheimer's Disease	**Phase 1**	$_{299}$HVPGG$_{305}$	Soluble, protofibrils prevent seeded aggregation and clearance by microglia	Ongoing	Roberts et al.
	Lu AF87908	Alzheimer's Disease		pS396	Fibrillar tau, prevent spreeding	Ongoing	Rensqevist et al
	PNT001	Alzheimer's Disease		Cis-pT231	Inhibits cistauosis effecting tau aggregation, tau oligomerization and thus fibril formation	1st Phase I adverse 2nd Phase 1 ongoing	Hamdane et al
	Gosuranemab	Alzheimer's Disease		$_{9}$EVMEDHAGTY$_{18}$	non-phosphorylated tau, extracellular tau	Reduced tau pathology	Bright et al.
	Semorinemab	Alzheimer's Disease		$_{15}$AGTYGLGDRK$_{24}$	Inhibiting microglial activation, clearance of extracellular tau	Ongoing	Lee et al., Adolfsson et al.
	Tilavonemab	Alzheimer's Disease	**Phase 2**	$_{25}$DQGGYT$_{30}$	Block uptake and seeding	Ongoing	Yanamandra et al
	Zagotenemab	Alzheimer's Disease		Conformational epitope, N-terminus (aa7-9) and 3R (aa313-322)	Block extracellular pathological tau, preventing propagation	Not reported	Chai et al.

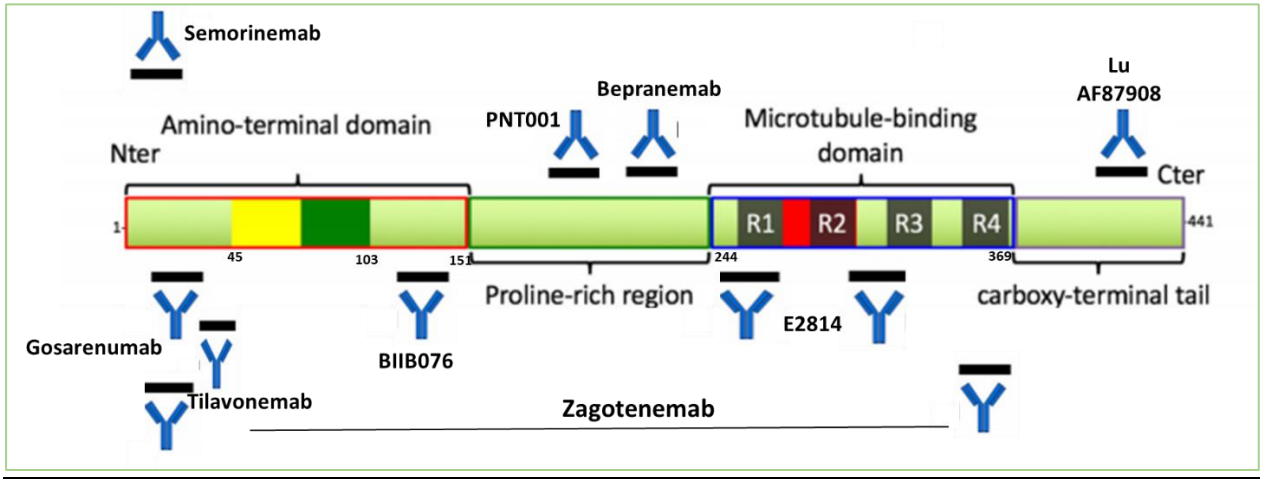

Figure 12 : Clinical anti-tau passive immunotherapies binding epitope on the full length of tau.

6.1.5 Targeting extracellular tau

Based on the prion-like hypothesis described above (Chapter 5), species with seeding capability can be transmitted from cell-to-cell and recruit soluble tau into growing aggregates. In line with this hypothesis tau species were identified in the extracellular space, supporting a role in cell to-cell transfer of pathology (Dujardin, Lécolle, et al., 2014). Extracellular tau is now considered to be the key driver in the spread of pathology making immunotherapy an attractive therapeutic approach. Up to now, there are a number of antibodies processed in clinical trials (Albert et al., 2019; Bright et al., 2015a; Chai et al., 2011b; Nobuhara et al., 2017; Rosenqvist et al., 2018; Yanamandra et al., 2013) as summarized in Table 1 targeting extracellular tau species, emphasizing the importance of blocking extracellular tau in reversing disease progression. The scope of blocking the initial uptake of the seeds is to break down the chain of spreading (Funk et al., 2015; Nobuhara et al., 2017). One more time, crucial for the activity to these studies, is the epitope of binding of the antibodies towards tau protein (Courade et al., 2018) with a special focus on the strains involved in uptake (Nobuhara et al., 2017). Antibodies targeting the mid-domain of tau protein seemed to be of high efficiency on blocking the uptake and subsequently aggregation, the latter aspect being tested in *in vitro* systems (Nobuhara et al., 2017; Roberts et al., 2020) but also in *in vivo* models (Albert et al., 2019; Chai et al., 2011b; Funk et al., 2015; Roberts et al., 2020). An extra reason regarding the better efficiency detected in mid-domain targeting antibodies compared to localized region spanning approximately 20aa in N-terminus (Bright et al., 2015a; Chai et al., 2011b), may come as the N-terminal tails are thought to be exposed outside the core of tau fibrils where they may be cleaved by proteases (Courade et al., 2018).

6.2 Therapeutic approaches for tau loss of function

6.2.1 Replace tau physiologic function- Microtubule stabilizers

If we approach tauopathies in the context of tau dysfunction, coming as a result of a loss of normal tau function, an agent that stabilizes microtubules and prevents axonal/dendritic degeneration may restore function and improve clinical symptoms. Despite of the number of attempts, only three entered in active development, but with no further success. Briefly, **Davunetide (NAP, AL-108)** is an eight amino acid peptide derived from the activity-dependent neurotrophic protein (ADNP), a growth factor with diverse neuroprotective activity (Gozes et al., 1999). Even though it had a good preclinical outcomes, by increasing the amount of microtubule-associated tau and reversed cognitive deficits (Matsuoka et al., 2008; Shiryaev et al., 2009), and Phase II improvement in working memory related to PSP patients, it discontinued in Phase II/III in clinical trial as there was no improvement (Boxer et al., 2015). Further, **Epothilone D (BMS-241027)**, a macrolide known for its strong antitumor activity and high BBB permeability, showed to act as a microtubule stabilizer as well. After an increased microtubule density and reduced cognitive deficits detected in preclinical study (Brunden et al., 2010), a Phase I clinical trial followed with minor side effects. Thus, it entered Phase I/II, but results were never published, and it was finally discontinued. Last, **abeotaxane (TPI 287**), is another drug used in cancer and specifically in brain metastases, which showed activity as a microtubule stabilizer. However, during Phase I tested in PSP and mild to mod AD patients, it showed an immune hypersensitivity reaction, ending up in discontinued clinical development (Tsai et al., 2019).

6.3 Clinical anti-tau antibodies and the BBB

The brain is isolated from serum by the blood-brain barrier (BBB), which is impermeable to large macromolecules including IgGs (mostly used in passive immunization). IgGs are found at around 10 mg/ml in serum while, their concentration in cerebrospinal fluid (CSF) is down a thousand times. Fc receptors (FcRn), which are highly abundant in BBB (Yun Zhang & Pardridge, 2001), seem to play a role in this low transit as they may perform reverse transcytosis (Abulrob et al., 2005). There is further evidence that antibody clearance from the brain is mediated by the antibody Fc domain (Yun Zhang & Pardridge, 2001). Thus, in terms of therapeutic antibodies in tauopathies, affinity for their antigens is an important element to gain sufficient exposure to ensure meaningful binding to intracerebral antigens. The successes achieved at targeting tau (Boutajangout et al., 2011; Yanamandra et al., 2013) as well as Aβ plaques (Klunk et al., 2014) in the brain stand as strong evidence that antibodies in circulation can penetrate the brain and engage their targets at a level sufficient to exert biologically relevant effects.

6.4 Fc receptors and their role

The Fc part of the IgGs bind to specific Fc gamma receptors (FcγRs) expressed on the surface of a wide range of immune effector cell types including neurons, microglia or astrocytes. The FcγRs activate immune response upon antibody binding (in humans these are FcγRI, FcγRIIa, FcγRIIc, and FcγRIIIa), do not activate immune response (FcγRIIb), or be neutral to activation as FcγRIIIa, which lacks cytoplasmic domains and is highly expressed on neutrophils (summarized in **Table 2**). Microglia express all types of FcγR, astrocytes the FcγRI, while for neurons it is debated (Andersson et al., 2019). There are four human IgG subtypes (IgG1, IgG2, IgG3, and IgG4), with variable affinity towards the different Fcγ receptors. All IgGs, except for IgG2, have high affinity towards FcγRI. The same occurs between FcγRIIIa and IgG3 (Vidarsson et al., 2014). The FcR system in mice is similar, with activating FcγRs (FcγRI, FcγRIII, and FcγRIV) and one with inhibitory activity (FcγRII) (summarized in Table 3). Again, there are four IgG subclasses, (IgG1, IgG2a, IgG2b, and IgG3) though the nomenclature differs between the species: for instance, mouse IgG2a is most similar in its effector functions to human IgG1 and mouse IgG1 to human IgG4. In humans, for IgG4 case, even-though it binds to all FcγRs on microglia, it has a slightly lower affinity than IgG1 (Vidarsson et al., 2014), and thus the its pro-inflammatory response is lower (Bruhns et al., 2009). In terms of therapeutics, it may be translated that not only IgG4 is a low immunogenic inducer but also that upon binding to the antigen, it limits the internalization through the Fc receptor (Lee et al., 2016b). Thus, the hypothesis raised regarding the mechanism of action in these cases is that upon binding to antigen they may probably inhibit the initial uptake, slowing down the disease progression. However, as most of the *in vivo* studies occur in mouse models, it is difficult to have a clear and direct conclusion of prospect outcomes to humans, even-though mouse IgG1 is closer to human IgG4 (Colin et al., 2020). This may explain though the low progression in clinical studies described above. The atypical Fc receptor TRIM21 is broadly expressed in the cytoplasm and mediates initiation of ubiquitin ligase activity culminating in the degradation of immune complexes at the proteasome (Mallery et al., 2010). TRIM21 can bind to all classes of IgG (Keeble et al., 2008). Of note, in a neurodegenerating brain, the levels of TRIM21 and cell surface FcγRs (McEwan, 2016) are both increased following microglial activation and production of inflammatory cytokines (E. Martin et al., 2017). Even if this seems to be of advantage as it could increase Fc mediated clearance, it may on the other hand drive inappropriate immune stimulation (Katsinelos et al., 2019) as already seen in Aβ cases (Mo et al., 2017). Thus, the anti-tau antibodies already in clinical trials are tested with modified effector functions (Lee et al., 2016b).

Table 2 : Human Fc Receptor

Name	Activity	High Affinity Ligands	Low affinity ligands	Brain expression
FcγRI	Activatory	IgG1, IgG3, IgG4		MG
FcγRIIa	Activatory		All IgG subtypes	MG
FcγRIIb	Inhibitory		All IgG subtypes	MG
FcRγIIc	Activatory		All IgG subtypes	-
FcRγIIIa	Activatory	IgG3	IgG1, IgG2, IgG4	MG
FcγRIIIb	Neutral		IgG1, IgG3	-
FcRn	Transcytosis recycling	All IgG subtypes		BBB enothelium
TRIM 21	Activation/degradation all IgG subclasses		IgA, IgM	MG, neurons

Summary of the localization of expression and binding characteristics of human cell surface FcγRs; the recycling Fc receptor, FcRn; and the cytoplasmic Fc receptor TRIM21. High affinity interaction are defined those of an dissociation constant (Kd) < 10^{-7}M. MG, microglia; BBB, blood-brain barrier. This table is adapted from (Katsinelos et al., 2019), based on (Bruhns et al., 2009), (Vidarsson et al., 2014) and (McEwan, 2016).

Table 3 : Mouse Fc receptor

Name	Activity	High Affinity Ligands	Low affinity ligands	Brain expression
FcγRI	Activatory	IgG2a	IgG2b	MG
FcγRII	Inhibitory		IgG1, IgG2a, IgG2b, IgE	MG
FcγRIII	Activatory		IgG1, IgG2a,IgG2b, IgE	MG
FcRγIV	Activatory	IgG2a, IgG2b	IgE	MG
FcRn	Transcytosis recycling	All IgG subtypes		BBB enothelium
TRIM 21	Activation/degradation all IgG subclasses	All IgG subtypes	IgA ?, IgM ?	MG, neurons

Summary of the murine Fc receptors, their high and low binding ligands and brain expression. High affinity interaction are defined those of an dissociation constant (Kd) < 10^{-7}M. MG, microglia; BBB, blood-brain barrier; ? refers to possible interaction but not yet demonstrated. This table is adapted from (Katsinelos et al., 2019), based on (Bruhns et al., 2009), (Vidarsson et al., 2014) and (McEwan, 2016).

6.5 Importance of affinity of therapeutic anti-tau antibodies

The antibody binding to the antigen is mediated by the contacts between the epitope and antibody's complementary regions (CDRs). It is the three-dimensional structure of the latest, together with its flexibility, that determine the three characteristics of this interaction: specificity, selectivity and strength, which are strongly related to each other (Jadhav et al., 2019b). Among the studies in clinical phase described above, the importance of specificity for the epitope is emphasized since the earliest studies (Yanamandra et al., 2013), and well established through the *in vitro* study published by (Courade et al., 2018). Selectivity between various epitopes, especially in tau cases where there is a continuous conformational change through disease progression for example in (Chai et al., 2011a) is also of importance. Determination of affinity is mostly performed by surface plasmon resonance technique (SPR) and quantified by determination of the dissociation constant K_D (known as affinity) by measuring the ratio of K_{off}/K_{on}. The affinity is a constant value, characteristic for the given antibody binding site-antigen epitope pair and can be used for comparison characteristic between antibodies. The immune system in case of conventional antibodies (IgGs) can reach an affinity between 10^{-8} to 10^{-10}M for one binding site but it gets even lower when both sites are binding, 10^{-12} to 10^{-15}M. In most of the cases for the antibodies that reached the clinical phase for anti-tau immunotherapy, K_D were measured in preclinical stage, Table 4 summarizes the immunotherapies currently in clinical phase, including the isotype of the antibody (for passive immunization the antibody delivered to patients, while for active immunization refers to the antibody response). The current FDA status is included in the table, epitope of binding, the animal model for the assays, and the affinity measurements coming from the immobilized antigen in SPR system.

Table 4 : Anti-tau immunotherapies currently in the clinical phase. It is included the isotype of the antibodies (for active immunization refers to the isotype of antibody response after peptide immunization), the affinity tested *in vitro,* and the animal models tested *in vivo*. The status of the therapeutic approaches is based on AlzForum.com, Aprile 2021.

Therapy	Name	FDA status	Epitope of binding	Animal model tested	Isotype	Affinity	SPR target
Active	AADvac1	**Phase 2** **Phase 1**	$_{294}$KDNIKHVPGGGS$_{305}$	Rat	IgG1 ( ) IgG2	1) 14nM 2) 91nM	1) Pathological tau (151-391/4R) 2) Human tau2N4R
	ACI-35	**Phase 1**	$_{393}$VYKpSPVVSGDTpSPRHL$_{408}$	C57BL/6 and Tau.P301L	IgG	ng	ng
	BIIB076		aa125-131,2N4R	rTg4510	IgG1	Sub-nM (not precized)	Recombinant human and cynomolgus tau
	Bepranemab		$_{235}$PSSAKSRLQTA $_{246}$	Tg30tau	IgG4	1)1.2nM 2) 0.8nM	1)Monomer tau 2) AD-PHF
	E2814	**Phase 1**	$_{299}$HVPGG$_{305}$	0N4R P301S	IgG1	88pM	Recombinant h-Tau 2N4R
	Lu AF87908		pS396	rTg4510	IgG1	27nM	(386-408) pS396 tau peptide
Passive	PNT001		Cis-pT231	C57BL/6 (induced TBI)	ng	ng	ng
	Gosuranemab		$_{9}$EVMEDHAGTY$_{18}$	JNPL3, tau-4R/2N-P301L	IgG4	0.11nM	Recombinant tau (rtau-383)
	Semorinemab		$_{2}$AEPRQEFEVMEDHAGTYGLGDRK$_{24}$	P301L	IgG4	ng	ng
		Phase 2					
	Tilavonemab		$_{25}$DQGGYT$_{30}$	P301S	IgG4	99pM	Human tau, 2N4R
	Zagotenemab		Conformational epitope, N-terminus (aa7-9) and 3R (aa313-322)	JNPL3	IgG4	220pM	Tau aggregates, h-PHFs

Ng: stands for not given; SPR: surface resonance plasmon spectroscopy

6.6 Mechanism of action of Immunotherapies

Even-though immunotherapy against tau protein is an interesting therapeutic strategy, it raises basic questions regarding the mechanism of action. Here, a number of hypotheses of how antibodies may act against tau protein in the brain will be presented.

6.6.1 Peripheral Sink

In immunotherapies targeting the CNS, whether the antibodies act in the circulation or cross the blood brain-barrier and exert effects locally in the brain parenchyma, remains an open question. The 'sink effect' states that immunotherapy of CNS targets, such as tau and Aβ, can be explained by antibodies in the circulation that capture antigens in the blood and thereby enhance their elimination from the CNS (Yan Zhang & Lee, 2011). This hypothesis has been mostly applied to Aβ, as it can be both detected in CSF and serum, and it was postulated for immunotherapy of protein tau (Nadege Zommer et al., 2012). It is therefore likely that in order to target CNS antigens effectively, local production of antibodies against proteopathic agents within the brain, or administration of antibodies directly to the CNS, could lead to higher levels of protection (W. Liu et al., 2016).

6.6.2 Neutralization

The definition of neutralization refers to the reduction in seeding potency observed following the binding of antibodies to proteinaceous assemblies in cell-based seeding or propagation assays in the absence of complement or cells of the professional immune system (Katsinelos et al., 2019). Thus, as the definition stands for, it excludes the effect of microglial clearance and other effector mechanisms likely to operate *in vivo*. However, it can still refer to several mechanisms related to seeding and propagation. As already developed on the above paragraphs many monoclonal anti-antibodies such as HJ9.3 (Funk et al., 2015; Yanamandra et al., 2013), have the potential to reduce or slow the uptake of tau to cells by this neutralization effect, which may further inhibit protein assemblies. However, entry blocking cannot be generally characterized as a potential mechanism as in the same study (Yanamandra et al., 2013), HJ8.5, which may neutralizes seeding fails to block tau uptake (Funk et al., 2015). However, in case of HJ9.3, the mechanism suggested for the inhibition of the protein uptake, is the one inhibiting the interactions with the HSPGs (Holmes et al., 2013; Rauch et al., 2018). Thus, even quite challenging, it has to be investigated the mechanism/s, which block the entry to the cytosol at a post-uptake stage, for example by blocking endosomal escape or inducing endolysosomal degradation (Katsinelos et al., 2019). Recently, it has been proposed a post-entry mechanism of neutralization that relies on engagement of the intracellular Fc receptor TRIM21. This potential mechanism suggest, the binding of the antibody (already in complex with the antigen) to the high-

affinity Fc receptor TRIM21, induces a rapid degradation response against the immune complex (Mallery et al., 2010), preventing the seeding (McEwan et al., 2017). The contribution of TREM21 to the overall *in vivo* protection afforded by an antibody remains to be determined.

6.6.3 Clearance by Microglia

Microglia represents the phagocytic immune effector cells of the CNS because it is able to induce the degradation of protein assemblies like tau (Majerova et al., 2014), and when tau is in complex with the anti-tau antibody then it enhances cellular uptake and degradation. Clearance by microglia thus represents a potential mechanism that can be stimulated for therapeutic clearance of protein deposits, mediated by FcγR. However, the FcγR-mediated clearance of protein/-complex may induce a damaging immune response (Mo et al., 2017; Sperling et al., 2014). For this reason, in immunotherapy approach, the IgG4 scaffold is preferred (Bright et al., 2015b; Chai et al., 2012; Yanamandra et al., 2013), with in few cases IgG1 (Nobuhara et al., 2017). Furthermore, IgG4 is the only among the IgG isotypes that undergoes arm exchange, resulting in chimeric, bispecific antibodies (Orren et al., 2007). In case of (Lee et al., 2016b), the problem was solved by the point mutations in Fc part that inhibit the FcγR binding, but maintain the prevention of tau spread and neurotoxicity. All together, these studies emphasize thus the importance of the selection of antibody isotypes for immunotherapy.

6.6.4 Intracellular sequestration or Clearance

In cell based systems and passive transfer in mice it is found that antibodies targeting tau can enter cells in complex with tau or not (Asuni et al., 2007; Collin et al., 2014; Congdon et al., 2013; Gu et al., 2013). Afterwards, they bind to intracellular tau and are found in endolysosomal/ macroautophagic pathways triggering thus degradation (Bi et al., 2011; Nobuhara et al., 2017). Involvement of FcRs in antibody uptake and protein clearance has been already examined utilizing Aβ antibodies in AD models. Furthermore, data from primary neuronal cultures showed that uptake is primarily occurring via receptor-mediated clathrin-dependent endocytosis and to a large extent by FcγII/III receptors (Congdon et al., 2013). It is unclear though, whether vesicles containing tau and antibody meet without cytoplasmic access or the intracellular antibodies are found directly in the cytoplasm, or (Katsinelos et al., 2019). In case of free antibody uptake, there are strong evidence of rapid engagement by TRIM21 inducing intracellular degradation (Kondo et al., 2015).

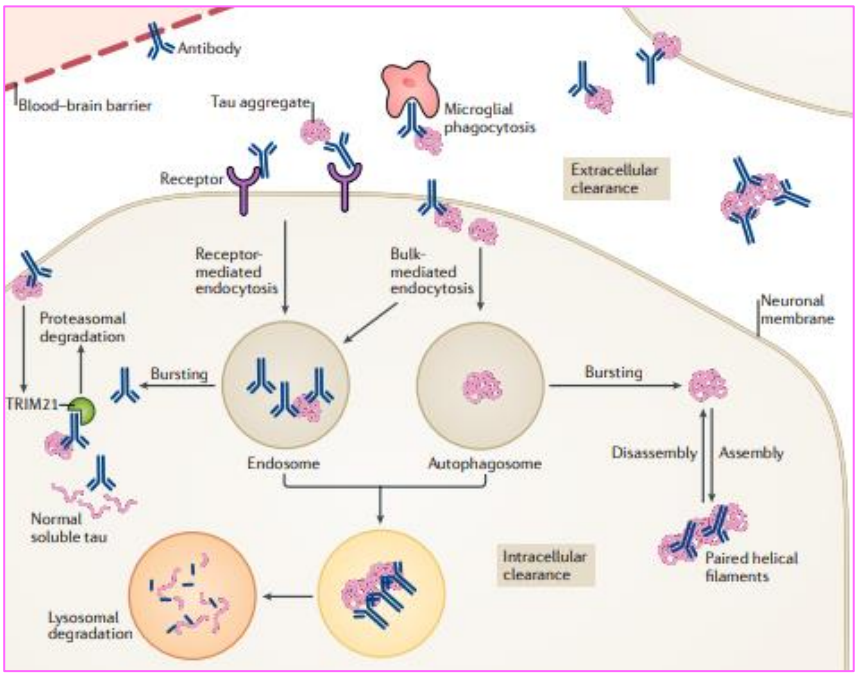

Figure 13 : Proposed mechanism of action of anti-tau antibodies. Antibodies can target tau both extracellularly and intracellularly. In the extracellular environment pathological sequestration of tau interferes with its assembly and promotes microglial phagocytosis, with the overall effect of blocking the spread of tau pathology between neurons. Within the cells, these antibodies could bind to tau aggregates within the endosomal–lysosomal system and promote their disassembly, leading to enhanced access of lysosomal enzymes to degrade the aggregates, to sequester tau assemblies in the cytosol and to prevent their release from the neuron, or to promote proteasomal degradation mediated by TRIM21 binding. The image is adjusted by (Congdon & Sigurdsson, 2018).

Chapter 7: Models used for studying tau aggregation in tauopathies

7.1 Advantages of use of animal models in research

To identify effective drugs in tauopathies, including the predominant AD, it is very important to better understand the pathophysiological mechanisms underlying each disease (Ribeiro et al., 2013). For this reason, the availability of animal models that can mimic the neuropathological and clinical features of these neurodegenerative diseases can help to get a step closer to these questions as well as can help to assess the efficacy of potential treatments before conducting clinical trials in humans. Another advantage of animal model is the wide range of studies that can be performed, such as behavior, lifespan and viability studies, live imaging, cellular and molecular analysis. However, the physiology of tau protein identified in adult mice is different of that in adult humans. Mouse brain contains the 4R tau isoforms exclusively, whereas levels of 3R and 4R are approximately equal in normal adult human brain of AD case, bringing thus a 14 amino acid differences in the N-terminal region (Andorfer et al., 2003).

7.1.1 Tau transgenic mouse model

Considering hyper-phosphorylation as the most important characteristics found in fibrillary tau, several animal models were generated to mimic hyper-phosphorylation of tau and the formation of NFTs as key aspects of tauopathies (Ribeiro et al., 2013). Phosphorylation of tau was detected at the well-known disease-related epitopes S202, T205, S212, S216, T231, S262, S356, S422, AT100 (Köhler et al., 2013). In the same line, overexpression of LRRK2 or p25/Cdk5 in mice resulted in hyper-phosphorylation of tau, tau aggregation into NFT-like structures, and neuronal death (Cruz et al., 2003). Some studies showed that the overexpression of human mutant tau in transgenic mice led to increased phosphorylation of tau and the formation of tau inclusions, aggregates, and fibrils. Almost all currently available tau animal models in AD are based on the over-expression of these pathogenic mutant tau forms. Therefore, it is still controversial how well these models mimic AD cases where there are no mutations in either tau or APP. However, the first models of tauopathy, based on the overexpression of either 3-repeat or 4-repeat human WT tau, presented tau hyper-phosphorylation but no NFT formation. Expression of tau-P301L, often in conjunction with other disease-associated proteins, is the most widely used (as seen in the clinical anti-tau therapies above) and most successful approach to recapitulate key aspects of AD such as tau hyper-phosphorylation, aggregation, and filament formation as well as neuron death. In these models, it is often not clear what drives tau hyper-phosphorylation. The well-known FTDP-17- associated missense tau mutations R406W, V337M, G272V, and P301L were shown to make tau a more favorable substrate for phosphorylation by rat brain kinases, in comparison to

WT tau protein (Allen et al., 2002; Alonso et al., 2004). Conversely, *in vitro* phosphorylation by recombinant GSK3β exerted reduced phosphorylation of the R406W mutated tau, probably through long-range conformational changes.

7.1.2 Non-transgenic mouse model

Non-transgenic models for studying AD are mainly obtained by injecting Aβ or tau directly into the brain via intra-cerebroventricular (i.c.v.) or intra-hippocampal injections (Puzzo et al., 2014). The advantages of the use of non-transgenic models include the possibility of (1) investigating Aβ and tau effects in animals different than mice for which transgenic models are not available; (2) excluding the confounding Huntington's Disease and Neurological Disease effects of overexpression of APP and its fragments; (3) investigating the specific roles of Aβ and tau species (monomers vs. oligomers vs. insoluble) at different concentrations; (4) investigating the difference between an acute and a chronic administration, and to clarify aspects of the molecular mechanisms underlying Aβ and tau pathology that cannot be investigated using transgenic models (Puzzo et al., 2015). However, acute models do not reproduce the gradual increase in Aβ deposition or tau pathology throughout the years as in humans.

7.1.3 Transgenic mouse models used in the current PhD project

There are numerous reports supporting the benefit of tau immunotherapy in various animal models (Asuni et al., 2007; Boutajangout et al., 2011; C. L. Dai et al., 2018). In this project, it will be used two transgenic mouse model, Tg30tau (Leroy et al., 2007) and Tg22tau. Tg30tau and Tg22tau express human 1N4R tau protein with two pathogenic mutations (P301S and G272V). The P301S causes frontotemporal dementia (FTD) or corticobasal degeneration (Bugiani et al. 1999) and is associated to widespread tau pathology and an early age onset. The G272V mutation was identified in a Dutch family with FTD with Parkinsonism linked to chromosome-17 (FTDP-17) (Heutink et al., 1997), which in mice is related to a delayed learning and reduced spatial memory but not to motor deficits. Older Tg30 mice develop brain atrophy and a motor neuron disease with axonopathy preceding neurofibrillary pathology and without overt neuronal loss in the hippocampus and the spinal cord, suggesting that these lesions can lead to neuronal dysfunction without cell death. THY-Tau22 shows hyperphosphorylation of tau on several Alzheimer's disease-relevant tau epitopes (AT8, AT100, AT180, AT270, 12E8, tau-pSer396, and AP422), neurofibrillary tangle-like inclusions (Gallyas and MC1-positive) with rare ghost tangles and PHF-like filaments, as well as mild astrogliosis. These mice also display deficits in hippocampal synaptic transmission and impaired behavior characterized by increased anxiety, delayed learning from 3 months, and reduced spatial memory at 10 months. There are no signs of motor deficits or changes in motor activity at any age investigated. This mouse model therefore displays the main features of tau pathology and several of the pathophysiological disturbances observed during neurofibrillary degeneration.

7.1.4 Drosophila models of tauopathy

Over the last years, a genetic model of tau-related neurodegenerative disease by expressing wild-type and mutant forms of human tau in the fruit fly Drosophila melanogaster is developed. Wild-type tau or Arg406 to Trp (R406W) mutant tau, an isoform associated with an early onset, familial form of dementia, was first expressed in a pan-neural pattern (elav-GAL4). The lifespan of the flies was moderately shortened by wild-type tau and severely shortened by the mutant tau. Thus, Drosophila represent a rapid and flexible system for investigating the mechanisms of tau-mediated neurodegeneration and the interaction between tau and other factors. Lately, it is been used with success on testing the therapeutic efficacy of several scFvs in tauopathies, improving survival rate and preventing developmental and progressive neurotoxicity in both models (Krishnaswamy et al., 2020; S. Li et al., 2021).

A detailed information regarding the models used in Alzheimer's Disease is given: Alzheimer's Disease Research Models | ALZFORUM.

7.2 Cellular model of tau seeding

As already described in Chapter 2 and Chapter 5 tau pathology do not appear randomly throughout the brain, but rather progress along distinct neural networks (Koenig SM, 2006; Toosi, 2014). This suggests that tau aggregates or aggregate prone seeds serve as this agent of spread, transmitting the aggregated state from cell to cell via prion-like mechanisms (Clavaguera et al., 2009; Frost et al., 2009; Prusiner, 1998). As already explained, the predominant concept is that tau seeds applied to the outside of cells bind the cell surface by attaching to HSPGs (Holmes & Diamond, 2017; Kfoury et al., 2012; Rauch et al., 2020), triggering uptake by micropinocytosis (Abulrob et al., 2005; Holmes et al., 2013). Upon internalization, tau aggregates or seeds nucleate the fibrillization of endogenous tau monomer via templated conformational change, or seeding (Frost et al., 2009). Furthermore, it is unclear whether seeding activity underlies progression of neurodegeneration, or is instead a consequence, or even more epiphenomenon. To test these hypotheses, a highly sensitive and quantitative assay using a novel FRET-based biosensor cell line that specifically reports tau seeding activity is created (Holmes et al., 2014). In detail, a monoclonal FRET biosensor HEK293T cell line, which stably express the MTBD with the disease associated P301S mutation fused to either CFP or YFP (C M Wischik et al., 1988) was engineered, referred to as “tau biosensor cells.” This line was selected for its optimized RD-CFP/YFP expression levels and minimal background FRET signal. Although at baseline the tau reporter proteins exist in a stable, soluble form within the cell, exposure to exogenous tau seeds leads to tau reporter protein aggregation, which generates a FRET signal. Mixing tau seeds with phospholipids (Lipofectamine 2000) before treating cells facilitates direct transduction of seeds into the biosensor cell line, thereby maximizing seed detection efficiency. The applied seeds nucleate aggregation of the tau FRET reporter proteins, which are further been detected by flow cytometry (Fig. 14 A). Importantly, cells treated with empty liposomes (vehicle) never converted to an inclusion-positive state (Fig. 14 B). To quantify the amount of seeded aggregation, a flow cytometry-based FRET measurement algorithm was developed (Banning et al., 2010). Further, to quantify the cellular FRET signal in the biosensor cell line, FACS was used to separate FRET-positive and FRET-negative cell populations.

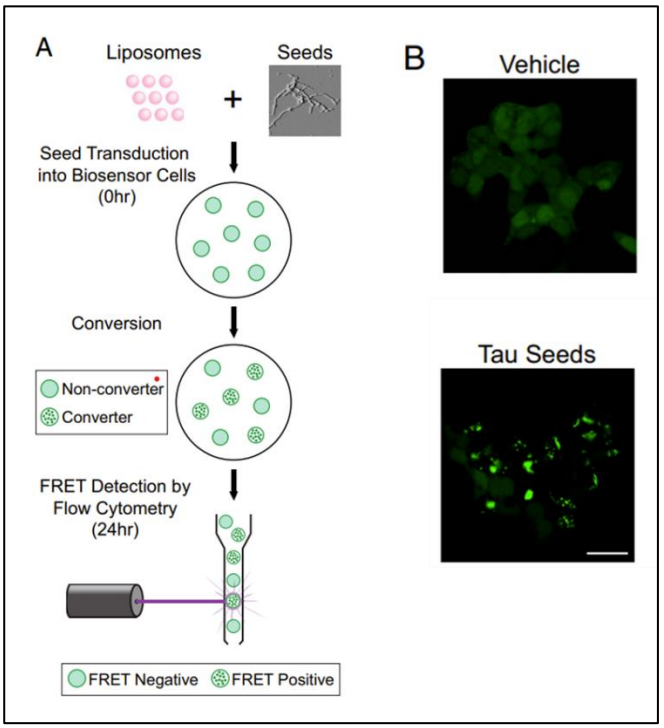

Figure 14. FRET flow cytometry detecting tau seeding. A. Schematic model of the FRET assay workflow. Lipofectamine/seed formulations are applied to biosensor cells for 24 h. Seeded aggregation produces a FRET signal that is measured by flow cytometry. **B.** Confocal microscopy of tau biosensor cells transduced with liposome vehicle or tau seeds (1 nM). Tau seed-treated cells exhibit intracellular tau inclusions. (Scale bar, 20 µm). Adjusted from (Holmes et al., 2014).

What is more with this assay was able to successfully detect the temporal evolution of tau seeding activity in the brains of P301S transgenic mic e(Holmes et al., 2014). This was later compared to standard measurements of histopathology taken from the same animals. This comparison implicates proteopathic tau seeding as a proximal cause of neurodegeneration, where results showed that proteopathic tau seeding occur far before (> 4 weeks) the onset of several standard histopathological markers, including AT-8. Emphasizing that it is a highly sensitive and specific to tau seeds method as well as quantitative as it can detect tau MTBD seeds at 316 fM (Holmes et al., 2014).

Chapter 8: Variable Heavy Chain of the Heavy Chain only Antibodies

8.1 Origin-General description

The conventional antibodies (IgG) consist of two identical heavy (H)-chain and two identical light (L)-chain polypeptides (Padlan et al., 1994). The L chain of these immunoglobulins comprises of two domains, whereas the H chain folds into four domains (Figure 15A). The sequence of the N-terminal domain of the H and L polypeptide chains varies between antibodies (designated as variable domains, i.e., VH and VL). The paired VH-VL domains constitute the variable fragment (Fv) that recognizes the antigen (Figure 15C). The remaining H and L sequences are more conserved (abbreviated as CH and CL, respectively). The two last CH regions named as crystallizable fragment (Fc) are important for recruitment of immune cells (e.g., macrophages and natural killer cells) or for effector functions (e.g., complement activation).

In the family of Camelidae (including camels, llamas and dromedaries) in addition to conventional antibodies there are antibodies that represent an exception of the conventional IgG structure (Muyldermans, 2013), known as heavy-chain antibodies (HCAbs), which lack the L chain polypeptide and the first constant domain (CH1) (Fig.15B). At its N-terminal region, the H chain of the homodimer protein contains a dedicated variable domain, referred to as VHH (Variable Heavy chain of the Heavy chain only antibody), which serves as the antigen binding domain. This domain is also known as a nanobody due to its small size (130aa, 14kDa) (Nb) or single-domain antibody (sdAb) (Fig.15D). HCAbs were first discovered in 1989 by the group of R. Hamers (1993), during a practical experiment conducted by undergraduate students at the Free University of Brussels, Belgium.

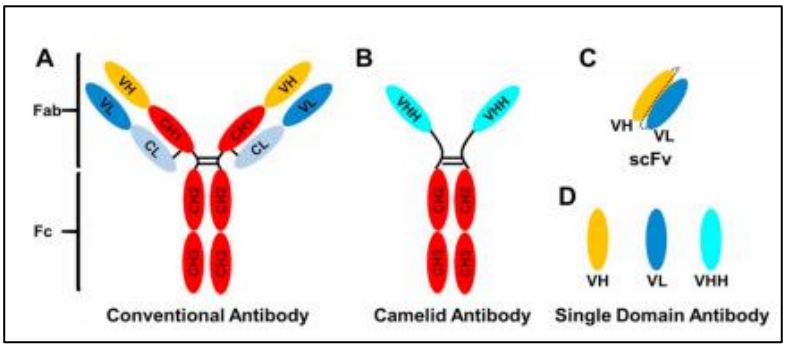

Figure 15 : Structure of antibody fragments. **A.** The conventional IgG antibodies consists of two heavy and two light chains. The heavy chains are composed of one variable domain (VH) and three constant domains (CH1, CH2, CH3). The light chains have only one variable domain (VL) and one constant domain (CL). The constant domains are joined by disulfide bonds. The antigen binding fragment (Fab) is the region of an antibody that binds to antigens and is composed of one constant and one variable domain, each with a heavy and a light chain. The crystallizable region (Fc region) is made up of only constant heavy domains. **B.** Camelid antibody consists of two heavy chains, with a single variable domain (VHH). **C.** An scFv is comprised of the shortest variable-region fragment (Fv) of the VH and VL joined together by a peptide linker, generally 3 or 5 copies of (Gly4Ser). **D.** Single domain antibodies (dAb), referred to as Nanobodies due to the small size (around 15kDa). Adjusted by (Messer & Butler, 2020).

8.2 Structure and biochemical properties of VHH

8.2.1 Three-dimensional structure of VHH

The tridimensional structure of VHHs corresponds to a typical immunoglobulin fold. It is composed of nine-strands organized into two β-sheets, stabilized by a conserved disulphide bridge between Cys23 and Cys94 (International ImMuno Genetics numbering, IMGT, Figure 16A). There is a high degree of identity between the amino acid sequence of the heavy chain of human conventional antibodies (VH) and VHH, reaching up to 80%. Similar to the conventional VH domains, VHHs contain four framework regions (FRs) that form the core structure of the immunoglobulin domain and three CDRs that are involved in antigen binding without requiring domain pairing (Figure 16B). However, they are adaptations to compensate the lack of the VL domain. In framework 2 (FR2) there are four VHH aa residues that differ from the VH ones (V42F or V42Y, G49E, L50R and W52G; IMGT numbering), located on the surface of VH that interacts with the VL. These amino acid substitutions increase the hydrophilicity of the VHH surface, in the absence of a VL domain. Thus, VHH are advantageous as they can be expressed in the periplasm and the cytoplasm of E. coli and eukaryotic cells (T. Li et al., 2012; Muyldermans, 2013). Additionally, the CDR regions that are responsible for antigen-antibody binding, are longer than those of VH, interaction being mainly mediated by the CDR3 region interacting. The larger size of the CDRs is believed to compensate for the absence of the three CDRs from the VLs, by providing a sufficiently large antigen-interacting surfaces (Muyldermans, 2013). In addition, the ability of these long chains to adopt a larger variety of conformations (Decanniere et al., 2000; Desmyter et al., 2002), results in a broad antigen-binding repertoire. The general size of CDR3 in VHH is around 16-18aa (Muyldermans, 2013), and can reach up to 25aa (Decanniere et al., 2000). Moreover, the long CDR3 can form a protruding loop, allowing VHHs to bind unique conformational epitopes, such as cryptic epitopes, inaccessible to conventional VH and VL pairs. Finally, another specific characteristic of VHH is of the presence of an extra disulphide bond, among the one usually found between Cys23 and Cys94. The extra one, in most of the cases it is located between CDR1 and CDR3 and - less frequently - between FR2 and CDR3 (10% of the cases). Although the position of the Cys in the CDR1 is restricted at positions: 30, 32, or 33 (or position 50 in FR2), in the CDR3 loop, the Cys residue occurs at nearly all possible positions (Saerens et al., 2008). The disulphide bond probably restricts the flexibility of long CDRs, which is expected to be entropically counterproductive for binding, leading to a stronger interaction. Furthermore, it allows the ability to adopt new conformations enabling the recognition of a variety of epitopes.

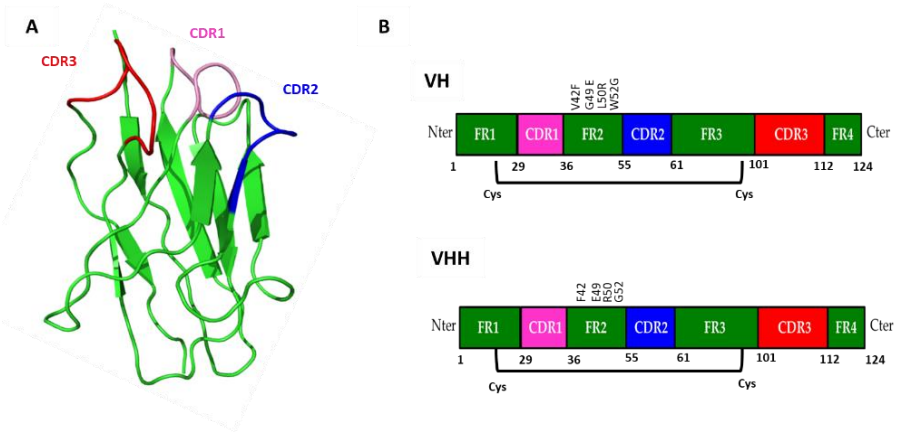

Figure 16: The structure of VHH. A. The three-dimensional structure of VHHs, convex architecture. **B.** The four Frameworks (FR1- FR4) and the three complementarity determining regions (CDRs) that form VH and VHH. In case of VHH as shown there are four single mutations (V42F, G49E, L50R and W52G), which correspond to the region of the VH domain that interacts with the VL. The disulphide bond created between Cysteine23 in FR1 and Cysteine94 in FR3 is indicated.

8.2.2 Biochemical properties

8.2.2.1 VHH are easy to generate, select and produce

There are currently several naïve and synthetic libraries available for *in vitro* screening. These are of advantage in case of toxic and non-immunogenic antigens, or when antigens are not available in the quantities requested for the immunization. Furthermore, once the libraries are prepared, they can be used to select binders with high affinity against any target (Pellis et al., 2012). They are different selection protocols, such as ribosome (T. Li et al., 2017), bacterial and yeast display and the phage display to select nanobodies from these libraries, phage display being the most popular. Briefly, as described (Pain, Dumont, & Dumoulin, 2015), in an animal from the family of Camelidae immunization are performed with the antigen of interest on a weekly basis and after the sixth week (Baral, Murad, Nguyen, Iqbal, & Zhang, 2011) lymphocytes are isolated, RNA extracted and cDNA prepared, with a further selection of those encoding single chain antibodies. The approximately 360bp encoding the VHH can be easily amplified by PCR from the single chain antibody genes and cloned into an appropriate vector (phagemid) coding for a coat protein of a filamentous phage (generally M13). The greatest advantage of nanobodies towards the conventional antibodies at this stage, in addition to the time and money saved, is the lack of random combination of VH and VL chains, which results in the generation of many non-productive combinations due to the loss of the original pairing. Last, the selected nanobodies can be expressed in high yield either in prokaryotic or in eukaryotic system, and the purification can be achieved by immobilized metal ion affinity chromatography (IMAC) via an engineered C-terminal His6 tag or by other affinity chromatography. Of importance, is the fact that in case of bacterial expression, the Nb is cloned after a secretion signal so that it is produced in the periplasm, where the oxidizing environment allows formation of disulphide bonds, avoiding at the same time the major contaminations with cytoplasmic proteins.

8.2.2.2 VHH are stable

Based on the structural characteristics described above, VHH has shown to have high conformational stability (30-60kJ/mol), leading to a high resistance in the denaturation effect that temperature (60-80^{o}C, Tm), chaotropic reagents (guanidinium chloride and urea, Cm) and high pressure (600- 750 MPa) may have. Thus, VHHs can be stored from a week at 37°C, up to months at 4°C, or even years at -20°C, without losing the ability to bind to their antigen. Furthermore, their stable character allows high concentrations in standard buffers, up to 15mg/ml, and several freeze-thaw cycles without any effect on the function.

8.2.2.3 Antigen specificity and affinity of the VHHs

Based on the protocol followed for generation and selection of the VHHs, it is more than clear that the nanobodies derived are of high specificity to their target antigen. Affinity is expected to be of good quality as well. The ranges of kinetic constants are for k_{on} of 10^5 to 10^6/Ms and for k_{off} of 10^{-2} to 10^{-4}/s, resulting in KD as low as 100pM (Dupré et al., 2019; Saerens et al., 2008), which equals the affinity ceiling proposed for natural antibodies.

8.2.2.4 VHHs lack immunogenicity

Mice and humans that were injected with VHH-containing constructs showed no immune response against them (Baral et al., 2011; Coppieters et al., 2006; Cortez-Retamozo et al., 2004). This can be easily related to their small size, short half-life in plasma as well as the high degree of identity with human VH. Furthermore, for 12 out of 14aa that differ between human VH and camelid VHH, mutations ensured " humanization", in the prospect of future use in therapeutics (Vincke et al., 2009). The term "humanized" refers to the replacement of one or more of these amino acid residues found naturally in camelid VHH by one or more of the amino acid residues, respectively, that occur at the corresponding positions in a VH from a conventional human antibody chain, ensuring that the solubility and high affinity will be un-affected. This technology is related to the ability of these sdAbs to be easily engineered as will be described at 8.2.2.5 part.

8.2.2.5 VHHs properties can be improved through protein engineering

Another advantage of the VHHs compared to the conventional antibodies (including Fab, scFv), is the fact that due to the single- domain composition of approximately 130aa, encoded by a short gene fragment, the properties of affinity, stability, immunogenicity, etc., can be easily improved. Thus, at first, a range of approaches such as: error-prone PCR, spiked mutagenesis combined with ribosome display (Yau et al., 2005) and Ala scanning-based mutations have been applied to identify the critical amino acids for antigen recognition. This may further impact specific residues in order to improve the stability of the domain and/or the affinity for their cognate antigen (Koide et al., 2007). For example, increasing the stability

of a high affinity VHH towards the antigen of interest can be achieved either by adding a new disulphide bridge between the two beta-sheets of its framework (i.e., between residues 54 and 78; IMTG numbering), or by grafting its CDRs to another robust VHH scaffold. This may result in a VHH highly resistant to degradation by pepsin or chymotrypsin (Hussack et al., 2011), suggesting that can be delivered orally in therapeutic uses. Furthermore, nanobodies can be used as modular building blocks to develop multidomain constructs 1) **multivalent** (recognize the same epitope), 2) **multispecific** (when two or more nanobodies linked together recognize different epitopes), increasing the avidity of the binding in both cases (Emmerson et al., 2011), or 3) **multifunctional** (when one nanobody is linked to an enzyme or toxin) entities for research, immuno-diagnosis or therapy. Furthermore, in order to improve the therapeutic effects of these small biological molecules, they have been fused to Fc domain of human, mouse or pig IgG (including the hinge region, CH2 and CH3). The gene of these constructs is then transfected in myeloma cell lines to reconstruct chimeric HCAbs (Bell et al., 2010). These techniques are of advantage by increasing the molecular weight, which ensures a prolonged half-life and the capacity to bind to Fc receptors (Alt et al., 1999; Rath et al., 2015).

8.3 Applications of VHHs

The beneficial properties developed on the above paragraphs stimulated further research on applying nanobodies as a research tool and/or to develop future diagnostic and therapeutic applications (de Marco, 2011; Harmsen & De Haard, 2007; Wesolowski et al., 2009)

8.3.1 Application as a research tool

The fact that Nbs are single antibody fragments with high affinity towards their target, including intracellular signaling molecules and cancer biomarkers, indicates a possible use as versatile tools. Therefore, the genetic fusion of a fluorescent protein with a Nb, and the ability to be expressed intracellularly, produces useful chromobodies or fluobodies to identify the antigen in various cellular compartments in living cells. Moreover, the use of GFP-binding Nbs coupled to organic dyes enables single-molecule localization with super-resolution imaging techniques of any GFP-tagged construct. Another important part of the characteristics of Nbs, is the specific conformational variant identification of its target as well as conformational changes that may occur on the target (Kirchhofer et al., 2010). Once expressed intracellularly, by binding to target antigen, VHH may deliver more information regarding the antigen interactions or get into interactions considered difficult to be pursued by a usual approach, like hidden epitopes (Pérez-Martínez et al., 2010; Tanaka et al., 2011). Another ability of these single domain antibodies is to trigger the UPS pathway, inducing the degradation of the antigen of binding (Causcinuss et al.2011). Last but not least, an important use of these antibodies it to assist the crystallization process and

structural determination of flexible or aggregating proteins (Pardon et al.). This comes through fixing highly dynamic proteins in a binder-preferred conformation and stabilize the intrinsic flexible regions or detergent-solubilized membrane proteins by shielding hydrophobic antigen surfaces from contact with solvent to allow the formation of effective crystal contacts.

8.3.2 Diagnostic application

Once again, the ability to have nanobodies with high affinity and specificity towards antigens and the inclusion of such groups at the opposite end of a domain permits their directional immobilization on the sensor surface for the maximal capacity of capturing and use as sensitive and selective biosensors. In other settings, Nanobodies were conjugated to either gold (Van De Broek et al., 2011) or magnetic nanoparticles (Pollithy et al., 2011), in order to produce an antigen-targeting photothermal therapeutic upon irradiation, or to capture and enrich analyte at low concentrations in complex mixtures, respectively. This conjugation capacity is highly valued in combination with the specificity, especially in industry, for generation of affinity adsorbents, like the one described at (Rothbauer et al., 2008) that recognizes GFP or that recognizes the C-terminal tetra-amino acids Glu-Pro-Glu-Ala (EPEA), that can be cloned as a tag behind any protein. Further, the low molecular weight offer numerous advantages for *in vivo*-imaging like positron emission tomography (PET) and computed tomography (de Vos et al., 2013; Vaneycken, D'huyvetter, et al., 2011), resulting in low radiation rate for the patient. This is also related to reduced time in blood as well as the ability to diffuse in tissues and potentially cross the BBB (M. David & Tayebi, 2014; T. Li et al., 2012). This was applied with success in mouse model for cases like breast cancer atherosclerotic plaques (Vaneycken, Devoogdt, et al., 2011). These are of great advantage if we consider that for brain imaging the compounds used require invasive techniques to penetrate in the brain and reach their target (e.g. BBB transient opening using hyperosmotic agents or ultrasound-associated microbubble injections (Santin et al., 2013; Sigurdsson et al., 2008). In addition, VHHs represent promising scaffolds for the development of imaging nanoprobes, particularly for intracerebral biomarkers, because they lack the Fc fragment. Thus, they cannot be exported outside the brain via the FcɣR mediated efflux system present at the BBB increasing their half- life (Rissiek et al., 2014). This comes to be ensured further by (T. Li et al., 2016), where two new VHHs that were designed to detect amyloid plaques and NFTs in brain tissue of patients with AD or mouse model with the disease, could visualize the pathological hallmarks after intravenous injection in mice. Becoming thus the first to show that VHH detect tau lesions in both tau transgenic mouse and human tauopathy brain tissues (Figure 17). The mechanism proposed of penetration through BBB is via transcytosis (Abulrob et al., 2005; Muruganandam et al., 2002; Rutgers et al., 2011).

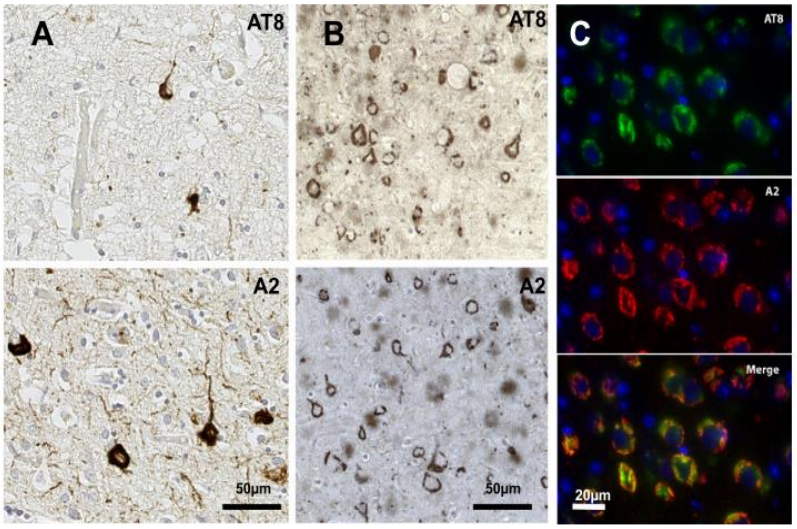

Figure 17 : Immunohistochemical characterization of VHH A2 as a specific probe for labeling neurofibrillary tangles. A2 shows similar sensitivity and selectivity to AT8 in detecting NFTs on both human AD (A) and Tg4510 mouse (B) brain sections. **C.** Double immunofluorescence staining of AT8 and A2 on Tg4510 mouse tissue confirmed the high specificity of A2. Adapted from (T. Li et al., 2016).

8.3.3 Therapeutic applications of VHHs

Nbs have been used for passive immunization to treat envenomed victims or infections (Harmsen et al., 2009; Stijlemans et al., 2004; Strokappe et al., 2012). To broaden their therapeutic use, it is important to determine the way of delivery and/or to improve their half-life. A potential use as will be seen (explained in 8.3.4) is for the treatment of neurodegenerative disorders.

8.3.4 Use of antibody fragments in neurodegenerative diseases

The term intrabody was initially described in 1988 (Carlson, 1988), and represents small antibody fragments (scFv, VH, VHH or VL), that are designed to be active intracellularly, offering distinct advantages over antisense and editing nucleic acid drugs, since they can target directly modified forms of proteins, including post-translational modifications and/or conformational epitope. This could be a powerful approach especially in neurodegenerative diseases, as the early steps of triggering the misfolding and aggregation of critical proteins are largely intracellular (Messer & Butler, 2020).

8.3.4.1 Development of bifunctional intrabodies

The antibody fragments upon binding to intracellular target antigen can inactivate the antigen, by the neutralization properties of the intrabody, effectively achieving protein knock-out, or knock-down *in vivo* (Melchionna & Cattaneo, 2007). Based on this, silencing intrabody technology (SIT) is developed, where an intrabody is equipped with sequences that triggers cellular proteolysis machinery. As a result, the desired protein is driven to degradation. This increases the effectivity of intrabody, knowing that neutralizing the aggregation of intracellular tau (for example) is challenging (Gallardo et al.,

2019), as well as minimizes the potential formation of irreversible fibrillary structures during the dissociation phase of the intrabodies (Messer & Butler, 2020). In case of Melchioma et al., a ubiquitin/proteasome-mediated proteolysis (UPP) substrate IkBα is fused to the C terminus of a scFv. scFV- IkBα, was transiently expressed in Hela cells and further treated with tumor necrosis factor alpha (TNFα), which activates the NF-kB signaling pathway, leading to IkBα degradation through the UPP (Osborn et al., 1989). Upon TNFα treatment, both the endogenous IkBα and the chimeric intrabody undergo ligand-induced degradation. This approach has been quite effective, also because the concentrations of the intracellular expressed antigen were much higher than the antibodies. In line with this study, an anti-tau intrabody fused to ubiquitin harboring a mutation prone for proteasome degradation was delivered into the brain via AAV, and shown to significantly reduced tauopathy in P301S mice (Gallardo et al., 2019). Thus, SIT greatly expands the potential of using intrabodies for protein function studies, target validation and therapy. While in other proteinopathies like Huntingtin and TAR DNA-binding protein 43 (TDP-43), where pathological proteins accumulate intracellularly, intrabody approach is especially appealing. In these cases, certain scFvs are fused to a PEST domain (Butler & Messer, 2011) (Tamaki et al., 2018). According to the PEST hypothesis, the presence of one or more regions rich in proline (P), glutamic acid (E), serine (S), and threonine (T) in the primary sequence of a protein confers susceptibility to rapid intracellular proteolysis (Rechsteiner and Rogers, 1996; Rogers et al., 1986). However, these are rapid degradation processes, which may finally be the reason of detecting an effect over the pathological protein only when tested in a cellular model. The structural information of tau aggregates could be helpful in rational design of specific tau aggregation inhibitors. These structures are also useful for the design of tau binders that can be used as part of the PROteolysis TArgeting Chimeras (PROTACs) approach. PROTACs is a strategy to degrade proteins by hijacking the ubiquitin-proteasome system (UPS). PROTAC is a bifunctional-hybrid molecule that on one side binds to E3 ubiquitin ligase and on the other side to a target protein. This bifunctional binder allows exposed lysine on the target protein to be ubiquitinated by the E3 ubiquitin ligase complex, followed by UPS-mediated protein degradation. In one example, PROTAC were designed to eliminate aberrant tau in frontotemporal dementia patient-derived neuronal cell models (Kargbo, 2019; Silva et al., 2019).

It has been shown also that Nbs can be used to silence gene expression and impart epigenetic memory, as well as enhance the function of commonly used transcriptional effectors in mammalian cells. Using Nbs to recruit endogenous chromatin regulators (CRs) to a gene of interest for transcriptional control could offer a better opportunity to recruit entire chromatin complexes, taking advantage of all domains essential for activity and their interactions (Van et al., 2021). Building this way

smaller tools for gene regulation: instead of fusing large CRs to the DNA-binding domain, a common issue also for CRISPRs (Adli, 2018).

8.3.4.2 Use of VHHs as a research tool in understanding the intracellular fibril formation

The formation of amyloid fibrils is a common biochemical characteristic that occurs in Alzheimer's disease and several other amyloidosis. The unifying structural feature of amyloid fibrils is their specific type of β-sheet conformation that differentiates these fibrils from the products of normal protein folding reactions. The formation of amyloid fibrils is characterized by a sigmoidal growth profile, involving a variety of conformational rearrangements and multiple steps of self-assembly, described as a nucleation/polymerization process (Figure 17A)(Friedhoff et al., 1998). The lag phase of this sigmoidal growth profile represents a slow nucleation step, where proteins misfold into aggregation prone species that auto-associate into pre-fibrillar species, also called oligomers. This represents the first step into formation of nuclei or seeds of aggregation. This phase can be shortened, or even eliminated, by the addition of seeds (Figure 18B) (Barghorn et al., 2000). During the elongation phase, there is a polymerization of the nuclei by addition of monomers or oligomers to form proto-fibrils, which represents an exponential growth, and finally fibrils. In the last stage, named as steady state, even though fibrils and monomers are in equilibrium, the structure of the fibrils can still evolve by rearrangement of the region of the protein that is not part of the core of the fibrils, leading to mature fibrils. The mature fibrils are highly insoluble with a variety in size and quantity and/or transient features, which leads to a difficulty of characterization by most of the conventional techniques, mostly because these require concentrated and homogeneous samples. In case fibril formation though, the related protein adopts a different conformation in its native, oligomeric and fibril forms, the characterization of which will be very valuable in investigating the mechanism of fibril formation in terms of structure, stability, kinetics of formation and toxicity, leading to early diagnostic tools and identification of targets for therapeutic treatments (Pain et al., 2015). Monoclonal conformational antibodies are promising to study these aspects since they can be raised against any conformational state of peptides or proteins. Furthermore, the binding properties of the antibodies specifically raised against various epitopes at the surface of the native state of a protein can be compared before and after the conformational changes leading successively to fibrillary intermediates, oligomeric species, and mature fibrils identification, even under conditions like in *in vivo* cases. In this way, the regions of the protein that are structurally re-organized during fibril formation or unfolded can be identified. Among the antibody formats used as molecular probes to investigate the mechanisms of misfolding and aggregation process, Nbs seemed to be of greater advantage (Figure 18C). This comes mainly because of their stability towards the harsh conditions of denaturation and/or long incubation time that needs to be used to trigger

the *in vitro* aggregation of target proteins (Dumoulin et al., 2003). Pain et al. have summarized a number of pathological conditions where the co-crystallization of Nbs with the target antigen gives a lot of information regarding the process of fibril formation and the mechanism of action of the scAbs into the protein related (i.e. monomers, oligomers and fibrils) (shown in Figure 18C).

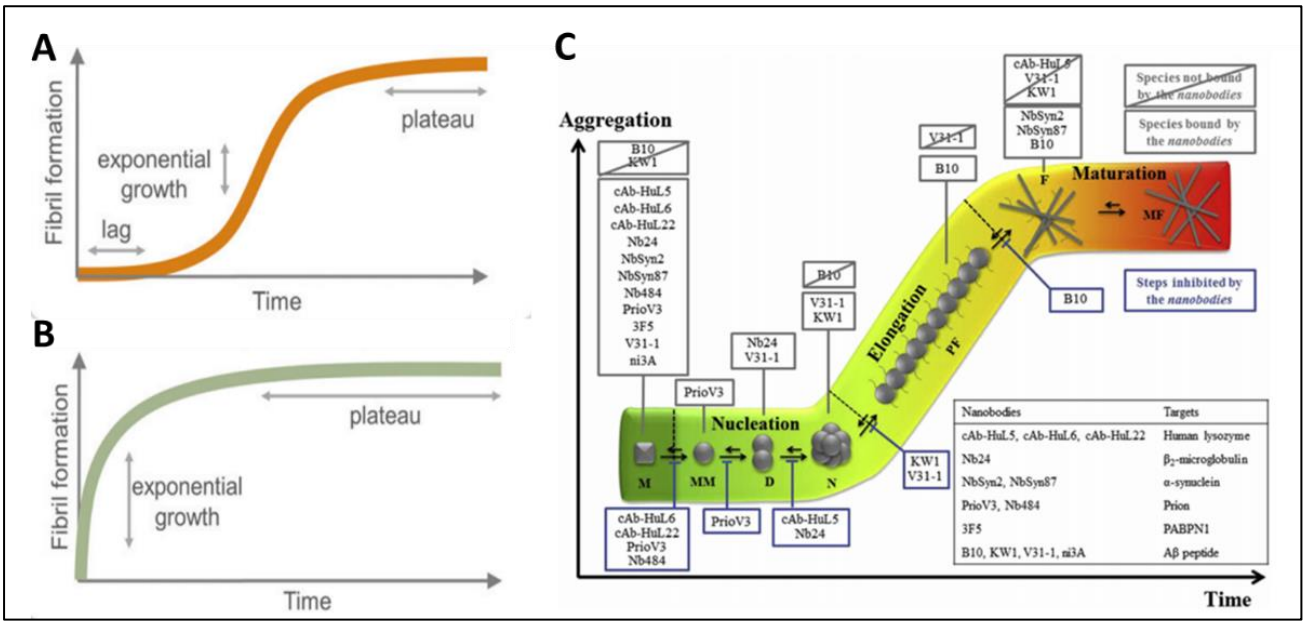

Figure 18 : Schematic representation of the S- shaped curve kinetics of fibril formation of an amyloidogenic protein. The formation of amyloid fibrils consists of three phases: (i) a nucleation phase or lag phase, during which monomers undergo conformational change and associate to form oligomeric nuclei, (ii) an elongation phase, during which the nuclei grow exponentially by further addition of monomers or oligomers to form protofibrils and fibrils, and (iii) a stationary phase, where monomers and fibrils are in equilibrium and during which fibrils formation has reached a plateau and can further mature. **A.** Kinetics of cofactor assisted protein fibrillization following the S-shaped curve kinetics. **B.** Seeded protein fibrillization follows exponential curve kinetics with the loss of the lag phase. **C.** The scheme is filled by different VHHs/Nbs currently under investigation, found to act in the different phases of the fibril formation. The grey boxes indicate the species which the different Nbs bind to, the crossed-out grey boxes indicate the species that are not recognized by the different nanobodies, and the blue boxes indicate the steps inhibited by the various nanobodies. M, monomers; MM, misfolded monomers; D, dimers; N, nuclei; PF, protofibrils; F, fibrils; MF, mature fibrils. Adapted from (Pain et al., 2015) and (Limorenko & Lashuel, 2021).

Among a number of Nbs used in neurodegenerative diseases, two of them named as KW1 and B10, showed of high interest in AD (Figure 19). KW1 and B10 come from synthetic library coding for nanobodies, using oligomers of Aβ40 and partially biotinylated fibrils, respectively, as targets (Habicht et al., 2007). A counter-selection was carried out in the presence of a 10-fold molar excess of freshly disaggregated Aβ40 peptide (i.e. largely monomeric) in order to avoid the selection of nanobodies that bind to the monomeric form of Aβ40 (Pain et al., 2015).

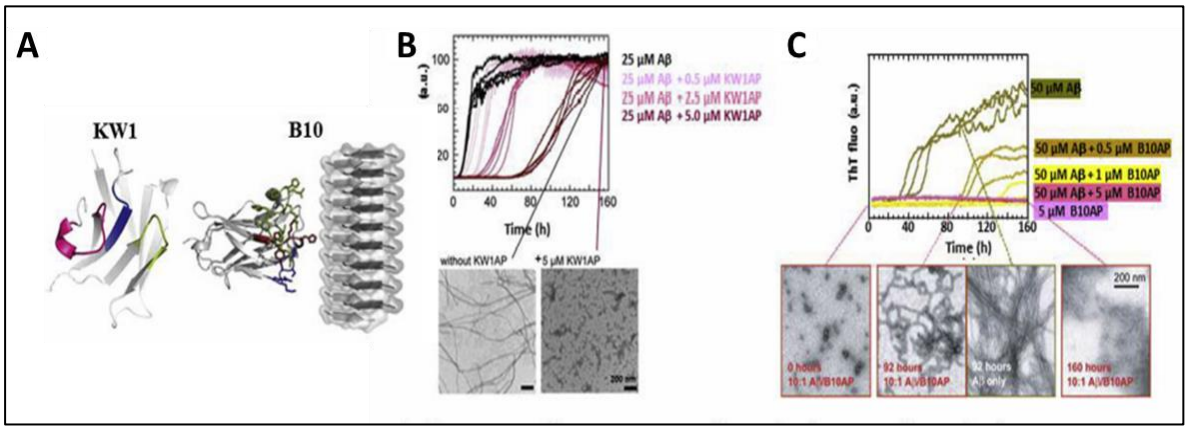

Figure 19 : Nanobodies use in understanding the fibrillary formation. A. The three-dimensional structure of KW1, B10 and amyloid fibrils. **B**. The *in vitro* aggregation of Aβ peptide, monitored by Th-T in the presence, or not, of KW1. **C.** The *in vitro* aggregation of Aβ peptide, monitored by Th-T in the presence or not of B10. Adjusted from (Pain et al., 2015), based on (Habicht et al., 2007).

KW1 interacts with oligomers through a hydrophobic and significantly aromatic surface motif formed by Aβ residues (Figure 19A). This specificity of KW1 to Aβ40 oligomers: binding neither to fibrils nor to disaggregated Aβ40 peptides, prevent the formation of mature fibrils, by increasing the lag phase, and leading to the formation of non-fibrillar aggregates (Figure 19B). On the other hand, B10 is specific for proto-fibrils and mature fibrils formed by the Aβ peptides, both *in vitro* and *in vivo*, indicating that in both these conditions the Aβ peptides share some basic structural features between them (Figure 19C) (Habicht et al., 2007). The B10 molecular recognition of amyloid fibrils, based on X-ray structure of B10, can be described as electrostatic interaction between the positively charged residues of CDRs with the anionic groups present on fibril surfaces. By further monitoring the formation of mature amyloid fibrils in the presence of B10, it was concluded that fibril formation is arrested at the proto-fibril stage by B10 preventing further self-association of proto-fibrils. These results are a proof of concept that nanobodies can target each species formed on the pathway of fibril formation and interfere with each step of the aggregation process (Friedhoff et al., 1998).

8.4 VHH against tau protein

Most widely used for VHHs selection is phage display library, as explained above. VHHs are presented at the tip surface of the phages, and the best binders are panned (two to three rounds) on antigens, which are most of the time immobilized in wells of a microtiter plate by passive adsorption or biotinylated on streptavidin-coated solid supports. In the same line in the current study have been selected 20 VHHs which by screening a synthetic phage-display library of humanized llama single-domain antibody (Moutel et al., 2016) against a biotinylated recombinant full-length tau protein (tau 2N4R) found to bind . After cross-validation by non-absorbed phage enzyme-linked immunosorbent assay (ELISA), these VHHs were selected for further analysis. Emphasizing though that the effect of the VHHs towards seeding and polymerization of tau is related to the recognized epitope (Courade et al., 2018; Yanamandra et al., 2013). Further, selectivity between various epitopes,

especially in tau cases where there is a continuous conformational change through disease progression for example in (Chai et al., 2011a), is also of importance. While nuclear magnetic resonance spectroscopy (NMR) is further used to define the binding region(s) on tau protein of the selected VHHs. The resonance perturbation mapping in ^{1}H, ^{15}N HSQC spectra of ^{15}N-Tau obtained allowed to define the various binding regions of the 20 VHHs selected along tau sequence. The initial screening of the different clones showed recognition of five different regions of tau from the proline-rich region to the C-terminus. Currently, it is described the series of tau-specific VHHs targeting the C-terminus of tau (Dupré et al., 2019). Even though, the parent F8-2 identified has no capacity to interfere with tau seeding and polymerization, showed interesting properties as a molecular tool to detect tau in research experiments. Interestingly, one among the selected VHHs, named VHH E4-1, detected to bind tau within the MTBD, which corresponds to the PHF6. However, VHH E4-1 was poorly binding tau intracellularly. Thus, an original round of optimization, using yeast two-hybrid system, to maximize its capacity to recognize tau when expressed in a cellular environment followed leading to a single optimized variant named VHH Z70. VHH Z70 differed by four mutations located outside the CDRs, in the framework domains (G12V, P16S, T81M and W114G), suggesting an unaltered epitope of recognition (PHF6), which was further confirmed by NMR resonance perturbation mapping. What is more, the characterization of the affinity of the VHH E4-1 and VHH Z70 towards full length tau showed an improvement of kinetic parameters of the VHH Z70 by 2.5 times (K_D 345 and 147nM, respectively). While the effect of VHH Z70 in tau seeding is to be determined as the main objective of the current study.

8.5 Nanobodies can cross membranes and the BBB and function intracellularly

As mentioned in (the Chapter 6), in the case of intracellular fibril aggregates and/or fibril aggregation in the brain, therapeutic antibodies must cross the BBB and/or be active in the cellular environment once inside the cells (Marschall & Dübel, 2016). Again, due to their small size, high stability and easiness to be engineered, the various approaches that have been reported to transduce proteins (i.e. coupling them to a shuttle peptide or protein to facilitate their passage through the BBB via receptor mediated transcytosis) should be easily transferable to Nbs (T. Li et al., 2012; Van Audenhove et al., 2013). It is known that only 0.1 to 0.2% of circulating conventional antibodies are found in brain at steady state concentrations. Recent studies have demonstrated that some VHHs are able to cross the blood-brain barrier (BBB) (T. Li et al., 2016; Muyldermans et al., 2001; Nguyen et al., 1998). The amount of transduced Nbs, as well as the mechanism by which they are transduced, vary significantly from one Nb sequence to another depending on physico-chemical characteristics like the isoelectric point (pI). Despite the observed intake, there is still a debate whether the transduced amount of Nbs is sufficient to allow imaging and therapy. Thus, a current strategy for the delivery of therapeutic antibodies

at a sufficient concentration, to reach a sufficient number of specific target cells for a sufficient time, is the use of adeno associated vectors (AAV). In addition, in the literature there are a number of other novel capsids reported to be appropriate for delivery of intrabodies in neurodegenerative diseases (Challis et al., 2019), which can be then easily been transformed to nanobodies case. Another issue for intracellular applications is related to the reducing cytosolic environment where the disulfide bonds are unable to form, affecting thus the folding or the ability of the protein to remain folded and thus impacting the function of conventional antibodies or antibody fragments (in our case VHH) (M. et al., 2010; Tanaka & Rabbitts, 2003). However, for some nanobodies, the disulphide bridge(s) is not necessary for the proper folding into cytosolic environment (T. Li et al., 2012) and the functionality of these nanobodies are conserved in cells (Saerens et al., 2008). Candidate clones must therefore be tested empirically, using model cells (preferable human stem cells differentiated along neuronal pathways) and animal systems that correlate as closely as possible with the proposed clinical use.

II. Objectives

The scope of this three-year project is to test the efficacy of VHH Z70 as a molecular tool to inhibit the seeding of tau. To reach that objective, we have first used a cellular assay. Taking into consideration that the recognition sequence of VHH Z70 on tau protein is the PHF6 peptide ($_{306}$VQIVYK$_{311}$) the ability of mitigating tau seeding will be tested first in a P301S FRET Biosensor aggregation reporter cells. This cell line constitutively expresses tau MTBD, containing the PHF6 peptide as well as a P301S mutation, fused to either CFP or YFP that together generate a FRET signal upon MTBD-P301S polymerization. The latest is induced by transfecting the cells with tau seeds (heparin induced MTBD fibrils), while in basal conditions, FRET signal is not detected by flow cytometry. To further test the ability of VHH Z70 to mitigate tau seeding in a more complex system, we have used in a second step a mouse model. Bilateral injection of LVV expressing VHH Z70 was performed in THY-tau30 Tg tau mouse model. In this case seeding was induced by injection (same coordinates as the LVV) of h- AD brain lysate. The selected h- AD brains was tested for pathological phosphorylated pattern of tau by WB and the ability to induce pathology in the current mouse model. We have also tested the ability for future use as control of h- AD brain lysates, which comes from healthy individuals, lack the pathological pattern of tau when tested in WB and do not induce pathology when injected intracranially. For the current study, injection of PBS instead of brain lysate was used as negative control of seeding. The identification of the effect of the VHH Z70 on tau seeding *in vivo* was checked by determining the pathology through specific phospho tau antibody (AT-8). Further, VHH Z70 was fused to Fc of a mouse IgG to try to detect the effect on extracellular tau, when expressed *in vivo* by LVV injections. A group of mice were injected with LVV expressing VHH Z70 fused to mCherry. An anti- mCherry immunohistofluorescence will ensure the expression level of VHH Z70 and diffusion pattern of the LVV. Finally, we have performed a preliminary experiment in a mouse model of aging, without injection of seeds, to assay the activity of VHH Z70. We also developed in parallel better tools to perform the experiments. The latest comes as a continue effort on developing monoclonal antibody detecting specifically VHH Z70 in the lab. Finally, we have also tried to improve the VHH Z70 affinity for tau. Random mutagenesis of VHH Z70 cDNA resulted in eight variants with increase affinity for tau. They were tested in the bio-sensor cellular model to evaluate whether this increase affinity was correlated to a better efficacy to mitigate seeding.

III. Materials and Methods

1. Cellular experiments

1.1 Seeding assay in HEK293 reporter cell-line

Stable HEK293 Tau RD P301S FRET Biosensor cells (ATCC CRL-3275) were plated at a density of 100k cells/well in 24-well plates. At ~60% confluency, cells were first transiently transfected with the various pmCherry-C plasmid constructs allowing expression of the VHHs fused to mCherry. Transfection complexes were obtained by mixing 500 ng of plasmid diluted in 40 µl of opti-MEM medium, which included 18.5 µL (46.25% v/v) of opti-MEM medium with 1.5 µL (3.75% v/v) Lipofectamine 2000 (Invitrogen). Resulting liposomes were incubated at room temperature for 20 min before addition to the cells. Cells were incubated for 24 hours with the liposomes and 1 ml/well of high glucose DMEM medium (ATCC) with Fetal Bovine Serum 1% (Life technologies). Eight µM of recombinant MTBD seeds were prepared *in vitro*, in the presence of 8 µM heparin, as described (Holmes et al., 2014). Cells were then treated with MTBD seeds (10 nM/well) in the presence of transfection reagents forming liposomes as here above described.

1.2 FRET Flow Cytometry

Cells were recovered with trypsin 0,05% and fixed in 2% PFA for 10 min, then suspended in PBS. Flow cytometry was performed on an ARIA SORP BD (acquisition software FACS DIVA V7.0 BD, Biosciences). To measure CFP (Cyan Fluorescent Protein) emission fluorescence and FRET (Forster Resonance Energy Transfer), cells were excited with a 405 nm laser. The fluorescence was captured with either a 466/40 or a 529/30 nm filter, respectively. To measure YFP (Yellow Fluorescent Protein) fluorescence, a 488 nm laser was used for excitation and emission fluorescence was captured with a 529/30 nm filter. mCherry cells were excited with a 561 nm laser and fluorescence was captured with a 610/20 nm filter. To selectively detect and quantify FRET, gating was used as described (Holmes et al., 2014). The FRET data were quantified using the KALUZA software analyze v2. Three independent experiments were done in triplicate or quadruplicate, with at least 10,000 cells per replicate analyzed.

1.3 MTBD seeds

The MTBD seeds used (or P301L-K18 domain) are composed of the four microtubule- binding regions of tau protein with a pro-aggregative and pathogenic P301L mutation found in frontotemporal dementia with parkinsonism-17 (Poorkaj et al., 1998; Spillantini et al., 1998). P301L-K18 tau fragment and expressed in *E.coli*. Before utilization in cell culture, DTT (1M) in final concentration of 10µM was added (5µl) and 30min of incubation in RT followed. Then, heparin was added to reach the final concentration of 8µM. Incubation for 48h at 37oC occurred, without shaking. The presence of fibrils is confirmed by

Thioflavin-T (Th-T) fluorescence in the end of the experiment with an aliquot of 100µl compared to a negative control without addition of heparin by addition of 50µM Th-T. The emission of Th-T was detected at 480nm after excitation at 440nm on a PHERAStar (BMG Labtech Gmbh, Ortenberg, Germany). Fibrils are sonicated each time before use.

2. *In vivo* experiments

2.1 Mouse model THY-tau30

The present experimental research was performed with the approval of an ethical committee and follows European guidelines for the use of animals. The animals were housed in a temperature-controlled (20–22°C) room maintained on a 12-h day/night cycle with food and water provided ad libitum in specific pathogen free animal facility (n= 5 mice, male or female per cage). Animals were allocated to experimental groups by randomization. THY-tau30 (Tg30tau) mice express human 1N4R tau protein with two pathogenic mutations (P301S and G272V) under the control of the neuron-specific Thy1.2 promoter (Leroy et al., 2007; Schindowski et al., 2006).

2.2 Human brain lysate

In this project were used human Alzheimer's Disease (h-AD) and human non AD brain lysates, the later as non-seeding control. For induction of the pathology in THY-tau30 mice, a mixture of two post-mortem human histological confirmed Alzheimer disease patients (frontal cortex area, Braak stage VI, Brodmann area 10) were used. This because the different filaments of human brains may exhibit a range of morphologies and distinct conformers may cause distinct tauopathies (Clavaguera et al., 2013; Nobuhara et al., 2017). The h-AD brains were obtained from the Lille Neurobank (fulfilling criteria of the French law on biological resources and declared to competent authority under the number DC-2008-642) with donor consent, data protection and ethical committee review. Samples were managed by the CRB/CIC1403 Biobank, BB- 0033-00030. To generate the human brain homogenates, tissues were weighed and homogenized on ice with a glass potter in five volumes (w/v) of phosphate-buffered saline (PBS). The homogenates were sonicated, followed by centrifugation at 4°C, 3000g for 5 min followed. The supernatant was aliquoted and frozen at -80°C.

2.3 Stereotaxic injection and sacrifice procedures

The *in vivo* studies occurred in anesthetized (Ketamine 100mg/kg, Xylazine 10mg/kg) transgenic mouse line, THY-tau30, one month-old (Leroy et al., 2007). Bilateral- intracranial injection of LV vector is performed. LVVs expressed either the anti-GFP VHH or the VHH Z70 fused to either mCherry or alone, for eight THY-tau30 mice assayed per condition. The production and use of the LVV VHH Z70-mCherry was to monitor the expression of the VHH Z70 by detection of the fusion protein. The

injection site was decided to be in the hippocampus area: anterio-posterior (AP): -2.5mm referred to Bregma; medio-lateral (ML): -1mm; dorso- ventral (DV): -2.3. The injection consisted of delivery of 2µl of 200ng/µL (based on viral capsid protein) of LVVs per hemisphere by using a 10µl glass syringe with a fixed needle (Hamilton). The rate of delivery is standardized at 250nl/min, followed by five minutes of rest into the injection site before removing. Two weeks after, bilateral injection (same site) of human AD brain homogenates (2µl/ hemisphere ; 7.5µg/µl) took place ensuring the induction of pathology (Albert et al., 2019; C. L. Dai et al., 2018; Vandermeeren et al., 2018). At 1-month-old, these mice have low endogenous tau pathology, which allowed to evaluate the seeding activity associated to the injected human-derived materials. Mice injected with LVV- anti-GFP VHH at the first injection and PBS (2µl/hemisphere) at the second one was used as negative control group, allowing to monitor the basal (non-seeded) development of the pathology. The protocol for brain recuperation and storage is as described in (Albert et al., 2019). Briefly, one-month post-injection, THY-tau30 mice were anaesthetized and transcardially perfused with ice-cold saline (0.9%) solution and subsequently with paraformaldehyde (4%, PFA) for 10min. The brains were then removed from skull and immediately post-fixed for 24h in PFA (4%), washed in PBS, placed in sucrose overnight and frozen in isopentane until free-floating coronal sections (40µm thickness) occurred by using cryostat microtome. Samples were stocked until use in PBS (Sigma P3813) +0,2 % Sodium Azide (Sigma S8032).

3. AT-8 immunohistochemical labeling, quantification, and statistical analysis

3.1 Immunohistochemistry

To remove Sodium Azide and proceed to immunohistochemistry, brain sections were washed in PBS- 0.2% Triton X-100 (PBS-T, 10minx3) (Sigma T9284). Then a 30 min of treatment with 0.3% H_2O_2 followed, blocking the endogenous peroxidase. After 3 washes in PBS-T, non-specific binding was blocked by using 'Mouse in Mouse' reagent (1:100 in PBS, Vector Laboratories) for 60 min and overnight incubation with AT-8 antibody as primary antibody (shaking at 4°C) in PBS-T occurred (1:500, Thermo MN1020). AT-8 is a mouse monoclonal antibody (M. Goedert et al., 1995) and one of the most widely used phosphorylation-dependent anti-tau antibodies specific for tau phosphorylated at Ser202, Thr205 and Ser208 (Despres et al., 2017). Next day, washings in PBS-T (10minx3) and labelling was amplified by incubation with an anti- mouse biotinylated IgG (1:400 in PBS-T, Vector) for 60 min followed by the application of the avidin-biotin-complex (ABC kit, 1:400 in PBS, Vector). Finally, to create a visible reaction product, sections were treated with DAB (3,3'-diaminobenzidine, Sigma) in Tris-HCl 0.1 M, pH 7.6, containing H_2O_2. Brain sections were mounted, air-dried, steadily dehydrated in ethanol (30%, 70%, 95%, 100%), cleared in toluene and coverslipped with VectaMount (Vector Laboratories).

3.2 Quantifications

Brain sections were blindly analyzed using quantification software (Mercator image analysis system, Explora Nova, La Rochelle, France). Threshold was established manually using identified objects on a set of slides and these remained constant throughout the analysis. Based on the injection site performed (AP:-2.5mm, ML:-1mm; DV:-2.3mm) and the area of diffusion where the LVV VHH- mCherry was detected, the zone of quantification is the early CA1 and Dentate Gyrus parts as well as Subiculum on posterior bregmas. Further, the sections of the bregma that were processed for quantification are between -2.06 and -2.92 (based on the Mouse Atlas, George Paxinos and Keith B.J. Franklin, Second Edition, Academic Press). This area actually represents four bregma anterior to the injection site (-2.06; -2.18; -2.3; -2.46) and four posterior to it (-2.5; -2.7; -2.8 and -2.92).

4. Cellular assay- infected with LVV

HEK293T cells, plated in six- well plates, were infected with 200 ng/well of LVV, expressing VHH anti-GFP or VHH Z70-mCherry intrabodies. The infection occurred in a minimal volume of medium (DMEM, Gilbco) and was increased up to 2ml 4-6 hours post-infection. The collection of the supernatant and the lysate occurred 48 hours after the infection. Samples were kept at -20^{o}C until further use.

5. Western Blotting

The dilution of the samples was done in LDS 2x (LDS NuPAGE® Buffer) and loading of 10µg of total protein was loaded per lane on 4–12% Bis-Tris NuPAGE Novex gel (Invitrogen). The total protein concentration was measured by BCA method. After the separation, the gel was blotted on a 0.45µm nitrocellulose membrane using the Novex system from Life Technologies (XCell IITM blot module). The membrane was then incubated for 1h at room temperature (RT) with blocking solution containing 5% non-fat dry milk before incubation overnight at 4^{o}C with primary antibody. Next day, the membrane was incubated for 1h with the corresponding (based on the primary antibody being used) secondary HRP- labelled antibody. After each incubation step, 3 washings of ten minutes in 1X Tris Buffer Solution (TBS) buffer followed. The signal was visualized using ECL western blotting detection reagents (GE Healthcare). Time of exposure was blot dependent.

6. Immunohistofluorescence

Brain sections were washed three times during 10min in PBS containing 0.2% Triton X-100 (SigmaT9284) to remove Sodium Azide and then saturated for 1h at Room Temperature (RT) with a 1% normal goat serum (Sigma-Aldrich) diluted in PBS, followed. Primary Antibody detecting the Red Fluorescence Probe (1:1000, rabbit, Polyclonal, Rockland) was incubated overnight at 4^{o}C and the next day the incubation of Alexa- Fluor 488 secondary antibody (anti rabbit, Invitrogen) was added

at dilution 1:1000 for 1h at RT. Samples were then washed in PBS-Triton X-100 0.2% (3x10min) and kept in saline 0.9% until mounting. Mounted brain sections were well air-dried and sudan black protocol was applied. Finally, slides were coverslipped using Vectashield with DAPI (Vector). Slide imaging was performed by microscopy using a slide scanner (Axioscan Z1-Zeiss) with a 20X objective.

7. Cloning of VHH Z70 Minibody

For expression of dimeric antibody (Minibody, Mb), VHH Z70 and VHH- anti GFP coding sequences were inserted in pFuse plasmid (Invivogen). Minibodies cloning, corresponding to bifunctional VHH Z70 or VHH anti GFP fused at their C-terminus to the Fc fragment of mouse IgG2, was performed according to Moutel et al. (Moutel et al., 2009).

8. Production and purification of the VHHs

Competent *E. Coli* BL21 (DE3) bacterial cells were transformed with the various PHEN2-VHH constructs. Recombinant *E. coli* cells produced proteins targeted to the periplasm after induction by 1 mM IPTG (isopropyl-thio-galactoside). Production was pursued for 4 h at 28 °C before centrifugation to collect the cell pellet. Pellet was suspended in 200 mM Tris-HCl, 500 mM sucrose, 0.5 mM EDTA, pH 8 and incubated 30 min on ice. Then 50 mM Tris-HCl, 125 mM sucrose, 0.125 mM EDTA, pH 8.0 and complete protease inhibitor (Roche) were added to the cells suspension and incubation continued for 30 min on ice. After centrifugation, the supernatant, corresponding to the periplasmic extract, was recovered. The VHHs were purified by immobilized-metal affinity chromatography (HisTrap HP, 1 mL, GE healthcare) followed by size exclusion chromatography (Hiload 16/ 60, Superdex 75, prep grade, GE healthcare) equilibrated in NMR buffer (50 mM NaPi pH 6.7, 30 mM NaCl, 2.5 mM EDTA, 1 mM DTT) (Dupré et al., 2019).

9. ELISA

NUNC F8 Maxisorp (ref: 469949) were coated with 200ng peptide diluted in carbonate buffer and stored overnight at 4°C. Saturation with PBS/Casein 0.1% followed the next day for 1h at 37°C. Following three washings steps with PBS/Tween 0.05%, incubation with either serum or cell supernatant for 2h at RT occurred. Finally, anti-mouse IgG-peroxidase conjugated diluted in PBS/BSA 0.2% (1:4000; Sigma, A3673) was added and incubation pursued for 1h at 37°C. Five washings with PBS/Tween 0.05% were performed before revelation by TMB in Citrate/Phosphate buffer containing H_2O_2 30% (incubating 30min at RT with shaking). This was ended by addition of 50µl/well of H_2SO_4 10%. Signal was detected at 450nm.

10. Immunocytochemistry

A 24- wells plate was prepared with lames, then 30.000 HEK293T cells were plated/ well. A day after, cells were infected with LVV expressing either VHH anti-GFP or VHH Z70 (50ng/well) and incubated for 48h. Then, medium was removed and

cells were fixed using 4% PAF for 30min. Afterwards, cells were washed and stored in DPBS. Immunocytochemistry followed shortly after to avoid any signal loss during delay. Cells were firstly washed with NH_4Cl 50 mM in PBS-BSA 1 % (3x5min), saturated with PBS-BSA 2% for 1h and incubated overnight with either serum (1/200) or supernatant (1/2) diluted in PBS-BSA 1% - triton 0,1%. The next day, wells were washed with NH_4Cl 50 mM in PBS-BSA1 %, and incubation with secondary antibody for 1h in dark was performed (dilution 1:1000, Invitrogen, Alexa 568). Washing and incubation with DAPI staining (1:5000) followed for 15min at RT. Wells were next washed once with NH_4Cl 50 mM in PBS-BSA 1% and once with PBS occurred. The slices were fixed, and microscope analysis followed (Apotome-Zeiss).

11. Statistical Analysis

Experiments of the reporter-cell seeding assays in HEK293T cells were performed at least in triplicate and obtained from three independent experiments. As non-normal distributed values, tested within the same group by using Shapiro-Wilk test, a Mann-Whitney U-test (non-parametric) was performed. Comparison between groups was done at the two-tailed, p value of 0.05. Data were analyzed using Prism Software. The same was followed for the immunohistochemistry analysis of the groups tested. Results of the *in vivo* analysis are presented either as the total signal of immunoreactive area or the total number of bodies detected normalized to the whole area analyzed, $\pm$ standard error bars (SD).

IV. Results

1.1 Preliminaries

My project is based on a synthetic VHH, VHH Z70, derived from the optimization for intracellular activity of a humanized synthetic single domain antibody, directed against tau microtubule binding domain. An initial clone, E4-1, was selected from the screen with Tau2N4R of a synthetic phage-display library of a humanized llama single-domain antibody (Moutel et al., 2016). E4-1 was shown to recognize tau MTBD domain, using NMR. However, this VHH showed to be a poor binder of tau when the Yeast 2-Hybrid (Y2-H) system was used to test its intracellular binding capacity. This may be due to improper folding and/or poor stability once expressed intracellularly (Dupré et al., 2019; T. Li et al., 2016). Thus, in order to maximize its capacity to recognize its intracellular target, a cDNA mutant library was constructed by random mutagenesis (Cadwell & Joyce, 1992). The library was transformed in yeast and was screened by cell-to- cell mating to get positive colonies. An optimized mutant, named VHH Z70, which resulted in four mutations in framework domain (G12V, P16S, T81M and W114G), outside of the CDRs, conserving thus the recognized epitope. The epitope conservation was further confirmed by resonance perturbation mapping, using isotopically labelled MTBD. Furthermore, the affinity towards tau was determined by surface plasmon resonance spectroscopy (SPR), showing VHH Z70 as a better binder (Lower K_D) than VHH E4-1, 147nM and 345nM, respectively. A yeast 2-hybrid was performed with a library of tau fragments and a minimal epitope was identified for VHH Z70. The sequence is localized in the R3 repeat and contains the PHF6 peptide, the nucleus of tau aggregation. To test the capacity of VHH Z70 to interfere with tau aggregation, an *in vitro* aggregation assay was used. The aggregation assays were carried out with recombinant tau protein in the presence of heparin, using Th-T as a dye whose fluorescence is increased in presence of aggregates. In addition VHH Z70 had the capacity to decrease the seeding in the fluorescent-based reporter cells (Holmes et al., 2013). The *in vitro* outcome was very encouraging showing that VHH Z70 had an efficient inhibitory effect.

1.2 Optimization of VHH Z70 to improve the affinity for its target

Based on the whole sequence of the VHH Z70 (as shown in Table 5, in separate has been given also the sequence of the CDRs), an optimization step to improve affinity in intracellular conditions was performed. The increased affinity parameter is desirable, as it may have effects on both sensitivity and specificity of the antibody. The strategy for optimization involved random mutagenesis (Cadwell & Joyce, 1992) coupled with Y2-H for selection (Dupré et al., 2019; Visintin et al., 1999). This experiment resulted in generation and selection of eight functional variants, here named as Mutants (Mut. 1, Mut. 3, Mut. 5, Mut. 9, Mut. 12, Mut. 14, Mut. 15 and Mut. 20). The point mutations (PMs) occurred mostly in the framework, with few

exceptions in the CDRs (Muts. 9/14 and 15). The mutated forms conserved the binding epitope on tau protein (PHF6). The affinities of the VHH Z70 and Mutants towards biotinylated full-length tau protein were determined by SPR and are summarized in **Table 6**, which also present the location of occurrence of PM as well as how the affinity parameters differ between derivates. The K_D of VHH cannot be directly compared to the usual apparent affinity used to define interaction of the IgGs, because the later are bivalent, resulting in an apparent higher affinity by an avidity effect. As presented in Table 5, Mutant 1 has a strong binding improvement (Lower K_D) compared to VHH Z70, about 6 times thanks to a point mutation in FR4, at the C-terminus of the CDR3. The same is identified for Mutant 12 with two-point mutations, in FR1 and FR4, the latest common with Mutant 1. In the case of Mutant 9, Mutant 14, and Mutant 15, additional mutations outside the FRs are found in the CDRs (CDR3 for Mut 9 and 15, CDR1 and 2 for Mut 14), which resulted in a decrease of the K_D without influencing the epitope of recognition. A gain of affinity was recorded also in the cases of Mut.3, Mut.5 and Mut.20 with point mutations occurring in the FR. These findings suggest that affinity towards epitope can be increased with or without changes in the CDR loops, as well as the role of CDR 1 and 2 in binding (Dupré et al., 2019). Of note, the overall negative charge detected in the CDRs of the VHH Z70, were not affected by the point mutations in resulting variants.

Table 5 : The amino acid sequence of the VHH Z70. The table presents the sequence of binding on tau by VHH Z70, the whole sequence of the VHH Z70 and the sequence of the CDR regions, mostly related to the antigen- antibody binding.

	Amino acid sequence
Epitope of binding (tau)	SVQIVYKPV
VHH Z70	MAEVQLQASGGVFVQSGGSLRLSCAASGATSTFDGMGWFRQ APGKEREFVSAISYEQGSYTYYADSVKGRFTISRDNSKNMVYLQ MNSLRAEDTATYYCAPAYEGDLYAFDSYGGQGTQVTVSSAA
VHH Z70 CDR1	ATSTFDG
VHH Z70 CDR2	YEQGSYT
VHH Z70 CDR3	PAYEGDLYAFD

Table 6 : Affinity determination for the series of VHHs binding tau, by surface plasmon resonance (SPR). Experiments were performed on immobilized biotinylated tau 2N4R (500 resonance units). Here are presented the mutations in the VHH Z70 sequence and the kinetic constants, k_{on} (kinetic association); k_{off} (kinetic dissociation) and dissociation equilibrium constant K_D, which is calculated as the ratio of the off-rate on the on-rate k_{off}/k_{on}.

VHH	Mutations	Region the PM occurred	K_{on} (1/Ms)	K_{off} (1/s)	K_D (nM)
VHH Z70	/	/	18100	0.0026	147
Mut 1	G115E	FR4	106744	0.0024	23
Mut 3	R47K	FR2	26042	0.0021	81
Mut 5	T96S	FR3	10918	0.0009	81
Mut 9	P101S, G115E	CDR3, FR4	40110	0.0020	51
Mut 12	S23C, G115E	FR1, FR4	33865	0.0021	61
Mut 14	T32I, E56G, G115E	CDR1, CDR2, FR4	18799	0.0014	74
Mut 15	R90G, P101S, G114E	FR3, CDR3, FR4	21264	0.0020	95
Mut 20	R47K, G115E	FR2, FR4	21285	0.0009	42

1.3 Inhibition of tau seeding in HEK293 tau repeat domain, P301S FRET Biosensor aggregation reporter cells

1.3.1 Test of the inhibition efficacy of VHH Z70 and Mutants towards tau seeding

VHH Z70 and the eight derived mutants were tested for their capacity to inhibit the intracellular seeding of tau protein. To evaluate this capacity of inhibition, a tau seeding assay modified from Holmes et al. 2014 was applied (explained in Chapter 7). Briefly, HEK293 is expressing the tau MTBD harboring a P301S mutation, fused to either CFP or YFP fluorophores that together generate a FRET signal in case of aggregation of the MTBD-P301S. The intracellular seeding of the MTBD-P301S protein is induced by treating the cells with tau seeds prepared *in vitro* (Narasimhan et al., 2017; Sanders et al., 2015*)* and incorporated in liposomes to increase their ability to penetrate into cells. A VHH named F8-2 was chosen as negative control of VHH activity as the binding site is in the C terminus of tau protein (373-378aa, based on the longest isoform of tau), outside the MTBD (Dupré et al., 2019). cDNAs of VHH Z70 and of the eight Mutants were cloned, to be expressed as fusion proteins (VHH-mCherry). Cells were transfected with these recombinant DNA constructs one day prior to the addition of tau seeds. The tau seeds are the recombinant *in vitro* aggregated MTBD of tau, fragmented by sonication (Holmes et al., 2013).

The intracellular seeding of the MTBD-P301S by treating the cells with the extracellular tau seeds, is leading to a FRET signal, with a detection signal at 12% $\pm$ 3.8% (S.D) in FRET gated positive cells, Figure 20. Treating the cells with both the seeds and the VHH used as negative control VHH-F8-2-mCherry detected to be at 11% $\pm$ 5.9% (S.D), showed no significant difference

compared to the cells treated with the seeds alone. This negative control also showed that the mCherry fluorophore did not interfere with the seeding, polymerization and/or FRET signal. Also, the VHH Z70 effect on tau seeding (8.8% ± 4% (S.D), resulted to be of no difference from the negative control (31.3% seeding inhibition, p value 0.0658), while the difference became significant when VHH F8-2 was compared to Mutant 1 (38.8% seeding inhibition, p value 0.0166) and Mutant 3 (42.8% seeding inhibition, p value 0.0025). Further, there was no significant difference in activity detected between VHH Z70 and Mutant 1, Mutant 3.

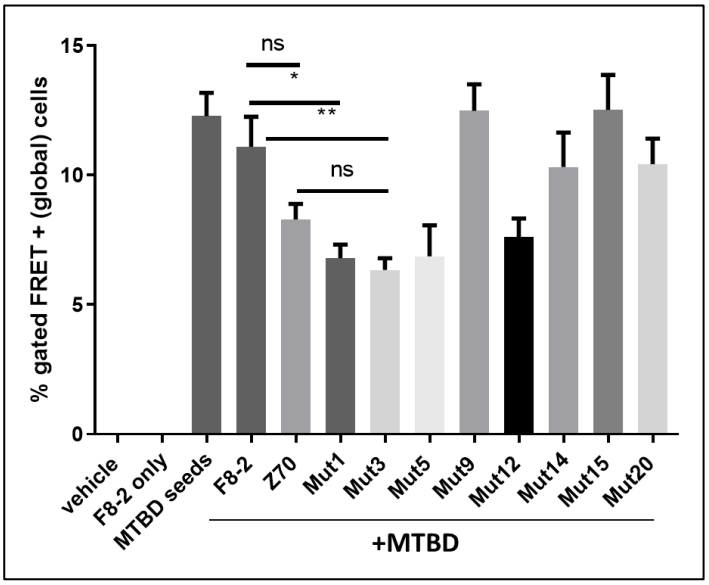

Figure 20 : VHH Z70 and Mutants effect on intracellular seeding of Tau MTBD in HEK293 TAU RD P301S FRET Biosensor cells. Percentage of FRET gated positive cells of HEK293 TAU RD P301S FRET Biosensor cells, determined from FACS data for cells transfected with VHH mCherry (F8-2, Z70 and Mutants) followed by MTBD seeds (n≥3). A significant decrease of FRET signal in FRET gated, report a decrease of intracellular MTBD seeding, observed in the presence of Mutants 1 and 3, but not detected when compared to VHH Z70. P value <0.05; **** P<0.0001; *0.0166; **0.0025; Ns: 0.0658; Error bars: S.D; Mann-Whitney U-Test, non-parametric.

Next, an additional mCherry gate was applied to detect FRET signal selectively in VHH-mCherry positive cells transfected with VHH Z70- mCherry or VHH- Mutants- mCherry (Figure 21). Thus, once again the FRET signal was detected, recording thus the effect of VHH Z70 and VHH- mutants on seeding. The VHH Z70 clearly affected the intra-cellular seeding, as the observed FRET signal for the corresponding transfected cells was significantly decreased from 15.3% ± 5% (S.D) for VHH F8-2 to 8.8% ± 3.1% (S.D) for VHH Z70 42% seeding inhibition, p value < 0.0001). Three of the derived mutants, VHH Mut.1, Mut.3 and Mut.12, also affected the intracellular aggregation, similarly to VHH Z70, as the observed FRET signals for the corresponding transfected cells were significantly decreased (p value <0.0001), where the seeding inhibition is translated to 49.6%, 51% and 48%, respectively. In contrast, no significant difference in activity of these mutants was detected compared to the primary VHH Z70 (p value > 0.05). What is more, the mutations occurring in the CDR region of Mutant 9,

Mutant 14 and Mutant 15 decreased significantly the effect of these mutants towards tau seeding, compared to the parent VHH Z70 (p value $\geq$ 0.2), where only in case of Mutant 14 a minor inhibition ability is kept, 12.6%. Further, VHH Mutant 5 and VHH Mutant 20, with mutations occurring in the framework regions (FR3 and FR2/FR4, respectively), also showed a decreased ability to block tau seeding (p value $\geq$ 0.2), where the seeding inhibition is translated to 26.5% and 17.8%, respectively. This might be due to improper folding or a partial destabilization of these VHH in a cellular context, although their selection in the Y2-H screen should have prevented this problem.

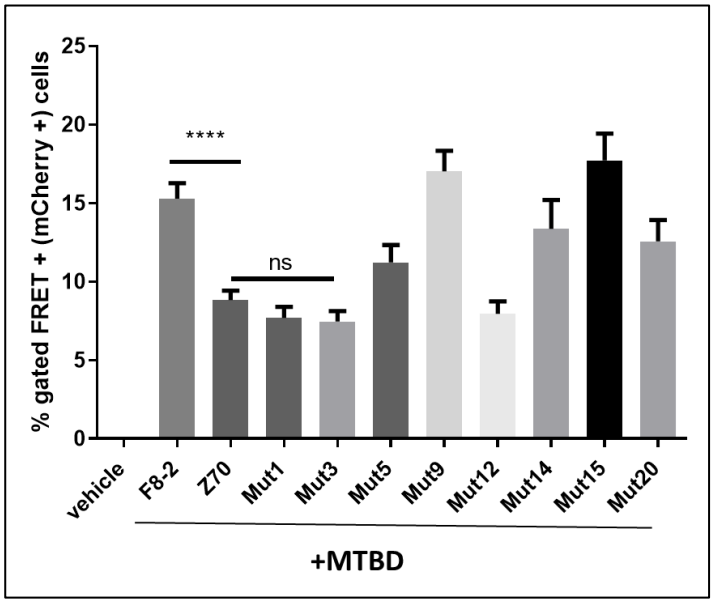

Figure 21 : VHH Z70 and Mutants block intracellular seeding of Tau MTBD in HEK293 TAU RD P301S FRET Biosensor cells. Percentage of mCherry gated FRET positive cells, determined from FACS data for cells transfected with VHH mCherry (F8-2, Z70 and Mutants) followed by MTBD seeds (n$\geq$3). A significant decrease of FRET signal in mCherry gate, report a decrease of intracellular MTBD aggregation, observed in the presence of- VHH Z70 and Mutants 1/3/12 fused to mCherry. Error bars: S.D, **** P<0.0001, Mann-Whitney U-Test.

For the derived Mutants showing a significant effect (Mutants 1, 3 and 12) in reduction of MTBD seeded aggregation, their efficacies in the absence of a carrier protein (mCherry) were next determined. To this effect, VHH cDNAs were cloned in a new plasmid, pcDNA3.1. The HEK293 cells were transfected with pcDNA3.1 VHH a day prior to transfection with tau seeds, with VHH F8-2 again serving as negative control. However, without the possibility to select the transfected cells by gating the mCherry fluorescence signal, FRET from intracellular aggregated tau being detected as a total signal, the experiments were not conclusive (total number of experiments 2). As shown in Figure 22, the FRET signal generated by the whole cell population of the VHH Z70 and the Mutants compared to the VHH F8- 2, is not significantly modified, despite a tendency for decrease of signal for Mutant 3 and Mutant 12.

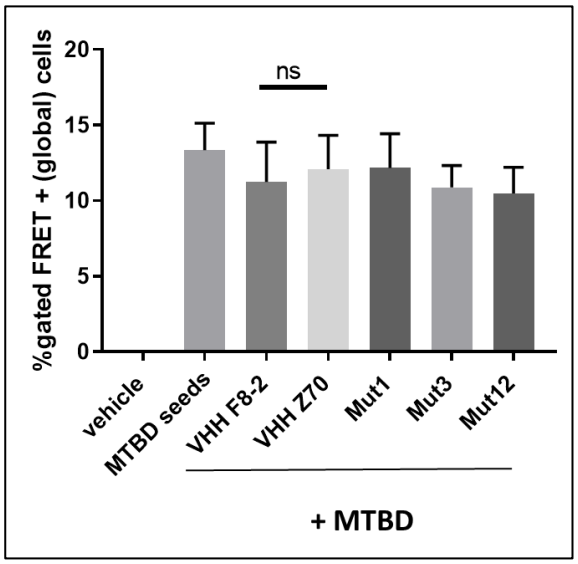

Figure 22 : Percentage of total FRET positive cells, determined from FACS data for cells transfected with pcDNA 3.1- VHH (F8-2, Z70 and Mutants) followed by MTBD seeds. There is no detection of significant decrease of total FRET signal between VHH F8-2 and VHH Z70, reporting an ability to detect the intracellular decrease of the MTBD aggregation. Error bars: S.D, ns (P value 0.3255), Mann-Whitney τ-Test. Vehicle stands for cells transfected with empty liposomes, while MTBD seeds stands for cells transfected with tau seeds only.

In order to overcome the inability of the detection of the effect of the VHH in the absence of a fusion reporter protein, experiments were performed by co-transfecting the HEK293 biosensor cells with empty mCherry-plasmid, together with the recombinant pcDNA 3.1 construct, which encodes the VHHs, to monitor the transfection. Our hypothesis was that co-transfection would be favored, and that the cells expressing mCherry were also expressing the VHHs. Comparison of the total FRET signal, or the mCherry-gated FRET signal, of the cells transfected with VHH Z70 and Mutants with the cells transfected with VHH F8-2 is shown in Figure 23. In the cherry-gated FRET signal measurements, significant difference was found between VHH F8-2 and VHH Z70/Mutant1/Mutant3 (p values of 0.0152, 0.0152 and 0.0173, respectively), showing an inhibition activity. For Mutant 12 transfection, analysis of the detected signal revealed two stars of significant difference compared to the control (p value 0.0022). However, only 3% of the alive cells were co-transfected, so that the analyzed population is small. Co-transfection with different concentration ratio between the two plasmids (now 1 to 5, in favor of pcDNA3.1) could be a better way to detect any difference on the effect of the various VHH in inhibiting Tau seeding in the biosensor cells.

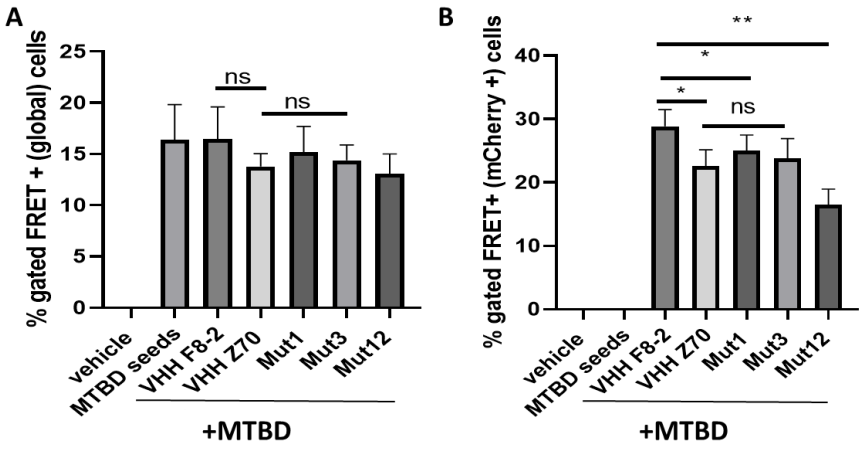

Figure 23 : Percentage of total FRET positive cells (A) and percentage of mCherry gated FRET positive cells (B), determined from FACS data for cells co-transfected with pcDNA 3.1- VHH and empty pmCherry followed by MTBD seeds. There is no detection of significant decrease of FRET (global) signal, while in mCherry gated FRET positive cells (B) was deteced a significant difference between VHH F8-2 and VHH Z70/ Mutant 1/Mutant 3 (P value 0.0152, 0.0152 and 0.0173, respectively) as well as Mutant 12 (P value 0.0022) , reporting an ability to detect the intracellular decrease of the MTBD aggregation. Error bars: S.D, P value <0.05; Mann-Whitney, non parametric. Vehicle stands for cells transfected with empty liposomes, while MTBD seeds stands for cells transfected with tau seeds only.

Of note, based on one preliminary single experiment, transfection with Mutant 12 seemed to decrease the number of HEK293T living cells 48h after transfection. This might indicate toxicity to the cells of this specific VHH. Mutant 12 has an extra cysteine, which usually are responsible for disulfide bonds created to afford stability in the cytoplasm. The same was checked for VHH F8-2 and Z70, where in these cases there was a steadily increase of alive cells over time related to the normal cell proliferation.

2.1 Inhibition of tau seeding *in vivo*

The ability of VHH Z70 to inhibit tau aggregation in *in vitro* aggregation assays (data shown in the publication) and *in cellular* model of seeding raises the hopes for a potential novel therapy in tauopathies. The main advantage is that VHH Z70 binds in the PHF6 in the MTBD, highly related to tau aggregation and seeding. Further, this hexapeptide is the binding site of a number of chaperons such as Hsp70, Hsp60 (Ciechanover & Kwon, 2017; Nachman et al., 2020). Chaperone proteins that act over protein aggregation play critical roles in neurodegeneration, and the roles of core classical chaperones such as Hsp's in the protection against neurotoxic protein deposits is firmly established. Also, Hsp70 was found to have disaggregate activity against Tau mature fibrils re-converting them into monomers (Nachman et al., 2020). These could suggest a mechanism for potential drug therapy. Thus, the next step followed is the determination of the inhibitory effect of VHH Z70 *in vivo*.

2.1.1 The efficacy of VHH Z70 expressed intracellularly (intrabody) in THY-tau30 Tg model

The *in vivo* testing occurred in one month old transgenic mouse line THY-tau30 Tg (Leroy et al., 2007), as summarized in scheme shown in Figure 26. Then, bilateral- intracranial injection of LVV expressing the VHH Z70, an anti-GFP VHH (green fluorescent probe as negative control) and a VHH Z70 fused to mCherry were performed (scheme of the injected groups of mice are shown in Table 7).

Table 7 : The scheme of the bilateral injected Tg30tau mice.

LVV injected (1st Inj)	2nd Injection	Number of mice
VHH Z70 intrabody	+AD	8
Anti GFP (44-4) intrabody	+AD	8
Anti GFP (44-4) intrabody	+PBS	8
mCherry-VHH Z70	+AD	8

LVVs have a limited diffusion capacity (Dujardin, Lécolle, et al., 2014), allowing to evaluate the local effect of VHH Z70 on tau seeding, while the mCherry fusion would help to make visible the extend of expression of the VHH Z70. Further, the LVVs infection of HEK293T cells showed expression of the VHH Z70, with no detection in the medium, confirming that VHH Z70 is well-expressed and not secreted.

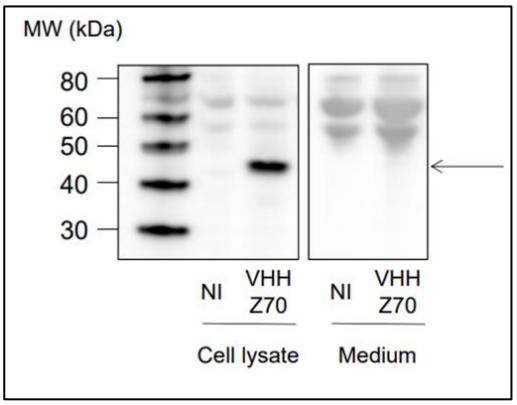

Figure 24 : Intracellular expression of VHH Z70: HEK293 cells were infected with LVVs encoding VHH Z70-mCherry or non- infected (NI). Forty- eight hours later, the cells were recovered and analyzed by Western Blotting. VHH 70 expression (black arrow) was revealed thanks to the mCherry tag using primary antibody against mCherry.

Two weeks after, bilateral injection (same site) of human AD brain extracts took place to induce tau pathology in Tg30tau (Albert et al., 2019; C. L. Dai et al., 2018; Vandermeeren et al., 2018). Mice injected with LVV VHH anti-GFP and PBS were used as control group. At 1-month-old, these mice have low endogenous tau pathology, which allowed to evaluate the

seeding activity associated to the injected human-derived materials. The selected AD brain homogenate used, is a mixture of two human brain lysates. This because the different filaments of human brains may exhibit a range of morphologies and distinct conformers may cause distinct tauopathies (Lasagna-Reeves et al., 2012; Mirbaha et al., 2017; Takeda et al., 2015). The selected ones are among several AD brains (frontal cortex, obtained from Lille Neurobank), giving a pattern indicative of the presence of the pathological isoforms of tau in Western Blot (Figure 25) and inducing the pathology when tested *in vivo* (data not shown).

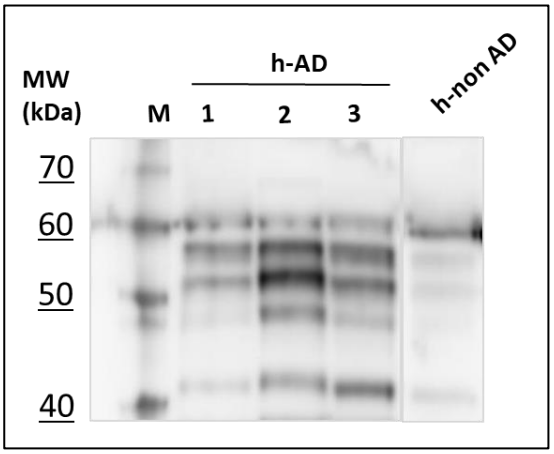

Figure 25 : Testing the pathological pattern of different human derived AD brains. Representing the PHFs derived from post-mortem human AD brain lysate (labelled as 1,2, 3), depicting the typical profile of the six hyperphosphorylated (full length) of tau isoforms running as a triplet between 50 and 70kDa. As negative control for tau recognition, is used brain-lysate derived from a non-AD patient. The h-AD homogenates 2 and 3, were combined and used as seeds in the in vivo experiments. For detection, primary antibody for the N-Terminus of tau (home- made, 12-21aa); Brain lysate 10µg/well; Rabbit, 1:10.000, o/n at 4oC and secondary Anti-Rabbit IgG, Made in Goat, Peroxidase (Thermofischer, labeled ZE0614), 1hRT; ECL: 1-2 min; Criterion 12%, Exposure time 30sec.

The sacrifice of mice occurred one-month post-injection and the level of pathology developed was quantified by immunohistochemistry with the monoclonal antibody AT- 8 (Despres et al., 2017). Of note, the injection site performed (AP: -2.5mm; ML:-1mm; DV:-2.3mm) was new and different of what was previously applied in the lab, where AP:-2.5mm; ML:-1mm; DV: -1.8mm (Figure 26). This choice was made to avoid any diffusion problems of the LVV during injection as the syringe passes through the elastic Corpus Callosum structure.

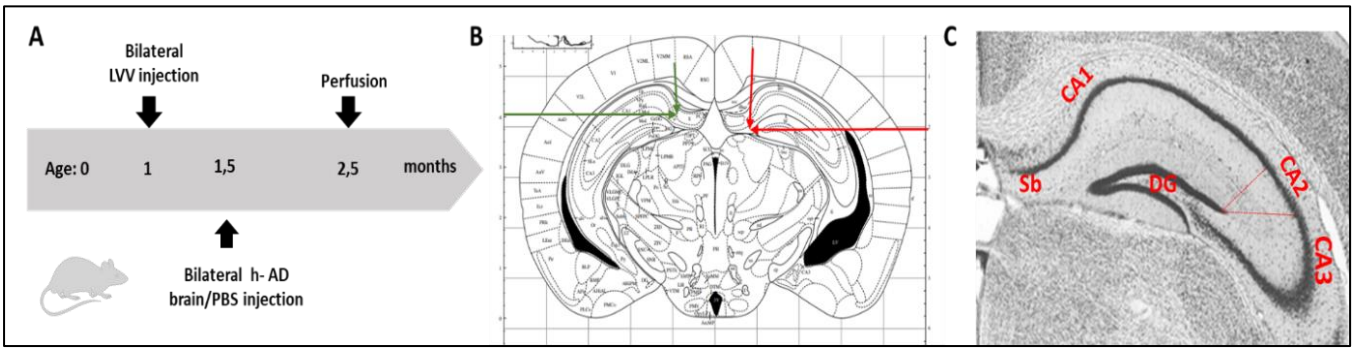

Figure 26 : Protocol of injection and the injection site in THY-tau30 Tg mouse hippocampus. A. Schematic representation of the injections in the bilateral intracranial injection of LVV (400ng/hemisphere) expressing either an anti-GFP VHH (two groups of eight) or mCherry- VHH Z70 (one group of eight) was performed in one month old mice. Induction of tau aggregation, occurred by a second bilateral injection, in the same site of injection, fifteen days after. For this, is used either human AD brain lysate (one anti-GFP VHH group and the mCherry- VHH Z70 group), or PBS buffer (in the remaining anti-GFP VHH group), ensuring a negative control for basal development of the tau pathology. The three groups were perfused one month later (aged 2.5 months). **B.** The bilateral injection occurred into the hippocampus area (presented in a coronal section) with the followed co-ordinates: AP:-2.5mm, ML:-1mm; DV:-1.8mm (named as old, left green arrows), and AP:-2.5mm, ML:-1mm; DV:-2.3mm (named as new, right red arrows). **C**. Schematic representation of the cellular layers of the mouse hippocampus. Bregma presented is the one of the injection site (AP:-2.5mm), including the subiculum (Sb), the cornu ammonis (CA, 1 to 3) and the dentate gyrus (DG). The B and C were adjusted from the *Mouse Brain Atlas of G. Paxinos & K.J. Franklin, Second edition*.

The detection of the diffusion of LVVs is between the -1.8 and -2.9 sections as shown by immunofluorescence labeling of the mCherry fusion, when analyzing mice injected with LVV expressing VHH Z70- mCherry (Figure 27). AT-8 immunostaining, showed the pathology, defined as AT-8 immunostaining, between -1.34 and -3.5 sections. However, the diffusion of the LVV appeared to be detected mostly in Dentate Gyrus part and slightly in CA1 (Figure 27), while the induction of pathology was the reversed case, showing thus sub-optimal conditions for this experiment. For the quantification, the region selected was between the bregmas -2.06 to -2.9, including the region of early CA1 and DG in the anterior bregmas and subiculum in the posterior sites, where both pathology and LVV expression were detected.

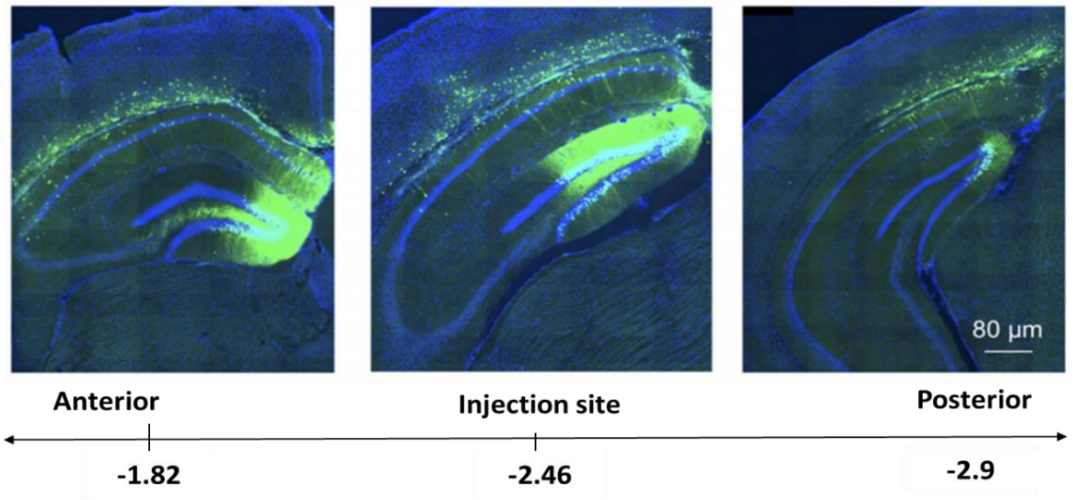

Figure 27 : Expression of the VHH Z70- fused to mCherry. Immunohistofluorescence of brain slices from intracranially injected mouse with LVV expressing mCherry VHH Z70 (AP: -2.5mm, DV:-1mm, ML: -2.3mm). Saturation with Normal Goat Serum, 1ry Polyclonal Anti-RFP (Rabbit, Rockland) and 2ry green fluorescence Alexa 488. The first section being well detected is -1.82 (left image) and the posterior part -2.9 (right image). Scale bar shown in the image.

The results of the quantification are shown either as AT-8 immunoreactivity (Figure 28A, C, E) or as number of stained bodies normalized to the total surface (Figure 28B, D, F), for VHH Z70 alone (Figure 28C, D) or fused to mCherry (Figure 28E, F), while images from the hippocampus area are shown in Figure 29. As shown in Figure 28E, analysis of brain sections from the animals injected with VHH Z70 fused to mCherry and further submitted to h-AD injection, showed a significant decrease of the detected AT-8 signal (p value of 0.0304) compared to positive control (mice injected with VHH-anti GFP and h-AD). This decrease was not significant when analyzing brain sections from the animals injected with VHH Z70, without the mCherry fusion. The number of stained bodies in both cases despite of the tendency of decrease (Figure 28D, F) did not seem to be significant compared to positive control, even if the effect is stronger in case of VHH Z70 fused to mCherry. This shows that the mCherry could be implicated in the stability of the VHH and/or affect the bioavailability parameters of the VHH Z70 protein. That we observed this effect in condition where the pathology induction and the VHH expression were not a perfect match is very encouraging. It will be of interest to improve the co-localization in future experiments.

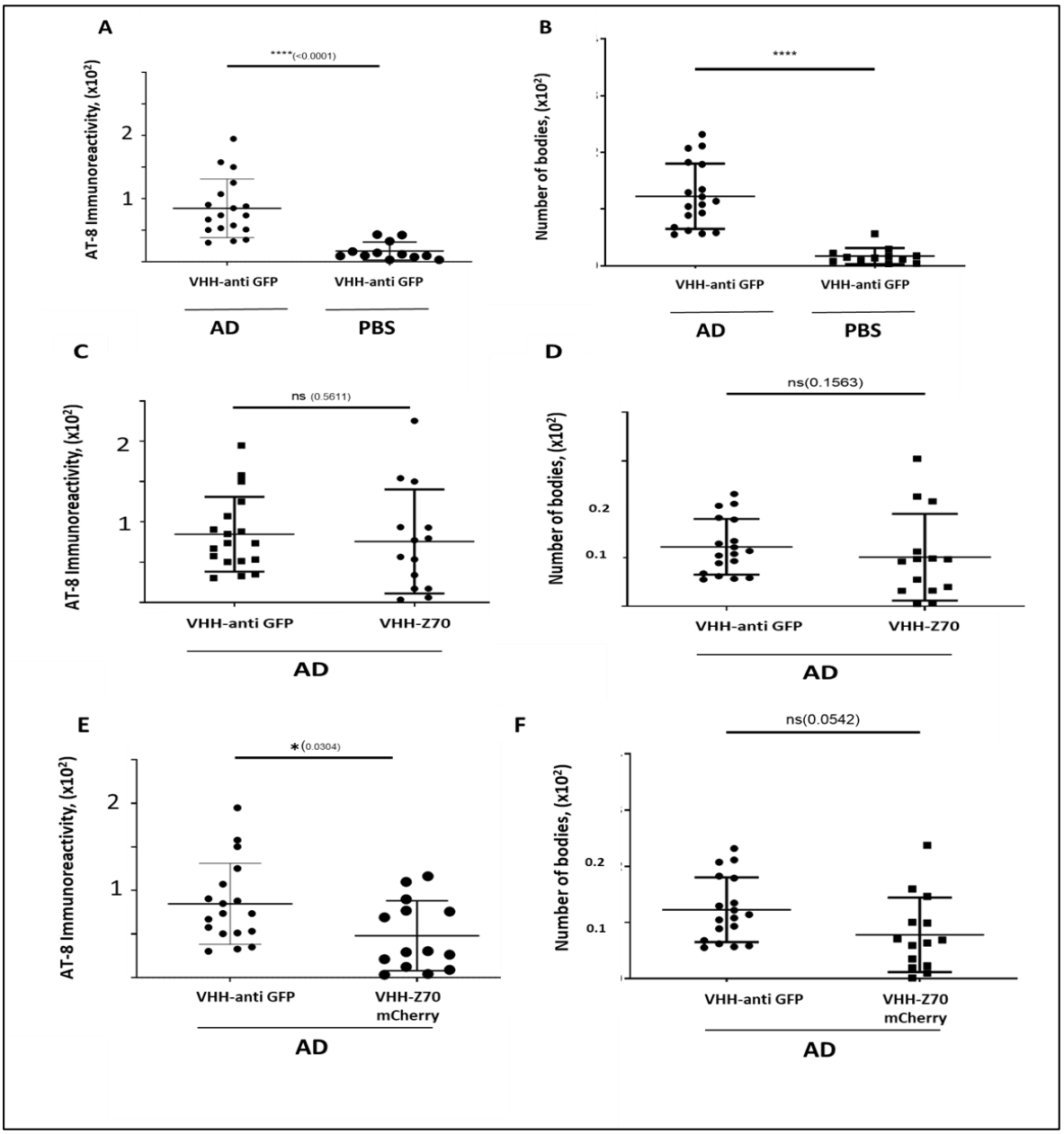

Figure 28 : Effect of VHH Z70 on seeding induced by h-AD brain in THY-tau30 Tg mouse model. The whole brain was processed for immunohistochemical analysis using AT8. Each data point corresponds to the quantification for one hemisphere. **A.** AT-8 immunoreactivity of the VHH anti-GFP on the group injected with h-AD (positive control group, n=9). No significant difference is observed compared to the VHH anti-GFP+PBS group (negative control group, n=6) (p value <0.0001). **B.** Number of bodies detected with AT-8 antibody in the VHH anti-GFP followed by h-AD compared to the PBS injection group (p value 0.0001). **C.** Effect of the VHH Z70 group on the group injected with h-AD (n=7) on AT-8 immunoreactivity, which shows of no difference to the VHH anti-GFP (p value 0.5611). **D.** The number of bodies identified with AT-8 immunostaining, for VHH Z70 + h AD group does not seem to be different compared to the positive control group (p value 0.1563). **E.** A significant effect on tau seeding of the VHH Z70 fused to mCherry group followed by h-AD injection (n=7), (p value 0.0304) is observed. **F.** Effect of the VHH Z70 fused to mCherry on the group injected with h-AD (n=7) on the number of detected bodies (P value 0.0542). Data are analyzed by Mann-Whitney U-test, non- parametric. * p value <0.05; error bars: (± S.D).

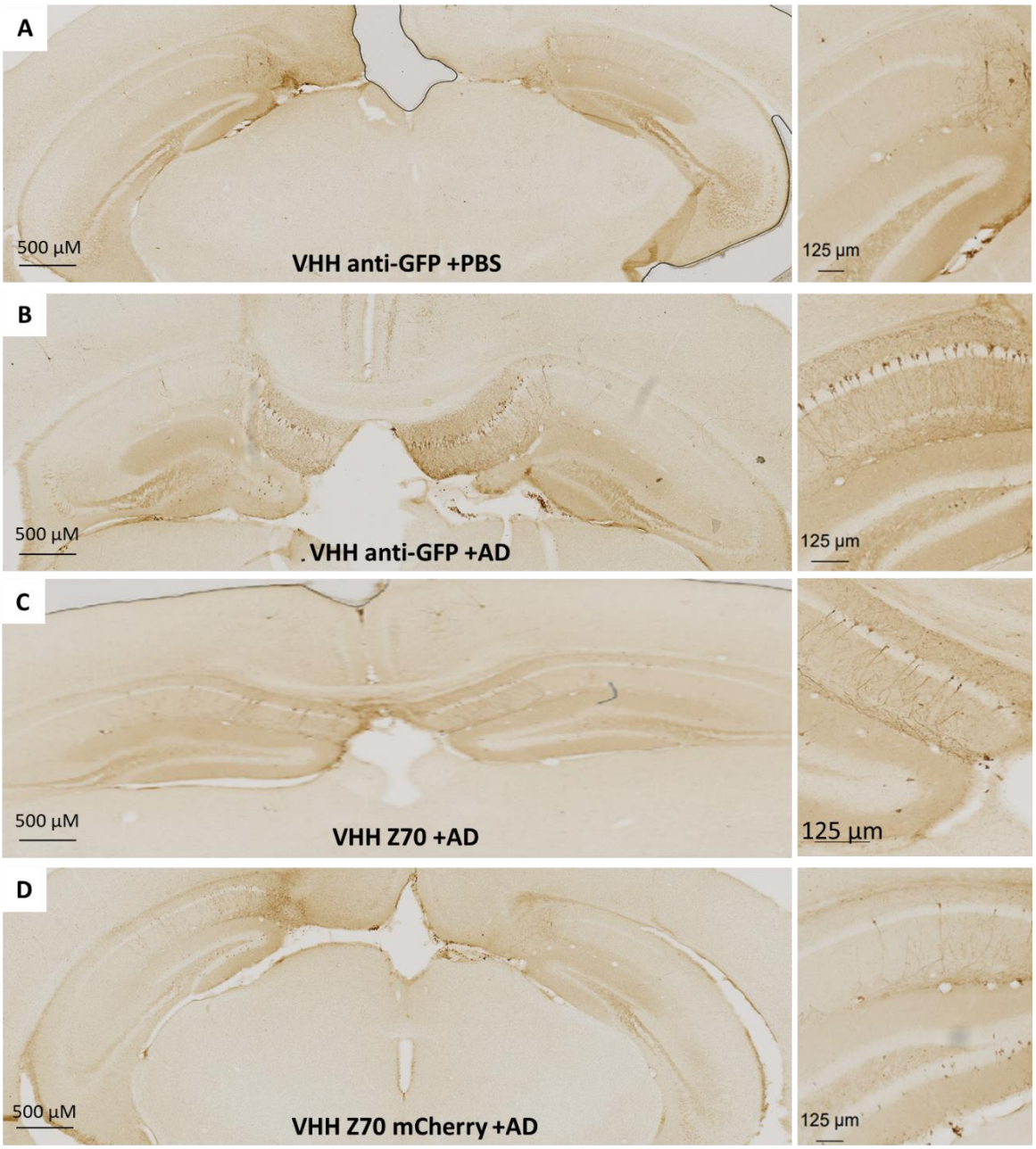

Figure 29 : VHH Z70 effect on human tau seeding induced by extracellular human pathological tau seeds. One month-old THY-tau30 mice were treated with bilateral injections of LVs **A-B:** encoding VHH-anti GFP or **C-D:** VHH Z70m fused or not to mCherry. Two weeks later mice received stereotaxic injection of PBS (A) or AD (B-D) brain lysate. Mice were sacrificed 4 weeks later and the whole brains were processed for immunohistochemical analysis using AT8. Sections from the hippocampus (injection site, AP: -2.46) are shown, while on the right are shown enlargements of these areas. Scale bars are as indicated in each figure.

2.1.2 Testing the ability of non-AD brain as negative control in *in vivo* experiments

In 2.3.1 part the induction of pathology in transgenic Tau30 mice by using AD brain as seed is presented. However, as a negative control of injection PBS was used instead of a non-AD control brain. The reason so far is the ability to have accessibility in such precious material as must be derived from a non-AD patient. Further, the control has to fulfill particular criteria like age (preferably between 45-50), no tangles or other protein aggregation found in histopathology examination and the possibility of having cortical region (as it is the part of the brain where the tauopathy is detected). Thus, it was

possible to have access in Lille Biobank to such samples and we received three non-AD brain parts, named here as N1/N2 and N3. The histopathological examination done by the neuropathologists upon reception of the donor brains, has shown that N1 and N2 have no tau or synuclein staining, while in N3 sample few tangles were detected. These outcomes were part of the selection criteria. The next step was to run a Western Blot and see if any pathology can be detected based on the pattern of tau protein migration, as was performed for the human AD brain (Figure 30).

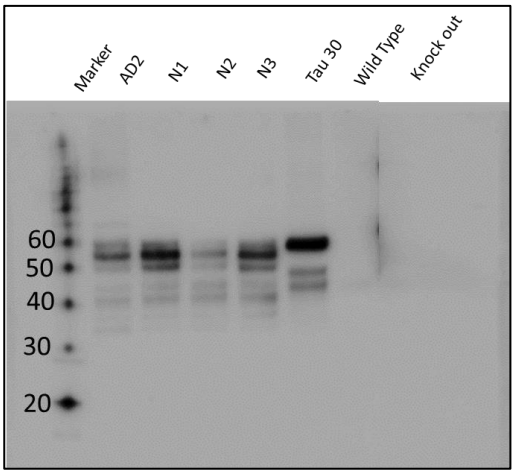

Figure 30 : Presentation of the tau pattern of three different human non- AD brains. Representing the profile of tau detected in post-mortem human non-AD brain lysate (labelled as N1, N2, N3). As positive control was used AD brain from the previous homogenization (AD2), which is one of the two used in animal experimentation. Further, as controls for tau recognition, are used mouse brain-lysate (wild-type, knock-out and Thy30tau). For detection, primary antibody for the N-Terminus of tau (home- made, 12-21aa); Brain lysate 10µg/well; Rabbit, 1:10.000, o/n at 4oC and secondary Anti-Rabbit IgG, Made in Goat, Peroxidase (Thermofischer, labeled ZE0614), 1hRT; ECL- Prime: 1 min; NuPage 4- 12%, Exposure time 30sec.

Besides the WB, which pattern seem to be difficult to differentiate from the AD2 brain, the three non-AD human brains (named as N1/2/3) were used for intracranial injection of Tg30tau mice to check the possibility of induction of the pathology. Thus, pooled N1/N2/N3 extracts were injected in one and a half month old transgenic mice (2mice/ condition), as well as the mixture of N1+N2 (mimicking the idea followed so far), AD2 (as positive control) and PBS (as current negative control). The mice were perfused one month after the injection. The protocol followed is as described above. Immunostaining with AT-8 antibody have been applied and representative images are shown in Figure 31. As shown in all cases also including the mix of two brain homogenates (indicated as N1 + N2) there was no pathology developed, which confirmed the validity of our control, and paved the way for more significant negative controls in future experiments.

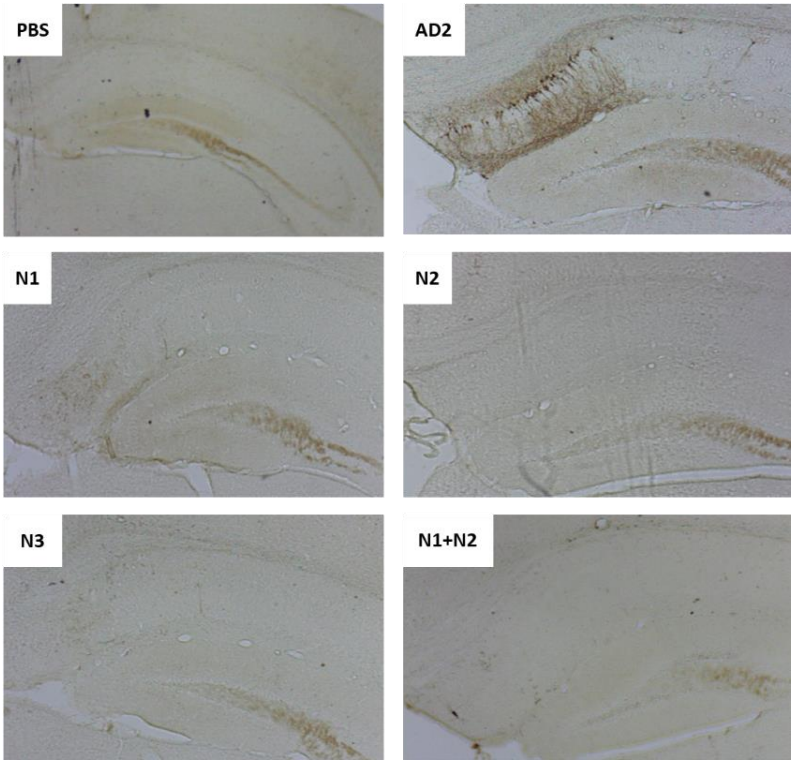

Figure 31 : Effect of different extracellular injected non-AD brain homogenates on inducing Tau seeding in THY-tau30 Tg mouse model. One month and a half-old THY-tau30 mice (2/condition) were treated with bilateral injections of PBS (negative control), h-AD brain as previously described (AD2, positive control), and the under investigation human non-AD brain lysates (named as N1, N2 and N3). The mixture of N1 and N2 was tried to mimic the conditions of the *in vivo* experiment followed in this project. Mice were sacrificed 4 weeks later and the whole brains were processed for immunohistochemical analysis using AT8. Sections from the hippocampus (injection site, AP: -2.46) are shown.

2.2 Use of the VHH Z70 to prevent propagation- Minibody Case

As described in chapter five, the prion-like propagation of tau involves transfer of abnormal tau seeds from a donor cell to recipient cell in which the recruitment of normal tau generates new tau seeds (Clavaguera et al., 2009, 2017). This hypothesis is supported by the latest findings of extracellular tau, which may be related to cell-to-cell transfer (Ahmed et al., 2014; Clavaguera et al., 2009; Clavaguera, Tolnay, & Goedert, 2017; Dujardin et al., 2014) and the main reason of the spread of the pathology. Thus, as already mentioned immunotherapy could be considered as a prospective approach in therapy. For this reason, another perspective of this project is to test the effect of VHH Z70 on extracellular tau. In order to do so, VHH Z70 was fused to an Fc domain derived from mouse IgG2a antibody and through a secretion signal sequence ((from IL-2, (Moutel et al., 2009)) allows the protein once expressed to be secreted in the extracellular space. This antibody engineer technology helps in keeping antibody specificity and gain in sensitivity. This methodology further confers the advantages of the IgG, concerning *in vivo* stability, and avidity through a possible dimerization in a redox free environment like the extracellular one (Figure 32), increasing the apparent binding affinity to the target antigen (Rath et al., 2015). Being

expressed intracellulary enables the correct conformation, proper folding, and posttranslational modifications of the protein (Jazayeri & Carroll, 2008).

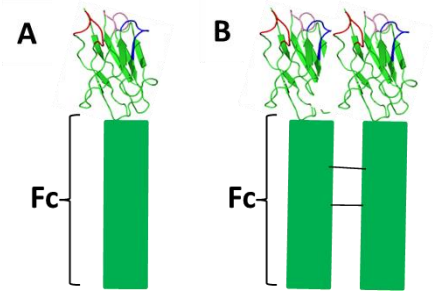

Figure 32 : Minibody structure. A. Molecularly engineered Minibody is formed with the fusion of VHH Z70 to Fc (fragment crystallizable) part of a mouse IgG2a**. B**. Minibody through disulfide bridges been created in Fc part may lead to a dimerization and mimicking thus a conventional IgG.

Thus, in the scheme of *in vivo* experiments in THY-tau30 Tg mice, there were two groups of eight mice that were injected with LVV-Minibody- VHH anti-GFP and LVV-Minibody- VHH Z70. In both cases the pathology was induced with h-AD brains injected at the same coordinates fifteen days later (described at 2.3.1 part). The procedure of animal handling and the AT-8 immunostaining is the same as described. Based on the quantification, there is no significant difference found between Minibody VHH anti-GFP and Minibody VHH Z70 for AT-8 immunoreactivity (p value 0.7277), as well as for the number of bodies quantified (p value 0.4726) as summarized in Figure 33.

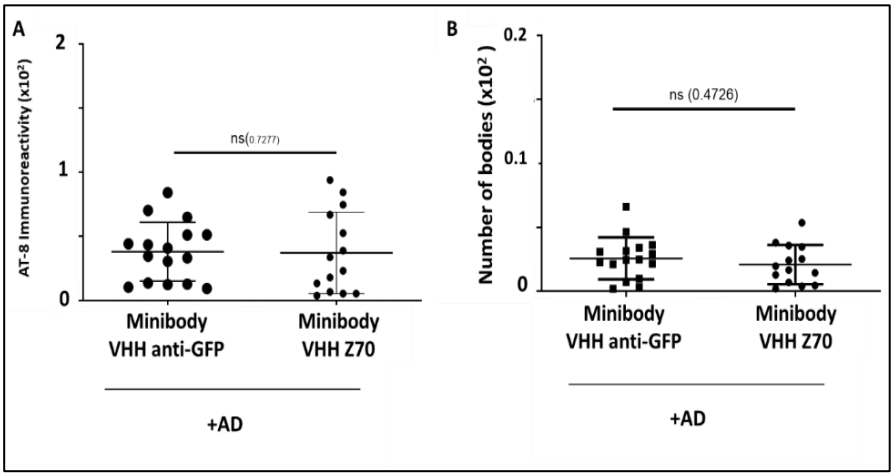

Figure 33 : Effect of the Minibody VHH Z70 on extracellular tau aggregates in THY-tau30 Tg mouse model. The whole brain was processed for immunohistochemical analysis using AT8. Each data point corresponds to the quantification for one hemisphere. **A.** It is shown the AT-8 immunoreactivity of the Minibody VHH Z70 group followed by h-AD injection (n=7), which had no significant difference compared to the Minibody VHH-anti GFP+AD (n=8) (P value of 0.7277). **B.** The number of bodies identified with AT-8 immunostaining, for Minibody VHH Z70 + AD group seem not to have any significant difference compared to Minibody VHH anti-GFP followed by h-AD injection. Data are analyzed by Mann-Whitney U-test. * p value <0.05; error bars: (± S.D).

The experiment was conducted by using a secondary anti-mouse IgG antibody, this may have been implicated to the signal detected and quantified with the AT-8 immunostaining applied. Thus, the experiment will be repeated by using AT-8

biotinylated and will be presented in the official presentation. However, the results may reflect to the fact that the seeds formed intracellularly by exogenous h-AD brain system were secreted in the extracellular environment during the experiment (total one month). In this case, the AT-8 immunostaining may still be mostly related to the injected exogenous seeds. Of interest in our case, is also the fact that Fc part is derived from an IgG2 antibody which may induce clearance by microglia.

2.3 Testing the long-term effect of VHH Z70 *in vivo*

In order to check the efficacy of the VHH Z70 expressed intracellularly in a long term time course in an *in vivo* mouse model of tauopathy, 3 month-old THY-tau22 Tg mice (Schindowski et al., 2006) were injected with LVV-VHH Z70 or LVV-VHH anti-GFP (as negative control). There were 4 mice for each condition. Pathology developed with age without further induction of pathology with extracellular seeds. The animals were perfused at the age of seven months. The procedure of animal handling and the AT-8 immunostaining is the same as described. This time the coordinates of injection were AP: -2.46, ML: -1 and DV: -1.8, leading to quantification of AT-8 immunoreactivity or number of bodies (normalized in both cases to the total surface) in the beginning of the CA1 part of the hippocampus. In both cases, a no-significant difference between groups was quantified (p value of 0.69). However, the low number of animals used in this preliminary experiment may be a reason for this poor outcome (Figure 34).

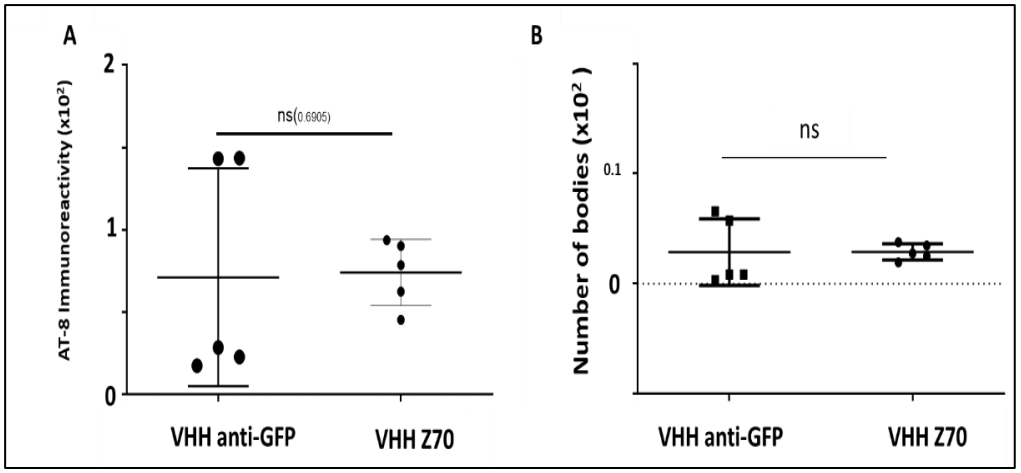

Figure 34 : Effect of the VHH Z70 on aged developed intracellular tau aggregates in THY-tau22 Tg mouse model. The whole brain was processed for immunohistochemical analysis using AT8. Each data point corresponds to the quantification for one hemisphere. **A.** It is shown the AT-8 immunoreactivity of the VHH Z70 group (n=3), which had no significant difference compared to the VHH-anti GFP (n=3) (P value of 0.6905). **B.** The number of bodies identified with AT-8 immunostaining, for VHH Z70 group seem not to have any significant difference compared to VHH anti-GFP (P value of 0.6905). Data are analyzed by Mann-Whitney U-test. * p value <0.05; error bars: (± S.D).

2.4 Generation of a monoclonal antibody

Given the difficulties in detecting VHH Z70, leading to the use of mCherry fusion protein, we have tried to generate a monoclonal antibody against VHH Z70. The peptide chosen for the immunization is part of the exposed at the surface of the VHH (a loop in Framework 2, based on the crystal structure of a VHH from our own humanized library, not published). The peptide was designed (Genecust) as a fusion with KLH for injection and with BSA for selection. Immunization was performed in Balb/c mice. During the first term, five injection of KLH-Peptide occurred in total in each mouse. Afterwards, serum was selected (labeled as S1) from these mice and the ability of detection of VHH Z70 was checked, taking as control the serum of each mouse before injection (labeled as So). The VHH Z70 loaded on the gel was either derived from cell lysates of HEK293 infected with LVV expressing VHH Z70 cell lysates (expected M.W around 15-20kDa), or purified bacteria-expressed VHH Z70 fused to a C-myc tag. The latest have an expected M.W. around 20-25kDa. The VHH- anti-GFP (labeled as LVV GFP) is used as negative control of VHH Z70 and was expressed the same way as VHH Z70 in HEK293T cell line (Figure 35).

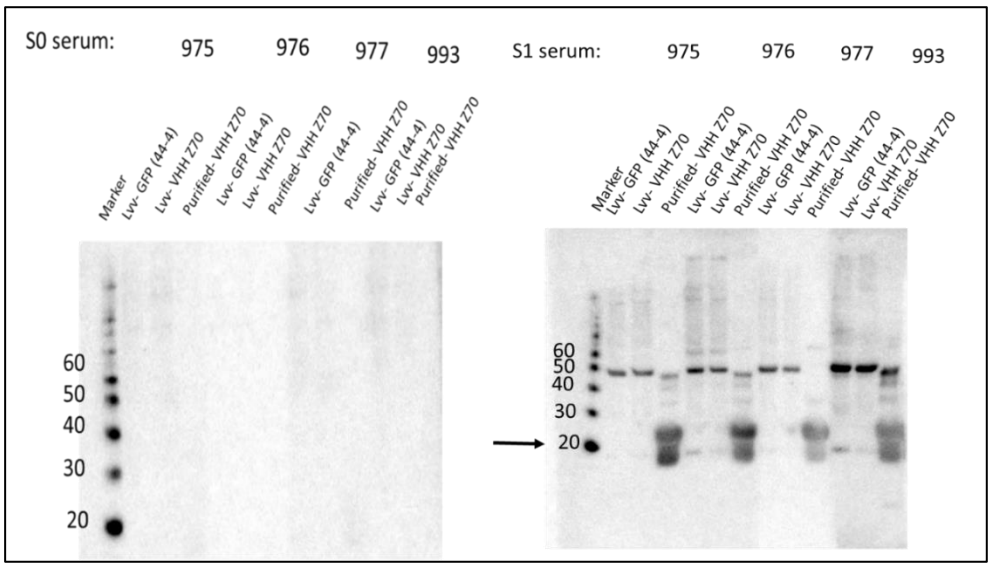

Figure 35 : Testing the ability of serum of immunized Balb/c mice, labeled as 975; 976; 977 and 993, to detect VHH Z70 and VHH anti-GFP. The VHHs are expressed after infection with LVV, HEK293 cells and lysates. The purified VHHZ70 refers to recombinant VHH expressed in bacteria. As 1ry Antibody is used the serum of the animals (1:1000), incubated o/n and as 2ry an Anti-Mouse (1:50000); ECL: 1min, NuPage 4- 12%. Exposure time 1 min 30sec. Serums were collected in two stages, before the immunization (S0, left image) and after the five immunizations (S1, right image).

Based on the outcome of the blot, we could see that there was no signal detection with the serum collected before immunization. This is not the case once the immunization occurred. The signal of detection of VHH anti-GFP and VHH Z70 as well as the purified VHH Z70 at expected M.W. (15kDa and 20kDa) was encouraging. The SO and S1 serums of the four animals were used in immunocytochemistry performed in HEK293T cells transfected with VHHZ70-mCherry (1000ng of plasmid/well) as well as in Immunocytochemistry (ICH) of brains injected with LVV expressing VHH Z70. The control in both cases was GFP. However, in ICH there was no signal at all, while for IHC it was detected but non-significant (data not shown).

Further, the mice labeled as 993 was selected and another immunization was performed. The serum was collected and labeled as S2. A Western Blot was performed as previously described, to see the detection ability of the VHH Z70, which seemed to have improved (Figure 36). Afterwards, the spleen of this mice was collected and hybridoma cell line were generated. The selection of the clones was tested with ELISA towards BSA-peptide, VHH Z70 and as control BSA. Although there was a number of subcloning taking place with a good detection ability of a few VHH Z70-specific clones, the signal originating from the last subclone was not encouraging.

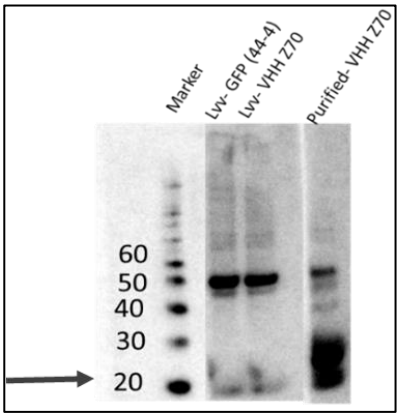

Figure 36 : Testing the ability of the serum of Balb/c mouse 993 (S2), to detect VHH Z70 and VHH anti-GFP. The VHHs which are expressed after infection with LVV, HEK293T cells and lysates. The purified VHHZ70 refers to bacteria cell line, which is further purified. As 1ry Antibody is used the serum of the animal (1:1000), incubated o/n and as 2ry and Anti-Mouse (1:50000); ECL: 1min, NuPage 4-12%. Exposure time 1 min 30sec.

Due to lock down this hybridoma cell line was discontinued. Thus, the same procedure for immunization and selection of the animal, which would undergo sacrifice for producing hybridoma cell line followed. This time, it was decided to boost the immunization by using three KLH-peptide injections, followed by injection with the full VHH Z70. However, because the injected VHH Z70 is protein expressed and purified from bacteria cells, a C-myc tag was present. Thus, while testing the ability of identification of candidate serums towards VHH Z70 in WBs and ELISA, it was observed that especially in ELISA there was a better recognition of the C-myc tagged VHH Z70. From that observation, we concluded that the antibody raised had a slight detection towards the tag. All the following selection of serum and later hybridoma were thus performed with c-myc-free VHH Z70. Here, the immunocytochemistry applied with three different supernatants of hybridoma cell lines tested for detection of HEK293 cells infected with LVV VHH Z70 are presented. As negative control, cells infected with LVV expressing VHH anti-GFP and incubated with serum of the selected animal are used, while cells infected with LVV VHH Z70 are used as positive control and incubated with the serum (Figure 37).

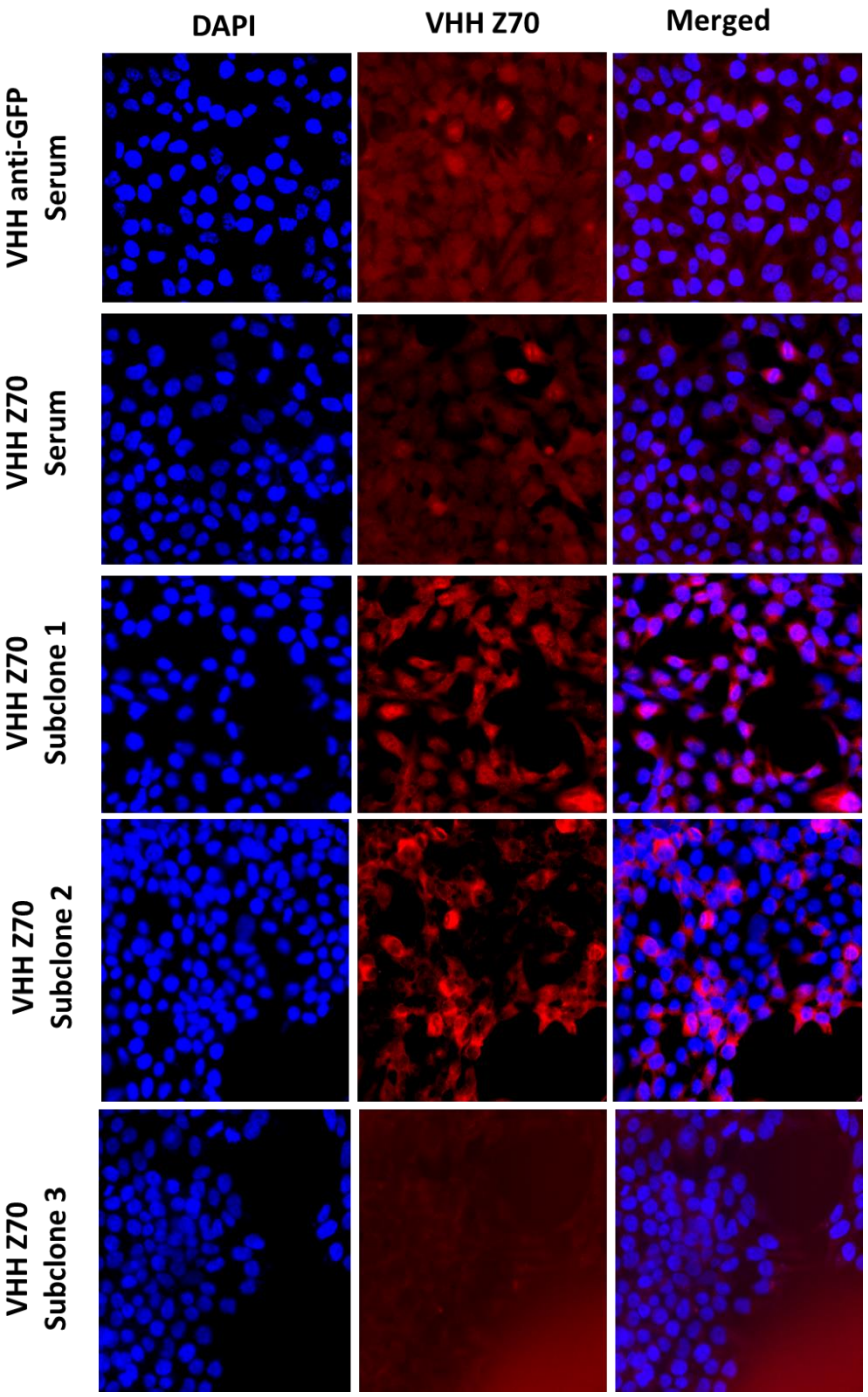

Figure 37 : Testing the detection of expressed VHH Z70 in HEK293 cell line with different subclones generated from hybridoma cell line. HEK293 cells infected with either LVV expressing VHH anti-GFP or VHH Z70 are incubated either with serum (control groups), or supernatant from subclones from hybridoma cell line developed (case of VHH Z70). Here presented three different subclones detecting the expressed VHH Z70. First line is shown DAPI staining, second is used anti mouse secondary antibody (Alexa 568) and the third one is merged. Scale bar of images is 50µm.

Even the results of two subclones showed in Figure 37 seemed to have a positive detection, among almost forty tested, further investigation did not show an optimistic outcome. Resulting in the fact of disability of generation of monoclonal antibodies towards VHH Z70.

2.4.1 Testing the monoclonal antibody generated for Minibody detection- Standardizing the conditions of expression of Minibody

As the Minibody- VHH Z70 shares the same sequence with the VHH Z70 itself we thought it would be good to test the generated potential VHH-Z70-specific monoclonal antibody towards the identification of the Minibody as well. To test the ability of the new generated monoclonal antibody, it was first important to standardize the production of the protein in the lab. For these reasons, we tried to express the Fc-Z70, which is fused in pFuse vector (Moutel et al., 2009), in different conditions and different methods of transfection in HEK293T cell line. First, the medium had to be standardized. Three conditions were followed A) DMEM Medium (Gibco, 1x (+4.5) g/L D glucose, L-glutamine (+) pyruvate), Harvest 3 days after transfection B) Hybridoma Medium, Harvest 3 days after transfection C) DMEM Medium to Hybridoma Medium, harvest 3 days after change of medium. In all these cases transfection occurred in 400.000 HEK293 cells, with 2μg pFUSE- Fc-VHH Z70 with Lipofectamine 2000 as transfection agent. After harvesting, part of the sample was concentrated (Amicon, Ultra 2ml centrifuged at 4500g at 4oC). Based on Western Blot outcome (data not shown), run in non-reductive conditions, the harvest of hybridoma medium switched from DMEM (condition C) seemed to have a better concentration of the protein. The non-reductive conditions were chosen with the possibility to detect both non-dimerized (expected M.W. 40kDa) and dimerized protein (expected M.W. 80kDa). Then to increase the level of expression, we tested a transfection protocol with a precipitating method by incubating cells with the DNA and mixture of HEPES and $CaCl_2$. The collected material was purified with A/G beads, but it was unsuccessful. Then, the ability of different serums of the Balb/C mice injected for the generation of monoclonal antibody to detect the expressed Fc-VHH Z70 was checked (Figure 38). The tested serums are not all due to low amount left. The outcome suggest that except of detection of the Minibody (non- and dimerized), probably the secondary Anti-Mouse antibody used is responsible for the detection of other non-specific signals.

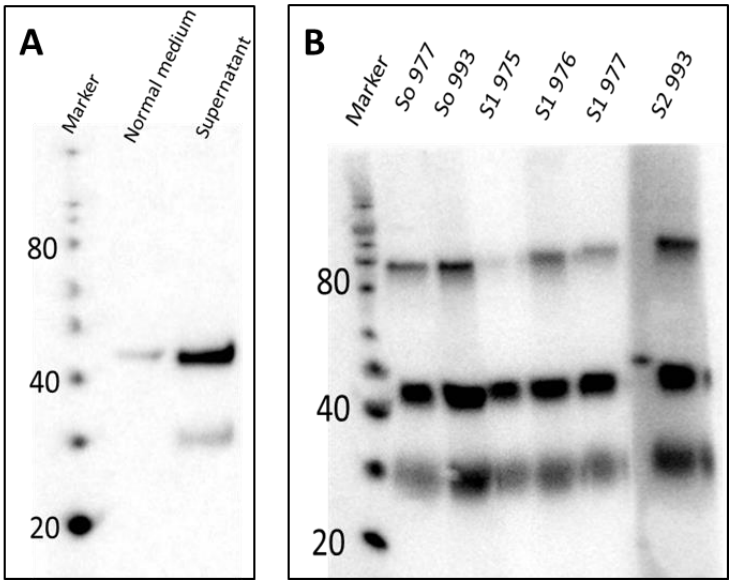

Figure 38 : Testing the ability of the serums of Balb/c mice, to detect Minibody-VHH Z70. A. Detection of the secreted Minibody VHH Z70 after transfection of pFuse–Fc-VHH Z70 in HEK293 cells and collection of the supernatant. Incubated directly with an Anti-Mouse-HRP (1:50000). **B.** Detection of Minibody-VHH Z70 by the serums of Balb/c mice (S0, S1 and S2). As 1ry Antibody is used the serum of the animal (1:1000), incubated o/n and as 2ry and Anti-Mouse (1:50000). Fc-VHH Z70 is expected at 40kDa, while probably to a dimerization of the protein we detect signal at 80kDa as well. The band lower than 40kDa may be related to unspecific binding or to a degradation of the protein. NuPage 4-12%. ECL: 1min; Exposure time 1min (A) and 30sec (B).

V. Discussion

Targeting tau protein has become a new strategy to alter disease progression in a number of tauopathies, including the most prevalent AD. Immunotherapy approach has been of great advantage in drug discovery lately and is proposed in tauopathies as well. In mouse models, both active and passive immunotherapies have been shown to be capable of reducing the formation of intracellular tau pathology as well as provided significant delays in the onset of the degenerative phenotype induced by tau (Asuni, Boutajangout, Quartermain, & Sigurdsson, 2007; Bi, Ittner, Ke, Götz, & Ittner, 2011; Boutajangout, Ingadottir, Davies, & Sigurdsson, 2011; Boutajangout, Quartermain, & Sigurdsson, 2010; Chai et al., 2011a; d'Abramo, Acker, Jimenez, & Davies, 2013; Sankaranarayanan et al., 2015; Theunis et al., 2017, 2013). The potential to reduce tau pathology has been also demonstrated by the use of antibody fragments like the single-chain variable fragments (scFvs) tested either in tau pathology mouse models (Gallardo et al., 2019; Goodwin et al., 2021; Ising et al., 2017; Vitale et al., 2020) or Drosophila models (S. Li et al., 2021). Tau is a complex therapeutic target for immunotherapies, as there are many factors that might influence the efficacy of individual antibody. In view of the therapeutic challenges that these diseases raise, we have used VHHs (or nanobodies, Variable domain of the Heavy- chain of the Heavy-chain-only-antibodies).

Choice of a tau epitope

Tau therapeutic antibodies target, neutralize and/or eliminate either monomeric (Boutajangout et al., 2010; Yanamandra et al., 2013), phospho-specific (Boutajangout et al., 2011; Chai et al., 2011b; Collin et al., 2014; D'Abramo et al., 2015; Sankaranarayanan et al., 2015; Umeda et al., 2015) or conformationally altered forms of tau protein (Castillo-Carranza et al., 2014; Walls et al., 2014), and thus prevent formation of neurofibrillary lesions. The identification of appropriate epitopes for the various tau species is essential to optimize tau immunotherapy strategy (Courade et al., 2018). This discrimination would be of great potential not only to the therapy of the disease but also to preventive strategy (Panza et al., 2016). The potential binding site of antibodies could be located either in the N-terminus (1-102aa), the central region (103-372aa) or the C-terminus (373-441aa). However, the majority of tau in the AD brain is truncated, at the N- and/or at the C-terminus, resulting in disability of antibodies targeting these regions to recognize all pathological tau species (H. H. Chen et al., 2018). Conversely, the antibodies targeting the central region might be better suited to recognize a broad range of tau species. In addition, the central region, which includes the MTBD, is responsible for the pathological tau-tau interaction. As described in Chapter 3, PHF6* and PHF6 peptides, positioned within MTBD, mediate self-assembly, driving amyloid formation *in vitro* (Carlomagno et al., 2021; Dimaio & Nogales, 2018) and promoting pathology *in vivo* (Martin Von Bergen et al., 2001) contrary to the full-length tau that is a highly soluble protein. Their atomic structures reveal the capacity of these segments

to form interdigitated steric-zipper interfaces that seed tau aggregation (X. Li, 2016; Sawaya et al., 2007). The structures of tau fibers isolated from patient brains affected by various tauopathies: AD (Fitzpatrick et al., 2017), corticobasal degeneration (Arakhamia et al., 2021) and Pick's disease (Falcon et al., 2018) were resolved by cryo-electron microscopy. The common core of these fibrillary structures is nevertheless composed of the subdomains R3 including the PHF6, R4 and a part of the C-terminal domain (V306-F378) that mainly form a β-sheet structure (Fitzpatrick et al., 2017). The subdomain of R3 is also part of the core the heparin-induced tau fibers, even differing from the structures of the human native fibers (Jiji et al., 2016). Emphasizing the importance of this region in fibril formation. This filament core has the ability to polymerize and form filaments *in vitro*, and act as seeds to recruit full-length tau to filaments, in the absence of an inducer such as heparin (Carlomagno et al., 2021). In addition, the accessibility of the PHF6*/ PHF6 peptides is proposed to be part of the mechanism leading to tau filament formation. The residues from these peptides are proposed to be shielded in a dynamic hairpin conformations in native tau, while exposed PHF6 residues would increase tau sensitivity to aggregation (Mirbaha et al., 2017). The conversion from an inert tau monomer to a seed-competent monomer would thus involve an increased accessibility of the PHF motifs (Mirbaha et al., 2017). Interestingly, several chaperons with tau anti-aggregation activities, such as Hsp70, Hsp60, DnaJA2 (Ciechanover & Kwon, 2017; Nachman et al., 2020a) and S100B (Moreira et al., 2021) bind to regions overlapping PHF6, and in a weaker manner PHF6*. Thus, one major mechanism of the anti-aggregation activities of these chaperons is likely the binding of tau in the PHF region (Mok et al., 2019). This leads to the consideration that binding PHF6 epitope of tau could be a potential anti-aggregation immunotherapeutic strategy. This is confirmed also by several studies, which tested in *in vivo* mouse models the effect of humanized and high- affinity IgG antibodies targeting the central domain (235-246aa) (Albert et al., 2019), or a particular sequence within MTBD (Roberts et al., 2020), resulting in inhibition of seeding. The PHF6 motif is predicted to be inaccessible in the structurally mature AD seeds, except at the extremity of the fibers. It is possible that binding by VHH Z70 at early stages of conformational conversion and misfolding could prevent nucleation. In addition, by binding at the extremity of the fibers, VHH Z70 could prevent elongation. It will remain to be demonstrated by in vitro assays of aggregation.

Assay of VHH Z70 in THY-tau30 Tg tau transgenic mouse model

As the majority of pathological tau remains intra-cellular in the cytosol, targeting intracellular tau with anti-tau antibodies may be more efficacious in preventing tauopathy progression and even in removing existing pathological forms of intracellular tau. With that point in mind, VHH E4-1 was optimized to improve its capacity to bind tau in the cellular environment. The optimization generated VHH Z70, which conserved the recognition epitope (PHF6), and showed improved affinity in tau binding than VHH E4-1. VHH Z70 has improved inhibitory effect towards tau aggregation *in vitro* and in a cellular model (P301S FRET Biosensor aggregation reporter cells) (Holmes et al., 2014), where in the latest recorded up to 42% seeding inhibition. The affinity may have played a role for the *in vitro* activity, as there is an improvement of K_D of 2.5 times (Rudnick et al., 2011). For the cellular assays, the better inhibition by VHH Z70 probably mostly arises due to the poor tau binding capacity of E4-1 in cells. Based on these encouraging results, VHH Z70 capacity of blocking tau seeding as possible immune-modulator was investigated in THY-tau30 Tg tau mouse model (Leroy et al., 2007). The induction of the endogenous aggregation process, which is low at one month old of this mouse model, occurred with exogenous human AD brain lysates injected fifteen days after at same site, promoting thus seeding (Clavaguera et al., 2009). As negative control for pathology induction was used PBS, but human brain lysates derived from non-AD patients as perfect negative control were also tested with success for future use. Animals injected with LVV expressing VHH Z70 had always a tendency to lower seeded pathology level compared to the negative control (VHH anti-GFP+AD), but this only became significant (p value of 0.0304) for the group of mice injected with LVV expressing VHH Z70 fused to mCherry. This shows that the mCherry could be implicated in the stability of the VHH and/or the effect of the bioavailability parameters of the VHH Z70 protein. Of note, the observation of this effect resulted in condition where the pathology induction and the VHH expression were not a perfect match is very encouraging. In future experiments, LVV will be replaced by AAV to allow a broader expression of the VHH, the LVV having a limited diffusion. This would ensure a better overlap of the brain regions where pathology developped and the VHH Z70 is expressed.

Choice of the intra *versus* extra cellular compartments

There are increasing evidence suggesting that tau pathology progressively spreads along connected neuronal pathways. It is also suggested that the spread of pathology occurs through extracellular pathological tau “seeds” that are transmitted from neuron to neuron (Ahmed et al., 2014; Clavaguera et al., 2009, 2017; Dujardin, Lécolle, et al., 2014). The precise molecular nature of the seeds is unknown (Lasagna-Reeves et al., 2012; Mirbaha et al., 2017; Takeda et al., 2015) but this

mechanism may provide several opportunities for therapeutic intervention, including passive immunization with appropriate monoclonal antibodies (Albert et al., 2019; Bright et al., 2015a; Chai et al., 2011b; Nobuhara et al., 2017; Rosenqvist et al., 2018; Yanamandra et al., 2013). One more time, crucial for the activity to these studies, is the epitope of binding of the antibodies towards tau protein (Courade et al., 2018) with a special focus on the strains involved in uptake (Nobuhara et al., 2017). Antibodies targeting the mid-domain of tau protein seemed to be the most efficient on blocking the uptake and subsequently aggregation, tested in *in vitro* systems (Nobuhara et al., 2017; Roberts et al., 2020) but also in *in vivo* models (Albert et al., 2019; Chai et al., 2011b; Funk et al., 2015; Roberts et al., 2020). Thus, we tested the ability of VHH Z70 to bind the extracellular tau and inhibit this way the propagation of it. For this reason, VHH Z70 was fused to an Fc domain of a mouse antibody, and the Minibody fragment produced can be expressed intracellularly and secreted extracellularly through a signal peptide (Moutel et al., 2009). This methodology confers the advantages of the IgG, concerning *in vivo* stability, and avidity through a possible dimerization in a redox free environment like the extracellular one, increasing the binding affinity to the target antigen (Rath et al., 2015). Theoretically, the intracellular expression would enable the correct conformation, proper folding and posttranslational modifications of the protein (Jazayeri & Carroll, 2008). However, the outcomes showed that the Minibody had no significant effect on seeding compared to the negative control (Minibody VHH anti-GFP), either because of lack of intracellular proper folding or because the evaluation period for the assay was not sufficient for the injected exogenous seeds to be secreted to the extracellular environment.

Functional variants of VHH 70

Based on the promising results of the *in vivo* experiments, optimizations of VHH Z70 activity in the intracellular compartment were performed. The determination of affinity of the eight functional variants that were selected from this screen with conserved epitope recognition suggested that the binding of the epitope can be improved by mutations located in both the complementary determining regions and the framework regions, reaching up to 6 times improvement in case of one variant (named as Mutant 1). Of note, the binding affinities recorded for the VHH- antigen interaction are high if we consider that the epitope do not consist of more than 5-8aa (De Genst et al., 2010; Dupré et al., 2019; Lutje Hulsik et al., 2013), which in case of intrinsically disordered proteins like tau represents a linear epitope. This ensures a limited interface with antibodies while retaining affinity and specificity, to compensate for the entropic cost of order gain due to the binding (Macraild, Richards, Anders, & Norton, 2016). Further, when tested in comparison with VHH Z70 for their ability to inhibit Tau

aggregation in fluorescence-based seeding reporter cells, three of these mutants (Mutant 1, Mutant 3 and Mutant 12) have an *in vitro* inhibitory activity reaching up to 51%.

To conclude, the results of this three-year project have established that VHH Z70 has potential in mitigating tau accumulation, at least in cellular and a mouse model of seeding. Suggesting thus that the tau specific VHHs are useful molecular tools to decipher the best target in Tau immunotherapies

VI. Perspectives

In future, as three Z70-derived variants matched VHH Z70 inhibitory effect on *in vitro* seeding, they are good candidates for further *in vivo* assays. Further, the analysis of the impact of VHH Z70 (or variants) on memory loss, in preventing either short or long-term memory, in *in vivo* models will be of importance. However, it would be of interest to test the affinity of VHH Z70 and the derived variants towards mutated forms of tau. The most widely used pre-clinical models of tauopathy (including the ones in the current study) employ cDNA-based transgenes overexpressing mostly P301S or P301L variants whereby the mutation lies in the middle of the R2 motif. This may lead or not, to weakened binding to tau of VHH Z70 and thus limit experimental outcomes.

Engineering of improved tau specific VHHs

Also, it is important to think about the steps that might be required to improve efficacy of the under investigation VHHs. Given the small size of these antibody fragments there are many functionalization's that might be considered, although they may be different for VHH Z70 and for VHH Z70 fused to Fc (Minibody). For Minibody, one might want to target microglial receptors and enhance the clearance of the complex Minibody-tau. For VHH Z70, one might want to add functional motifs that increase protein clearance, degradation (Gallardo et al., 2019; Goodwin et al., 2021) and/or stability (Dinkus J. et al., 2021). Furthermore, engineering of anti-tau intrabodies that are prone to target tau for either proteasome or lysosomal- degradation may result in a possible reduction of the intracellular tau protein levels leading to a greater neuroprotective effect relative to conventional immunotherapeutic approaches for tauopathies, even though it has to be tested if this degradation system is affecting also the VHH. VHH Z70 could also be combined with one other VHH, through genetic or (bio)-chemical engineering. The added VHH, connected by a suitable peptide linker, may be identical (monospecific polypeptide) or different (multispecific polypeptide). Thus, these polypeptides provide at least one other binding site (towards same form/ epitope of tau or not), increasing avidity and specificity for targeted tau. However, due to *in vivo* findings regarding the VHH Z70 fused to mCherry, a possible proposal would be to have two VHH Z70 linked with a suitable linker that would favor solubility and stability in cells, while keeping the binding epitope.

Delivery of the tau specific VHHs to the CNS

When referring to tau immunotherapies, efficacy is first confronted to the limiting step of the necessity for the antibodies to reach the brain. Indeed, only 0.1% of the peripheral levels of the antibodies are reported to be found in the CNS. Even

though, single domain antibodies are able to transmigrate across human cerebral endothelial cells *in vitro* and across the BBB *in vivo* with good efficiency but peripheral diffusion and lack of stability can be a limitation. Lately, gene therapy has gained a lot of importance, mainly using recombinant adeno-associated virus (rAAV) that are considered safer than LVs for medical applications. Thus, a deeper research of the potential use of rAAV vectors encoding tau-targeted antibodies or antibody fragments, like in the case of VHH Z70, could be used to more directly target tau within the mouse brain (Ising et al., 2017; Vitale et al., 2020), via one-time intracranial injection. However, peripheral administration provides obvious advantages compared to AAV gene therapy: a non-invasive route of injection, lack of surgery-related side effects, improved patient compliance and costs. Intramuscular injection (Vitale et al., 2020) could be an effective, feasible and safe delivery approach, which has as well broader diffusion from the point of injection compared to LVV.

VII. References

2. (2019). 乳鼠心肌提取 HHS Public Access. *Physiology & Behavior*, *176*(3), 139–148. https://doi.org/10.1016/j.physbeh.2017.03.040

Abulrob, A., Sprong, H., Van Bergen En Henegouwen, P., & Stanimirovic, D. (2005). The blood-brain barrier transmigrating single domain antibody: Mechanisms of transport and antigenic epitopes in human brain endothelial cells. *Journal of Neurochemistry*, *95*(4), 1201–1214. https://doi.org/10.1111/j.1471-4159.2005.03463.x

Abushouk, A. I., Elmaraezy, A., Aglan, A., Salama, R., Fouda, S., Fouda, R., & AlSafadi, A. M. (2017). Bapineuzumab for mild to moderate Alzheimer's disease: A meta-analysis of randomized controlled trials. *BMC Neurology*, *17*(1), 1–13. https://doi.org/10.1186/s12883-017-0850-1

Adli, M. (2018). The CRISPR tool kit for genome editing and beyond. *Nature Communications*, *9*(1). https://doi.org/10.1038/s41467-018-04252-2

Adolfsson, O., Pihlgren, M., Toni, N., Varisco, Y., Buccarello, A. L., Antoniello, K., Lohmann, S., Piorkowska, K., Gafner, V., Atwal, J. K., Maloney, J., Chen, M., Gogineni, A., Weimer, R. M., Mortensen, D. L., Friesenhahn, M., Ho, C., Paul, R., Pfeifer, A., … Watts, R. J. (2012). An effector-reduced anti-β-amyloid (Aβ) antibody with unique Aβ binding properties promotes neuroprotection and glial engulfment of Aβ. *Journal of Neuroscience*, *32*(28), 9677–9689. https://doi.org/10.1523/JNEUROSCI.4742-11.2012

Agarwal, M., Alam, M. R., Haider, M. K., Malik, M. Z., & Kim, D. K. (2021). Alzheimer's disease: An overview of major hypotheses and therapeutic options in nanotechnology. *Nanomaterials*, *11*(1), 1–18. https://doi.org/10.3390/nano11010059

Ahlijanian, M. K., Barrezueta, N. X., Williams, R. D., Jakowski, A., Kowsz, K. P., McCarthy, S., Coskran, T., Carlo, A., Seymour, P. A., Burkhardt, J. E., Nelson, R. B., & McNeish, J. D. (2000). Hyperphosphorylated tau and neurofilament and cytoskeletal disruptions in mice overexpressing human p25, an activator of cdk5. *Proceedings of the National Academy of Sciences of the United States of America*, *97*(6), 2910–2915. https://doi.org/10.1073/pnas.040577797

Ahmed, Z., Cooper, J., Murray, T. K., Garn, K., McNaughton, E., Clarke, H., Parhizkar, S., Ward, M. A., Cavallini, A., Jackson, S., Bose, S., Clavaguera, F., Tolnay, M., Lavenir, I., Goedert, M., Hutton, M. L., & O'Neill, M. J. (2014). A novel in vivo model of tau propagation with rapid and progressive neurofibrillary tangle pathology: The pattern of spread is determined by connectivity, not proximity. *Acta Neuropathologica*, *127*(5), 667–683. https://doi.org/10.1007/s00401-014-1254-6

Alafuzoff, I., Arzberger, T., Al-Sarraj, S., Bodi, I., Bogdanovic, N., Braak, H., Bugiani, O., Del-Tredici, K., Ferrer, I., Gelpi, E., Giaccone, G., Graeber, M. B., Ince, P., Kamphorst, W., King, A., Korkolopoulou, P., Kovács, G. G., Larionov, S., Meyronet, D., … Kretzschmar, H. (2008). Staging of neurofibrillary pathology in Alzheimer's disease: A study of the BrainNet Europe consortium. *Brain Pathology*, *18*(4), 484–496. https://doi.org/10.1111/j.1750-3639.2008.00147.x

Alam, R., Driver, D., Wu, S., Lozano, E., Key, S. L., Hole, J. T., Hayashi, M. L., & Lu, J. (2017). Preclinical Characterization of an Antibody [Ly3303560] Targeting Aggregated Tau. *Alzheimer's & Dementia*, *13*(7), P592–P593. https://doi.org/10.1016/j.jalz.2017.07.227

Albayram, O., Kondo, A., Mannix, R., Smith, C., Tsai, C. Y., Li, C., Herbert, M. K., Qiu, J., Monuteaux, M., Driver, J., Yan, S., Gormley, W., Puccio, A. M., Okonkwo, D. O., Lucke-Wold, B., Bailes, J., Meehan, W., Zeidel, M., Lu, K. P., & Zhou, X. Z. (2017). Cis P-tau is induced in clinical and preclinical brain injury and contributes to post-injury sequelae. *Nature Communications*, *8*(1). https://doi.org/10.1038/s41467-017-01068-4

Albayram, O., MacIver, B., Mathai, J., Verstegen, A., Baxley, S., Qiu, C., Bell, C., Caldarone, B. J., Zhou, X. Z., Lu, K. P., & Zeidel, M. (2019). Traumatic Brain Injury-related voiding dysfunction in mice is caused by damage to rostral pathways, altering inputs to the reflex pathways. *Scientific Reports*, *9*(1), 1–12. https://doi.org/10.1038/s41598-019-45234-8

Albert, M., Mairet-Coello, G., Danis, C., Lieger, S., Caillierez, R., Carrier, S., Skrobala, E., Landrieu, I., Michel, A., Schmitt, M., Citron, M., Downey, P., Courade, J. P., Buée, L., & Colin, M. (2019). Prevention of tau seeding and propagation by immunotherapy with a central tau epitope antibody. *Brain : A Journal of Neurology*, *142*(6), 1736–1750. https://doi.org/10.1093/brain/awz100

Alicea, J. V., Diamond, M. I., & Joachimiak, L. A. (2021). Tau strains shape disease. *Acta Neuropathologica*, *0123456789*.

https://doi.org/10.1007/s00401-021-02301-7

Allen, B., Ingram, E., Takao, M., Smith, M. J., Jakes, R., Virdee, K., Yoshida, H., Holzer, M., Craxton, M., Emson, P. C., Atzori, C., Migheli, A., Crowther, R. A., Ghetti, B., Spillantini, M. G., & Goedert, M. (2002). Abundant tau filaments and neurodegeneration in mice transgenic for human P301S tau. *Journal of Neuropathology and Experimental Neurology*, *22*(21), 9340–9351. isi:000175724500174

Alonso, A. D. C., Mederlyova, A., Novak, M., Grundke-Iqbal, I., & Iqbal, K. (2004). Promotion of hyperphosphorylation by frontotemporal dementia tau mutations. *Journal of Biological Chemistry*, *279*(33), 34873–34881. https://doi.org/10.1074/jbc.M405131200

Alt, M., Müller, R., & Kontermann, R. E. (1999). Novel tetravalent and bispecific IgG-like antibody molecules combining single-chain diabodies with the immunoglobulin γ1 Fc or CH3 region. *FEBS Letters*, *454*(1–2), 90–94. https://doi.org/10.1016/S0014-5793(99)00782-6

Andersson, C. R., Falsig, J., Stavenhagen, J. B., Christensen, S., Kartberg, F., Rosenqvist, N., Finsen, B., & Pedersen, J. T. (2019). Antibody-mediated clearance of tau in primary mouse microglial cultures requires Fcγ-receptor binding and functional lysosomes. *Scientific Reports*, *9*(1), 1–12. https://doi.org/10.1038/s41598-019-41105-4

Andorfer, C., Kress, Y., Espinoza, M., De Silva, R., Tucker, K. L., Barde, Y. A., Duff, K., & Davies, P. (2003). Hyperphosphorylation and aggregation of tau in mice expressing normal human tau isoforms. *Journal of Neurochemistry*, *86*(3), 582–590. https://doi.org/10.1046/j.1471-4159.2003.01879.x

Arai, T., Guo, J., Mcgeer, P. L., Thr, A., Ser, L., & Ser, L. (2005). Proteolysis of Non-phosphorylated and Phosphorylated Tau by Thrombin * that thrombin proteolyzed tau at multiple arginine and. *Journal of Biological Chemistry*, *280*(7), 5145–5153. https://doi.org/10.1074/jbc.M409234200

Arai, T., Ikeda, K., Akiyama, H., & Nonaka, T. (2004). *Identification of Amino-Terminally Cleaved Tau Fragments That Distinguish Progressive Supranuclear Palsy from Corticobasal Degeneration*. 72–79.

Arakhamia, T., Lee, C. E., Carlomagno, Y., Duong, D. M., Sean, R., Wang, K., Williams, D., Deture, M., Dickson, D. W., Cook, C. N., Seyfried, N. T., Petrucelli, L., & Anthony, W. P. (2021). *of tauopathy strains*. *180*(4), 633–644. https://doi.org/10.1016/j.cell.2020.01.027.Posttranslational

Arendt, T., Stieler, J. T., & Holzer, M. (2016). Tau and tauopathies. *Brain Research Bulletin*, *126*, 238–292. https://doi.org/10.1016/j.brainresbull.2016.08.018

Asai, H., Ikezu, S., Tsunoda, S., Medalla, M., Luebke, J., Haydar, T., Wolozin, B., Butovsky, O., Kügler, S., & Ikezu, T. (2015). Depletion of microglia and inhibition of exosome synthesis halt tau propagation. *Nature Neuroscience*, *18*(11), 1584–1593. https://doi.org/10.1038/nn.4132

Assaf-Casals, A., & Dbaibo, G. (2016). Meningococcal quadrivalent tetanus toxoid conjugate vaccine (MenACWY-TT, Nimenrix™): A review of its immunogenicity, safety, co-administration, and antibody persistence. *Human Vaccines and Immunotherapeutics*, *12*(7), 1825–1837. https://doi.org/10.1080/21645515.2016.1143157

Asuni, A. A., Boutajangout, A., Quartermain, D., & Sigurdsson, E. M. (2007). Immunotherapy targeting pathological tau conformers in a tangle mouse model reduces brain pathology with associated functional improvements. *Journal of Neuroscience*, *27*(34), 9115–9129. https://doi.org/10.1523/JNEUROSCI.2361-07.2007

Augustinack, J. C., Schneider, A., Mandelkow, E. M., & Hyman, B. T. (2002). Specific tau phosphorylation sites correlate with severity of neuronal cytopathology in Alzheimer's disease. *Acta Neuropathologica*, *103*(1), 26–35. https://doi.org/10.1007/s004010100423

Baddeley, T. C., McCaffrey, J., Storey, J. M. D., Cheung, J. K. S., Melis, V., Horsley, D., Harrington, C. R., & Wischik, C. M. (2015). Complex disposition of methylthioninium redox forms determines efficacy in tau aggregation inhibitor therapy for Alzheimer's disease. *Journal of Pharmacology and Experimental Therapeutics*, *352*(1), 110–118. https://doi.org/10.1124/jpet.114.219352

Banks, W. A., Kovac, A., Majerova, P., Bullock, K. M., Shi, M., & Zhang, J. (2016). Tau proteins cross the blood-brain barrier. *Journal of Alzheimer's Disease*, *55*(1), 411–419. https://doi.org/10.3233/JAD-160542

Banning, C., Votteler, J., Hoffmann, D., Koppensteiner, H., Warmer, M., Reimer, R., Kirchhoff, F., Schubert, U., Hauber, J., & Schindler, M. (2010). A flow cytometry-based FRET assay to identify and analyse protein-protein interactions in living

cells. *PLoS ONE*, *5*(2). https://doi.org/10.1371/journal.pone.0009344

Baral, T. N., Murad, Y., Nguyen, T. D., Iqbal, U., & Zhang, J. (2011). Isolation of functional single domain antibody by whole cell immunization: Implications for cancer treatment. *Journal of Immunological Methods*, *371*(1–2), 70–80. https://doi.org/10.1016/j.jim.2011.06.017

Barbier, P., Zejneli, O., Martinho, M., Lasorsa, A., Belle, V., Smet-Nocca, C., Tsvetkov, P. O., Devred, F., & Landrieu, I. (2019). Role of Tau as a Microtubule-Associated Protein: Structural and Functional Aspects. *Frontiers in Aging Neuroscience*, *11*(August), 1–14. https://doi.org/10.3389/fnagi.2019.00204

Barghorn, S., Zheng-Fischhofer, Q., Ackmann, M., Biernat, J., Von Bergen, M., Mandelkow, E. M., & Mandelkow, E. (2000). Structure, microtubule interactions, and paired helical filament aggregation by tau mutants of frontotemporal dementias. *Biochemistry*, *39*(38), 11714–11721. https://doi.org/10.1021/bi000850r

Bednarski, E., Lynch, G., & Ted, C. D. (1996). *Cytosolic Proteolysis of r by Cathepsin D in Hippocampus Following Suppression of Cathepsins B and L*. 1846–1855.

Bell, A., Wang, Z. J., Arbabi-Ghahroudi, M., Chang, T. A., Durocher, Y., Trojahn, U., Baardsnes, J., Jaramillo, M. L., Li, S., Baral, T. N., O'Connor-McCourt, M., MacKenzie, R., & Zhang, J. (2010). Differential tumor-targeting abilities of three single-domain antibody formats. *Cancer Letters*, *289*(1), 81–90. https://doi.org/10.1016/j.canlet.2009.08.003

Bi, M., Ittner, A., Ke, Y. D., Götz, J., & Ittner, L. M. (2011). Tau-targeted immunization impedes progression of neurofibrillary histopathology in aged P301L tau transgenic mice. *PLoS ONE*, *6*(12). https://doi.org/10.1371/journal.pone.0026860

Bibow, S., Mukrasch, M. D., Chinnathambi, S., Biernat, J., Griesinger, C., Mandelkow, E., & Zweckstetter, M. (2011). The dynamic structure of filamentous Tau. *Angewandte Chemie - International Edition*, *50*(48), 11520–11524. https://doi.org/10.1002/anie.201105493

Bibow, S., Ozenne, V., Biernat, J., Blackledge, M., Mandelkow, E., & Zweckstetter, M. (2011). Structural impact of proline-directed pseudophosphorylation at AT8, AT100, and PHF1 epitopes on 441-residue tau. *Journal of the American Chemical Society*, *133*(40), 15842–15845. https://doi.org/10.1021/ja205836j

Blennow, K., Zetterberg, H., Rinne, J. O., Salloway, S., Wei, J., Black, R., Grundman, M., & Liu, E. (2012). Effect of immunotherapy with bapineuzumab on cerebrospinal fluid biomarker levels in patients with mild to moderate alzheimer disease. *Archives of Neurology*, *69*(8), 1002–1010. https://doi.org/10.1001/archneurol.2012.90

Boche, D., Denham, N., Holmes, C., & Nicoll, J. A. R. (2010). Neuropathology after active Aβ42 immunotherapy: Implications for Alzheimer's disease pathogenesis. *Acta Neuropathologica*, *120*(3), 369–384. https://doi.org/10.1007/s00401-010-0719-5

Boche, D., Donald, J., Love, S., Harris, S., Neal, J. W., Holmes, C., & Nicoll, J. A. R. (2010). Reduction of aggregated Tau in neuronal processes but not in the cell bodies after Aβ42 immunisation in Alzheimer's disease. *Acta Neuropathologica*, *120*(1), 13–20. https://doi.org/10.1007/s00401-010-0705-y

Bourré, G., Cantrelle, F. X., Kamah, A., Chambraud, B., Landrieu, I., & Smet-Nocca, C. (2018). Direct crosstalk between O-GlcNAcylation and phosphorylation of tau protein investigated by NMR spectroscopy. *Frontiers in Endocrinology*, *9*(OCT), 1–13. https://doi.org/10.3389/fendo.2018.00595

Boutajangout, A., Ingadottir, J., Davies, P., & Sigurdsson, E. M. (2011). Passive immunization targeting pathological phospho-tau protein in a mouse model reduces functional decline and clears tau aggregates from the brain. *Journal of Neurochemistry*, *118*(4), 658–667. https://doi.org/10.1111/j.1471-4159.2011.07337.x

Boutajangout, A., Quartermain, D., & Sigurdsson, E. M. (2010). Immunotherapy targeting pathological tau prevents cognitive decline in a new tangle mouse model. *Journal of Neuroscience*, *30*(49), 16559–16566. https://doi.org/10.1523/JNEUROSCI.4363-10.2010

Boxer, A. L., Lang, A. E., Grossman, M., David, S., Miller, B. L., Schneider, L. S., Doody, R. S., Lees, A., Golbe, L. I., Williams, D. R., Lobach, I. V, Heuer, H. W., & Gozes, I. (2015). *NIH Public Access*. *13*(7), 676–685. https://doi.org/10.1016/S1474-4422(14)70088-2.Davunetide

Boxer, A. L., Qureshi, I., Ahlijanian, M., Grundman, M., Golbe, L. I., Litvan, I., Honig, L. S., Tuite, P., McFarland, N. R., O'Suilleabhain, P., Xie, T., Tirucherai, G. S., Bechtold, C., Bordelon, Y., Geldmacher, D. S., Grossman, M., Isaacson, S.,

Zesiewicz, T., Olsson, T., … Dam, T. (2019). Safety of the tau-directed monoclonal antibody BIIB092 in progressive supranuclear palsy: a randomised, placebo-controlled, multiple ascending dose phase 1b trial. *The Lancet Neurology*, *18*(6), 549–558. https://doi.org/10.1016/S1474-4422(19)30139-5

Braak, H., Alafuzoff, I., Arzberger, T., Kretzschmar, H., & Tredici, K. (2006). Staging of Alzheimer disease-associated neurofibrillary pathology using paraffin sections and immunocytochemistry. *Acta Neuropathologica*, *112*(4), 389–404. https://doi.org/10.1007/s00401-006-0127-z

Braak, H., & Del Tredici, K. (2013). Reply: The early pathological process in sporadic Alzheimer's disease. *Acta Neuropathologica*, *126*(4), 615–618. https://doi.org/10.1007/s00401-013-1170-1

Braak, H., Thal, D. R., Ghebremedhin, E., & Del Tredici, K. (2011). Stages of the pathologic process in alzheimer disease: Age categories from 1 to 100 years. *Journal of Neuropathology and Experimental Neurology*, *70*(11), 960–969. https://doi.org/10.1097/NEN.0b013e318232a379

Bramblett, G. T., Goedert, M., Jakes, R., Merrick, S. E., Trojanowski, J. Q., & Lee, V. M. Y. (1993). Abnormal tau phosphorylation at Ser396 in alzheimer's disease recapitulates development and contributes to reduced microtubule binding. *Neuron*, *10*(6), 1089–1099. https://doi.org/10.1016/0896-6273(93)90057-X

Bright, J., Hussain, S., Dang, V., Wright, S., Cooper, B., Byun, T., Ramos, C., Singh, A., Parry, G., Stagliano, N., & Griswold-Prenner, I. (2015a). Human secreted tau increases amyloid-beta production. *Neurobiology of Aging*, *36*(2), 693–709. https://doi.org/10.1016/j.neurobiolaging.2014.09.007

Bright, J., Hussain, S., Dang, V., Wright, S., Cooper, B., Byun, T., Ramos, C., Singh, A., Parry, G., Stagliano, N., & Griswold-Prenner, I. (2015b). Human secreted tau increases amyloid-beta production. *Neurobiology of Aging*, *36*(2), 693–709. https://doi.org/10.1016/j.neurobiolaging.2014.09.007

Bruhns, P., Iannascoli, B., England, P., Mancardi, D. A., Fernandez, N., Jorieux, S., & Daëron, M. (2009). Specificity and affinity of human Fcγ receptors and their polymorphic variants for human IgG subclasses. *Blood*, *113*(16), 3716–3725. https://doi.org/10.1182/blood-2008-09-179754

Brunden, K. R., Zhang, B., Carroll, J., Yao, Y., Potuzak, J. S., Hogan, A. M. L., Iba, M., James, M. J., Xie, S. X., Ballatore, C., Smith, A. B., Lee, V. M. Y., & Trojanowski, J. Q. (2010). Epothilone D improves microtubule density, axonal integrity, and cognition in a transgenic mouse model of tauopathy. *Journal of Neuroscience*, *30*(41), 13861–13866. https://doi.org/10.1523/JNEUROSCI.3059-10.2010

Buée-Scherrer, V., Condamines, O., Mourton-Gilles, C., Jakes, R., Goedert, M., Pau, B., & Delacourte, A. (1996). AD2, a phosphorylation-dependent monoclonal antibody directed against tau proteins found in Alzheimer's disease. *Molecular Brain Research*, *39*(1–2), 79–88. https://doi.org/10.1016/0169-328X(96)00003-4

Buée, L., Bussière, T., Buée-Scherrer, V., Delacourte, A., & Hof, P. R. (2000). Tau protein isoforms, phosphorylation and role in neurodegenerative disorders11These authors contributed equally to this work. *Brain Research Reviews*, *33*(1), 95–130. https://doi.org/10.1016/S0165-0173(00)00019-9

Butler, D. C., & Messer, A. (2011). Bifunctional anti-huntingtin proteasome-directed intrabodies mediate efficient degradation of mutant huntingtin exon 1 protein fragments. *PLoS ONE*, *6*(12). https://doi.org/10.1371/journal.pone.0029199

Butterfield, D. A., Abdul, H. M., Opii, W., Newman, S. F., Joshi, G., Ansari, M. A., & Sultana, R. (2006). Pin1 in Alzheimer's disease. *Journal of Neurochemistry*, *98*(6), 1697–1706. https://doi.org/10.1111/j.1471-4159.2006.03995.x

Caccamo, A., Magrì, A., Medina, D. X., Wisely, E. V., López-Aranda, M. F., Silva, A. J., & Oddo, S. (2013). mTOR regulates tau phosphorylation and degradation: Implications for Alzheimer's disease and other tauopathies. *Aging Cell*, *12*(3), 370–380. https://doi.org/10.1111/acel.12057

Cadwell, R. C., & Joyce, G. F. (1992). Randomization of genes by PCR mutagenesis. *Genome Research*, *2*(1), 28–33. https://doi.org/10.1101/gr.2.1.28

Cairns, N. J., Ph, D., Xie, X., Blazey, T. M., Holtzman, D. M., Aisen, P. S., Ghetti, B., Klunk, W. E., Mcdade, E., Rossor, M. N., Schofield, P. R., Ph, D., Sc, D., & Sperling, R. A. (2013). *Bateman et al Biomarker Changes AD 2012*. *367*(9), 795–804. https://doi.org/10.1056/NEJMoa1202753.Clinical

Carare, R. O., Hawkes, C. A., Jeffrey, M., Kalaria, R. N., & Weller, R. O. (2013). Review: Cerebral amyloid angiopathy, prion

angiopathy, CADASIL and the spectrum of protein elimination failure angiopathies (PEFA) in neurodegenerative disease with a focus on therapy. *Neuropathology and Applied Neurobiology*, *39*(6), 593–611. https://doi.org/10.1111/nan.12042

Carlomagno, Y., Manne, S., DeTure, M., Prudencio, M., Zhang, Y. J., Hanna Al-Shaikh, R., Dunmore, J. A., Daughrity, L. M., Song, Y., Castanedes-Casey, M., Lewis-Tuffin, L. J., Nicholson, K. A., Wszolek, Z. K., Dickson, D. W., Fitzpatrick, A. W. P., Petrucelli, L., & Cook, C. N. (2021). The AD tau core spontaneously self-assembles and recruits full-length tau to filaments. *Cell Reports*, *34*(11), 108843. https://doi.org/10.1016/j.celrep.2021.108843

Castillo-Carranza, D. L., Sengupta, U., Guerrero-Muñoz, M. J., Lasagna-Reeves, C. A., Gerson, J. E., Singh, G., Mark Estes, D., Barrett, A. D. T., Dineley, K. T., Jackson, G. R., & Kayed, R. (2014). Passive immunization with tau oligomer monoclonal antibody reverses tauopathy phenotypes without affecting hyperphosphorylated neurofibrillary tangles. *Journal of Neuroscience*, *34*(12), 4260–4272. https://doi.org/10.1523/JNEUROSCI.3192-13.2014

Chai, X., Dage, J. L., & Citron, M. (2012). Constitutive secretion of tau protein by an unconventional mechanism. *Neurobiology of Disease*, *48*(3), 356–366. https://doi.org/10.1016/j.nbd.2012.05.021

Chai, X., Wu, S., Murray, T. K., Kinley, R., Cella, C. V., Sims, H., Buckner, N., Hanmer, J., Davies, P., O'Neill, M. J., Hutton, M. L., & Citron, M. (2011a). Passive immunization with anti-tau antibodies in two transgenic models: Reduction of tau pathology and delay of disease progression. *Journal of Biological Chemistry*, *286*(39), 34457–34467. https://doi.org/10.1074/jbc.M111.229633

Chai, X., Wu, S., Murray, T. K., Kinley, R., Cella, C. V., Sims, H., Buckner, N., Hanmer, J., Davies, P., O'Neill, M. J., Hutton, M. L., & Citron, M. (2011b). Passive immunization with anti-tau antibodies in two transgenic models: Reduction of tau pathology and delay of disease progression. *Journal of Biological Chemistry*, *286*(39), 34457–34467. https://doi.org/10.1074/jbc.M111.229633

Challis, R. C., Ravindra Kumar, S., Chan, K. Y., Challis, C., Beadle, K., Jang, M. J., Kim, H. M., Rajendran, P. S., Tompkins, J. D., Shivkumar, K., Deverman, B. E., & Gradinaru, V. (2019). Systemic AAV vectors for widespread and targeted gene delivery in rodents. *Nature Protocols*, *14*(2), 379–414. https://doi.org/10.1038/s41596-018-0097-3

Chen, G., Huang, L. D., Jiang, Y. M., & Manji, H. K. (2000). The mood-stabilizing agent valproate inhibits the activity of glycogen synthase kinase-3. *Journal of Neurochemistry*, *72*(3), 1327–1330. https://doi.org/10.1046/j.1471-4159.2000.0721327.x

Chen, H. H., Liu, P., Auger, P., Lee, S. H., Adolfsson, O., Rey-Bellet, L., Lafrance-Vanasse, J., Friedman, B. A., Pihlgren, M., Muhs, A., Pfeifer, A., Ernst, J., Ayalon, G., Wildsmith, K. R., Beach, T. G., & van der Brug, M. P. (2018). Calpain-mediated tau fragmentation is altered in Alzheimer's disease progression. *Scientific Reports*, *8*(1), 1–15. https://doi.org/10.1038/s41598-018-35130-y

Cho, H., Choi, J. Y., Hwang, M. S., Kim, Y. J., Lee, H. M., Lee, H. S., Lee, J. H., Ryu, Y. H., Lee, M. S., & Lyoo, C. H. (2016). In vivo cortical spreading pattern of tau and amyloid in the Alzheimer disease spectrum. *Annals of Neurology*, *80*(2), 247–258. https://doi.org/10.1002/ana.24711

Chohan, M. O., Khatoon, S., Iqbal, I. G., & Iqbal, K. (2006). Involvement of I2PP2A in the abnormal hyperphosphorylation of tau and its reversal by Memantine. *FEBS Letters*, *580*(16), 3973–3979. https://doi.org/10.1016/j.febslet.2006.06.021

Ciechanover, A., & Kwon, Y. T. (2017). Protein quality control by molecular chaperones in neurodegeneration. *Frontiers in Neuroscience*, *11*(APR), 1–18. https://doi.org/10.3389/fnins.2017.00185

Clavaguera, F., Akatsu, H., Fraser, G., Crowther, R. A., Frank, S., Hench, J., Probst, A., Winkler, D. T., Reichwald, J., Staufenbiel, M., Ghetti, B., Goedert, M., & Tolnay, M. (2013). Brain homogenates from human tauopathies induce tau inclusions in mouse brain. *Proceedings of the National Academy of Sciences of the United States of America*, *110*(23), 9535–9540. https://doi.org/10.1073/pnas.1301175110

Clavaguera, F., Bolmont, T., Crowther, R. A., Abramowski, D., Frank, S., Probst, A., Fraser, G., Stalder, A. K., Beibel, M., Staufenbiel, M., Jucker, M., Goedert, M., & Tolnay, M. (2009). Transmission and spreading of tauopathy in transgenic mouse brain. *Nature Cell Biology*, *11*(7), 909–913. https://doi.org/10.1038/ncb1901

Clavaguera, F., Hench, J., Lavenir, I., Schweighauser, G., Frank, S., Goedert, M., & Tolnay, M. (2014). Peripheral administration of tau aggregates triggers intracerebral tauopathy in transgenic mice. *Acta Neuropathologica*, *127*(2), 299–301. https://doi.org/10.1007/s00401-013-1231-5

Clavaguera, F., Tolnay, M., & Goedert, M. (2017). The prion-like behavior of assembled tau in transgenic mice. *Cold Spring Harbor Perspectives in Medicine*, *7*(10), 1–13. https://doi.org/10.1101/cshperspect.a024372

Colin, M., Dujardin, S., Schraen-Maschke, S., Meno-Tetang, G., Duyckaerts, C., Courade, J. P., & Buée, L. (2020). From the prion-like propagation hypothesis to therapeutic strategies of anti-tau immunotherapy. *Acta Neuropathologica*, *139*(1), 3–25. https://doi.org/10.1007/s00401-019-02087-9

Collin, L., Bohrmann, B., Göpfert, U., Oroszlan-Szovik, K., Ozmen, L., & Grüninger, F. (2014). Neuronal uptake of tau/pS422 antibody and reduced progression of tau pathology in a mouse model of Alzheimer's disease. *Brain*, *137*(10), 2834–2846. https://doi.org/10.1093/brain/awu213

Congdon, E. E., Gu, J., Sait, H. B. R., & Sigurdsson, E. M. (2013). Antibody uptake into neurons occurs primarily via clathrin-dependent Fcα receptor endocytosis and is a prerequisite for acute tau protein clearance. *Journal of Biological Chemistry*, *288*(49), 35452–35465. https://doi.org/10.1074/jbc.M113.491001

Congdon, E. E., & Sigurdsson, E. M. (2018). Tau-targeting therapies for Alzheimer disease. *Nature Reviews Neurology*, *14*(7), 399–415. https://doi.org/10.1038/s41582-018-0013-z

Coppieters, K., Dreier, T., Silence, K., De Haard, H., Lauwereys, M., Casteels, P., Beirnaert, E., Jonckheere, H., Van De Wiele, C., Staelens, L., Hostens, J., Revets, H., Remaut, E., Elewaut, D., & Rottiers, P. (2006). Formatted anti-tumor necrosis factor α VHH proteins derived from camelids show superior potency and targeting to inflamed joints in a murine model of collagen-induced arthritis. *Arthritis and Rheumatism*, *54*(6), 1856–1866. https://doi.org/10.1002/art.21827

Corcoran, N. M., Martin, D., Hutter-Paier, B., Windisch, M., Nguyen, T., Nheu, L., Sundstrom, L. E., Costello, A. J., & Hovens, C. M. (2010). Sodium selenate specifically activates PP2A phosphatase, dephosphorylates tau and reverses memory deficits in an Alzheimer's disease model. *Journal of Clinical Neuroscience*, *17*(8), 1025–1033. https://doi.org/10.1016/j.jocn.2010.04.020

Corey, D. R. (2017). Nusinersen, an antisense oligonucleotide drug for spinal muscular atrophy. *Nature Neuroscience*, *20*(4), 497–499. https://doi.org/10.1038/nn.4508

Cortez-Retamozo, V., Backmann, N., Senter, P. D., Wernery, U., De Baetselier, P., Muyldermans, S., & Revets, H. (2004). Efficient Cancer Therapy with a Nanobody-Based Conjugate. *Cancer Research*, *64*(8), 2853–2857. https://doi.org/10.1158/0008-5472.CAN-03-3935

Couch, J. A., Yu, Y. J., Zhang, Y., Tarrant, J. M., Fuji, R. N., Meilandt, W. J., Solanoy, H., Tong, R. K., Hoyte, K., Luk, W., Lu, Y., Gadkar, K., Prabhu, S., Ordonia, B. A., Nguyen, Q., Lin, Y., Lin, Z., Balazs, M., Scearce-Levie, K., … Watts, R. J. (2013). Addressing safety liabilities of TfR bispecific antibodies that cross the blood-brain barrier. *Science Translational Medicine*, *5*(183). https://doi.org/10.1126/scitranslmed.3005338

Courade, J. P., Angers, R., Mairet-Coello, G., Pacico, N., Tyson, K., Lightwood, D., Munro, R., McMillan, D., Griffin, R., Baker, T., Starkie, D., Nan, R., Westwood, M., Mushikiwabo, M. L., Jung, S., Odede, G., Sweeney, B., Popplewell, A., Burgess, G., … Citron, M. (2018). Epitope determines efficacy of therapeutic anti-Tau antibodies in a functional assay with human Alzheimer Tau. *Acta Neuropathologica*, *136*(5), 729–745. https://doi.org/10.1007/s00401-018-1911-2

Crowther, R. A. (1991). Straight and paired helical filaments in Alzheimer disease have a common structural unit. *Proceedings of the National Academy of Sciences of the United States of America*, *88*(6), 2288–2292. https://doi.org/10.1073/pnas.88.6.2288

Cruz, J. C., Tseng, H. C., Goldman, J. A., Shih, H., & Tsai, L. H. (2003). Aberrant Cdk5 activation by p25 triggers pathological events leading to neurodegeneration and neurofibrillary tangles. *Neuron*, *40*(3), 471–483. https://doi.org/10.1016/S0896-6273(03)00627-5

Cummings, J., Lee, G., Ritter, A., & Zhong, K. (2018). Alzheimer's disease drug development pipeline: 2018. *Alzheimer's and Dementia: Translational Research and Clinical Interventions*, *4*(2018), 195–214. https://doi.org/10.1016/j.trci.2018.03.009

D'Abramo, C., Acker, C. M., Jimenez, H., & Davies, P. (2015). Passive immunization in JNPL3 transgenic mice using an array of phospho-tau specific antibodies. *PLoS ONE*, *10*(8), 1–12. https://doi.org/10.1371/journal.pone.0135774

d'Abramo, C., Acker, C. M., Jimenez, H. T., & Davies, P. (2013). Tau Passive Immunotherapy in Mutant P301L Mice: Antibody Affinity versus Specificity. *PLoS ONE*, *8*(4), 1–10. https://doi.org/10.1371/journal.pone.0062402

Dai, C. L., Chen, X., Kazim, S. F., Liu, F., Gong, C. X., Grundke-Iqbal, I., & Iqbal, K. (2015). Passive immunization targeting the N-terminal projection domain of tau decreases tau pathology and improves cognition in a transgenic mouse model of Alzheimer disease and tauopathies. *Journal of Neural Transmission*, *122*(4), 607–617. https://doi.org/10.1007/s00702-014-1315-y

Dai, C. L., Hu, W., Tung, Y. C., Liu, F., Gong, C. X., & Iqbal, K. (2018). Tau passive immunization blocks seeding and spread of Alzheimer hyperphosphorylated Tau-induced pathology in 3 × Tg-AD mice. *Alzheimer's Research and Therapy*, *10*(1), 1–14. https://doi.org/10.1186/s13195-018-0341-7

Dai, C. ling, Tung, Y. C., Liu, F., Gong, C. X., & Iqbal, K. (2017). Tau passive immunization inhibits not only tau but also Aβ pathology. *Alzheimer's Research and Therapy*, *9*(1), 1–16. https://doi.org/10.1186/s13195-016-0227-5

David, D. C., Layfield, R., Serpell, L., Narain, Y., Goedert, M., & Spillantini, M. G. (2002). *Proteasomal degradation of tau protein*. 176–185.

David, M., & Tayebi, M. (2014). Detection of protein aggregates in brain and cerebrospinal fluid derived from multiple sclerosis patients. *Frontiers in Neurology*, *5*(NOV), 1–7. https://doi.org/10.3389/fneur.2014.00251

De Calignon, A., Polydoro, M., Suárez-Calvet, M., William, C., Adamowicz, D. H., Kopeikina, K. J., Pitstick, R., Sahara, N., Ashe, K. H., Carlson, G. A., Spires-Jones, T. L., & Hyman, B. T. (2012). Propagation of Tau Pathology in a Model of Early Alzheimer's Disease. *Neuron*, *73*(4), 685–697. https://doi.org/10.1016/j.neuron.2011.11.033

de Marco, A. (2011). Biotechnological applications of recombinant single-domain antibody fragments. *Microbial Cell Factories*, *10*(1), 44. https://doi.org/10.1186/1475-2859-10-44

De Saint-Vis, B., Vincent, J., Vandenabeele, S., Vanbervliet, B., Pin, J. J., Aït-Yahia, S., Patel, S., Mattei, M. G., Banchereau, J., Zurawski, S., Davoust, J., Caux, C., & Lebecque, S. (1998). A novel lysosome-associated membrane glycoprotein, DC-LAMP, induced upon DC maturation, is transiently expressed in MHC class II compartment. *Immunity*, *9*(3), 325–336. https://doi.org/10.1016/S1074-7613(00)80615-9

de Vos, J., Devoogdt, N., Lahoutte, T., Muyldermans, S., & Muyldermans, S. (2013). Camelid single-domain antibody-fragment engineering for (pre)clinical in vivo molecular imaging applications: Adjusting the bullet to its target. *Expert Opinion on Biological Therapy*, *13*(8), 1149–1160. https://doi.org/10.1517/14712598.2013.800478

Decanniere, K., Muyldermans, S., & Wyns, L. (2000). Canonical antigen-binding loop structures in immunoglobulins: More structures, more canonical classes? *Journal of Molecular Biology*, *300*(1), 83–91. https://doi.org/10.1006/jmbi.2000.3839

Deger, J. M., Gerson, J. E., & Kayed, R. (2015). *The interrelationship of proteasome impairment and oligomeric intermediates in neurodegeneration*. *April*, 715–724. https://doi.org/10.1111/acel.12359

Del Ser, T., Steinwachs, K. C., Gertz, H. J., Andrés, M. V., Gómez-Carrillo, B., Medina, M., Vericat, J. A., Redondo, P., Fleet, D., & León, T. (2013). Treatment of Alzheimer's disease with the GSK-3 inhibitor tideglusib: A pilot study. *Journal of Alzheimer's Disease*, *33*(1), 205–215. https://doi.org/10.3233/JAD-2012-120805

Desmyter, A., Spinelli, S., Payan, F., Lauwereys, M., Wyns, L., Muyldermans, S., & Cambillau, C. (2002). Three camelid VHH domains in complex with porcine pancreatic α-amylase: Inhibition and versatility of binding topology. *Journal of Biological Chemistry*, *277*(26), 23645–23650. https://doi.org/10.1074/jbc.M202327200

Despres, C., Byrne, C., Qi, H., Cantrelle, F. X., Huvent, I., Chambraud, B., Baulieu, E. E., Jacquot, Y., Landrieu, I., Lippens, G., & Smet-Nocca, C. (2017). Identification of the Tau phosphorylation pattern that drives its aggregation. *Proceedings of the National Academy of Sciences of the United States of America*, *114*(34), 9080–9085. https://doi.org/10.1073/pnas.1708448114

Devos, S. L., Miller, R. L., Schoch, K. M., Holmes, B. B., Kebodeaux, S., Wegener, A. J., Chen, G., Shen, T., Tran, H., Nichols, B., Zanardi, T. A., Kordasiewicz, H. B., Swayze, E. E., Bennett, C. F., Marc, I., & Miller, T. M. (2018). *HHS Public Access*. *9*(374), 1–30. https://doi.org/10.1126/scitranslmed.aag0481.Tau

Dimaio, F., & Nogales, E. (2018). *Near-atomic model of microtubule-tau interactions*. *1246*(June), 1242–1246.

Dujardin, S., Bégard, S., Caillierez, R., Lachaud, C., Delattre, L., Carrier, S., Loyens, A., Galas, M. C., Bousset, L., Melki, R., Aurégan, G., Hantraye, P., Brouillet, E., Buée, L., & Colin, M. (2014). Ectosomes: A new mechanism for non-exosomal secretion of Tau protein. *PLoS ONE*, *9*(6), 28–31. https://doi.org/10.1371/journal.pone.0100760

Dujardin, S., Lécolle, K., Caillierez, R., Bégard, S., Zommer, N., Lachaud, C., Carrier, S., Dufour, N., Aurégan, G., Winderickx, J., Hantraye, P., Déglon, N., Colin, M., & Buée, L. (2014). Neuron-to-neuron wild-type Tau protein transfer through a trans-synaptic mechanism: Relevance to sporadic tauopathies. *Acta Neuropathologica Communications*, *2*(1), 1–14. https://doi.org/10.1186/2051-5960-2-14

Dumoulin, M., Last, A. M., Desmyter, A., Decanniere, K., Canet, D., Larsson, G., Spencer, A., Archer, D. B., Sasse, J., Muyldermans, S., Wyns, L., Redfield, C., Matagne, A., Robinson, C. V., & Dobson, C. M. (2003). A camelid antibody fragment inhibits the formation of amyloid fibrils by human lysozyme. *Nature*, *424*(6950), 783–788. https://doi.org/10.1038/nature01870

Dupré, E., Danis, C., Arrial, A., Hanoulle, X., Homa, M., Cantrelle, F.-X., Merzougui, H., Colin, M., Rain, J.-C., Buée, L., & Landrieu, I. (2019). Single Domain Antibody Fragments as New Tools for the Detection of Neuronal Tau Protein in Cells and in Mice Studies. *ACS Chemical Neuroscience*. https://doi.org/10.1021/acschemneuro.9b00217

Duran, J. M., Anjard, C., Stefan, C., Loomis, W. F., & Malhotra, V. (2010). Unconventional secretion of Acb1 is mediated by autophagosomes. *Journal of Cell Biology*, *188*(4), 527–536. https://doi.org/10.1083/jcb.200911154

Duyckaerts, C., & Hauw, J. J. (1997). Prevalence, incidence and duration of Braak's stages in the general population: Can we know? [2]. *Neurobiology of Aging*, *18*(4), 362–369. https://doi.org/10.1016/S0197-4580(97)00047-X

Eidenmüller, J., Fath, T., Maas, T., Pool, M., Sontag, E., & Brandt, R. (2001). Phosphorylation-mimicking glutamate clusters in the proline-rich region are sufficient to simulate the functional deficiencies of hyperphosphorylated tau protein. *Biochemical Journal*, *357*(3), 759–767. https://doi.org/10.1042/0264-6021:3570759

Eliezer, D., Barré, P., Kobaslija, M., Chan, D., Li, X., & Heend, L. (2005). Residual structure in the repeat domain of tau: Echoes of microtubule binding and paired helical filament formation. *Biochemistry*, *44*(3), 1026–1036. https://doi.org/10.1021/bi048953n

Emmerson, C. D., Vlist Els J., van der, Braam, M. R., Vanlandschoot, P., Merchiers, P., Haard Hans J. W., de J. W., Verrips, C. T., Henegouwen Paul M. P., van B. en, & Dolk, E. (2011). Enhancement of polymeric immunoglobulin receptor transcytosis by biparatopic vhh. *PLoS ONE*, *6*(10), 1–10. https://doi.org/10.1371/journal.pone.0026299

Evans, L. D., Wassmer, T., Fraser, G., Smith, J., Perkinton, M., Billinton, A., & Livesey, F. J. (2018). Extracellular Monomeric and Aggregated Tau Efficiently Enter Human Neurons through Overlapping but Distinct Pathways. *Cell Reports*, *22*(13), 3612–3624. https://doi.org/10.1016/j.celrep.2018.03.021

Falcon, B., Cavallini, A., Angers, R., Glover, S., Murray, T. K., Barnham, L., Jackson, S., O'Neill, M. J., Isaacs, A. M., Hutton, M. L., Szekeres, P. G., Goedert, M., & Bose, S. (2015). Conformation determines the seeding potencies of native and recombinant Tau aggregates. *Journal of Biological Chemistry*, *290*(2), 1049–1065. https://doi.org/10.1074/jbc.M114.589309

Falcon, B., Zhang, W., Murzin, A. G., Murshudov, G., Garringer, H. J., Vidal, R., Crowther, R. A., Ghetti, B., Scheres, S. H. W., & Goedert, M. (2018). Structures of filaments from Pick's disease reveal a novel tau protein fold. *Nature*, *561*(7721), 137–140. https://doi.org/10.1038/s41586-018-0454-y

Ferrer, I., Rovira, M. B., Luisa, M., Guerra, S., Rey, M. J., & Costa-jussá, F. (n.d.). *Neuropathology and Pathogenesis of Encephalitis Following Amyloid-β Immunization in AD-Ferrer et al 11*. 11–20.

Finkel, R. S., Mercuri, E., Darras, B. T., Connolly, A. M., Kuntz, N. L., Kirschner, J., Chiriboga, C. A., Saito, K., Servais, L., Tizzano, E., Topaloglu, H., Tulinius, M., Montes, J., Glanzman, A. M., Bishop, K., Zhong, Z. J., Gheuens, S., Bennett, C. F., Schneider, E., … De Vivo, D. C. (2017). Nusinersen versus Sham Control in Infantile-Onset Spinal Muscular Atrophy. *New England Journal of Medicine*, *377*(18), 1723–1732. https://doi.org/10.1056/nejmoa1702752

Fitzpatrick, A. W. P., Falcon, B., He, S., Murzin, A. G., Murshudov, G., Garringer, H. J., Crowther, R. A., Ghetti, B., Goedert, M., & Scheres, S. H. W. (2017). Cryo-EM structures of tau filaments from Alzheimer's disease. *Nature*, *547*(7662), 185–190. https://doi.org/10.1038/nature23002

Friedhoff, P., Von Bergen, M., Mandelkow, E. M., Davies, P., & Mandelkow, E. (1998). A nucleated assembly mechanism of Alzheimer paired helical filaments. *Proceedings of the National Academy of Sciences of the United States of America*, *95*(26), 15712–15717. https://doi.org/10.1073/pnas.95.26.15712

Frost, B., Jacks, R. L., & Diamond, M. I. (2009). Propagation of Tau misfolding from the outside to the inside of a cell.

Journal of Biological Chemistry, *284*(19), 12845–12852. https://doi.org/10.1074/jbc.M808759200

Fuhrman, Jed; McCallum, Kirk; Davis, A. (1992). ²»ÉøÍ¸ÐÔµÄ © 19 9 2 Nature Publishing Group. *Nature*, *359*, 710–713.

Funk, K. E., Mirbaha, H., Jiang, H., Holtzman, D. M., & Diamond, M. I. (2015). Distinct therapeutic mechanisms of Tau antibodies: Promoting microglial clearance versus blocking neuronal uptake. *Journal of Biological Chemistry*, *290*(35), 21652–21662. https://doi.org/10.1074/jbc.M115.657924

Gallardo, G., Wong, C. H., Ricardez, S. M., Mann, C. N., Lin, K. H., Leyns, C. E. G., Jiang, H., & Holtzman, D. M. (2019). Targeting tauopathy with engineered tau-degrading intrabodies. *Molecular Neurodegeneration*, *14*(1), 1–12. https://doi.org/10.1186/s13024-019-0340-6

Gamblin, T. C., Chen, F., Zambrano, A., Abraha, A., Lagalwar, S., Guillozet, A. L., Lu, M., Fu, Y., Garcia-sierra, F., Lapointe, N., Miller, R., Berry, R. W., Binder, L. I., & Cryns, V. L. (2003). *Caspase cleavage of tau : Linking amyloid and neurofibrillary tangles in Alzheimer ' s disease*.

Gauthier, S., Feldman, H. H., Schneider, L. S., Wilcock, G. K., Giovanni, B., Hardlund, J. H., Moebius, H. J., Bentham, P., Kook, K. A., Wischik, D. J., Schelter, B. O., Davis, C. S., Staff, R. T., Bracoud, L., Shamsi, K., John, M. D., Harrington, C. R., & Wischik, C. M. (2016). *27863809*. *388*(10062), 2873–2884. https://doi.org/10.1016/S0140-6736(16)31275-2.Efficacy

Goedert, M., Jakes, R., & Vanmechelen, E. (1995). Monoclonal antibody AT8 recognises tau protein phosphorylated at both serine 202 and threonine 205. *Neuroscience Letters*, *189*(3), 167–170. https://doi.org/10.1016/0304-3940(95)11484-E

Goedert, Michel, Eisenberg, D. S., & Crowther, R. A. (2017). Propagation of Tau Aggregates and Neurodegeneration. *Annual Review of Neuroscience*, *40*, 189–210. https://doi.org/10.1146/annurev-neuro-072116-031153

Gong, C. X., Liu, F., & Iqbal, K. (2016). O-GlcNAcylation: A regulator of tau pathology and neurodegeneration. *Alzheimer's and Dementia*, *12*(10), 1078–1089. https://doi.org/10.1016/j.jalz.2016.02.011

Goodwin, M. S., Sinyavskaya, O., Burg, F., O'Neal, V., Ceballos-Diaz, C., Cruz, P. E., Lewis, J., Giasson, B. I., Davies, P., Golde, T. E., & Levites, Y. (2021). Anti-tau scFvs Targeted to the Cytoplasm or Secretory Pathway Variably Modify Pathology and Neurodegenerative Phenotypes. *Molecular Therapy*, *29*(2), 859–872. https://doi.org/10.1016/j.ymthe.2020.10.007

Gozes, I., Bassan, M., Zamostiano, R., Pinhasov, A., Davidson, A., Giladi, E., Perl, O., Glazner, G. W., & Brenneman, D. E. (1999). A novel signaling molecule for neuropeptide action: Activity-dependent neuroprotective protein. *Annals of the New York Academy of Sciences*, *897*, 125–135. https://doi.org/10.1111/j.1749-6632.1999.tb07884.x

Griswold-prenner, I. I., San, S., Us, C. A., Nancy, E., Francisco, S. S., Dang, V., Francisco, S. S., Us, C. A., Hussain, S., Francisco, S., Us, C. A., Bright, J. M., Us, C. A., Mullins, N., Llp, S., Remillard, J. E., & Sloper, J. G. (2015). *(12) United States Patent*. *2*(12).

Grundke-Iqbal, I., Iqbal, K., & Tung, Y. C. (1986). Abnormal phosphorylation of the microtubule-associated protein τ (tau) in Alzheimer cytoskeletal pathology. *Proceedings of the National Academy of Sciences of the United States of America*, *83*(13), 44913–44917. https://doi.org/10.1097/00002093-198701030-00020

Gu, J., Congdon, E. E., & Sigurdsson, E. M. (2013). Two novel Tau antibodies targeting the 396/404 region are primarily taken up by neurons and reduce Tau protein pathology. *Journal of Biological Chemistry*, *288*(46), 33081–33095. https://doi.org/10.1074/jbc.M113.494922

Guo, T., Noble, W., & Hanger, D. P. (2017). Roles of tau protein in health and disease. *Acta Neuropathologica*, *133*(5), 665–704. https://doi.org/10.1007/s00401-017-1707-9

Habicht, G., Haupt, C., Friedrich, R. P., Hortschansky, P., Sachse, C., Meinhardt, J., Wieligmann, K., Gellermann, G. P., Brodhun, M., Götz, J., Halbhuber, K. J., Röcken, C., Horn, U., & Fändrich, M. (2007). Directed selection of a conformational antibody domain that prevents mature amyloid fibril formation by stabilizing Aβ protofibrils. *Proceedings of the National Academy of Sciences of the United States of America*, *104*(49), 19232–19237. https://doi.org/10.1073/pnas.0703793104

Hamdane, M., Dourlen, P., Bretteville, A., Sambo, A. V., Ferreira, S., Ando, K., Kerdraon, O., Bégard, S., Geay, L., Lippens, G., Sergeant, N., Delacourte, A., Maurage, C. A., Galas, M. C., & Buée, L. (2006). Pin1 allows for differential Tau

dephosphorylation in neuronal cells. *Molecular and Cellular Neuroscience*, *32*(1–2), 155–160. https://doi.org/10.1016/j.mcn.2006.03.006

Hamdane, M., Sambo, A. V., Delobel, P., Bégard, S., Violleau, A., Delacourte, A., Bertrand, P., Benavides, J., & Buée, L. (2003). Mitotic-like Tau Phosphorylation by p25-Cdk5 Kinase Complex. *Journal of Biological Chemistry*, *278*(36), 34026–34034. https://doi.org/10.1074/jbc.M302872200

Hanger, D. P., Anderton, B. H., & Noble, W. (2009). Tau phosphorylation: the therapeutic challenge for neurodegenerative disease. *Trends in Molecular Medicine*, *15*(3), 112–119. https://doi.org/10.1016/j.molmed.2009.01.003

Hanger, D. P., Hughes, K., Woodgett, J. R., Brion, J. P., & Anderton, B. H. (1992). Glycogen synthase kinase-3 induces Alzheimer's disease-like phosphorylation of tau: Generation of paired helical filament epitopes and neuronal localisation of the kinase. *Neuroscience Letters*, *147*(1), 58–62. https://doi.org/10.1016/0304-3940(92)90774-2

Hansen, A. K., Brooks, D. J., & Borghammer, P. (2018). MAO-B Inhibitors Do Not Block In Vivo Flortaucipir([18F]-AV-1451) Binding. *Molecular Imaging and Biology*, *20*(3), 356–360. https://doi.org/10.1007/s11307-017-1143-1

Hardy, J. A., & Higgins, G. A. (1992). Alzheimer's Disease: The Amyloid Alzheimer's disease. *Science*, *256*, 184–185.

Harley, C. W., Walling, S. G., Yuan, Q., & Martin, G. M. (2021). The 'a, b, c's of pretangle tau and their relation to aging and the risk of Alzheimer's Disease. *Seminars in Cell and Developmental Biology*, *December 2020*. https://doi.org/10.1016/j.semcdb.2020.12.010

Harmsen, M. M., & De Haard, H. J. (2007). Properties, production, and applications of camelid single-domain antibody fragments. *Applied Microbiology and Biotechnology*, *77*(1), 13–22. https://doi.org/10.1007/s00253-007-1142-2

Harmsen, M. M., Fijten, H. P. D., Engel, B., Dekker, A., & Eblé, P. L. (2009). Passive immunization with llama single-domain antibody fragments reduces foot-and-mouth disease transmission between pigs. *Vaccine*, *27*(13), 1904–1911. https://doi.org/10.1016/j.vaccine.2009.01.110

Hart, G. W. (1997). Dynamic O-linked glycosylation of nuclear and cytoskeletal proteins. *Annual Review of Biochemistry*, *66*, 315–335. https://doi.org/10.1146/annurev.biochem.66.1.315

Hasegawa, M., Smith, M. J., & Goedert, M. (1998). Tau proteins with FTDP-17 mutations have a reduced ability to promote microtubule assembly. *FEBS Letters*, *437*(3), 207–210. https://doi.org/10.1016/S0014-5793(98)01217-4

Heiss, W. D., Szelies, B., Kessler, J., & Herholz, K. (1991). Abnormalities of energy metabolism in Alzheimer's disease studied with PET. *Annals of the New York Academy of Sciences*, *640*(070), 65–71. https://doi.org/10.1111/j.1749-6632.1991.tb00192.x

Hochgräfe, K., Sydow, A., Matenia, D., Cadinu, D., Könen, S., Petrova, O., Pickhardt, M., Goll, P., Morellini, F., Mandelkow, E., & Mandelkow, E. M. (2015). Preventive methylene blue treatment preserves cognition in mice expressing full-length pro-aggregant human Tau. *Acta Neuropathologica Communications*, *3*, 25. https://doi.org/10.1186/s40478-015-0204-4

Hoffman, A., Taleski, G., & Sontag, E. (2017). The protein serine/threonine phosphatases PP2A, PP1 and calcineurin: A triple threat in the regulation of the neuronal cytoskeleton. *Molecular and Cellular Neuroscience*, *84*, 119–131. https://doi.org/10.1016/j.mcn.2017.01.005

Holmes, B. B., DeVos, S. L., Kfoury, N., Li, M., Jacks, R., Yanamandra, K., Ouidja, M. O., Brodsky, F. M., Marasa, J., Bagchi, D. P., Kotzbauer, P. T., Miller, T. M., Papy-Garcia, D., & Diamond, M. I. (2013). Heparan sulfate proteoglycans mediate internalization and propagation of specific proteopathic seeds. *Proceedings of the National Academy of Sciences of the United States of America*, *110*(33). https://doi.org/10.1073/pnas.1301440110

Holmes, B. B., & Diamond, M. I. (2017). Cellular models for the study of prions. *Cold Spring Harbor Perspectives in Medicine*, *7*(2), 1–10. https://doi.org/10.1101/cshperspect.a024026

Holmes, B. B., Furman, J. L., Mahan, T. E., Yamasaki, T. R., Mirbaha, H., Eades, W. C., Belaygorod, L., Cairns, N. J., Holtzman, D. M., & Diamond, M. I. (2014). Proteopathic tau seeding predicts tauopathy in vivo. *Proceedings of the National Academy of Sciences of the United States of America*, *111*(41), E4376–E4385. https://doi.org/10.1073/pnas.1411649111

Horowitz, P. M., Patterson, K. R., Guillozet-bongaarts, A. L., Reynolds, M. R., Carroll, C. A., Weintraub, S. T., Bennett, D. A.,

Cryns, V. L., Berry, R. W., & Binder, L. I. (2004). *Early N-Terminal Changes and Caspase-6 Cleavage of Tau in Alzheimer ' s Disease*. *24*(36), 7895–7902. https://doi.org/10.1523/JNEUROSCI.1988-04.2004

Hussack, G., Hirama, T., Ding, W., MacKenzie, R., & Tanha, J. (2011). Engineered single-domain antibodies with high protease resistance and thermal stability. *PLoS ONE*, *6*(11). https://doi.org/10.1371/journal.pone.0028218

Hyman, B. T. (1997). The neuropathological diagnosis of Alzheimer's disease: Clinical- pathological studies. *Neurobiology of Aging*, *18*(4 SUPPL.). https://doi.org/10.1016/S0197-4580(97)00066-3

Iba, M., Guo, J. L., McBride, J. D., Zhang, B., Trojanowski, J. Q., & Lee, V. M. Y. (2013). Synthetic tau fibrils mediate transmission of neurofibrillary tangles in a transgenic mouse model of alzheimer's-like tauopathy. *Journal of Neuroscience*, *33*(3), 1024–1037. https://doi.org/10.1523/JNEUROSCI.2642-12.2013

Iqbal, K., Liu, F., & Gong, C. X. (2016). Tau and neurodegenerative disease: The story so far. *Nature Reviews Neurology*, *12*(1), 15–27. https://doi.org/10.1038/nrneurol.2015.225

Ising, C., Gallardo, G., Leyns, C. E. G., Wong, C. H., Jiang, H., Stewart, F., Koscal, L. J., Roh, J., Robinson, G. O., Serrano, J. R., & Holtzman, D. M. (2017). Correction: AAV-mediated expression of anti-tau scFvs decreases tau accumulation in a mouse model of tauopathy [The Journal of Experimental Medicine, 214, 5 (2017) (1227-1238)] DOI:10.1084/jem.20162125. *Journal of Experimental Medicine*, *214*(7), 2163. https://doi.org/10.1084/jem.2016212505192017c

Ittner, A., Bertz, J., Suh, L. S., Stevens, C. H., Götz, J., & Ittner, L. M. (2015). Tau-targeting passive immunization modulates aspects of pathology in tau transgenic mice. *Journal of Neurochemistry*, *132*(1), 135–145. https://doi.org/10.1111/jnc.12821

Jackson, S. J., Kerridge, C., Cooper, J., Cavallini, A., Falcon, B., Cella, C. V., Landi, A., Szekeres, P. G., Murray, T. K., Ahmed, Z., Goedert, M., Hutton, M., O'Neill, M. J., & Bose, S. (2016). Short fibrils constitute the major species of seed-competent tau in the brains of mice transgenic for human p301s tau. *Journal of Neuroscience*, *36*(3), 762–772. https://doi.org/10.1523/JNEUROSCI.3542-15.2016

Jadhav, S., Avila, J., Schöll, M., Kovacs, G. G., Kövari, E., Skrabana, R., Evans, L. D., Kontsekova, E., Malawska, B., de Silva, R., Buee, L., & Zilka, N. (2019a). A walk through tau therapeutic strategies. *Acta Neuropathologica Communications*, *7*(1), 22. https://doi.org/10.1186/s40478-019-0664-z

Jadhav, S., Avila, J., Schöll, M., Kovacs, G. G., Kövari, E., Skrabana, R., Evans, L. D., Kontsekova, E., Malawska, B., de Silva, R., Buee, L., & Zilka, N. (2019b). A walk through tau therapeutic strategies. *Acta Neuropathologica Communications*, *7*(1), 22. https://doi.org/10.1186/s40478-019-0664-z

Jeganathan, S., Hascher, A., Chinnathambi, S., Biernat, J., Mandelkow, E. M., & Mandelkow, E. (2008). Proline-directed pseudo-phosphorylation at AT8 and PHF1 epitopes induces a compaction of the paperclip folding of tau and generates a pathological (MC-1) conformation. *Journal of Biological Chemistry*, *283*(46), 32066–32076. https://doi.org/10.1074/jbc.M805300200

Jeklin, A. (2016). *済無No Title No Title No Title*. *July*, 1–23.

Jellinger, K. A. (2000). Clinical validity of Braak staging in the oldest-old. *Acta Neuropathologica*, *99*(5), 583–584. https://doi.org/10.1007/s004010051164

Jiang, J., & Jiang, H. (2015). Efficacy and adverse effects of memantine treatment for Alzheimer's disease from randomized controlled trials. *Neurological Sciences*, *36*(9), 1633–1641. https://doi.org/10.1007/s10072-015-2221-2

Jicha, G. A., Bowser, R., Kazam, I. G., & Davies, P. (1997). Alz-50 and MC-1, a new monoclonal antibody raised to paired helical filaments, recognize conformational epitopes on recombinant tau. *Journal of Neuroscience Research*, *48*(2), 128–132. https://doi.org/10.1002/(SICI)1097-4547(19970415)48:2<128::AID-JNR5>3.0.CO;2-E

Jiji, A. C., Shine, A., & Vijayan, V. (2016). Direct Observation of Aggregation-Induced Backbone Conformational Changes in Tau Peptides. *Angewandte Chemie - International Edition*, *55*(38), 11562–11566. https://doi.org/10.1002/anie.201606544

Johnson, G. V. W., & Stoothoff, W. H. (2004). Tau phosphorylation in neuronal cell function and dysfunction. *Journal of Cell Science*, *117*(Pt 24), 5721–5729. https://doi.org/10.1242/jcs.01558

Joie, R. La, Visani, A. V, Baker, S. L., Brown, J. A., Cha, J., Chaudhary, K., Edwards, L., Iaccarino, L., Janabi, M., Lesman-segev, O., Miller, Z., Perry, D. C., Neil, J. P. O., Pham, J., Rojas, J. C., Rosen, H. J., Seeley, W. W., Tsai, R. M., Miller, B. L., … Rabinovici, G. D. (2020). *HHS Public Access*. *12*(524), 1–25. https://doi.org/10.1126/scitranslmed.aau5732.Prospective

Jouanne, M., Rault, S., & Voisin-Chiret, A. S. (2017). Tau protein aggregation in Alzheimer's disease: An attractive target for the development of novel therapeutic agents. *European Journal of Medicinal Chemistry*, *139*(October), 153–167. https://doi.org/10.1016/j.ejmech.2017.07.070

Karch, C. M., Jeng, A. T., & Goate, A. M. (2012). Extracellular tau levels are influenced by variability in tau that is associated with tauopathies. *Journal of Biological Chemistry*, *287*(51), 42751–42762. https://doi.org/10.1074/jbc.M112.380642

Kargbo, R. B. (2019). Treatment of Alzheimer's by PROTAC-Tau Protein Degradation [Editorial]. *ACS Medicinal Chemistry Letters*, *10*, 699–700. https://doi.org/10.1021/acsmedchemlett.9b00083

Karlawish, J., Jack, C. R., Rocca, W. A., Snyder, H. M., & Carrillo, M. C. (2017). Alzheimer's disease: The next frontier—Special Report 2017. *Alzheimer's and Dementia*, *13*(4), 374–380. https://doi.org/10.1016/j.jalz.2017.02.006

Katsinelos, T., Tuck, B. J., Mukadam, A. S., & McEwan, W. A. (2019). The role of antibodies and their receptors in protection against ordered protein assembly in neurodegeneration. *Frontiers in Immunology*, *10*(MAY), 1–15. https://doi.org/10.3389/fimmu.2019.01139

Katsinelos, T., Zeitler, M., Dimou, E., Karakatsani, A., Müller, H. M., Nachman, E., Steringer, J. P., Ruiz de Almodovar, C., Nickel, W., & Jahn, T. R. (2018). Unconventional Secretion Mediates the Trans-cellular Spreading of Tau. *Cell Reports*, *23*(7), 2039–2055. https://doi.org/10.1016/j.celrep.2018.04.056

Ke, Y. D., Suchowerska, A. K., Van Der Hoven, J., De Silva, D. M., Wu, C. W., Van Eersel, J., Ittner, A., & Ittner, L. M. (2012). Lessons from Tau-deficient mice. *International Journal of Alzheimer's Disease*, *2012*. https://doi.org/10.1155/2012/873270

Keeble, A. H., Khan, Z., Forster, A., & James, L. C. (2008). Trim21 Conserved. *Proceedings of the National Academy of Sciences of the United States of America*, *105*(16), 6045–6050. http://www.pnas.org/content/105/16/6045.long%0Apapers2://publication/doi/10.1073/pnas.0800159105

Kfoury, N., Holmes, B. B., Jiang, H., Holtzman, D. M., & Diamond, M. I. (2012). Trans-cellular propagation of Tau aggregation by fibrillar species. *Journal of Biological Chemistry*, *287*(23), 19440–19451. https://doi.org/10.1074/jbc.M112.346072

Kins, S., Kurosinski, P., Nitsch, R. M., & Götz, J. (2003). Activation of the ERK and JNK signaling pathways caused by neuron-specific inhibition of PP2A in transgenic mice. *American Journal of Pathology*, *163*(3), 833–843. https://doi.org/10.1016/S0002-9440(10)63444-X

Kirchhofer, A., Helma, J., Schmidthals, K., Frauer, C., Cui, S., Karcher, A., Pellis, M., Muyldermans, S., Casas-Delucchi, C. S., Cardoso, M. C., Leonhardt, H., Hopfner, K. P., & Rothbauer, U. (2010). Modulation of protein properties in living cells using nanobodies. *Nature Structural and Molecular Biology*, *17*(1), 133–139. https://doi.org/10.1038/nsmb.1727

Klunk, W., Raskind, M., Sabbagh, M., Honig, L. S., Ph, D., Porsteinsson, A. P., Ferris, S., Ph, D., Reichert, M., Ph, D., Grundman, M., Yuen, E., Black, R., & Robert, H. (2014). *Two Phase 3 Trials of Bapineuzumab for AD - NEJM 2014*. *370*(4), 322–333. https://doi.org/10.1056/NEJMoa1304839.Two

Koenig SM, T. J. (2006). Ventilator-Associated Pneumonia: Diagnosis, Treatment, and Prevention. Clin Microbiol Rev 2006; 19:637-57. *Clin Microbiol Rev*, *19*(1), 637–657. https://doi.org/10.1016/j.neuron.2009.03.024.Neurodegenerative

Köhler, C., Dinekov, M., & Götz, J. (2013). Active glycogen synthase kinase-3 and tau pathology-related tyrosine phosphorylation in pR5 human tau transgenic mice. *Neurobiology of Aging*, *34*(5), 1369–1379. https://doi.org/10.1016/j.neurobiolaging.2012.11.010

Koide, A., Tereshko, V., Uysal, S., Margalef, K., Kossiakoff, A. A., & Koide, S. (2007). Exploring the Capacity of Minimalist Protein Interfaces: Interface Energetics and Affinity Maturation to Picomolar KD of a Single-domain Antibody with a Flat Paratope. *Journal of Molecular Biology*, *373*(4), 941–953. https://doi.org/10.1016/j.jmb.2007.08.027

Kondo, A., Shahpasand, K., Mannix, R., Qiu, J., Moncaster, J., Chen, C., Yao, Y., Lin, Y., Driver, J. A., Sun, Y., Wei, S., Luo, M., Albayram, O., Huang, P., Rotenberg, A., Ryo, A., Goldstein, L. E., Pascual-leone, A., Mckee, A. C., … Lu, K. P. (2015). Cis

P-Tau: Early Driver of Brain Injury and Tauopathy Blocked By Antibody. *Nature*, *523*(7561), 431–436. https://doi.org/10.1038/nature14658.cis

Kontsekova, E., Zilka, N., Kovacech, B., Novak, P., & Novak, M. (2014). First-in-man tau vaccine targeting structural determinants essential for pathological tau-tau interaction reduces tau oligomerisation and neurofibrillary degeneration in an Alzheimer's disease model. *Alzheimer's Research and Therapy*, *6*(4), 1–12. https://doi.org/10.1186/alzrt278

Kopke, E., Tung, Y. C., Shaikh, S., Del Alonso, C. A., Iqbal, K., & Grundke-Iqbal, I. (1993a). Microtubule-associated protein tau. Abnormal phosphorylation of a non- paired helical filament pool in Alzheimer disease. *Journal of Biological Chemistry*, *268*(32), 24374–24384. https://doi.org/10.1016/s0021-9258(20)80536-5

Kopke, E., Tung, Y. C., Shaikh, S., Del Alonso, C. A., Iqbal, K., & Grundke-Iqbal, I. (1993b). Microtubule-associated protein tau. Abnormal phosphorylation of a non- paired helical filament pool in Alzheimer disease. *Journal of Biological Chemistry*, *268*(32), 24374–24384.

Kosik, K. S., & Shimura, H. (2005). Phosphorylated tau and the neurodegenerative foldopathies. *Biochimica et Biophysica Acta - Molecular Basis of Disease*, *1739*(2), 298–310. https://doi.org/10.1016/j.bbadis.2004.10.011

Kovacs, G. G., Xie, S. X., Robinson, J. L., Lee, E. B., Smith, D. H., Schuck, T., Lee, V. M. Y., & Trojanowski, J. Q. (2018). Sequential stages and distribution patterns of aging-related tau astrogliopathy (ARTAG) in the human brain. *Acta Neuropathologica Communications*, *6*(1), 50. https://doi.org/10.1186/s40478-018-0552-y

Krishnaswamy, S., Huang, H. W., Marchal, I. S., Ryoo, H. D., & Sigurdsson, E. M. (2020). Neuronally expressed anti-tau scFv prevents tauopathy-induced phenotypes in Drosophila models. *Neurobiology of Disease*, *137*(October 2019), 104770. https://doi.org/10.1016/j.nbd.2020.104770

Lasagna-Reeves, C. A., Castillo-Carranza, D. L., Sengupta, U., Guerrero-Munoz, M. J., Kiritoshi, T., Neugebauer, V., Jackson, G. R., & Kayed, R. (2012). Alzheimer brain-derived tau oligomers propagate pathology from endogenous tau. *Scientific Reports*, *2*. https://doi.org/10.1038/srep00700

Lee, S. H., Le Pichon, C. E., Adolfsson, O., Gafner, V., Pihlgren, M., Lin, H., Solanoy, H., Brendza, R., Ngu, H., Foreman, O., Chan, R., Ernst, J. A., DiCara, D., Hotzel, I., Srinivasan, K., Hansen, D. V., Atwal, J., Lu, Y., Bumbaca, D., … Ayalon, G. (2016a). Antibody-Mediated Targeting of Tau In Vivo Does Not Require Effector Function and Microglial Engagement. *Cell Reports*, *16*(6), 1690–1700. https://doi.org/10.1016/j.celrep.2016.06.099

Lee, S. H., Le Pichon, C. E., Adolfsson, O., Gafner, V., Pihlgren, M., Lin, H., Solanoy, H., Brendza, R., Ngu, H., Foreman, O., Chan, R., Ernst, J. A., DiCara, D., Hotzel, I., Srinivasan, K., Hansen, D. V., Atwal, J., Lu, Y., Bumbaca, D., … Ayalon, G. (2016b). Antibody-Mediated Targeting of Tau In Vivo Does Not Require Effector Function and Microglial Engagement. *Cell Reports*, *16*(6), 1690–1700. https://doi.org/10.1016/j.celrep.2016.06.099

Lefebvre, T., Ferreira, S., Dupont-Wallois, L., Bussière, T., Dupire, M. J., Delacourte, A., Michalski, J. C., & Caillet-Boudin, M. L. (2003). Evidence of a balance between phosphorylation and O-GlcNAc glycosylation of Tau proteins - A role in nuclear localization. *Biochimica et Biophysica Acta - General Subjects*, *1619*(2), 167–176. https://doi.org/10.1016/S0304-4165(02)00477-4

Leroux, E., Perbet, R., Caillierez, R., Richetin, K., Lieger, S., Espourteille, J., Bouillet, T., Bégard, S., Danis, C., Loyens, A., Toni, N., Déglon, N., Deramecourt, V., Schraen-Maschke, S., Buée, L., & Colin, M. (2021). Extracellular vesicles: Major actors of heterogeneity in tau spreading among human tauopathies. *Molecular Therapy*. https://doi.org/10.1016/j.ymthe.2021.09.020

Leroy, K., Ando, K., Héraud, C., Yilmaz, Z., Authelet, M., Boeynaems, J. M., Buée, L., De Decker, R., & Brion, J. P. (2010). Lithium treatment arrests the development of neurofibrillary tangles in mutant tau transgenic mice with advanced neurofibrillary pathology. *Journal of Alzheimer's Disease*, *19*(2), 705–719. https://doi.org/10.3233/JAD-2010-1276

Leroy, K., Bretteville, A., Schindowski, K., Gilissen, E., Authelet, M., De Decker, R., Yilmaz, Z., Buée, L., & Brion, J. P. (2007). Early axonopathy preceding neurofibrillary tangles in mutant tau transgenic mice. *American Journal of Pathology*, *171*(3), 976–992. https://doi.org/10.2353/ajpath.2007.070345

Lewis, J., & Dickson, D. W. (2016). Propagation of tau pathology: hypotheses, discoveries, and yet unresolved questions from experimental and human brain studies. *Acta Neuropathologica*, *131*(1), 27–48. https://doi.org/10.1007/s00401-015-1507-z

Li, S., Yi, Y., Cui, K., Zhang, Y., Chen, Y., Han, D., Sun, L., Zhang, X., Chen, F., Zhang, Y., & Yang, Y. (2021). A Single-Chain Variable Fragment Antibody Inhibits Aggregation of Phosphorylated Tau and Ameliorates Tau Toxicity in vitro and in vivo. *Journal of Alzheimer's Disease*, *79*(4), 1613–1629. https://doi.org/10.3233/JAD-191266

Li, T., Bourgeois, J. P., Celli, S., Glacial, F., Le Sourd, A. M., Mecheri, S., Weksler, B., Romero, I., Couraud, P. O., Rougeon, F., & Lafaye, P. (2012). Cell-penetrating anti-GFAP VHH and corresponding fluorescent fusion protein VHH-GFP spontaneously cross the blood-brain barrier and specifically recognize astrocytes: Application to brain imaging. *FASEB Journal*, *26*(10), 3969–3979. https://doi.org/10.1096/fj.11-201384

Li, T., Vandesquille, M., Koukouli, F., Dudeffant, C., Youssef, I., Lenormand, P., Ganneau, C., Maskos, U., Czech, C., Grueninger, F., Duyckaerts, C., Dhenain, M., Bay, S., Delatour, B., & Lafaye, P. (2016). Camelid single-domain antibodies: A versatile tool for in vivo imaging of extracellular and intracellular brain targets. *Journal of Controlled Release*, *243*, 1–10. https://doi.org/10.1016/j.jconrel.2016.09.019

Li, X. (2016). 乳鼠心肌提取 HHS Public Access. *Physiology & Behavior*, *176*(3), 139–148. https://doi.org/10.1038/nchem.2889.Structure-based

Limorenko, G., & Lashuel, H. A. (2021). *Revisiting the grammar of Tau aggregation and pathology formation : How new insights from brain pathology are shaping how we study and target Tauopathies*. 1–80. https://doi.org/10.1039/d1cs00127b

Liu, C., & Götz, J. (2013). Profiling murine tau with 0N, 1N and 2N isoform-specific antibodies in brain and peripheral organs reveals distinct subcellular localization, with the 1N isoform being enriched in the nucleus. *PLoS ONE*, *8*(12), 1–18. https://doi.org/10.1371/journal.pone.0084849

Liu, F., Grundke-Iqbal, I., Iqbal, K., & Gong, C. X. (2005). Contributions of protein phosphatases PP1, PP2A, PP2B and PP5 to the regulation of tau phosphorylation. *European Journal of Neuroscience*, *22*(8), 1942–1950. https://doi.org/10.1111/j.1460-9568.2005.04391.x

Liu, F., Li, B., Tung, E. J., Grundke-Iqbal, I., Iqbal, K., & Gong, C. X. (2007). Site-specific effects of tau phosphorylation on its microtubule assembly activity and self-aggregation. *European Journal of Neuroscience*, *26*(12), 3429–3436. https://doi.org/10.1111/j.1460-9568.2007.05955.x

Liu, F., Shi, J., Tanimukai, H., Gu, J., Gu, J., Grundke-Iqbal, I., Iqbal, K., & Gong, C. X. (2009). Reduced O-GlcNAcylation links lower brain glucose metabolism and tau pathology in Alzheimer's disease. *Brain*, *132*(7), 1820–1832. https://doi.org/10.1093/brain/awp099

Liu, W., Zhao, L., Blackman, B., Parmar, M., Wong, M. Y., Woo, T., Yu, F., Sondhi, D., Kaminsky, S. M., Crystal, R. G., & Paul, S. M. (2016). Vectored intracerebral immunization with the anti-tau monoclonal antibody PHF1 markedly reduces tau pathology in mutant tau transgenic mice. *Journal of Neuroscience*, *36*(49), 12425–12435. https://doi.org/10.1523/JNEUROSCI.2016-16.2016

Lobello, K., Ryan, J. M., Liu, E., Rippon, G., & Black, R. (2012). Targeting beta amyloid: A clinical review of immunotherapeutic approaches in Alzheimer's disease. *International Journal of Alzheimer's Disease*, *2012*. https://doi.org/10.1155/2012/628070

Loscalzo, D. E. H. R. C. J. (2011). 基因的改变NIH Public Access. *Bone*, *23*(1), 1–7. https://doi.org/10.1016/j.pnpbp.2013.03.004.Anesthesia

M., N., O., V., C., N., A., E., B., G., J., C., P., T., J., R., & F., P. (2010). Characterization of single chain antibody targets using the yeast two-hybrid technology. *Molecular Biology of the Cell*, *21*(24), 1–13. http://www.molbiolcell.org/content/suppl/2010/12/11/21.24.4299.DC1/2010_Late_Abstracts.pdf%5Cnhttp://ovidsp.ovid.com/ovidweb.cgi?T=JS&PAGE=reference&D=emed10&NEWS=N&AN=70668827

Ma, X., Li, H., He, Y., & Hao, J. (2017). The emerging link between O-GlcNAcylation and neurological disorders. *Cellular and Molecular Life Sciences*, *74*(20), 3667–3686. https://doi.org/10.1007/s00018-017-2542-9

Mah, D., Zhao, J., Liu, X., Zhang, F., Liu, J., & Wang, L. (2021). *The Sulfation Code of Tauopathies : Heparan Sulfate Proteoglycans in the Prion Like Spread of Tau Pathology*. *8*(May), 1–12. https://doi.org/10.3389/fmolb.2021.671458

Majerova, P., Zilkova, M., Kazmerova, Z., Kovac, A., Paholikova, K., Kovacech, B., Zilka, N., & Novak, M. (2014). Microglia display modest phagocytic capacity for extracellular tau oligomers. *Journal of Neuroinflammation*, *11*(1), 1–12.

https://doi.org/10.1186/s12974-014-0161-z

Mallery, D. L., McEwan, W. A., Bidgood, S. R., Towers, G. J., Johnson, C. M., & James, L. C. (2010). Antibodies mediate intracellular immunity through tripartite motif-containing 21 (TRIM21). *Proceedings of the National Academy of Sciences of the United States of America*, *107*(46), 19985–19990. https://doi.org/10.1073/pnas.1014074107

Malpas, C. B., Vivasha, L., Genc, S., Saling, M. M., Desmond, P., Steward, C., Hicks, R. J., Callahan, J., Brodtmann, A., Collins, S., MacFarlane, S., Corcoran, N. M., Hovens, C. M., Velakoulis, D., & O'Brien, T. J. (2016). A phase iia randomized control trial of VEL015 (sodium selenate) in mild-moderate Alzheimer's disease. *Journal of Alzheimer's Disease*, *54*(1), 223–232. https://doi.org/10.3233/JAD-160544

Mandelkow, E., & Mandelkow, E. (2012). Biochemistry and cell biology of Tau protein in neurofibrillary degeneration_Cold Spring Harb Perspect Med-2012-Mandelkow-cshperspect.a006247. *Cold Sping Harbor Perspectives in Medicine*, *2*(7), 1–25.

Manuscript, A. (2015). *Pardon et al. - 2014 - A general protocol for the generation of Nanobodies for structural biology(3)*. *9*(3), 674–693. https://doi.org/10.1038/nprot.2014.039.A

Maphis, N., Xu, G., Kokiko-Cochran, O. N., Jiang, S., Cardona, A., Ransohoff, R. M., Lamb, B. T., & Bhaskar, K. (2015). Reactive microglia drive tau pathology and contribute to the spreading of pathological tau in the brain. *Brain*, *138*(6), 1738–1755. https://doi.org/10.1093/brain/awv081

Marschall, A. L. J., & Dübel, S. (2016). Antibodies inside of a cell can change its outside: Can intrabodies provide a new therapeutic paradigm? *Computational and Structural Biotechnology Journal*, *14*, 304–308. https://doi.org/10.1016/j.csbj.2016.07.003

Martin, E., Boucher, C., Fontaine, B., & Delarasse, C. (2017). Distinct inflammatory phenotypes of microglia and monocyte-derived macrophages in Alzheimer's disease models: effects of aging and amyloid pathology. *Aging Cell*, *16*(1), 27–38. https://doi.org/10.1111/acel.12522

Martin, L., Latypova, X., Wilson, C. M., Magnaudeix, A., Perrin, M. L., Yardin, C., & Terro, F. (2013). Tau protein kinases: Involvement in Alzheimer's disease. *Ageing Research Reviews*, *12*(1), 289–309. https://doi.org/10.1016/j.arr.2012.06.003

Masliah, E., Hansen, L., Adame, A., Crews, L., Bard, F., Lee, C., Seubert, P., Games, D., Kirby, L., & Schenk, D. (2005). Aβ vaccination effects on plaque pathology in the absence of encephalitis in Alzheimer disease. *Neurology*, *64*(1), 129–131. https://doi.org/10.1212/01.WNL.0000148590.39911.DF

Matsunaga, S., Kishi, T., & Iwata, N. (2015). Memantine monotherapy for Alzheimer's Disease:A systematic review and meta-analysis. *PLoS ONE*, *10*(4), 1–16. https://doi.org/10.1371/journal.pone.0123289

Matsuo, E. S., Shin, R. W., Billingsley, M. L., Van deVoorde, A., O'Connor, M., Trojanowski, J. Q., & Lee, V. M. Y. (1994). Biopsy-derived adult human brain tau is phosphorylated at many of the same sites as Alzheimer's disease paired helical filament tau. *Neuron*, *13*(4), 989–1002. https://doi.org/10.1016/0896-6273(94)90264-X

Matsuoka, Y., Jouroukhin, Y., Gray, A. J., Ma, L., Hirata-Fukae, C., Li, H. F., Feng, L., Lecanu, L., Walker, B. R., Planel, E., Arancio, O., Gozes, I., & Aisen, P. S. (2008). A neuronal microtubule-interacting agent, NAPVSIPQ, reduces tau pathology and enhances cognitive function in a mouse model of Alzheimer's disease. *Journal of Pharmacology and Experimental Therapeutics*, *325*(1), 146–153. https://doi.org/10.1124/jpet.107.130526

Mawal-Dewan, M., Henley, J., Van De Voorde, A., Trojanowski, J. Q., & Lee, V. M. Y. (1994). The phosphorylation state of tau in the developing rat brain is regulated by phosphoprotein phosphatases. *Journal of Biological Chemistry*, *269*(49), 30981–30987. https://doi.org/10.1016/s0021-9258(18)47378-4

McEwan, W. A. (2016). Surveillance for intracellular antibody by cytosolic Fc receptor TRIM21. *Antibodies*, *5*(4). https://doi.org/10.3390/antib5040021

McEwan, W. A., Falcon, B., Vaysburd, M., Clift, D., Oblak, A. L., Ghetti, B., Goedert, M., & James, L. C. (2017). Cytosolic Fc receptor TRIM21 inhibits seeded tau aggregation. *Proceedings of the National Academy of Sciences of the United States of America*, *114*(3), 574–579. https://doi.org/10.1073/pnas.1607215114

Melková, K., Zapletal, V., Narasimhan, S., Jansen, S., Hritz, J., Škrabana, R., Zweckstetter, M., Jensen, M. R., Blackledge, M., & Žídek, L. (2019). Structure and functions of microtubule associated proteins tau and map2c: Similarities and

differences. *Biomolecules*, *9*(3), 1–32. https://doi.org/10.3390/biom9030105

Mendelkow Phosp.pdf. (n.d.).

Messer, A., & Butler, D. C. (2020). Optimizing intracellular antibodies (intrabodies/nanobodies) to treat neurodegenerative disorders. *Neurobiology of Disease*, *134*(July 2019), 104619. https://doi.org/10.1016/j.nbd.2019.104619

Mirbaha, H., Chen, D., Morozova, O. A., Ruff, K. M., Sharma, A., Liu, X., Pappu, R. V., Colby, D. W., Mirzaei, H., Joachimiak, L. A., & Diamond, M. I. (2017). Inert and seed-competent tau monomers suggest structural origins of aggregation. *BioRxiv*, 1–29. https://doi.org/10.1101/163394

Mo, J. J., Li, J. Y., Yang, Z., Liu, Z., & Feng, J. S. (2017). Efficacy and safety of anti-amyloid-β immunotherapy for Alzheimer's disease: a systematic review and network meta-analysis. *Annals of Clinical and Translational Neurology*, *4*(12), 931–942. https://doi.org/10.1002/acn3.469

Moreira, G. G., Cantrelle, F. X., Quezada, A., Carvalho, F. S., Cristóvão, J. S., Sengupta, U., Puangmalai, N., Carapeto, A. P., Rodrigues, M. S., Cardoso, I., Fritz, G., Herrera, F., Kayed, R., Landrieu, I., & Gomes, C. M. (2021). Dynamic interactions and Ca2+-binding modulate the holdase-type chaperone activity of S100B preventing tau aggregation and seeding. *Nature Communications*, *12*(1), 1–16. https://doi.org/10.1038/s41467-021-26584-2

Morishima-Kawashima, M., Hasegawa, M., Takio, K., Suzuki, M., Yoshida, H., Titani, K., & Ihara, Y. (1995). Proline-directed and non-proline-directed phosphorylation of PHF-tau. *Journal of Biological Chemistry*, *270*(2), 823–829. https://doi.org/10.1074/jbc.270.2.823

Morozova, O. A., March, Z. M., Robinson, A. S., & Colby, D. W. (2013). Conformational features of tau fibrils from alzheimer's disease brain are faithfully propagated by unmodified recombinant protein. *Biochemistry*, *52*(40), 6960–6967. https://doi.org/10.1021/bi400866w

Morris, R. G., & Salmon, D. P. (2007). The centennial of Alzheimer's disease and the publication of "Über eine eigenartige erkankung der hirnrinde" by Alöis Alzheimer. *Cortex*, *43*(7), 821–825. https://doi.org/10.1016/S0010-9452(08)70681-6

Moutel, S., Bery, N., Bernard, V., Keller, L., Lemesre, E., De Marco, A., Ligat, L., Rain, J. C., Favre, G., Olichon, A., & Perez, F. (2016). NaLi-H1: A universal synthetic library of humanized nanobodies providing highly functional antibodies and intrabodies. *ELife*, *5*(JULY), 1–31. https://doi.org/10.7554/eLife.16228

Moutel, S., El Marjou, A., Vielemeyer, O., Nizak, C., Benaroch, P., Dübel, S., & Perez, F. (2009). A multi-Fc-species system for recombinant antibody production. *BMC Biotechnology*, *9*, 1–9. https://doi.org/10.1186/1472-6750-9-14

Mudher, A., Colin, M., Dujardin, S., Medina, M., Dewachter, I., Alavi Naini, S. M., Mandelkow, E. M., Mandelkow, E., Buée, L., Goedert, M., & Brion, J. P. (2017). What is the evidence that tau pathology spreads through prion-like propagation? *Acta Neuropathologica Communications*, *5*(1), 99. https://doi.org/10.1186/s40478-017-0488-7

Mukrasch, M. D., Bibow, S., Korukottu, J., Jeganathan, S., Biernat, J., Griesinger, C., Mandelkow, E., & Zweckstetter, M. (2009). Structural polymorphism of 441-residue Tau at single residue resolution. *PLoS Biology*, *7*(2), 0399–0414. https://doi.org/10.1371/journal.pbio.1000034

Mukrasch, M. D., Biernat, J., Von Bergen, M., Griesinger, C., Mandelkow, E., & Zweckstetter, M. (2005). Sites of tau important for aggregation populate β-structure and bind to microtubules and polyanions. *Journal of Biological Chemistry*, *280*(26), 24978–24986. https://doi.org/10.1074/jbc.M501565200

Murphy, D. B., Johnson, K. A., & Borisy, G. G. (1977). Role of tubulin-associated proteins in microtubule nucleation and elongation. *Journal of Molecular Biology*, *117*(1), 33–52. https://doi.org/10.1016/0022-2836(77)90021-3

Muruganandam, A., Tanha, J., Narang, S., & Stanimirovic, D. (2002). Selection of phage-displayed llama single-domain antibodies that transmigrate across human blood-brain barrier endothelium. *The FASEB Journal : Official Publication of the Federation of American Societies for Experimental Biology*, *16*(2), 240–242. https://doi.org/10.1096/fj.01-0343fje

Muyldermans, S. (2013). Nanobodies: Natural Single-Domain Antibodies. *Annual Review of Biochemistry*, *82*(1), 775–797. https://doi.org/10.1146/annurev-biochem-063011-092449

Muyldermans, S., Cambillau, C., & Wyns, L. (2001). Recognition of antigens by single-domain antibody fragments: The

superfluous luxury of paired domains. *Trends in Biochemical Sciences*, *26*(4), 230–235. https://doi.org/10.1016/S0968-0004(01)01790-X

Nachman, E., Wentink, A. S., Madiona, K., Bousset, L., Katsinelos, T., Allinson, K., Kampinga, H., McEwan, W. A., Jahn, T. R., Melki, R., Mogk, A., Bukau, B., & Nussbaum-Krammer, C. (2020a). Disassembly of Tau fibrils by the human Hsp70 disaggregation machinery generates small seeding-competent species. *Journal of Biological Chemistry*, *295*(28), 9676–9690. https://doi.org/10.1074/jbc.RA120.013478

Nachman, E., Wentink, A. S., Madiona, K., Bousset, L., Katsinelos, T., Allinson, K., Kampinga, H., McEwan, W. A., Jahn, T. R., Melki, R., Mogk, A., Bukau, B., & Nussbaum-Krammer, C. (2020b). Disassembly of Tau fibrils by the human Hsp70 disaggregation machinery generates small seeding-competent species. *Journal of Biological Chemistry*, *295*(28), 9676–9690. https://doi.org/10.1074/jbc.RA120.013478

Nadege Zommer, Nicolas Sergeant, Susanna Schraen-Maschke, David Blum, & Luc Buee. (2012). Targeting Phospho-Ser422 by Active Tau Immunotherapy in the THYTau22 Mouse Model: A Suitable Therapeutic Approach. *Current Alzheimer Research*, *9*(4), 397–405. https://doi.org/10.2174/156720512800492503

Narasimhan, S., Guo, J. L., Changolkar, L., Stieber, A., McBride, J. D., Silva, L. V., He, Z., Zhang, B., Gathagan, R. J., Trojanowski, J. Q., & Lee, V. M. Y. (2017). Pathological tau strains from human brains recapitulate the diversity of tauopathies in nontransgenic mouse brain. *Journal of Neuroscience*, *37*(47), 11406–11423. https://doi.org/10.1523/JNEUROSCI.1230-17.2017

Nemade, R. V., Carrette, O., Larsen, W. J., & Markoff, E. (2002). Involvement of nitric oxide and the ovarian blood follicle barrier in murine follicular cyst development. *Fertility and Sterility*, *78*(6), 1301–1308. https://doi.org/10.1016/S0015-0282(02)04340-6

Nguyen, V. K., Muyldermans, S., & Hamers, R. (1998). The specific variable domain of camel heavy-chain antibodies is encoded in the germline. *Journal of Molecular Biology*, *275*(3), 413–418. https://doi.org/10.1006/jmbi.1997.1477

Nicolll, J. A. R., Wilkinson, D., Holmes, C., Steart, P., Markham, H., & Weller, R. O. (2003). Neuropathology of human Alzheimer disease after immunization with amyloid-β peptide: A case report. *Nature Medicine*, *9*(4), 448–452. https://doi.org/10.1038/nm840

Noble, W., Hanger, D. P., Miller, C. C. J., & Lovestone, S. (2013). The importance of tau phosphorylation for neurodegenerative diseases. *Frontiers in Neurology*, *4 JUL*(July), 1–11. https://doi.org/10.3389/fneur.2013.00083

Noble, W., Planel, E., Zehr, C., Olm, V., Meyerson, J., Suleman, F., Gaynor, K., Wang, L., LaFrancois, J., Feinstein, B., Burns, M., Krishnamurthy, P., Wen, Y., Bhat, R., Lewis, J., Dickson, D., & Duff, K. (2005). Inhibition of glycogen synthase kinase-3 by lithium correlates with reduced tauopathy and degeneration in vivo. *Proceedings of the National Academy of Sciences of the United States of America*, *102*(19), 6990–6995. https://doi.org/10.1073/pnas.0500466102

Nobuhara, C. K., DeVos, S. L., Commins, C., Wegmann, S., Moore, B. D., Roe, A. D., Costantino, I., Frosch, M. P., Pitstick, R., Carlson, G. A., Hock, C., Nitsch, R. M., Montrasio, F., Grimm, J., Cheung, A. E., Dunah, A. W., Wittmann, M., Bussiere, T., Weinreb, P. H., … Takeda, S. (2017). Tau Antibody Targeting Pathological Species Blocks Neuronal Uptake and Interneuron Propagation of Tau in Vitro. *American Journal of Pathology*, *187*(6), 1399–1412. https://doi.org/10.1016/j.ajpath.2017.01.022

Norrbom, M., Wozniak, D. F., Ph, D., Dawson, H. N., Ph, D., & Frank, C. (2016). Increased 4R-tau induces pathological changes in a human-tau mouse model. *Neuron*, *90*(5), 941–947. https://doi.org/10.1016/j.neuron.2016.04.042.Increased

Novak, P., Schmidt, R., Kontsekova, E., Zilka, N., Kovacech, B., Skrabana, R., Vince-Kazmerova, Z., Katina, S., Fialova, L., Prcina, M., Parrak, V., Dal-Bianco, P., Brunner, M., Staffen, W., Rainer, M., Ondrus, M., Ropele, S., Smisek, M., Sivak, R., … Novak, M. (2017). Safety and immunogenicity of the tau vaccine AADvac1 in patients with Alzheimer's disease: a randomised, double-blind, placebo-controlled, phase 1 trial. *The Lancet Neurology*, *16*(2), 123–134. https://doi.org/10.1016/S1474-4422(16)30331-3

Orgogozo, J. M., Gilman, S., Dartigues, J. F., Laurent, B., Puel, M., Kirby, L. C., Jouanny, P., Dubois, B., Eisner, L., Flitman, S., Michel, B. F., Boada, M., Frank, A., & Hock, C. (2003). Subacute meningoencephalitis in a subset of patients with AD after Aβ42 immunization. *Neurology*, *61*(1), 46–54. https://doi.org/10.1212/01.WNL.0000073623.84147.A8

Orren, A., Lachmann, P. J., Welbaum, B. E., Sodetz, J. M., Boyle, M. D., Borsos, T., Podack, E. R., Hugli, T. E., Qiao, F., Abagyan, R., Hazard, S., Tomlinson, S., Dennert, G., Podack, E. R., Hengartner, H., Lichtenheld, M. G., Chiswell, B., Sodetz, J. M., Feil, S. C., … Tweten, R. K. (2007). *Anti-Inflammatory Activity of Human*. *317*(September), 1554–1558.

Osborn, L., Kunkel, S., & Nabel, G. J. (1989). Tumor necrosis factor α and interleukin 1 stimulate the human immunodeficiency virus enhancer by activation of the nuclear factor κB. *Proceedings of the National Academy of Sciences of the United States of America*, *86*(7), 2336–2340. https://doi.org/10.1073/pnas.86.7.2336

Otth, C., Concha, I. I., Arendt, T., Stieler, J., Schliebs, R., González-Billault, C., & Maccionia, R. B. (2002). AβPP induces cdk5-dependent tau hyperphosphorylation in transgenic mice Tg2576. *Journal of Alzheimer's Disease*, *4*(5), 417–430. https://doi.org/10.3233/JAD-2002-4508

Pain, C., Dumont, J., & Dumoulin, M. (2015). Camelid single-domain antibody fragments: Uses and prospects to investigate protein misfolding and aggregation, and to treat diseases associated with these phenomena. *Biochimie*, *111*, 82–106. https://doi.org/10.1016/j.biochi.2015.01.012

Panza, F., Solfrizzi, V., Imbimbo, B. P., & Logroscino, G. (2014). Amyloid-directed monoclonal antibodies for the treatment of Alzheimer's disease: The point of no return? *Expert Opinion on Biological Therapy*, *14*(10), 1465–1476. https://doi.org/10.1517/14712598.2014.935332

Panza, F., Solfrizzi, V., Seripa, D., Imbimbo, B. P., Lozupone, M., Santamato, A., Tortelli, R., Galizia, I., Prete, C., Daniele, A., Pilotto, A., Greco, A., & Logroscino, G. (2016). Tau-based therapeutics for Alzheimer's disease: Active and passive immunotherapy. *Immunotherapy*, *8*(9), 1119–1134. https://doi.org/10.2217/imt-2016-0019

Patton, R. L., Kalback, W. M., Esh, C. L., Kokjohn, T. A., Van Vickle, G. D., Luehrs, D. C., Kuo, Y. M., Lopez, J., Brune, D., Ferrer, I., Masliah, E., Newel, A. J., Beach, T. G., Castaño, E. M., & Roher, A. E. (2006). Amyloid-β peptide remnants in AN-1792-immunized Alzheimer's disease patients: A biochemical analysis. *American Journal of Pathology*, *169*(3), 1048–1063. https://doi.org/10.2353/ajpath.2006.060269

Pérez-Martínez, D., Tanaka, T., & Rabbitts, T. H. (2010). Intracellular antibodies and cancer: New technologies offer therapeutic opportunities. *BioEssays*, *32*(7), 589–598. https://doi.org/10.1002/bies.201000009

Pérez, M., Valpuesta, J. M., Medina, M., Montejo de Garcini, E., & Avila, J. (2002). Polymerization of τ into Filaments in the Presence of Heparin: The Minimal Sequence Required for τ - τ Interaction. *Journal of Neurochemistry*, *67*(3), 1183–1190. https://doi.org/10.1046/j.1471-4159.1996.67031183.x

Pernègre, C., Duquette, A., & Leclerc, N. (2019). Tau secretion: Good and bad for neurons. *Frontiers in Neuroscience*, *13*(JUN), 1–11. https://doi.org/10.3389/fnins.2019.00649

Picci, P. (2019). Staging. *Diagnosis of Musculoskeletal Tumors and Tumor-like Conditions: Clinical, Radiological and Histological Correlations - the Rizzoli Case Archive*, *16*(3), 31–33. https://doi.org/10.1007/978-3-030-29676-6_8

Planel, E., Richter, K. E. G., Nolan, C. E., Finley, J. E., Liu, L., Wen, Y., Krishnamurthy, P., Herman, M., Wang, L., Schachter, J. B., Nelson, R. B., Lau, L. F., & Duff, K. E. (2007). Anesthesia leads to tau hyperphosphorylation through inhibition of phosphatase activity by hypothermia. *Journal of Neuroscience*, *27*(12), 3090–3097. https://doi.org/10.1523/JNEUROSCI.4854-06.2007

Plotkin, S. S., & Cashman, N. R. (2020). Passive immunotherapies targeting Aβ and tau in Alzheimer's disease. *Neurobiology of Disease*, *144*(July), 105010. https://doi.org/10.1016/j.nbd.2020.105010

Pollithy, A., Romer, T., Lang, C., Müller, F. D., Helma, J., Leonhardt, H., Rothbauer, U., & Schüler, D. (2011). Magnetosome expression of functional camelid antibody fragments (nanobodies) in Magnetospirillum gryphiswaldense. *Applied and Environmental Microbiology*, *77*(17), 6165–6171. https://doi.org/10.1128/AEM.05282-11

Pooler, A. M., Phillips, E. C., Lau, D. H. W., Noble, W., & Hanger, D. P. (2013). Physiological release of endogenous tau is stimulated by neuronal activity. *EMBO Reports*, *14*(4), 389–394. https://doi.org/10.1038/embor.2013.15

Poorkaj, P., Bird, T. D., Wijsman, E., Nemens, E., Garruto, R. M., Anderson, L., Andreadis, A., Wiederholt, W. C., Raskind, M., & Schellenberg, G. D. (1998). Tau is a candidate gene for chromosome 17 frontotemporal dementia. *Annals of Neurology*, *43*(6), 815–825. https://doi.org/10.1002/ana.410430617

Prusiner, S. B. (1998). Prions. *Proceedings of the National Academy of Sciences of the United States of America*.

Puzzo, D., & Arancio, O. (2013). Amyloid-β peptide: Dr. Jekyll or Mr. Hyde? *Journal of Alzheimer's Disease*, *33*(SUPPL. 1). https://doi.org/10.3233/JAD-2012-129033

Puzzo, D., Gulisano, W., Palmeri, A., & Arancio, O. (2015). Rodent models for Alzheimer's disease drug discovery. *Expert Opinion on Drug Discovery*, *10*(7), 703–711. https://doi.org/10.1517/17460441.2015.1041913

Qiao, S., Qin, M., & Wang, H. (2016). Analysis of knee infrared image based on sample entropy algorithm. *Proceedings - 8th International Conference on Intelligent Networks and Intelligent Systems, ICINIS 2015*, 1–4. https://doi.org/10.1109/ICINIS.2015.10

Qing, H., He, G., Ly, P. T. T., Fox, C. J., Staufenbiel, M., Cai, F., Zhang, Z., Wei, S., Sun, X., Chen, C. H., Zhou, W., Wang, K., & Song, W. (2008). Valproic acid inhibits aβ production, neuritic plaque formation, and behavioral deficits in alzheimer's disease mouse models. *Journal of Experimental Medicine*, *205*(12), 2781–2789. https://doi.org/10.1084/jem.20081588

Qureshi, I. A., Tirucherai, G., Ahlijanian, M. K., Kolaitis, G., Bechtold, C., & Grundman, M. (2018). A randomized, single ascending dose study of intravenous BIIB092 in healthy participants. *Alzheimer's and Dementia: Translational Research and Clinical Interventions*, *4*, 746–755. https://doi.org/10.1016/j.trci.2018.10.007

Rabouille, C. (2017). Pathways of Unconventional Protein Secretion. *Trends in Cell Biology*, *27*(3), 230–240. https://doi.org/10.1016/j.tcb.2016.11.007

Ramakrishnan, P., Dickson, D. W., & Davies, P. (2003). Pin1 colocalization with phosphorylated tau in Alzheimer's disease and other tauopathies. *Neurobiology of Disease*, *14*(2), 251–264. https://doi.org/10.1016/S0969-9961(03)00109-8

Rath, T., Baker, K., Dumont, J. A., Peters, R. T., Jiang, H., Qiao, S. W., Lencer, W. I., Pierce, G. F., & Blumberg, R. S. (2015). Fc-fusion proteins and FcRn: Structural insights for longer-lasting and more effective therapeutics. *Critical Reviews in Biotechnology*, *35*(2), 235–254. https://doi.org/10.3109/07388551.2013.834293

Rauch, J. N., Chen, J. J., Sorum, A. W., Miller, G. M., Sharf, T., See, S. K., Hsieh-Wilson, L. C., Kampmann, M., & Kosik, K. S. (2018). Tau Internalization is Regulated by 6-O Sulfation on Heparan Sulfate Proteoglycans (HSPGs). *Scientific Reports*, *8*(1), 1–10. https://doi.org/10.1038/s41598-018-24904-z

Rauch, J. N., Luna, G., Guzman, E., Audouard, M., Challis, C., Sibih, Y. E., Leshuk, C., Hernandez, I., Wegmann, S., Hyman, B. T., Gradinaru, V., Kampmann, M., & Kosik, K. S. (2020). LRP1 is a master regulator of tau uptake and spread. *Nature*, *580*(7803), 381–385. https://doi.org/10.1038/s41586-020-2156-5

Ribeiro, F. M., Camargos, E. R. da S., De Souza, L. C., & Teixeira, A. L. (2013). Animal models of neurodegenerative diseases. *Revista Brasileira de Psiquiatria*, *35*(SUPPL.2), 82–91. https://doi.org/10.1590/1516-4446-2013-1157

Richards et al. (2018a). 乳鼠心肌提取 HHS Public Access. *Physiology & Behavior*, *176*(5), 139–148. https://doi.org/10.1038/nrneurol.2017.96.A

Richards et al. (2018b). 乳鼠心肌提取 HHS Public Access. *Physiology & Behavior*, *176*(5), 139–148. https://doi.org/10.1038/nrg3978.Knocking

Richards et al. (2018c). 乳鼠心肌提取 HHS Public Access. *Physiology & Behavior*, *176*(5), 139–148. https://doi.org/10.3233/JAD-151208.Selenoprotein

Richter, M., Mewes, A., Fritsch, M., Krügel, U., Hoffmann, R., & Singer, D. (2014). Doubly phosphorylated peptide vaccines to protect transgenic P301S mice against Alzheimer's disease like tau aggregation. *Vaccines*, *2*(3), 601–623. https://doi.org/10.3390/vaccines2030601

Rissiek, B., Koch-Nolte, F., & Magnus, T. (2014). Nanobodies as modulators of inflammation: Potential applications for acute brain injury. *Frontiers in Cellular Neuroscience*, *8*(OCT), 1–7. https://doi.org/10.3389/fncel.2014.00344

Robert Cronin Yung Peng, Rose Khavari, N. D. (2017). 乳鼠心肌提取 HHS Public Access. *Physiology & Behavior*, *176*(3), 139–148. https://doi.org/10.1159/000444169.Carotid

Roberts, M., Sevastou, I., Imaizumi, Y., Mistry, K., Talma, S., Dey, M., Gartlon, J., Ochiai, H., Zhou, Z., Akasofu, S., Tokuhara, N., Ogo, M., Aoyama, M., Aoyagi, H., Strand, K., Sajedi, E., Agarwala, K. L., Spidel, J., Albone, E., … de Silva, R. (2020). Pre-clinical characterisation of E2814, a high-affinity antibody targeting the microtubule-binding repeat domain of tau for passive immunotherapy in Alzheimer's disease. *Acta Neuropathologica Communications*, *8*(1), 13.

https://doi.org/10.1186/s40478-020-0884-2

Robertson, L. A., Moya, K. L., & Breen, K. C. (2004). The potential role of tau protein O-glycosylation in Alzheimer's disease. *Journal of Alzheimer's Disease*, *6*(5), 489–495. https://doi.org/10.3233/JAD-2004-6505

Roder, H. M., Fracasso, R. P., Hoffman, F. J., Witowsky, J. A., Davis, G., & Pellegrino, C. B. (1997). Phosphorylation-dependent monoclonal tau antibodies do not reliably report phosphorylation by extracellular signal-regulated kinase 2 at specific sites. *Journal of Biological Chemistry*, *272*(7), 4509–4515. https://doi.org/10.1074/jbc.272.7.4509

Rodríguez-martín, T., Cuchillo-ibáñez, I., Noble, W., Nyenya, F., Anderton, B. H., & Hanger, D. P. (2013). Neurobiology of Aging Tau phosphorylation affects its axonal transport and degradation. *Neurobiology of Aging*, *34*(9), 2146–2157. https://doi.org/10.1016/j.neurobiolaging.2013.03.015

Rosenqvist, N., Asuni, A. A., Andersson, C. R., Christensen, S., Daechsel, J. A., Egebjerg, J., Falsig, J., Helboe, L., Jul, P., Kartberg, F., Pedersen, L., Sigurdsson, E. M., Sotty, F., Skjødt, K., Stavenhagen, J. B., Volbracht, C., & Pedersen, J. T. (2018). Highly specific and selective anti-pS396-tau antibody C10.2 targets seeding-competent tau. *Alzheimer's and Dementia: Translational Research and Clinical Interventions*, *4*, 521–534. https://doi.org/10.1016/j.trci.2018.09.005

Rothbauer, U., Zolghadr, K., Muyldermans, S., Schepers, A., Cardoso, M. C., & Leonhardt, H. (2008). A versatile nanotrap for biochemical and functional studies with fluorescent fusion proteins. *Molecular and Cellular Proteomics*, *7*(2), 282–289. https://doi.org/10.1074/mcp.M700342-MCP200

Rudnick, S. I., Lou, J., Shaller, C. C., Tang, Y., Klein-Szanto, A. J. P., Weiner, L. M., Marks, J. D., & Adams, G. P. (2011). Influence of affinity and antigen internalization on the uptake and penetration of anti-HER2 Antibodies in Solid Tumors. *Cancer Research*, *71*(6), 2250–2259. https://doi.org/10.1158/0008-5472.CAN-10-2277

Rutgers, K. S., van Remoortere, A., van Buchem, M. A., Verrips, C. T., Greenberg, S. M., Bacskai, B. J., Frosch, M. P., van Duinen, S. G., Maat-Schieman, M. L., & Van der Maarel, S. M. (2011). Differential recognition of vascular and parenchymal beta amyloid deposition. *Neurobiology of Aging*, *32*(10), 1774–1783. https://doi.org/10.1016/j.neurobiolaging.2009.11.012

Saerens, D., Conrath, K., Govaert, J., & Muyldermans, S. (2008). Disulfide Bond Introduction for General Stabilization of Immunoglobulin Heavy-Chain Variable Domains. *Journal of Molecular Biology*, *377*(2), 478–488. https://doi.org/10.1016/j.jmb.2008.01.022

Sahlins, D. M. (2004). *Cosac Naify | Esperando Foucault , ainda*. *88*(4), 450–467. https://doi.org/10.1016/j.bcp.2014.01.011.Behavioral

Saito, T., Iwata, N., Tsubuki, S., Takaki, Y., Takano, J., Huang, S. M., Suemoto, T., Higuchi, M., & Saido, T. C. (2005). Somatostatin regulates brain amyloid β peptide Aβ42 through modulation of proteolytic degradation. *Nature Medicine*, *11*(4), 434–439. https://doi.org/10.1038/nm1206

Sanders, D. W., Kaufman, S. K., Devos, S. L., Sharma, A. M., Li, A., Barker, S. J., Foley, A., Thorpe, J. R., Serpell, L. C., Miller, T. M., Grinberg, L. T., Seeley, W. W., & Diamond, M. I. (2015). *NIH Public Access*. *82*(6), 1271–1288. https://doi.org/10.1016/j.neuron.2014.04.047.Distinct

Sankaranarayanan, S., Barten, D. M., Vana, L., Devidze, N., Yang, L., Cadelina, G., Hoque, N., DeCarr, L., Keenan, S., Lin, A., Cao, Y., Snyder, B., Zhang, B., Nitla, M., Hirschfeld, G., Barrezueta, N., Polson, C., Wes, P., Rangan, V. S., … Ahlijanian, M. (2015). Passive immunization with phospho-tau antibodies reduces tau pathology and functional deficits in two distinct mouse tauopathy models. *PLoS ONE*, *10*(5), 1–28. https://doi.org/10.1371/journal.pone.0125614

Santin, M. D., Debeir, T., Bridal, S. L., Rooney, T., & Dhenain, M. (2013). Fast in vivo imaging of amyloid plaques using μ-MRI Gd-staining combined with ultrasound-induced blood-brain barrier opening. *NeuroImage*, *79*, 288–294. https://doi.org/10.1016/j.neuroimage.2013.04.106

Santos, C. R. A., Duarte, A. C., Quintela, T., Tomás, J., Albuquerque, T., Marques, F., Palha, J. A., & Gonçalves, I. (2017). The choroid plexus as a sex hormone target: Functional implications. *Frontiers in Neuroendocrinology*, *44*, 103–121. https://doi.org/10.1016/j.yfrne.2016.12.002

Sawaya, M. R., Sambashivan, S., Nelson, R., Ivanova, M. I., Sievers, S. A., Apostol, M. I., Thompson, M. J., Balbirnie, M., Wiltzius, J. J. W., McFarlane, H. T., Madsen, A., Riekel, C., & Eisenberg, D. (2007). Atomic structures of amyloid cross-β spines reveal varied steric zippers. *Nature*, *447*(7143), 453–457. https://doi.org/10.1038/nature05695

Scheltens, P., Blennow, K., Breteler, M. M. B., de Strooper, B., Frisoni, G. B., Salloway, S., & Van der Flier, W. M. (2016). Alzheimer's disease. *The Lancet*, *388*(10043), 505–517. https://doi.org/10.1016/S0140-6736(15)01124-1

Scheres, S. H., Zhang, W., Falcon, B., & Goedert, M. (2020). Cryo-EM structures of tau filaments. *Current Opinion in Structural Biology*, *64*(October), 17–25. https://doi.org/10.1016/j.sbi.2020.05.011

Schindowski, K., Bretteville, A., Leroy, K., Bégard, S., Brion, J. P., Hamdane, M., & Buée, L. (2006). Alzheimer's disease-like tau neuropathology leads to memory deficits and loss of functional synapses in a novel mutated tau transgenic mouse without any motor deficits. *American Journal of Pathology*, *169*(2), 599–616. https://doi.org/10.2353/ajpath.2006.060002

Schwalbe, M., Biernat, J., Bibow, S., Ozenne, V., Jensen, M. R., Kadavath, H., Blackledge, M., Mandelkow, E., & Zweckstetter, M. (2013). Phosphorylation of human tau protein by microtubule affinity-regulating kinase 2. *Biochemistry*, *52*(50), 9068–9079. https://doi.org/10.1021/bi401266n

Segat, L., Pontillo, A., Annoni, G., Trabattoni, D., Vergani, C., Clerici, M., Arosio, B., & Crovella, S. (2007). PIN1 promoter polymorphisms are associated with Alzheimer's disease. *Neurobiology of Aging*, *28*(1), 69–74. https://doi.org/10.1016/j.neurobiolaging.2005.11.009

Serenó, L., Coma, M., Rodríguez, M., Sánchez-Ferrer, P., Sánchez, M. B., Gich, I., Agulló, J. M., Pérez, M., Avila, J., Guardia-Laguarta, C., Clarimón, J., Lleó, A., & Gómez-Isla, T. (2009). A novel GSK-3β inhibitor reduces Alzheimer's pathology and rescues neuronal loss in vivo. *Neurobiology of Disease*, *35*(3), 359–367. https://doi.org/10.1016/j.nbd.2009.05.025

Sergeant, N., Bretteville, A., Hamdane, M., Caillet-Boudin, M. L., Grognet, P., Bombois, S., Blum, D., Delacourte, A., Pasquier, F., Vanmechelen, E., Schraen-Maschke, S., & Buée, L. (2008). Biochemistry of Tau in Alzheimer's disease and related neurological disorders. *Expert Review of Proteomics*, *5*(2), 207–224. https://doi.org/10.1586/14789450.5.2.207

Serrano-Pozo, A., Frosch, M. P., Masliah, E., & Hyman, B. T. (2011). Neuropathological alterations in Alzheimer disease. *Cold Spring Harbor Perspectives in Medicine*, *1*(1), 1–23. https://doi.org/10.1101/cshperspect.a006189

Serrano-Pozo, A., William, C. M., Ferrer, I., Uro-Coste, E., Delisle, M. B., Maurage, C. A., Hock, C., Nitsch, R. M., Masliah, E., Growdon, J. H., Frosch, M. P., & Hyman, B. T. (2010). Beneficial effect of human anti-amyloid-β active immunization on neurite morphology and tau pathology. *Brain*, *133*(5), 1312–1327. https://doi.org/10.1093/brain/awq056

Seubert, P., Mawal-Dewan, M., Barbour, R., Jakes, R., Goedert, M., Johnson, G. V. W., Litersky, J. M., Schenk, D., Lieberburg, I., Trojanowski, J. Q., & Lee, V. M. Y. (1995). Detection of phosphorylated Ser262 in fetal tau, adult tau, and paired helical filament tau. *Journal of Biological Chemistry*, *270*(32), 18917–18922. https://doi.org/10.1074/jbc.270.32.18917

Shiryaev, N., Jouroukhin, Y., Giladi, E., Polyzoidou, E., Grigoriadis, N. C., Rosenmann, H., & Gozes, I. (2009). NAP protects memory, increases soluble tau and reduces tau hyperphosphorylation in a tauopathy model. *Neurobiology of Disease*, *34*(2), 381–388. https://doi.org/10.1016/j.nbd.2009.02.011

Sigurdsson, E. M., Wadghiri, Y. Z., Mosconi, L., Blind, J. A., Knudsen, E., Asuni, A., Scholtzova, H., Tsui, W. H., Li, Y., Sadowski, M., Turnbull, D. H., de Leon, M. J., & Wisniewski, T. (2008). A non-toxic ligand for voxel-based MRI analysis of plaques in AD transgenic mice. *Neurobiology of Aging*, *29*(6), 836–847. https://doi.org/10.1016/j.neurobiolaging.2006.12.018

Silva, M. C., Ferguson, F. M., Cai, Q., Donovan, K. A., Nandi, G., Patnaik, D., Zhang, T., Huang, H. T., Lucente, D. E., Dickerson, B. C., Mitchison, T. J., Fischer, E. S., Gray, N. S., & Haggarty, S. J. (2019). Targeted degradation of aberrant tau in frontotemporal dementia patient-derived neuronal cell models. *ELife*, *8*, 1–31. https://doi.org/10.7554/eLife.45457

Šimić, G., Babić Leko, M., Wray, S., Harrington, C., Delalle, I., Jovanov-Milošević, N., Bažadona, D., Buée, L., de Silva, R., Giovanni, G. Di, Wischik, C., & Hof, P. R. (2016). Tau protein hyperphosphorylation and aggregation in alzheimer's disease and other tauopathies, and possible neuroprotective strategies. *Biomolecules*, *6*(1), 2–28. https://doi.org/10.3390/biom6010006

Skachokova, Z., Martinisi, A., Flach, M., Sprenger, F., Naegelin, Y., Steiner-Monard, V., Sollberger, M., Monsch, A. U., Goedert, M., Tolnay, M., & Winkler, D. T. (2019). Cerebrospinal fluid from Alzheimer's disease patients promotes tau

aggregation in transgenic mice. *Acta Neuropathologica Communications*, *7*(1), 72. https://doi.org/10.1186/s40478-019-0725-3

Smet, C., Leroy, A., Sillen, A., Wieruszeski, J. M., Landrieu, I., & Lippens, G. (2004). Accepting its random coil nature allows a partial NMR assignment of the neuronal Tau protein. *ChemBioChem*, *5*(12), 1639–1646. https://doi.org/10.1002/cbic.200400145

Sontag, J. M., & Sontag, E. (2014). Protein phosphatase 2A dysfunction in Alzheimer's disease. *Frontiers in Molecular Neuroscience*, *7*(MAR), 1–10. https://doi.org/10.3389/fnmol.2014.00016

Soto, C. (2003). Unfolding the role of protein misfolding in neurodegenerative diseases. *Nature Reviews Neuroscience*, *4*(1), 49–60. https://doi.org/10.1038/nrn1007

Sperling, R., Salloway, S., Brooks, D. J., Tampieri, D., Barakos, J., Fox, N. C., Raskind, M., Sabbagh, M., Honig, L. S., Porsteinsson, A. P., & Lieberburg, I. (2014). *NIH Public Access analysis*. *11*(3), 241–249. https://doi.org/10.1016/S1474-4422(12)70015-7.Amyloid-related

Spillantini, M. G., Murrell, J. R., Goedert, M., Farlow, M. R., Klug, A., & Ghetti, B. (1998). Mutation in the tau gene in familial multiple system tauopathy with presenile dementia. *Proceedings of the National Academy of Sciences of the United States of America*, *95*(13), 7737–7741. https://doi.org/10.1073/pnas.95.13.7737

Stack, C., Jainuddin, S., Elipenahli, C., Gerges, M., Starkova, N., Starkov, A. A., Jové, M., Portero-Otin, M., Launay, N., Pujol, A., Kaidery, N. A., Thomas, B., Tampellini, D., Flint Beal, M., & Dumont, M. (2014). Methylene blue upregulates Nrf2/ARE genes and prevents tau-related neurotoxicity. *Human Molecular Genetics*, *23*(14), 3716–3732. https://doi.org/10.1093/hmg/ddu080

Stijlemans, B., Conrath, K., Cortez-Retamozo, V., Van Xong, H., Wyns, L., Senter, P., Revets, H., De Baetselier, P., Muyldermans, S., & Magez, S. (2004). Efficient targeting of conserved cryptic epitopes of infectious agents by single domain antibodies: African trypanosomes as paradigm. *Journal of Biological Chemistry*, *279*(2), 1256–1261. https://doi.org/10.1074/jbc.M307341200

Strokappe, N., Szynol, A., Aasa-Chapman, M., Gorlani, A., Quigley, A., Hulsik, D. L., Chen, L., Weiss, R., de Haard, H., & Verrips, T. (2012). Llama antibody fragments recognizing various epitopes of the CD4bs neutralize a broad range of HIV-1 subtypes A, B and C. *PLoS ONE*, *7*(3). https://doi.org/10.1371/journal.pone.0033298

Tabrizi, S. J., Leavitt, B. R., Landwehrmeyer, G. B., Wild, E. J., Saft, C., Barker, R. A., Blair, N. F., Craufurd, D., Priller, J., Rickards, H., Rosser, A., Kordasiewicz, H. B., Czech, C., Swayze, E. E., Norris, D. A., Baumann, T., Gerlach, I., Schobel, S. A., Paz, E., … Lane, R. M. (2019). Targeting Huntingtin Expression in Patients with Huntington's Disease. *New England Journal of Medicine*, *380*(24), 2307–2316. https://doi.org/10.1056/nejmoa1900907

Takeda, S., Wegmann, S., Cho, H., Devos, S. L., Commins, C., Roe, A. D., Nicholls, S. B., Carlson, G. A., Pitstick, R., Nobuhara, C. K., Costantino, I., Frosch, M. P., Muller, D. J., Irimia, D., & Hyman, B. T. (2015). Neuronal uptake and propagation of a rare phosphorylated high-molecular-weight tau derived from Alzheimer's disease brain. *Nature Communications*, *6*. https://doi.org/10.1038/ncomms9490

Takei, Y. (2000). Defects in axonal elongation and neuronal migration in mice with disrupted tau and map1b genes. *Neuroscience Research*, *38*(5), S105. https://doi.org/10.1016/s0168-0102(00)81476-5

Tamaki, Y., Shodai, A., Morimura, T., Hikiami, R., Minamiyama, S., Ayaki, T., Tooyama, I., Furukawa, Y., Takahashi, R., & Urushitani, M. (2018). Elimination of TDP-43 inclusions linked to amyotrophic lateral sclerosis by a misfolding-specific intrabody with dual proteolytic signals. *Scientific Reports*, *8*(1), 1–16. https://doi.org/10.1038/s41598-018-24463-3

Tanaka, T., & Rabbitts, T. H. (2003). Intrabodies based on intracellular capture frameworks that bind the RAS protein with high affinity and impair oncogenic transformation. *EMBO Journal*, *22*(5), 1025–1035. https://doi.org/10.1093/emboj/cdg106

Tanaka, T., Sewell, H., Waters, S., Phillips, S. E. V., & Rabbitts, T. H. (2011). Single domain intracellular antibodies from diverse libraries: Emphasizing dual functions of LMO2 protein interactions using a single VH domain. *Journal of Biological Chemistry*, *286*(5), 3707–3716. https://doi.org/10.1074/jbc.M110.188193

Tardivel, M., Bégard, S., Bousset, L., Dujardin, S., Coens, A., Melki, R., Buée, L., & Colin, M. (2016). Tunneling nanotube (TNT)-mediated neuron-to neuron transfer of pathological Tau protein assemblies. *Acta Neuropathologica*

Communications, *4*(1), 117. https://doi.org/10.1186/s40478-016-0386-4

Tariot, P. N., Schneider, L. S., Cummings, J., Thomas, R. G., Raman, R., Jakimovich, L. J., Loy, R., Bartocci, B., Fleisher, A., Ismail, M. S., Porsteinsson, A., Weiner, M., Jack, C. R., Thal, L., & Aisen, P. S. (2011). Chronic divalproex sodium to attenuate agitation and clinical progression of Alzheimer disease. *Archives of General Psychiatry*, *68*(8), 853–861. https://doi.org/10.1001/archgenpsychiatry.2011.72

Tenreiro, S., Eckermann, K., & Outeiro, T. F. (2014). Protein phosphorylation in neurodegeneration: Friend or foe? *Frontiers in Molecular Neuroscience*, *7*(MAY), 1–30. https://doi.org/10.3389/fnmol.2014.00042

Tepper, K., Biernat, J., Kumar, S., Wegmann, S., Timm, T., Hübschmann, S., Redecke, L., Mandelkow, E. M., Müller, D. J., & Mandelkow, E. (2014). Oligomer formation of tau protein hyperphosphorylated in cells. *Journal of Biological Chemistry*, *289*(49), 34389–34407. https://doi.org/10.1074/jbc.M114.611368

Terwel, D., Lasrado, R., Snauwaert, J., Vandeweert, E., Van Haesendonck, C., Borghgraef, P., & Van Leuven, F. (2005). Changed conformation of mutant tau-P301L underlies the moribund tauopathy, absent in progressive, nonlethal axonopathy of tau-4R/2N transgenic mice. *Journal of Biological Chemistry*, *280*(5), 3963–3973. https://doi.org/10.1074/jbc.M409876200

Terwel, D., Muyllaert, D., Dewachter, I., Borghgraef, P., Croes, S., Devijver, H., & Van Leuven, F. (2008). Amyloid activates GSK-3β to aggravate neuronal tauopathy in bigenic mice. *American Journal of Pathology*, *172*(3), 786–798. https://doi.org/10.2353/ajpath.2008.070904

Thal, D. R., Rüb, U., Orantes, M., & Braak, H. (2002). *Thal et al., 2002-Phases of Aß-deposition in the human brain and its relevance for the development of AD*.

Theunis, C., Adolfsson, O., Crespo-Biel, N., Piorkowska, K., Pihlgren, M., Hickman, D. T., Gafner, V., Borghgraef, P., Devijver, H., Pfeifer, A., Van Leuven, F., & Muhs, A. (2017). Novel Phospho-Tau Monoclonal Antibody Generated Using a Liposomal Vaccine, with Enhanced Recognition of a Conformational Tauopathy Epitope. *Journal of Alzheimer's Disease*, *56*(2), 585–599. https://doi.org/10.3233/JAD-160695

Theunis, C., Crespo-Biel, N., Gafner, V., Pihlgren, M., López-Deber, M. P., Reis, P., Hickman, D. T., Adolfsson, O., Chuard, N., Ndao, D. M., Borghgraef, P., Devijver, H., Van Leuven, F., Pfeifer, A., & Muhs, A. (2013). Efficacy and safety of a liposome-based vaccine against protein Tau, assessed in Tau.P301L mice that model tauopathy. *PLoS ONE*, *8*(8). https://doi.org/10.1371/journal.pone.0072301

Toosi, K. (2014). 基因的改变NIH Public Access. *Bone*, *23*(1), 1–7. https://doi.org/10.1016/j.neuron.2012.03.004.Predicting

Torreilles, F., Roquet, F., Granier, C., Pau, B., & Mourton-Gilles, C. (2000). Binding specificity of monoclonal antibody AD2: influence of the phosphorylation state of tau. *Molecular Brain Research*, *78*(1–2), 181–185. https://doi.org/10.1016/S0169-328X(00)00073-5

Trinczek, B., Biernat, J., Baumann, K., Mandelkow, E., & Mandelkow, E. M. (1995). Domains of tau protein, differential phosphorylation, and dynamic instability of microtubules. *Molecular Biology of the Cell*, *6*(12), 1887–1902. https://doi.org/10.1091/mbc.6.12.1887

Tsoi, K. K. F., Chan, J. Y. C., Leung, N. W. Y., Hirai, H. W., Wong, S. Y. S., & Kwok, T. C. Y. (2016). Combination Therapy Showed Limited Superiority Over Monotherapy for Alzheimer Disease: A Meta-analysis of 14 Randomized Trials. *Journal of the American Medical Directors Association*, *17*(9), 863.e1-863.e8. https://doi.org/10.1016/j.jamda.2016.05.015

Umeda, T., Eguchi, H., Kunori, Y., Matsumoto, Y., Taniguchi, T., Mori, H., & Tomiyama, T. (2015). Passive immunotherapy of tauopathy targeting pSer413-tau: a pilot study in mice. *Annals of Clinical and Translational Neurology*, *2*(3), 241–255. https://doi.org/10.1002/acn3.171

Valera, E., Spencer, B., & Masliah, E. (2016). Immunotherapeutic Approaches Targeting Amyloid-β, α-Synuclein, and Tau for the Treatment of Neurodegenerative Disorders. *Neurotherapeutics*, *13*(1), 179–189. https://doi.org/10.1007/s13311-015-0397-z

Van Audenhove, I., Van Impe, K., Ruano-Gallego, D., De Clercq, S., De Muynck, K., Vanloo, B., Verstraete, H., Fernández, L. Á., & Gettemans, J. (2013). Mapping cytoskeletal protein function in cells by means of nanobodies. *Cytoskeleton*, *70*(10), 604–622. https://doi.org/10.1002/cm.21122

Van De Broek, B., Devoogdt, N., Dhollander, A., Gijs, H. L., Jans, K., Lagae, L., Muyldermans, S., Maes, G., & Borghs, G. (2011). Specific cell targeting with nanobody conjugated branched gold nanoparticles for photothermal therapy. *ACS Nano*, *5*(6), 4319–4328. https://doi.org/10.1021/nn1023363

Van Eersel, J., Ke, Y. D., Liu, X., Delerue, F., Kril, J. J., Götz, J., & Ittner, L. M. (2010). Sodium selenate mitigates tau pathology, neurodegeneration, and functional deficits in Alzheimer's disease models. *Proceedings of the National Academy of Sciences of the United States of America*, *107*(31), 13888–13893. https://doi.org/10.1073/pnas.1009038107

Van, M. V., Fujimori, T., & Bintu, L. (2021). Nanobody-mediated control of gene expression and epigenetic memory. *Nature Communications*, *12*(1). https://doi.org/10.1038/s41467-020-20757-1

Vandermeeren, M., Borgers, M., Van Kolen, K., Theunis, C., Vasconcelos, B., Bottelbergs, A., Wintmolders, C., Daneels, G., Willems, R., Dockx, K., Delbroek, L., Marreiro, A., Ver Donck, L., Sousa, C., Nanjunda, R., Lacy, E., Van De Casteele, T., Van Dam, D., De Deyn, P. P., … Mercken, M. H. (2018). Anti-tau monoclonal antibodies derived from soluble and filamentous tau show diverse functional properties in vitro and in vivo. *Journal of Alzheimer's Disease*, *65*(1), 265–281. https://doi.org/10.3233/JAD-180404

VandeVrede, L., Boxer, A. L., & Polydoro, M. (2020). Targeting tau: Clinical trials and novel therapeutic approaches. *Neuroscience Letters*, *731*(July 2019), 134919. https://doi.org/10.1016/j.neulet.2020.134919

Vaneycken, I., D'huyvetter, M., Hernot, S., de Vos, J., Xavier, C., Devoogdt, N., Caveliers, V., & Lahoutte, T. (2011). Immuno-imaging using nanobodies. *Current Opinion in Biotechnology*, *22*(6), 877–881. https://doi.org/10.1016/j.copbio.2011.06.009

Vaneycken, I., Devoogdt, N., Van Gassen, N., Vincke, C., Xavier, C., Wernery, U., Muyldermans, S., Lahoutte, T., & Caveliers, V. (2011). Preclinical screening of anti-HER2 nanobodies for molecular imaging of breast cancer. *The FASEB Journal*, *25*(7), 2433–2446. https://doi.org/10.1096/fj.10-180331

Vidarsson, G., Dekkers, G., & Rispens, T. (2014). IgG subclasses and allotypes: From structure to effector functions. *Frontiers in Immunology*, *5*(OCT), 1–17. https://doi.org/10.3389/fimmu.2014.00520

Vincke, C., Loris, R., Saerens, D., Martinez-Rodriguez, S., Muyldermans, S., & Conrath, K. (2009). General strategy to humanize a camelid single-domain antibody and identification of a universal humanized nanobody scaffold. *Journal of Biological Chemistry*, *284*(5), 3273–3284. https://doi.org/10.1074/jbc.M806889200

Visintin, M., Tse, E., Axelson, H., Rabbitts, T. H., & Cattaneo, A. (1999). Selection of antibodies for intracellular function using a two-hybrid in vivo system. *Proceedings of the National Academy of Sciences of the United States of America*, *96*(21), 11723–11728. https://doi.org/10.1073/pnas.96.21.11723

Vitale, F., Ortolan, J., Volpe, B. T., Marambaud, P., Giliberto, L., & D'Abramo, C. (2020). Intramuscular injection of vectorized-scFvMC1 reduces pathological tau in two different tau transgenic models. *Acta Neuropathologica Communications*, *8*(1), 1–19. https://doi.org/10.1186/s40478-020-01003-7

Von Bergen, M., Friedhoff, P., Biernat, J., Heberle, J., Mandelkow, E. M., & Mandelkow, E. (2000). Assembly of τ protein into Alzheimer paired helical filaments depends on a local sequence motif (306VQIVYK311) forming β structure. *Proceedings of the National Academy of Sciences of the United States of America*, *97*(10), 5129–5134. https://doi.org/10.1073/pnas.97.10.5129

Von Bergen, Martin, Barghorn, S., Li, L., Marx, A., Biernat, J., Mandelkow, E. M., & Mandelkow, E. (2001). Mutations of Tau Protein in Frontotemporal Dementia Promote Aggregation of Paired Helical Filaments by Enhancing Local β-Structure. *Journal of Biological Chemistry*, *276*(51), 48165–48174. https://doi.org/10.1074/jbc.M105196200

Walls, K. C., Ager, R. R., Vasilevko, V., Cheng, D., Medeiros, R., & LaFerla, F. M. (2014). P-Tau immunotherapy reduces soluble and insoluble tau in aged 3xTg-AD mice. *Neuroscience Letters*, *575*, 96–100. https://doi.org/10.1016/j.neulet.2014.05.047

Wang, X., Smith, K., Pearson, M., Hughes, A., Cosden, M. L., Marcus, J., Fred Hess, J., Savage, M. J., Rosahl, T., Smith, S. M., Schachter, J. B., & Uslaner, J. M. (2018). Early intervention of tau pathology prevents behavioral changes in the rTg4510 mouse model of tauopathy. *PLoS ONE*, *13*(4), 1–15. https://doi.org/10.1371/journal.pone.0195486

Wang, Y., Zhang, Y., Hu, W., Xie, S., Gong, C. X., Iqbal, K., & Liu, F. (2015). Rapid alteration of protein phosphorylation

during postmortem: Implication in the study of protein phosphorylation. *Scientific Reports*, *5*(September), 1–11. https://doi.org/10.1038/srep15709

Wang, Z., Gucek, M., & Hart, G. W. (2008). Cross-talk between GlcNAcylation and phosphorylation: Site-specific phosphorylation dynamics in response to globally elevated O-GlcNAc. *Proceedings of the National Academy of Sciences of the United States of America*, *105*(37), 13793–13798. https://doi.org/10.1073/pnas.0806216105

Wegmann, S., Eftekharzadeh, B., Tepper, K., Zoltowska, K. M., Bennett, R. E., Dujardin, S., Laskowski, P. R., MacKenzie, D., Kamath, T., Commins, C., Vanderburg, C., Roe, A. D., Fan, Z., Molliex, A. M., Hernandez-Vega, A., Muller, D., Hyman, A. A., Mandelkow, E., Taylor, J. P., & Hyman, B. T. (2018). Tau protein liquid–liquid phase separation can initiate tau aggregation. *The EMBO Journal*, *37*(7), 1–21. https://doi.org/10.15252/embj.201798049

Wei Qiang1, † W.-M. Y., Jun-Xia Lu1, † J. C., & & Robert Tycko. (2017). Structural variation in amyloid-β fibrils from Alzheimer's disease clinical subtypes. *Nature*, *541*(7636), 217–221. https://doi.org/10.1038/nature20814.Structural

Wesolowski, J., Alzogaray, V., Reyelt, J., Unger, M., Juarez, K., Urrutia, M., Cauerhff, A., Danquah, W., Rissiek, B., Scheuplein, F., Schwarz, N., Adriouch, S., Boyer, O., Seman, M., Licea, A., Serreze, D. V., Goldbaum, F. A., Haag, F., & Koch-Nolte, F. (2009). Single domain antibodies: Promising experimental and therapeutic tools in infection and immunity. *Medical Microbiology and Immunology*, *198*(3), 157–174. https://doi.org/10.1007/s00430-009-0116-7

Wilcock, G. K., Gauthier, S., Frisoni, G. B., Jia, J., Hardlund, J. H., Moebius, H. J., Bentham, P., Kook, K. A., Schelter, B. O., Wischik, D. J., Davis, C. S., Staff, R. T., Vuksanovic, V., Ahearn, T., Bracoud, L., Shamsi, K., Marek, K., Seibyl, J., Riedel, G., … Wischik, C. M. (2018). Potential of Low Dose Leuco-Methylthioninium Bis(Hydromethanesulphonate) (LMTM) Monotherapy for Treatment of Mild Alzheimer's Disease: Cohort Analysis as Modified Primary Outcome in a Phase III Clinical Trial. *Journal of Alzheimer's Disease*, *61*(1), 435–457. https://doi.org/10.3233/JAD-170560

Wilkaniec, A., Czapski, G. A., & Adamczyk, A. (2016). Cdk5 at crossroads of protein oligomerization in neurodegenerative diseases: Facts and hypotheses. *Journal of Neurochemistry*, *136*(2), 222–233. https://doi.org/10.1111/jnc.13365

Williams, B., Jalilianhasanpour, R., Matin, N., Fricchione, G. L., Sepulcre, J., Keshavan, M. S., ... & Perez, D. L. (2018). Individual differences in corticolimbic structural profiles linked to insecure attachment and coping styles in motor functional ne, 230-237. (2019). 乳鼠心肌提取 HHS Public Access. *Physiology & Behavior*, *176*(3), 139–148. https://doi.org/10.1038/s41594-018-0057-1.Mapping

Wintjens, R., Wieruszeski, J. M., Drobecq, H., Rousselot-Pailley, P., Buée, L., Lippens, G., & Landrieu, I. (2001). 1H NMR Study on the Binding of Pin1 Trp-Trp Domain with Phosphothreonine Peptides. *Journal of Biological Chemistry*, *276*(27), 25150–25156. https://doi.org/10.1074/jbc.M010327200

Wischik, C. M., Edwards, P. C., Lai, R. Y. K., Roth, M., & Harrington, C. R. (1996). Selective inhibition of Alzheimer disease-like tau aggregation by phenothiazines. *Proceedings of the National Academy of Sciences of the United States of America*, *93*(20), 11213–11218. https://doi.org/10.1073/pnas.93.20.11213

Wischik, C M, Novak, M., Edwards, P. C., Klug, A., Tichelaar, W., & Crowther, R. A. (1988). Structural characterization of the core of the paired helical filament of Alzheimer disease (molecular pathology/neurodegenerative disease/neurofibrillary tangles/snnng transmission electron microscopy). *Medical Sciences*, *85*(July), 4884–4888.

Wischik, Claude M., Harrington, C. R., & Storey, J. M. D. (2014). Tau-aggregation inhibitor therapy for Alzheimer's disease. *Biochemical Pharmacology*, *88*(4), 529–539. https://doi.org/10.1016/j.bcp.2013.12.008

Wolozin, B. L., Pruchnicki, A., Dickson, D. W., & Davies, P. (1986). A neuronal antigen in the brains of Alzheimer patients. *Science*, *232*(4750), 648–650. https://doi.org/10.1126/science.3083509

Wu, J. W., Hussaini, S. A., Bastille, I. M., Rodriguez, G. A., Mrejeru, A., Rilett, K., Sanders, D. w., Cook, C., Fu, H., Boonen, R., Herman, M., Nahmani, E., Emrani, S., Figueroa, H., Diamond, M. I., Clelland, C., Wray, S., & Duff, K. E. (2016). Neuronal activity enhances tau propagation and tau pathology in vivo conducted the experiments and data analyses HHS Public Access Author manuscript. *Nat Neurosci*, *19*(8), 1085–1092. https://doi.org/10.1038/nn.4328.Neuronal

Yamada, K., Cirrito, J. R., Stewart, F. R., Jiang, H., Finn, M. B., Holmes, B. B., Binder, L. I., Mandelkow, E. M., Diamond, M. I., Lee, V. M. Y., & Holtzman, D. M. (2011). In vivo microdialysis reveals age-dependent decrease of brain interstitial fluid tau levels in P301S human tau transgenic mice. *Journal of Neuroscience*, *31*(37), 13110–13117. https://doi.org/10.1523/JNEUROSCI.2569-11.2011

Yanamandra, K., Jiang, H., Mahan, T. E., Maloney, S. E., Wozniak, D. F., Diamond, M. I., & Holtzman, D. M. (2015). Anti-tau antibody reduces insoluble tau and decreases brain atrophy. *Annals of Clinical and Translational Neurology*, *2*(3), 278–288. https://doi.org/10.1002/acn3.176

Yanamandra, K., Kfoury, N., Jiang, H., Mahan, T. E., Ma, S., Maloney, S. E., Wozniak, D. F., Diamond, M. I., & Holtzman, D. M. (2013). Anti-tau antibodies that block tau aggregate seeding invitro markedly decrease pathology and improve cognition in vivo. *Neuron*, *80*(2), 402–414. https://doi.org/10.1016/j.neuron.2013.07.046

Yang, T., Dang, Y., Ostaszewski, B., Mengel, D., Steffen, V., Rabe, C., Bittner, T., Walsh, D. M., & Selkoe, D. J. (2019). Target engagement in an alzheimer trial: Crenezumab lowers amyloid β oligomers in cerebrospinal fluid. *Annals of Neurology*, *86*(2), 215–224. https://doi.org/10.1002/ana.25513

Yau, K. Y. F., Dubuc, G., Li, S., Hirama, T., MacKenzie, C. R., Jermutus, L., Hall, J. C., & Tanha, J. (2005). Affinity maturation of a VHH by mutational hotspot randomization. *Journal of Immunological Methods*, *297*(1–2), 213–224. https://doi.org/10.1016/j.jim.2004.12.005

Yu, Y., Zhang, L., Li, X., Run, X., Liang, Z., Li, Y., Liu, Y., Lee, M. H., Grundke-Iqbal, I., Iqbal, K., Vocadlo, D. J., Liu, F., & Gong, C. X. (2012). Differential effects of an o-glcnacase inhibitor on tau phosphorylation. *PLoS ONE*, *7*(4), 1–8. https://doi.org/10.1371/journal.pone.0035277

Yuzwa, S. A., Cheung, A. H., Okon, M., McIntosh, L. P., & Vocadlo, D. J. (2014). O-GlcNAc Modification of tau Directly Inhibits Its Aggregation without Perturbing the Conformational Properties of tau Monomers. *Journal of Molecular Biology*, *426*(8), 1736–1752. https://doi.org/10.1016/j.jmb.2014.01.004

Yuzwa, S. A., Shan, X., MacAuley, M. S., Clark, T., Skorobogatko, Y., Vosseller, K., & Vocadlo, D. J. (2012). Increasing O-GlcNAc slows neurodegeneration and stabilizes tau against aggregation. *Nature Chemical Biology*, *8*(4), 393–399. https://doi.org/10.1038/nchembio.797

Zhang, W., Falcon, B., Murzin, A. G., Fan, J., Crowther, R. A., Goedert, M., & Scheres, S. H. W. (2019). Heparin-induced tau filaments are polymorphic and differ from those in alzheimer's and pick's diseases. *ELife*, *8*, 1–24. https://doi.org/10.7554/eLife.43584

Zhang, Yan, & Lee, D. H. S. (2011). Sink hypothesis and therapeutic strategies for attenuating Aβ levels. *Neuroscientist*, *17*(2), 163–173. https://doi.org/10.1177/1073858410381532

Zhang, Yun, & Pardridge, W. M. (2001). Mediated efflux of IgG molecules from brain to blood across the blood-brain barrier. *Journal of Neuroimmunology*, *114*(1–2), 168–172. https://doi.org/10.1016/S0165-5728(01)00242-9

Zhou, X. Z., Kops, O., Werner, A., Lu, P. J., Shen, M., Stoller, G., Küllertz, G., Stark, M., Fischer, G., & Lu, K. P. (2000). Pin1-dependent prolyl isomerization regulates dephosphorylation of Cdc25C and Tau proteins. *Molecular Cell*, *6*(4), 873–883. https://doi.org/10.1016/S1097-2765(05)00083-3

Zhu, Y., Shan, X., Yuzwa, S. A., & Vocadlo, D. J. (2014). The emerging link between O-GlcNAc and Alzheimer disease. *Journal of Biological Chemistry*, *289*(50), 34472–34481. https://doi.org/10.1074/jbc.R114.601351

Zuckerman, J. E., & Davis, M. E. (2015). Clinical experiences with systemically administered siRNA-based therapeutics in cancer. *Nature Reviews Drug Discovery*, *14*(12), 843–856. https://doi.org/10.1038/nrd4685

VIII. Publications

Inhibition of Tau seeding by targeting Tau nucleation core within neurons with a single domain antibody fragment

Clément Danis[1,2,3*], Elian Dupré[1,2,3*], Orgeta Zejneli[1,2,3*], Raphaëlle Caillierez[3], Alexis Arrial[4], Séverine Bégard[3], Justine Mortelecque[1,2], Sabiha Eddarkaoui[3], Anne Loyens[3], François-Xavier Cantrelle[1,2], Xavier Hanoulle[1,2], Jean-Christophe Rain[4], Morvane Colin[3§], Luc Buée[3§‡], Isabelle Landrieu[1,2§‡]

[1]*CNRS ERL9002 BSI Integrative Structural Biology F-59000 Lille, France*

[2]*Univ. Lille, Inserm, CHU Lille, Institut Pasteur de Lille, U1167 - RID-AGE - Risk Factors and Molecular Determinants of Aging-Related Diseases, F-59000 Lille, France*

[3]*Univ. Lille, Inserm, CHU Lille, U1172 - LilNCog - Lille Neuroscience & Cognition, F-59000 Lille, France*

[4]*Hybrigenic Services, F-91000 Evry*-Courcouronnes*, France*

*,§ Equal contributions

‡Correspondence should be addressed to:

I.L.(isabelle.landrieu@univ-lille.fr)

50, Avenue de Halley

59658 Villeneuve d'Ascq France, Tel +33362531712

L.B. (luc.buee@inserm.fr)

1, place de Verdun

59045 Lille, France, Tel +33320298670

Short Title : Tau-specific Nanobodies

Tau proteins aggregate into filaments in brain cells in Alzheimer's disease and related disorders referred to as tauopathies. Here, we used fragments of camelid heavy-chain-only antibodies (VHHs or single domain antibody fragments) targeting Tau as immuno-modulators of its pathologic seeding. A VHH issued from the screen against Tau of a synthetic phage-display library of humanized VHHs was selected for its capacity to bind Tau microtubule-binding domain, composing the core of Tau fibrils. This parent VHH was optimized to improve its biochemical properties and to act in the intra-cellular compartment, resulting in VHH Z70. VHH Z70 precisely binds the PHF6 sequence, known for its nucleation capacity, as shown by the crystal structure of the complex. VHH Z70 was more efficient than the parent VHH to inhibit *in vitro* Tau aggregation in heparin-induced assays. Expression of VHH Z70 in a cellular model of Tau seeding also decreased the aggregation-reporting fluorescence signal. Finally, intra-cellular expression of VHH Z70 in the brain of an established tauopathy mouse seeding model demonstrated its capacity to mitigate accumulation of pathological Tau. VHH Z70, by targeting Tau inside brain neurons, where most of the pathological Tau resides, provides a new immunological tool to target the intra-cellular compartment in tauopathies.

INTRODUCTION

In neurodegenerative disorders, immunotherapy is currently actively explored as a disease-modifying treatment. Improving immunological tools to treat these disorders is thus a key challenge. Next to classical vaccination or the use of immunoglobulin (Ig) in passive immunotherapies, new approaches are now available. The Fv variable domains, which determine antibody specificity, can now be expressed independently of the Ig framework. These fragments - as single chain fragments of the Fv in scFvs or single domain fragments in VHHs[1] (Variable Heavy-chain of the Heavy-chain-only antibodies) - can be engineered to be active intracellularly. Such immunological tools are likely to be useful given that the protein aggregates in neurodegenerative proteinopathy disorders are mostly found within neuronal cells.[2] In this work, we have explored the use of VHHs in one group of these disorders, referred to as tauopathies.

Aggregation of the intrinsically disordered neuronal Tau protein to form fibrillar amyloid structures is related to these tauopathies, including the most prevalent, Alzheimer's disease (AD). AD is characterized by both extracellular amyloid deposits made of Aß (amyloid) peptides and intra-neuronal neurofibrillary tangles (NFTs) formed by Tau protein aggregates.[3] In the pathological context, Tau is the principal component of paired helical filaments (PHFs) and straight filaments,[4,5] which form the intra-cellular fibrillar deposits leading to the neuropathological lesions. In addition, it has been proposed that extracellular pathological Tau species are taken up in cells, leading to intra-cellular Tau seeding and the polymerization process.[6–8] Intervention strategies based on the amyloid cascade hypothesis had, up to date, limited success despite their being the primary target of clinical assays.[9] In AD, the severity of cognitive decline is better correlated with the evolution of NFTs than amyloid deposits.[10–12] In other tauopathies, no amyloid deposition is observed. This emphasizes the need to pursue other biological hypotheses than the amyloid cascade, including Tau-based ones, in search for disease-modifying treatments for tauopathies.

The compelling results of immunotherapies directed against Tau in several transgenic (Tg) mouse models of tauopathies, in decreasing Tau accumulation and in some case ensuring recovery of cognitive or motor functions,[13–20] have motivated several pharmaceutical companies to launch clinical trials of active and passive immunization, the latter with various Tau-specific monoclonal antibodies.[21,22] However, advances in the field still require deciphering key aspects of efficient Tau-specific immunotherapies and to develop their full potential to target tauopathies. The road to anti-Tau immunotherapies is opened based on the evidence of both Tau seeding capacity and Tau propagation.[23–26] Yet, most pathological Tau assemblies remains intra-cellular in the cytoplasm, where it is not the primary target of Tau-specific conventional immunotherapies using Ig. In addition, the extracellular Tau could, at least partly, remains unattainable to Tau-specific antibodies, as would be the case for Tau in extracellular vesicles[27,28] or nanotubes.[29] Finally, the propagation pattern related to extracellular Tau, clearly defined in AD, could also be less relevant in pure and more acute tauopathies, for which the time frame restrains the propagation.[25] In these latter cases, the rational to target extracellular Tau is weaker.

Exploring the capacity to use immunotherapies targeting the intra-neuronal Tau has thus become an important challenge to further explore. With that in mind, we have chosen VHHs, commonly called nanobodies, to target new and original epitopes of Tau, and to optimize their intra-cellular activity. VHHs consist in a unique heavy-chain

that corresponds to the variable heavy-chain from *Camelidae* immunoglobulins[1]. The interest of using the VHHs instead of the classical antibodies stand in their easy generation, from a synthetic library, involving no animal handling, their selection using phage-display, their production in periplasm of bacteria, as well as the multiple possibilities offered by modification using protein engineering.[30] They can be modified to penetrate into the cytoplasm of cells,[31,32] or to be expressed inside the cells,[33] and bind specifically to their target epitope. Additionally, VHHs showed their potential as diagnostic tools to target NFTs with an affinity and specificity very close to antibodies already used for detecting these pathologic features by immunochemistry, opening the way for new probes in *in vivo* imaging experiments.[34] As demonstrated with scFvs,[35,36] we here showed that it is also possible to select, to optimize and to consider VHHs as therapeutic tools in tauopathies.

Besides the Tau location targeted by the VHHs, the epitope recognition is another parameter of crucial interest to mitigate the seeding and polymerization of the intra-cellular Tau. Tau can be divided into 4 domains comprising the N-terminal domain (N1-N2), the proline-rich domain (P1-P2), the microtubule-binding domain (MTBD) constituted itself of 4 partially repeated regions, R1 to R4, and the C-terminal domain (**Figure 1b** scheme). Two homologous hexapeptides named PHF6* ($_{275}$VQIINK$_{280}$) and PHF6 ($_{306}$VQIVYK$_{311}$) located respectively at the beginning of R2 and R3 repeat regions (**Figure 1b** scheme) of Tau MTBD are nuclei of Tau aggregation.[37]

Taking that into consideration, a Tau-specific VHH targeting the MTBD was selected from a screen of a humanized naive synthetic library initially performed to obtain VHHs targeting the different Tau domains. In addition, we optimized this parent VHH by a yeast two-hybrid approach to obtain VHH Z70, which efficiently binds Tau once expressed in the intra-cellular environment. VHH Z70 decreased Tau fibrils assembly *in vitro* and in HEK293 seeding-reporting cellular model. After transduction by lentiviral vectors (LVs) in the hippocampal formation of a tauopathy mouse model, the expressed VHH Z70 significantly reduced Tau seeding induced by human AD brain homogenates. Z70 antibody fragment thus provides a new immunological tool to target Tau in cells and to open the way for future gene therapy.

RESULTS

Identification of synthetic VHHs directed against Tau microtubule-binding domain

To generate original VHHs targeting various Tau domains, ~~with the potential to block its aggregation,~~ 20 clones resulting from the screen of a synthetic phage-display library of humanized llama single-domain antibody[38] against recombinant Tau protein (Tau 2N4R longest isoform) were initially selected for further analysis. Definition of the region recognized by each of these VHHs was a first step in assessing their properties. Resonance perturbation mapping in ^{1}H, ^{15}N HSQC spectra of ^{15}N-Tau, obtained by nuclear magnetic resonance (NMR) spectroscopy, allowed to define the various binding regions of the VHHs along Tau sequence. Comparison of the spectra of Tau alone in solution or in the presence of a VHH identified the spectral perturbations that are used to define the binding region. The initial screening of the different clones showed recognition of five different regions of Tau from the proline-rich region to the C-terminus (**Figures 1** and **S1**). We have previously described the series of Tau-specific VHHs targeting the C-terminus of Tau, and parent VHH F8-2, which shows interesting properties as molecular tool to detect Tau in research experiments. Nevertheless, F8-2 has no capacity to interfere with Tau seeding and polymerization.[39]

Interestingly, one VHH, named VHH E4-1, affected resonances in Tau spectrum corresponding to residues within the R2-R3 repeats of the MTBD (**Figure 1**). The binding mapping was confirmed using a Tau fragment that corresponded to the isolated MTBD. The smaller size of this Tau fragment (124 amino acid residues instead of 441) resulted in fewer resonances and less resonance overlap in the corresponding Tau[245-368] ^{1}H, ^{15}N spectrum, facilitating the identification of the binding region (**Figures S2** and **S3**). The affected resonances corresponded to amino acid residues located in a stretch expanding from residue V275 to K317 including the two aggregation nuclei PHF6* and PHF6 (**Figure S3b**). VHH E4-1 thus bound within the R2-R3 repeats of the MTBD.

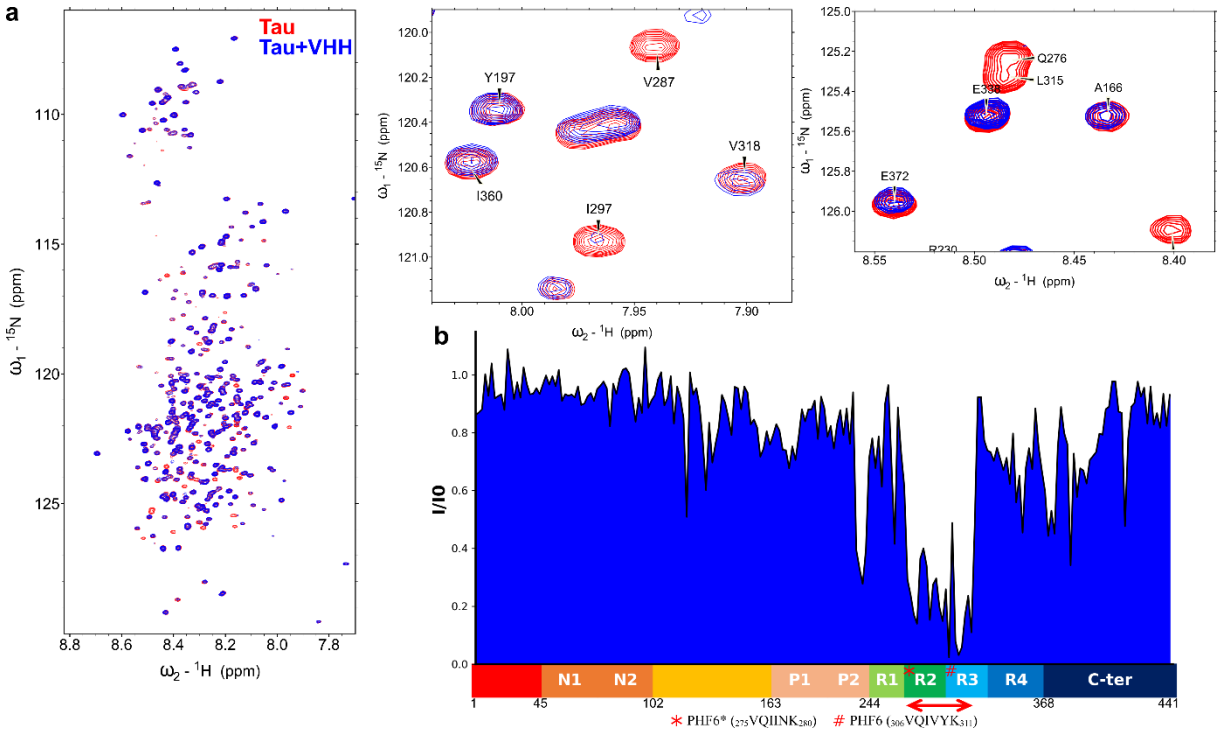

Figure 1 VHH E4-1 binds to the MTBD of Tau. (**a**) Overlay of ^{1}H, ^{15}N HSQC two-dimensional full spectra and enlargements of free full-length Tau2N4R (in red) or Tau2N4R mixed with non-labelled VHH E4-1 (in blue) (n=1). In the spectrum of Tau in the presence of VHH E4-1, multiple resonances are broadened beyond detection compared to the Tau control spectrum. (**b**) Normalized NMR intensities (I/I0) along the Tau sequence with (I0) and (I) corresponding to the resonance intensity when Tau is free in solution or mixed with equimolar quantity of VHH E4-1 (I), respectively. The normalized intensity ratios (I/I0) plot allowed the identification of the Tau MTBD domain as the target of VHH E4-1 interaction. A red double-arrow indicates the region containing the corresponding major broadened resonances, which was mapped to the R2-R3 repeats in the MTBD. N1 and N2 are two inserted sequences in the N-terminal domain (1-163) that are not present in all Tau isoforms (named Tau 0N, Tau 1N or Tau 2N), the proline-rich domain is subdivided in P1 and P2 regions, the MTBD consists of 4 partially repeated regions, R1 to R4 (in Tau 4R). The R2 repeat is not present in Tau 3R. C-ter is for the C-terminal domain.

Optimization of parent VHH E4-1 into variant VHH Z70

An important property of the VHHs is their capacity to be expressed and to recognize their target in the cellular environment. However, some VHHs might be ineffective in binding once expressed in a cell due to their improper folding leading to aggregation or instability.[40] For instance, VHH E4-1 did not bind Tau in yeast two-hybrid assays that require the interaction to take place in the yeast nucleus, providing an evaluation of VHH E4-1 intra-cellular

binding capacity[41] (**Figure 2a**). VHH E4-1 was thus next submitted to an original round of optimization, using yeast two-hybrid system, to maximize its capacity to recognize its target when expressed in a cellular environment. First, we built a cDNA mutant library by random mutagenesis, targeting the whole sequence of VHH E4-1 to produce a variety of VHH preys (VHH-Gal4-activation domain fusion) against the Tau bait (LexA-Tau fusion). The library of 1.5 million variants was transformed in yeast and screen by cell-to-cell mating to get positive colonies under the pressure of selection conditions corresponding to undetected VHH E4-1-Tau interaction (**Figure 2a**). A single optimized variant named VHH Z70 was obtained, resulting from 4 mutations G12V, P16S, T81M and W114G located in the framework domains (FR) (**Figure 2b**). Fluorescence imaging of HEK cells expressing mCherry-VHH E4-1 showed focal inclusion bodies illustrated by the detection of fluorescent puncta aggregates (**Figures 2c and S4**). In contrast, most cells transfected with mCherry-VHH Z70 construct clearly showed the intracellular solubility of VHH Z70 because a homogenous strong fluorescence signal filled the cells (**Figure 2d and S4**). The optimization of parent VHH E4-1 for intracellular applications thus succeeded in providing the VHH Z70 with good stability in cells (**Figure 2e**). Location of the 4 stabilizing mutations outside the recognition loops (CDR) (**Figure 2b**) suggest that the epitope recognized by VHH Z70 mutant is unaltered. Conservation of the binding region was confirmed by NMR resonance perturbation mapping, using labelled Tau and MTBD in the same manner as for the parent VHH E4-1 (**Figures S5 and S6**). Interactions of VHH E4-1 and VHH Z70 with full-length Tau2N4R were further characterized using surface plasmon resonance spectroscopy (SPR) with biotinylated-Tau immobilized at the surface of a streptavidin-functionalized chip. The assay provided the kinetic parameters of the interactions, characterized by dissociation constants Kd of 345 nM for VHH E4-1 (**Figure 2f**) and Kd of 147 nM for variant VHH Z70 (**Figure 2g**). VHH Z70, optimized for intra-cellular activity, had a better affinity for its target than its parent VHH E4-1, the major optimization concerning the association constant (k_{on}) (**Figure S7**). SPR was additionally performed with biotinylated VHH Z70 immobilized on the chips. A Tau peptide [273-318] corresponding to the NMR-identified VHH binding site, fused to a SUMO domain to improve its solubility, was injected into the flux. VHH Z70 interacted with the fused peptide with a Kd of 21 nM (**Figure 3a and S7**), confirming that this peptide in Tau sequence was self-sufficient for VHH-Z70 binding.

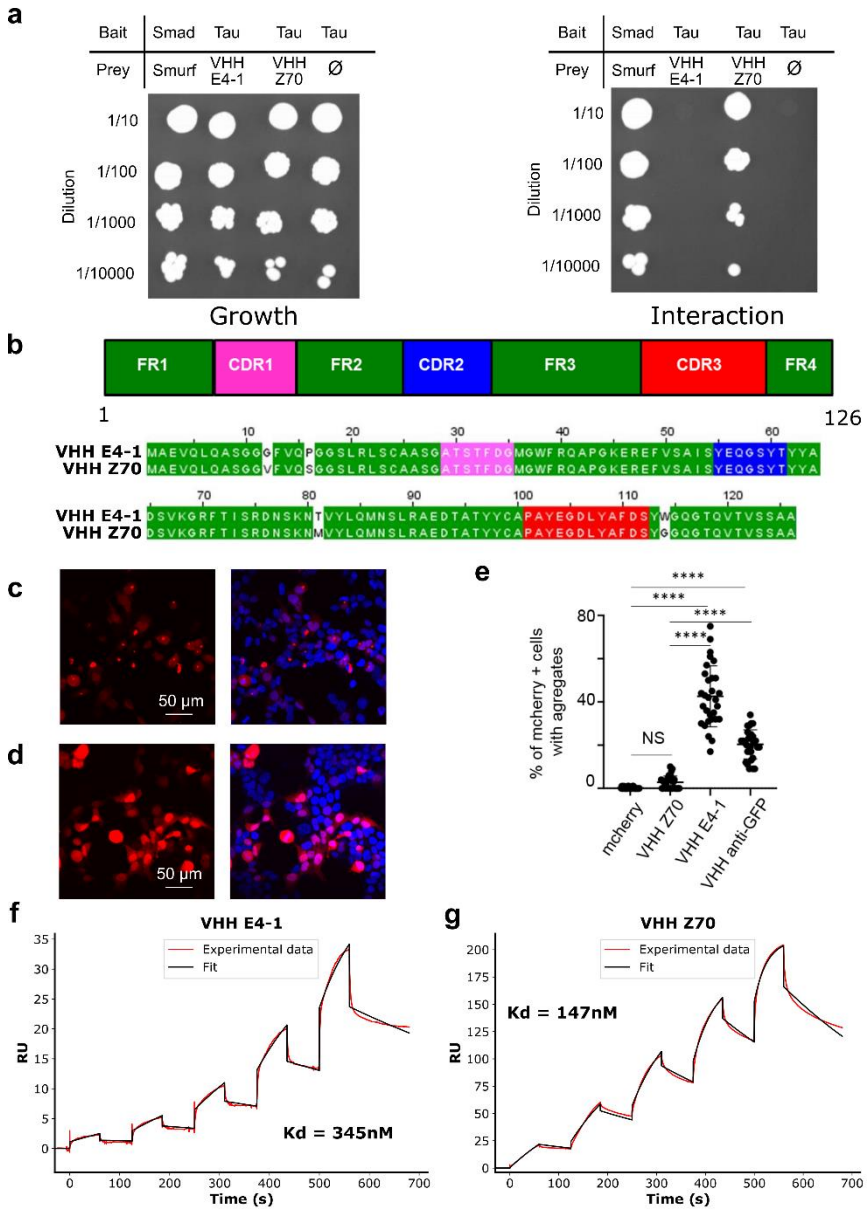

Figure 2 VHH Z70 is optimized for intra-cellular binding and has a better affinity for Tau than VHH E4-1. (**a**) Results from yeast two-hybrid. A growth test on non-selective medium (*left panel*, lacking only leucine and tryptophan) or on selective medium (*right panel,* lacking leucine, tryptophan and histidine) was performed with dilution (*top to bottom*) of the diploid yeast culture expressing both bait and prey constructs. Positive and negative controls of interaction consist respectively in Smad/Smurf interaction[42] and Tau alone (empty vector). VHH E4-1 did not interact with Tau in yeast (no growth on selective medium) whereas VHH Z70 did. (**b**) Domain organization of the VHHs (CDR are for complementarity-determining regions and FR for framework regions) and sequence alignment between VHH E4-1 and VHH Z70 showing 4 mutations in the FR: G12V, P16S, T81M and W114G. (**c-d**) HEK293 cells were transfected with plasmid encoding either (**c**) mCherry-VHH E4.1 or (**d**) mCherry-VHH Z70 and mCherry or mCherry GFP-specific VHH (**Figure S4**). mCherry is visualized in red and nuclei in blue. The scale bar is indicated on the figure. (**e**) Percentage of mCherry positive cells with puncta is provided for 10 images per group and three independent experiments (30 points) (**f-g**) Sensorgrams (reference subtracted data) of single

cycle kinetics analysis performed on immobilized biotinylated Tau, with five injections of (**f**) VHH E4-1 or (**g**) VHH Z70 at 0.125 µM, 0.25 µM, 0.5 µM, 1 µM, and 2 µM (n=1). Dissociation equilibrium constant Kd were calculated from the ratio of off-rate and on-rate kinetic constants k_{off}/k_{on}. k_{on}, k_{off} and Kd are included in the table in **Figure S7**. Black lines correspond to the fitted curves, red lines to the measurements.

Identification of the minimal Tau epitope recognized by VHH Z70

To determine the minimal sequence that VHH Z70 binds within the R2-R3 Tau repeats, an epitope mapping was performed using yeast two-hybrid (267.10^3 tested interactions) with VHH Z70 as bait (LexA-VHH fusion) against a library of Tau fragments as preys (GAL4 activation domain-Tau fragments fusion). 90 positive clones were selected for their growth in the selection conditions, evidencing binding of VHH Z70 to Tau fragments of various length, from a small-scale cell-to-cell mating screen. Comparison of the Tau prey fragment sequences corresponding to these 90 interactions identified peptide $_{305}$SVQIVYKPV$_{313}$ as the minimal common recognition motif of Tau that VHH Z70 can bind (**Figure S8**). The sequence is localized in the R3 repeat of the MTBD domain and contains the PHF6 peptide $_{306}$VQIVYK$_{311}$. We next used Tau2N3R isoform that lacks the R2 repeat and so does not contain the PHF6* peptide, to confirm that the R3 repeat that contains the PHF6 peptide was sufficient for the interaction. As observed in the NMR resonance intensity profile, the interaction of VHH Z70 with Tau2N3R is maintained, and the most affected resonances in the Tau NMR spectrum corresponded to the PHF6 residues in the R3 repeats (**Figure S9**), confirming that PHF6* is not necessary for VHH Z70 binding to Tau. In the yeast two-hybrid system, we next used chimeric constructs of the MTBD that have been modified to display two PHF6 or two PHF6* instead of the wild-type PHF6 and PHF6* (**Figures 3b and S10a)**. VHH Z70 did not interact with chimeric MTBD with two PHF6* (PHF6*x2) in yeast (no growth on selective medium) whereas it did interact with Tau and chimeric MTBD with two PHF6 (PHF6x2) (**Figure 3b**). VHH Z70 was thus not able to bind the double PHF6* construct, in conditions corresponding to positive binding to Tau or to the double PHF6 chimeric MTBD. SPR was additionally performed with biotinylated VHH Z70 immobilized on the chip while the MTBD or each of these chimeric constructs were injected in the flux. VHH Z70 interacted with the MTBD or the chimeric MTBD with two PHF6 with Kd of 146 nM and 34 nM, respectively (**Figure S10b-c**), while interaction with the PHF6* is characterized by a Kd of 398 nM (**Figure S10d**). The rate of dissociation (koff) was the major parameter that explained the Kd differences. In conclusion, the epitope of the VHH Z70 was defined as the PHF6 sequence by

several concurring approaches and in *in vitro* conditions, residual interaction of VHH Z70 is detected with the PHF6* sequence.

Structure of VHH Z70 in complex with a PHF6 peptide

To obtain further atomic detail on the PHF6 recognition by VHH Z70, the structure of the complex between VHH Z70 and a Tau[301-312] peptide, including the PHF6 sequence, was solved by X-ray crystallography at a resolution of 1.7Å. Structure of this complex clearly demonstrated the direct interaction of residues from the CDR3 loop with each residue of the PHF6 sequence. The complex assembly was characterized by the formation of a three-stranded ß-sheet formed by two strands from the CDR3 folded in a β hairpin and one strand formed by the PHF6 sequence that adopts an elongated conformation (**Figures 3c and S11a**). CDR1 and CDR2 loops are not participating directly in the interaction but we cannot exclude that they might be involved in the interaction with full length Tau. The interface area is 480 Å², corresponding to 526 Å² of buried accessible surface area from the peptide (38% of total peptide surface, residues 305 to 312) and 434 Å² buried accessible surface area from the VHH (7% of total, residues 39, 47-49, 63-65, 68, 104-110) (**Figure S11b**). Residues 111 to 115 of VHH Z70 were not resolved, indicating a high degree of flexibility of this region corresponding to the last 2 residues of CDR3 and the first 3 residues of FR4. One of the mutations (W114G) that distinguished VHH E4-1 from VHH Z70 was in this segment, indicating that the observed flexibility might be important for CDR3 positioning. The interaction with the CDR3 was stabilized by formation of five intermolecular hydrogen-bonds (**Figure S11c**) involving atoms of the backbone of PHF6 peptide, residues S305 to P312, through a β-augmentation mechanism (**Figure 3c**). Structure of the complex confirmed that the S305 to P312 sequence was sufficient for VHH Z70 binding, although binding might also be partly context-dependent and optimal when the recognition segment is embedded in the full-length protein (or at least MTBD).

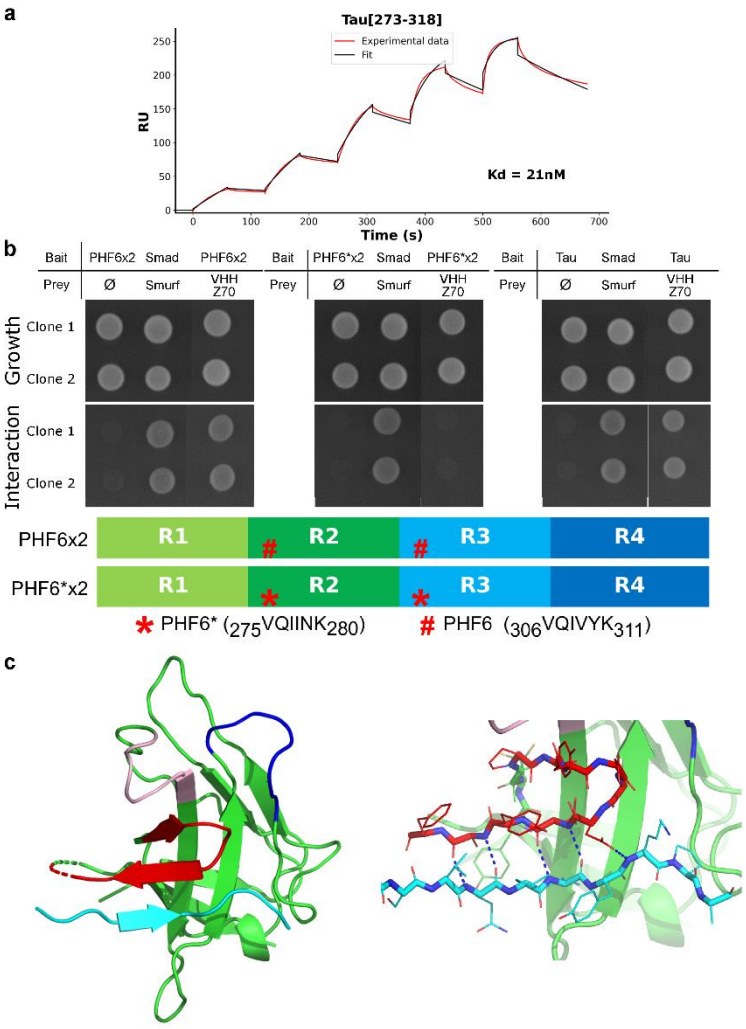

Figure 3 The PHF6 peptide sequence is essential for VHH Z70 binding to Tau MTBD.

(a) Sensorgram (reference subtracted data) of single-cycle kinetics analysis performed on immobilized biotinylated VHH Z70, with five injections of peptide Tau[273-318] fused at its N-terminus with the SUMO protein (n=1) at 31.25 nM, 62.5 nM, 125 nM, 250 nM and 500 nM. Tau peptide sequence and, k_{on}, k_{off} and Kd are included in the table in **Figure S7**. Black lines correspond to the fitted curves, red lines to the measurements. (**b**) Results from yeast two-hybrid. The VHH are expressed as preys, with a C-terminal Gal4-activation domain fusion (VHH-Gal4AD) and Tau0N4R/MTBD as bait with a C-terminal fusion with lexA (Tau0N4R/MTBD-LexA). A growth test on non-selective medium (*upper panel Growth*, lacking only leucine and tryptophane) or on selective medium (*lower panel Interaction,* lacking leucine, tryptophane and histidine) was performed of the diploid yeast culture expressing both bait and prey constructs. Positive and negative controls of interaction consist respectively in Smad/Smurf interaction and Tau or chimeric MTBD alone (empty vector). (**c**) Ribbon representation of the crystal structure of the complex between VHH Z70 and the PHF6 peptide. The CDR1, CDR2 and CDR3 loops of VHH 70 are coloured in pink, in dark blue and in red, respectively. Framework regions of the VHH are represented in green

and the PHF6 Tau peptide in cyan. The right panel shows the five intermolecular H-bonds (dashed blue lines) between VHH Z70 and Tau peptide. See **Figure S11** for 90°-rotation view and surface representation.

Inhibition of *in vitro* Tau aggregation

VHH E4-1 and VHH Z70 recognizing Tau peptide PHF6, which is known to nucleate the aggregation process and to form the core of Tau fibers, were assayed for their capacity to interfere with Tau *in vitro* polymerization. The assays were carried out with recombinant Tau protein in the presence of heparin, using thioflavin T as a dye whose fluorescence is increased in presence of aggregates **(Figure 4**). Negative and positive controls consisted in Tau without or with heparin, respectively. An additional control was performed in the presence of VHH F8-2, a VHH issued from the initial phage-library screen (**Figure S1**), which targets Tau C-terminal domain[39]. At 10 µM of Tau, the observed amount of aggregates was maximal (defined as 100%) for the positive control (Tau with heparin, blue line) after 8 h of incubation at 37°C, while no fluorescence change was detected for the negative control (Tau without heparin, black line) (**Figure 4**). At equimolar concentration of Tau:VHH F8-2, the fluorescence signal reached 91.2 % (± 3.8%), showing that VHH F8-2 did not affect the aggregation of Tau (**Figure 4a**, orange line). In contrast, at a molar ratio of 1:0.25 Tau:VHH E4-1, the maximal fluorescence signal reached 86.9 % (± 2.4%). Additionally, about 3.8h were needed to gain 50% of maximal signal, compare to 2.5h for the positive control, showing a slower aggregation kinetic in the presence of VHH E4-1 (**Figure 4b,** green line). At a 1:1 Tau:VHH E4-1 molar ratio, the fluorescence signal only reached 58.3 % (± 3.9%) and more than 12.8h were necessary to gain 50% of maximal signal (**Figure 4b,** orange line). VHH Z70 had an even stronger inhibition effect on the aggregation of Tau than the parent VHH E4-1. At a 1:1 Tau:VHH Z70 molar ratio, the maximal fluorescence signal barely reached above the negative control level, at 4.1 % (± 0.1%) (**Figure 4c,** orange line). The link between the thioflavin T fluorescence measurements in our assays and the formation of Tau fibrils at the end-point of each aggregation assay was confirmed by transmission electron microscopy imaging (**Figure S12**). Whereas no fibrils were detected without heparin (**Figure S12a,** negative control), large amounts were observed for Tau in the presence of heparin only (**Figure S12b**, positive control) or in the additional presence of VHH F8-2 (**Figure S12c**). Shorter filaments were detected with VHH E4-1 (**Figure S12d**) and practically none with VHH Z70 (**Figure S12e**).

In conclusion, parent VHH E4-1 and its optimized variant VHH Z70 have both the capacity to interfere with Tau fibrils assembly *in vitro.*

Figure 4 VHH E4-1 and VHH Z70 inhibit *in vitro* Tau aggregation.

Aggregation of Tau (10 µM) in the absence of heparin (black curve), in the presence of heparin and of increasing concentration of (**a**) VHH F8-2 (**b**) VHH E4-1 and (**c**) VHH Z70 (0, 1, 2.5, 5 and 10 µM) monitored by Thioflavin T fluorescence at 490 nm (n=3). Error bars: s.e.m,

Inhibition of Tau seeding in FRET Biosensor reporter cells

The capacity of VHH Z70 and its parent VHH E4-1 to block Tau seeding by using the HEK293 Tau RD P301S FRET Biosensor reporter cell line model was next investigated. This cell line constitutively expresses Tau RD (MTBD), with a P301S mutation, fused to either CFP (Cyan Fluorescent Protein) or YFP (Yellow Fluorescent Protein)

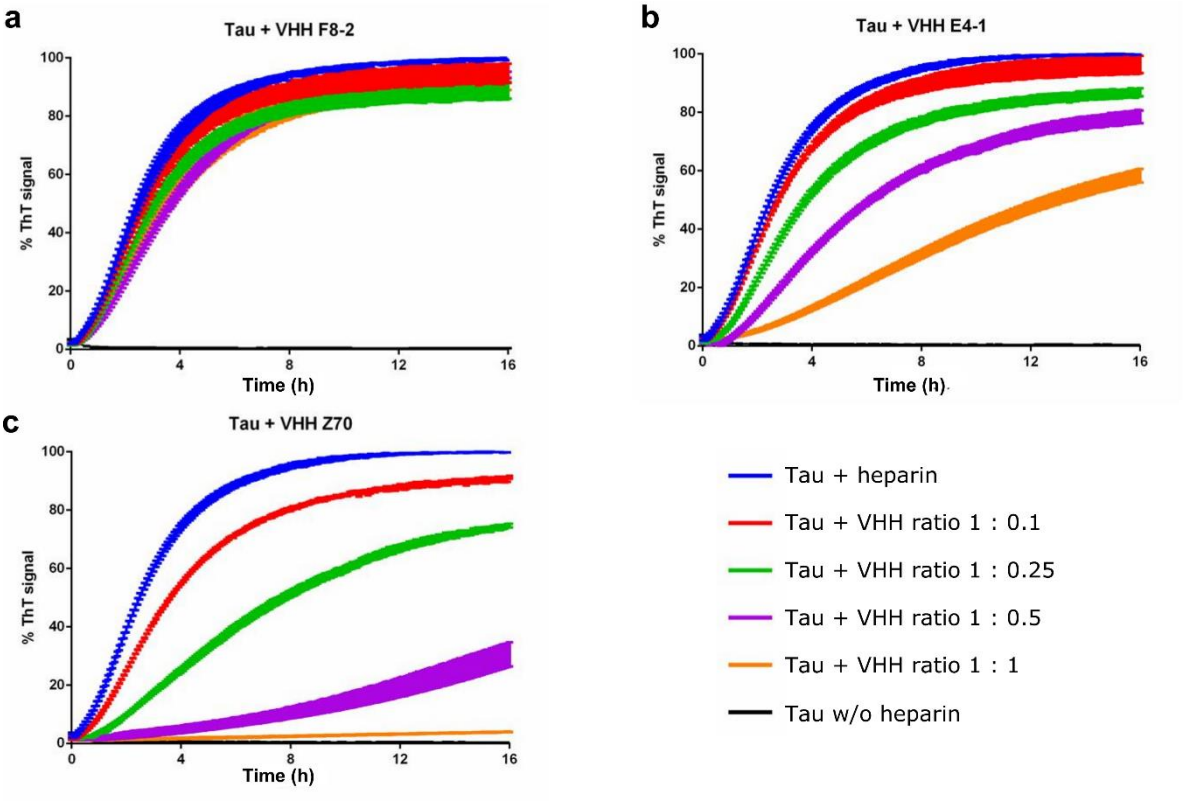

that together generate a FRET (Forster Resonance Energy Transfer) signal upon MTBD-P301S polymerization.[43] The MTBD-P301S contains the PHF6 peptide $_{306}$VQIVYK$_{311}$ identified as the recognition sequence of VHH-Z70[43]. In basal conditions, FRET signal is not detected by flow cytometry (**Figure 5a,** vehicle). The intra-cellular polymerization of MTBD-P301S protein is induced by treating the cells with Tau seeds (heparin-induced MTBD fibrils)[43], leading to a FRET signal (16.0% ± 0.8% FRET- gated positive cells, **Figure 5a,** grey column). In addition,

VHH F8-2 was transfected one day prior to MTBD seed treatment as negative control since its binding is outside the MTBD. As expected, VHH F8-2 did not affect the seeding in the reporter cells (15.4% ± 1.0% FRET-gated positive cells, **Figure 5a,** white column). This negative control also showed that the mCherry fluorophore did not interfere with the seeding, polymerization and/or FRET signal. We next used the mCherry-VHH fusion proteins to select the transfected cells and to detect FRET signal selectively in mCherry-VHH positive cells (mCherry-gated and FRET-gated positive cells **Figure 5b**). As expected, given that VHH E4-1 did not bind Tau in cells (**Figure 2a**), the FRET signal reduction for VHH E4-1 transfected cells was not significant, with a percentage of FRET decreasing to 15.6% ± 0.9%, compared to 18.5% ± 1.3% FRET signal for the VHH F8-2 negative control (**Figure 5b**). In contrast, VHH Z70 clearly affected the intra-cellular seeding of MTBD-P301S polymerization, as the observed FRET signal for the corresponding transfected cells was significantly decreased to 10.9% ± 0.7% (41% seeding inhibition, p value = 0.0003, **Figure 5b**). Based on these measurements, we concluded that VHH Z70 has reduced the association of MTBD-P301S CFP and YFP by 40%, showing the efficiency of VHH Z70 to inhibit Tau seeding in this cellular model.

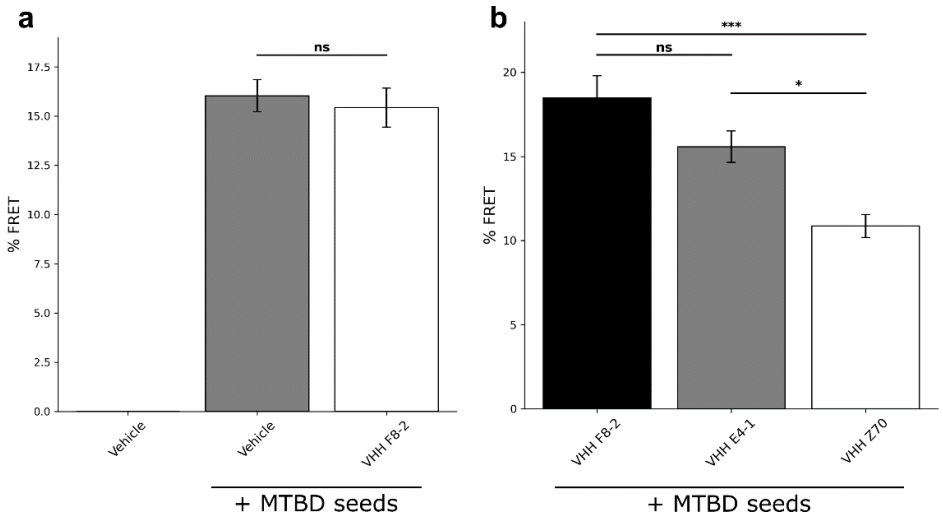

Figure 5 VHH Z70 blocks intra-cellular seeding of Tau MTBD in HEK293 biosensor cells.

(**a-b**) Analysis of Tau seeding in HEK293 Tau RD P301S FRET Biosensor cells. (**a**) Percentage of FRET positive cells in the whole population determined from flow cytometry data for cells transfected with vehicle or transfected with vehicle and VHH F8-2 followed by MTBD seeds (n=3). (**b**) Percentage of FRET positive cells in the mCherry-gated population determined from flow cytometry data for cells transfected with VHH F8-2, VHH E4-1 and VHH Z70 followed by MTBD seeds (n=3). A significant decrease of FRET signal, reporting a decrease intra-cellular

MTBD aggregation, is observed in the presence of VHH Z70. *p value < 0.05, ***p value<0.001, ns not significant. Error bars: s.e.m.

Inhibition of Tau seeding in the Tg tauopathy mouse model THY-tau 30

The next step was to test the capacity of VHH Z70 to block Tau seeding in a well-characterized model[19]. This model consists in the intra-cranial injection of human AD (h-AD) brain-derived materials to robustly induce Tau pathology on a relatively short time scale (1 month), in young Tg THY-tau30 mice (1-month-old).[19,44] At 1-month-old, these mice have low endogenous Tau pathology, which allowed to evaluate the seeding activity associated to the injected human-derived materials. To assay the capacity of VHH Z70 to mitigate the tauopathy in this model, VHH Z70 was expressed as a fusion protein with mCherry inside brain cells, following infection by LVs. LVs were used for their limited diffusion capacity, allowing to evaluate the local effect of VHH Z70 on Tau seeding. LVs infection of HEK293 cells showed expression of VHH Z70 in the cell fraction, with no detection in the medium, confirming that Z70 VHHs are well-expressed and are not secreted (**Figure S13**).

LVs were next delivered using intra-cranial injection in each brain hemisphere, 2 weeks prior to the stereotaxic h-AD seed delivery at the same coordinates in the hippocampus region (**Figure 6a**). Negative control experiments consisted in injection of a VHH directed against GFP (VHH anti-GFP), which is not present in mouse brains, instead of VHH Z70. The expression of VHH Z70 in the brain was monitored in both hemispheres using the mCherry fusion as a reporter (**Figure S14**). The level of Tau pathology was evaluated, 1-month post-injection of the seeds, by immunohistochemistry with the monoclonal AT8 antibody.[10,45] In the animals injected with h-AD brain extract and expressing VHH Z70, a significant decrease of the AT8 labeling compared to the negative control group is observed (**Figures 6b-c,** p value=0.019, **6d and S15**). The decrease detected in the area where the LVs expressing VHH Z70 had diffused and the pathology had spread following injections showed the positive effect of VHH Z70 on mitigating the seeded pathology. Accordingly, when brain tissue sections were double-stained, almost no co-localisation of signals was observed in neurons: most neurons expressing VHH Z70 (mCherry positive) had no Tau pathology as defined based on the AT8 signal (**Figures 6d** and **S16**). We concluded that intra-cellular immunization with VHH Z70 slows the seeding induced by injection of extracellular h-AD brain extract in THY-tau30.

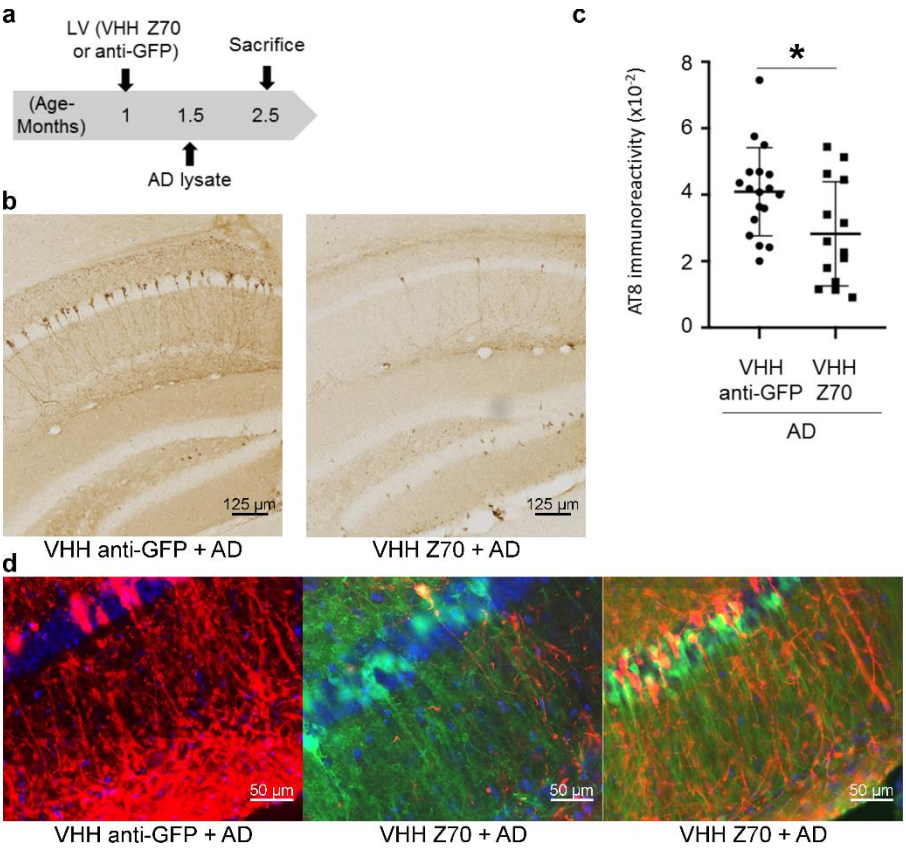

Figure 6 VHH Z70 reduces human Tau seeding activity induced by h-AD brain-derived material in THY-tau30 Tg mouse model. (**a**) Bilateral intra-cranial injection of LVs to express either VHH anti-GFP or VHH Z70 was performed in one-month old THY-tau30 mice. Induction of the tauopathy occurred by a second bilateral injection, at the same coordinates, fifteen days after with human h-AD. Mice were sacrificed and perfused one-month latter (aged 2.5 months). (**b**) The whole brain was processed for immunohistochemical analysis using AT8 for the control group (labelled VHH anti-GFP+AD; n=9) corresponding to injection of LVs VHH anti-GFP followed by h-AD injection and the group (labelled VHH Z70+AD ; n=7) corresponding to LVs VHH Z70 followed by h-AD injection. Enlarged images are taken from the hippocampus (injection site, AP : -2.46). Scale bars are indicated on the figure. (**c)** Each data point corresponds to the quantification for one hemisphere. Results are presented as AT8 immunoreactivity (immunoreactive area normalized to the whole area). * p value < 0.05. Error bars : S.D. **(d)** In a region of the hippocampus (molecular layer) with strong induction of the pathology (detected using AT-8 antibodies, visualised in red, see VHH anti-GFP + AD) and good diffusion of LVs expressing Z70 (detected using mCherry antibodies, visualised in green, see VHH Z70 + AD), there is no Tau pathology (red labelling) in neurons positive for VHH-Z70 expression (green labelling). Immunohistochemical analysis is shown for two animals (VHH Z70 + AD) with different levels of pathology. Larger views of the analysis are shown in **Figure S16**.

DISCUSSION

Tau immunotherapy is an attractive strategy in tauopathies to bind to and to clear extracellular and/or intra-cellular pathological species of the Tau protein to slow disease progression. Indeed, by targeting different Tau epitopes, immunotherapy studies showed a reduction of Tau pathology and cognitive deficit in different mouse models of tauopathy[13–20]. Nevertheless, the mechanistic detail of their mode of action is only recently emerging.

Indeed, it remains difficult to evaluate whether detection of an intra-cellular Ig results from uptake of the Ig by itself or of the immune complex, and thus whether their primary target is Tau in the intra- or extra-cellular compartment. One study with systematic comparison of intra-neuronal *versus* extraneuronal-acting equivalent Tau-specific scFvs showed a significant improved effect of the intra-neuronal modified scFvs against the tauopathy, in two tauopathy mouse models[36]. Intra-neuronal chimeric scFvs are another successful example, designed to target Tau to the proteasome or lysosomal pathway in human Tau Tg mice.[46]

We succeeded in selecting a VHH targeted to a specific region in a rather large intrinsically disordered protein, in one single screen. NMR interaction mapping was particularly helpful to select for VHHs binding the MTBD (**Figure 1** and **S1**). Yeast two-hybrid combined with molecular strategies has allowed for the identification of a major binding site $_{306}$VQIVYK$_{311}$ (**Figures 3 and S7**). In addition, a weaker secondary interaction was detected with PHF6* (VQIINK) when using sensitive *in vitro* methods (NMR in **Figures 5** and **6**). This secondary binding site might contribute to the overall VHH Z70 activity by slowing-down dissociation and by doing so, increase the apparent affinity for Tau.

The main interest is that VHH Z70 binds in the MTBD, while the majority of epitopes targeted in clinical trial are located in the N- or C-terminal regions[21]. Some studies show that targeting N-terminal species could block Tau uptake and its transfer between neurons,[47] and could reduce accumulation of Tau in the brain of mouse model of tauopathy.[48] Nevertheless, antibodies targeting N- and C-terminal epitopes bring the risk of binding Tau sequences eliminated by proteolysis.[49] They are also unlikely to interfere with seeding and polymerization, other crucial aspects of the pathology. Two phase II trials of passive immunotherapies with monoclonal antibodies targeting the N-terminal part of Tau in supranuclear palsy, gosuranemab[50] and tilavonemab,[51] reported no clinical treatment effect despite target engagement. Both assays rationales were the removal of the extracellular Tau to slow

progression of the disease. Although multiple parameters could explain these results,[52] the N-terminal part of Tau remains unlikely to be the mediator of Tau toxicity.[22] Conversely, Bepranemab, a humanized monoclonal IgG4 antibody binding to the central region of Tau (235–246), near the MTBD, was reported to inhibit seeding in a cellular assay and a mouse model.[19,53] Similarly, treatment with a humanized IgG antibody, binding the R2 and R4 repeats within the MTBD, decreases the level of sarkosyl-insoluble Tau in brain of a mouse model of Tau seeding.[54] These antibody are being proposed for clinical development and their capacity to attenuate the spread of Tau supports the hypothesis that the MTBD provides an efficient target for therapeutic antibodies. VHH Z70 has similar properties but by acting directly intra-cellularly.

Here, we demonstrated the interest of targeting the Tau PHF6 motif, which participates to the aggregation process[37] and which is found in the core of Tau fibrils in AD.[55–58] PHF6* and PHF6 peptides spontaneously aggregate in solution contrary to the full-length Tau that is a highly soluble protein. Their atomic structures reveal the capacity of these segments to form interdigitated steric-zipper interfaces that seed Tau aggregation.[59,60] In addition, the accessibility of the PHF6*/ PHF6 peptides is proposed to be part of the mechanism leading to Tau filament formation. The residues from these peptides are proposed to be shielded in a dynamic hairpin conformations in native Tau, while exposed PHF6 residues would increase Tau sensitivity to aggregation.[61] The conversion from an inert Tau monomer to a seed-competent monomer would thus involve an increased accessibility of the PHF motifs.[61] Interestingly, several chaperons with Tau anti-aggregation activities, such as Hsc70, Hsp60, DnaJA2 and S100B[62] proteins, bind to regions overlapping PHF6, and in a weaker manner PHF6*. Thus, one major mechanism of the anti-aggregation activities of these chaperons is likely the binding of Tau in the PHF region.[63]

The cryo-electron microscopy structures of Tau fibers isolated from patient brains affected by various tauopathies: AD,[55] corticobasal degeneration,[56] Pick's disease,[57] chronic traumatic encephalopathy[58] and progressive supranuclear palsy[64] show distinct folds. The common core of these fibrillary structures is nevertheless composed of the subdomains R3 including the PHF6, R4 and a part of the C-terminal domain (V306-F378) that mainly form a β-sheet unit.[55] This filament core has the ability to polymerize and form filaments *in vitro*, and act as seeds to recruit full-length Tau to filaments, in the absence of an inducer such as heparin[65]. To form these fibers, a mechanism of ß-augmentation is responsible for the stacking of the ß-sheet units on top of one-another to ensure elongation of the fiber. The PHF6 sequence is thus forming in this process the same type of interactions as those

observed with the VHH Z70 (**Figure S17**). Although it will remain to be demonstrated, the specific ß-strand conformation adopted by the PHF6 sequence in the complex suggests that VHH Z70 might not be able to interact with the fibers, except at the free extremity. However, by interacting with the PHF6 at the extremity of Tau oligomers or fibers, VHH Z70 might interfere with the elongation mechanism by competing with the ß-sheet augmentation.

Additionally, the properties of the parent VHH (E4-1) were improved. VHH Z70 has indeed been selected for its capacity to bind Tau in the intra-cellular compartment, using yeast two-hybrid (**Figure 2a**). The four mutations differentiating VHH Z70 from the E4-1 are in the framework region and allow the active conformation to be achieved once expressed in cells. This can result either because the cysteine residues are well-positioned to form disulfide bridges, despite the reductive environment, or because the mutations allow a disulfide-independent folding. VHH Z70 indeed showed improve solubility when express in cells compare to VHH E4-1 that formed aggregates, observed in the experimental conditions as puncta of mCherry fluorescence (**Figures 2c-e** and **S4**). Although we succeeded, the process remains challenging, as a single clone was selected out of the 1.5 million variants screened by two-hybrid. In addition, the affinity reached the 100 nM range and remained an important parameter to optimize as we observed a higher inhibition activity for VHH Z70 compared to VHH-E4-1 in the *in vitro* aggregation assay (**Figure 4**). The heparin-induced Tau fibers that are formed in this assay are heterogeneous and have been shown to differ from the structures of the human native fibers.[66] Nevertheless, even if not recapitulating all the structural features, the heparin-induced fibers still contain the R3 repeat at the core of a ß-sheet unit and fibers are formed by stacking these ß-sheet units on one-another. Consequently, although the model has limitations, the *in vitro* heparin-induced aggregation remains of interest when targeting the PHF6 sequence as its key-role in nucleation is conserved in this assay. In addition, VHH Z70 was shown to inhibit seeding in an established cellular model that does not use heparin as inducer of the aggregation. The poor seeding inhibition capacity of VHH-E4-1 in this model (**Figure 5**) is likely due to its poor intra-cellular activity compared to VHH Z70 (**Figure 2a-c**).

Importantly, VHH Z70 decreases the Tau pathology in an established mouse model of tauopathy[19] (**Figure 6**). In this injection model, VHH Z70 mechanism of action likely results from blocking Tau seeding, limiting the accumulation of pathological Tau. Interestingly, the hippocampal neurons expressing VHH Z70 did not show signs

of the Tau pathology based on the AT8 labelling (**Figures 6d** and **S16**). According to our *in vitro* results, nucleation is probably blocked by the binding of the VHH Z70 to monomeric Tau, preventing its recruitment by the seeds. We cannot however exclude the possibility that VHH Z70 also binds to the seeds, given the lack of a precise definition of the nature of these seeds: seed-competent monomeric, oligomeric or fibrillar Tau.

VHHs have entered the real world of therapeutics,[67] and as they can be delivered as genes, the synergy with the progress in viral vector-mediated gene delivery could open the way for feasible treatments of tauopathies.

MATERIALS AND METHODS

Screening and Selection of VHHs directed against Tau protein

The Nali-H1 library of VHHs ($3x10^{11}$ phages) was screened against the recombinant biotinylated-Tau 2N4R as described previously.[38,39] EZ-Link™ Sulfo-NHS-Biotin (Thermo Fisher Scientific) was used for the biotinylation following manufacturer protocol except for a two-fold molar excess of Sulfo-NHS-Biotin. The unreacted Sulfo-NHS-Biotin was eliminated by desalting on Sepadextran™ 25 Medium SC (Proteigene). Biotinylated-Tau protein was bound to Dynabeads™ M-280 Streptavidin (Invitrogen) at a concentration gradually decreasing at each round of selection: 100nM in first round, 50nM in second round and 10nM in third round. Biotinylated-Tau binding was verified by Western Blot using Streptavidin Protein, HRP (Thermo Fisher Scientific). Non-absorbed Phage ELISA assay using avidin-plates and biotinylated-Tau Antigen (5µg/ml) was used for cross-validation of 186 randomly picked clones.[68]

Production and purification of VHHs

Competent *Escherichia coli* BL21 (DE3) bacterial cells were transformed with the various PHEN2-VHH constructs. Recombinant *E. coli* cells produced proteins targeted to the periplasm after induction by 1 mM IPTG (isopropylthiogalactoside). Production was pursued for 4 hours at 28°C before centrifugation to collect the cell pellet. Pellet was suspended in 200 mM Tris-HCl, 500 mM sucrose, 0.5 mM EDTA, pH 8 and incubated 30 min on ice. 50 mM Tris-HCl, 125 mM sucrose, 0,125 mM EDTA, pH 8 and complete protease inhibitor (Roche) were then added to the cells suspension and incubation continued 30 min on ice. After centrifugation, the supernatant, corresponding to the periplasmic extract, was recovered. The VHHs were purified by immobilized-metal affinity chromatography (HisTrap HP, 1mL, Cytiva) followed by size exclusion chromatography (Hiload 16/60, Superdex

75, prep grade, Cytiva) in NMR buffer (50 mM sodium phosphate buffer (NaPi) pH 6.7, 30 mM NaCl, 2.5 mM EDTA, 1 mM DTT).

Production and purification of Tau 2N4R, Tau 2N3R, Tau MTBD and Tau [208-324]

pET15b-Tau recombinant T7lac expression plasmid was transformed into competent *E. coli* BL21 (DE3) bacterial cells. A small-scale culture was grown in LB medium at 37 °C and was added at 1:10 V/V to 1L of a modified M9 medium containing MEM vitamin mix 1X (Sigma-Aldrich), 4 g of glucose, 1 g of ^{15}N-NH_4Cl (Sigma-Aldrich), 0.5 g of ^{15}N-enriched Isogro (Sigma-Aldrich), 0.1 mM $CaCl_2$ and 2 mM $MgSO_4$. Recombinant ^{15}N Tau production was induced with 0.5 mM IPTG when the culture reached an optical density at 600nm of 0.8. Proteins were first purified by heating the bacterial extract, obtained in 50 mM NaPi pH 6.5, 2.5 mM EDTA and supplemented with complete protease inhibitors cocktail (Sigma-Aldrich), 15 min at 75 °C. The resulting supernatant was next passed on a cation exchange chromatography column (Hitrap SP sepharose FF, 5mL, Cytiva) with 50 mM NaPi pH 6.5 and eluted with a NaCl gradient. Tau proteins were buffer-exchanged against 50 mM ammonium bicarbonate (Hiload 16/60 desalting column, Cytiva) for lyophilization. The same protocol[69] was used to produce and purify Tau 2N3R isoform, Tau[245-368] (designated MTBD, also called K18 fragment), chimeric Tau[245-368] with two PHF6 or PHF6* peptide sequences instead of PHF6* and PHF6 sequences (**Figure S10a**) and Tau [208-324].

Production and purification of SUMO-Tau peptides

cDNA encoding peptide Tau[273-318] was amplified from Tau 2N4R cDNA by PCR. cDNA was cloned by a ligation independent protocol into vector pETNKI-HisSUMO3-LIC as described.[70] Tau peptide was expressed as a C-terminal SUMO protein fusion with a N-terminal HisTag. His-SUMO-Tau peptide was purified by affinity chromatography on Ni-NTA resin followed by size exclusion chromatography (Hiload 16/60, Superdex 75, prep grade, Cytiva) in SPR buffer (HBS-EP+, GE Healthcare).

Nuclear Magnetic Resonance Spectroscopy Experiments

Analysis of the ^{15}N Tau/VHH interactions were performed at 298K on a Bruker Avance Neo 900MHz spectrometer equipped with cryogenic probe. TMSP (trimethyl silyl propionate) was used as internal reference. Lyophilized ^{15}N Tau were diluted in a buffer containing 50 mM NaPi, 30 mM NaCl, 2.5 mM EDTA, 1 mM DTT, and 10% D_2O,

pH 6.7 and mixed with VHH at 100 μM final concentration for each protein. 200 μL of each mix in 3 mm tubes were sufficient to obtain the 2D ^{1}H, ^{15}N HSQC spectra with 32 scans. ^{1}H, ^{15}N HSQC were acquired with 3072 and 416 points in the direct and indirect dimensions, for 12.6 and 25 ppm spectral windows, in the ^{1}H and ^{15}N dimensions respectively. Each resonance in Tau spectra can be linked to a specific amino acid residue in Tau sequence,[71,72] allowing to map the binding region based on the observed differences of chemical shift value and/or intensity for each resonance in the bound *versus* free condition. Data were processed with Bruker Topspin 3.6 and analyzed with Sparky (T. D. Goddard and D. G. Kneller, SPARKY 3, University of California, San Francisco).

Optimization of VHH E4-1 for intra-cellular expression

VHH E4-1 was amplified from pHEN2 plasmid (oligonucleotides 3390 and 3880 in **Figure S18**) using Taq polymerase with 14 mM $MgCl_2$ and 0.2 mM $MnCl_2$ and a modified nucleotide pool[73]. The amplified cDNAs were transformed in yeast Y187 strain, together with a digested empty derivative of pGADGH vector[74], allowing recombination by gap repair in the vector. The VHH cDNAs are expressed as preys, with a C-terminal Gal4-activation domain fusion (E4-1-Gal4AD). A library of 2.1 million clones was obtained, collected and aliquoted. Tau variant 0N4R isoform (NM_016834.4) was expressed as bait with a C-terminal fusion with lexA (Tau-LexA) from pB29 vector, which is derived from the original pBTM116.[75] The library was screened at saturation, with 20 million tested diploids, using cell-to-cell mating protocol.[76] A single clone was obtained, named VHH Z70.

One-to-one interaction by yeast two-hybrid

A one-to-one mating assay was used to test for interaction using a mating protocol with L40ΔGal4 (mata) transformed with the bait (C-terminal fusion with lexA) and Y187 (matα) yeast strains transformed with the prey (C-terminal Gal4-activation domain fusion).[76] The interaction pairs were tested in triplicate on selective media by streak.

mCherry intracellular aggregation assays

HEK293 cells were seeded in 12-well plates (10^6 cells per well). 24 hours later, cells were transfected with plasmids encoding mCherry, mCherry-VHH Z70, mCherry-VHH E4-1 or mCherry-VHH anti-GFP together with lipofectamine in optiMEM, as recommended by the manufacturer (Invitrogen). 48 hours later, medium was removed, and cells were washed in pre-warmed PBS before 30-min fixation at RT with 4% PFA. After three successive washes in pre-warmed PBS, the nuclei were stained with DAPI (1/10 000) for 15 min at RT. Cells were

cover-slipped with VectaMount. 10 images per condition (n=3 independent experiences) were acquired using a Zeiss AxioObserver Z1 (spinning disk Yokogawa CSU-X1, camera sCMOS Photometrics Prime 95B). The number of mCherry positive cells containing puncta was quantified from the 3 independent experiments, 10 images per experiment and per group (n=862 cells for mCherry, n=932 for VHH-Z70), n=995 for VHH E4.1 and n=977 for VHH anti-GFP).

Tau fragment library construction

Tau cDNA (NM_016834.4) was amplified from Tau-LexA bait vector (oligonucleotides 6690 and 6972 in **Figure S18**). 5 µg of the PCR product was subjected to Fragmentase® treatment (New England Biolab, NEB) until a smear of fragments was detected around 400-500pb by agarose gel electrophoresis. The DNA fragments were purified by phenol/chloroform extraction and ethanol precipitation. The DNA fragments were next subjected to end repair (NEB) and dA-tailing adaptation, using Blunt/TA ligase master mix with NEBNext® Adaptor hairpin loop (NEB), followed by AMPure XP bead (Beckman Coulter) purification. After USER® enzyme digestion (NEB), DNA fragments were amplified (oligonucleotides 10829 and 10830 in **Figure S18**) with 15 cycles of PCR using NEBNext® Q5® Hot Start HiFi PCR Master Mix (NEB), which allowed to add Gap Repair recombination sequences for the cloning in Gal4-AD prey plasmid pP7. The library comprised 50000 independent clones.

Tau fragment library screening

The coding sequence for VHH Z70 was PCR-amplified and cloned into pB27 as a C-terminal fusion to LexA (LexA-VHHZ70). The construct was used to produce a bait to screen the Tau fragments library constructed into pP7. pB27 and pP7 derived from the original pBTM116[75] and pGADGH[74] plasmids, respectively. The Tau fragment library was screened using a mating approach with YHGX13 (Y187 ade2-101::loxP-kanMX-loxP, matα) and L40ΔGal4 (mata) yeast strains.[76] 90 His+ colonies corresponding to 267.10^3 tested diploids were selected on a medium lacking tryptophan, leucine and histidine. The prey fragments of the positive clones were amplified by PCR and sequenced at their 5' and 3' junctions.

Surface Plasmon Resonance experiments

Affinity measurements were performed on a BIAcore T200 optical biosensor instrument (Cytiva). Full-length recombinant Tau 2N4R proteins were biotinylated with 5 molar excess of NHS-biotin conjugates (Thermofisher)

during 4 hours at 4 °C. Capture of biotinylated Tau was performed on a streptavidin SA sensorchip in HBS-EP+ buffer (Cytiva). One flow cell was used as a reference to evaluate non-specific binding and provide background correction. Biotinylated-Tau was injected at a flow-rate of 30 µL/min, until the total amount of captured Tau reached 500 resonance units (RUs). VHHs were injected sequentially with increasing concentrations ranging between 0.125 and 2 µM in a single cycle, with regeneration (3 successive washes of 1M NaCl) between each VHH. On the other hand, a VHH Z70 construct, containing a single C-terminal cysteine, was biotinylated using EZ-Link Maleimide-PEG2-Biotin (Thermo Scientific) and was immobilized on a SA (Streptavidin) chip in HBS-EP+ buffer (Cytiva). Increasing concentrations, ranging between 31.25 and 500 nM of the SUMO-Tau peptide, were successively injected. The same functionalized SA chip was also used to inject increasing concentrations of 3 different MTBD constructs, ranging between 62.5 nM and 1 µM. Single-Cycle Kinetics (SCK) analysis[52] was performed to determine association k_{on} and dissociation K_{off} rate constants by curve fitting of the sensorgrams using the 1:1 Langmuir model of interaction of the BIAevaluation sotware 2.0 (Cytiva). Dissociation equilibrium constants (Kd) were calculated as K_{off}/k_{on}.

VHH Z70/PHF6 Tau peptide complex crystallization and structure determination.

VHH Z70 protein solution was dialyzed against 10 mM HEPES pH 7.4, 50 mM NaCl then concentrated to 250 µM and incubated with 1 mM of PHF6 peptide for 30 minutes prior crystallization screening. The PHF6 peptide sequence was $_{301}$PGGGSVQIVYKP$_{312}$KK (Genecust, France), with the last two peptide residues added compare to the native Tau sequence for solubility purposes. From an initial screening of around 600 conditions, optimal crystallization conditions were found to be 0.17 M ammonium sulfate, 25.5% PEG 4000 and 15% glycerol (found in the Cryos Suite, Qiagen). Crystals were evaluated at SOLEIL synchrotron beamline PX1. Crystals belonged to space group P6522 with cell parameters suggesting that the asymmetric unit contains one VHH monomer (98% probability estimated from Matthews coefficient). The best diffraction dataset was obtained at a resolution of 1.7 Å. Structure was solved using molecular replacement (MOLREP[78]) with pdb 1ol0 as template and refined to a Rwork of 0.2 and Rfree of 0.21 using REFMAC5[79] and COOT[80]. The structure was deposited in the Worldwide protein data bank (wwpdb) with access code 7QCQ.

In vitro kinetic aggregation assays

Tau 2N4R aggregation assays were performed with 10 µM Tau and with increasing concentrations of VHHs (between 0 and 10 µM) in buffer containing 50 mM MES pH 6.9, 30 mM NaCl, 2.5 mM EDTA, 0.3 mM freshly prepared DTT, 2.5 mM heparin H3 (Sigma-Aldrich) and 50 µM Thioflavin T (Sigma-Aldrich), at 37°C. Experiments were reproduced 3 times in triplicates for each condition. The resulting fluorescence of Thioflavin T was recorded every 5 min/cycle within 200 cycles using PHERAstar microplate-reader (BMG labtech). The measures were normalized in fluorescence percentage, 100% being defined as the maximum value reached in the positive Tau control, in each experiment.

Transmission Electron Microscopy

The same samples from the *in vitro* aggregation assays were recovered and a 10 µl sample of Tau or Tau:VHH ratio 1:1 condition was loaded on a formvar/carbon-coated grid (for 5 min and rinsed twice with water). After drying, the grids were stained with 1% uranyl acetate for 1 min. Tau fibrils were observed under a transmission electron microscope (EM 900 Zeiss equipped with a Gatan Orius 1000 camera).

Seeding assays in HEK293 reporter cell-line

Stable HEK293 Tau RD P301S FRET Biosensor cells (ATCC CRL-3275) were plated at a density of 100k cells/well in 24-well plates. For confocal analysis, cells were plated on glass slides coated with poly-D-lysine and laminin at a density of 100k cells/well in 24-well plates. At 60% confluency, cells were first transiently transfected with the various pmCherry-N1 plasmid constructs allowing expression of the mCherry-fused VHHs. Transfection complexes were obtained by mixing 500 ng of plasmid diluted in 40 µl of opti-MEM medium, which included 18.5 µL (46.25% v/v) of opti-MEM medium with 1.5 µL (3.75% v/v) Lipofectamine 2000 (Invitrogen). Resulting liposomes were incubated at room temperature for 20 min before addition to the cells. Cells were incubated for 24 hours with the liposomes and 1 ml/well of high glucose DMEM medium (ATCC) with Fetal Bovine Serum 1% (Life technologies). The transfection efficiency was estimated to reach about 46%, for all mCherry-fused VHH plasmids (**Figure S19**). Eight µM of recombinant MTBD seeds were prepared *in vitro*, in the presence of 8 µM heparin, as described.[43] Cells were then treated with MTBD seeds (10 nM/well) in the presence of transfection reagents forming liposomes as here above described.

FRET Flow Cytometry

Cells were recovered with trypsin 0,05% and fixed in 2% PFA for 10 min, then suspended in PBS. Flow cytometry was performed on an ARIA SORP BD (acquisition software FACS DIVA V7.0 BD, Biosciences). To measure CFP emission fluorescence and FRET, cells were excited with a 405 nm laser. The fluorescence was captured with either a 466/40 or a 529/30 nm filter, respectively. To measure YFP fluorescence, a 488 nm laser was used for excitation and emission fluorescence was captured with a 529/30 nm filter. mCherry cells were excited with a 561 nm laser and fluorescence was captured with a 610/20 nm filter. To selectively detect and quantify FRET, gating was used as described.[43,81] The FRET data were quantified using the KALUZA software analyze v2. Three independent experiments were done in triplicate or quadruplicate, with at least 10,000 cells per replicate analyzed.

Animals

The study was performed in accordance with the ethical standards as laid down in the 1964 Declaration of Helsinki and its later amendments or comparable ethical standards. The experimental research has been performed with the approval of an ethical committee (agreement APAFIS#2264-2015101320441671 from CEEA75, Lille, France) and follows European guidelines for the use of animals. The animals (males and females) were housed in a temperature-controlled (20-22°C) room maintained on a 12 h day/night cycle with food and water provided *ad libitum* in specific pathogen free animal facility (n=5 mice per cage). Animals were allocated to experimental groups by randomization. AD brain extracts were obtained from the Lille Neurobank (fulfilling criteria of the French law on biological resources and declared to competent authority under the number DC-2008-642) with donor consent, data protection and ethical committee review. Samples were managed by the CRB/CIC1403 Biobank, BB-0033-00030.

Stereotaxic injection of THY-tau30 Tg Mice

THY-tau30 Tg mice express human 1N4R Tau protein with two pathogenic mutations (P301S and G272V) under the control of the neuron-specific Thy1.2 promoter.[82,83] 1-month-old anesthetized THY-tau30 mice were submitted to stereotaxic intra-cerebrocranial injections (400ng in 2µl at 250nl/min with a Hamilton glass syringe) at the coordinates posterior AP: -2.46, midline ML: -1 and vertical depth DV: -2.3 of both brain hemispheres with LVs expressing either VHH Z70 with a N-terminal mCherry fusion protein (VHH Z70) or a VHH directed against the green fluorescent protein (VHH anti-GFP).

2 weeks later, these mice were submitted to injections of human AD brain homogenate (h-AD, 15 µg in 2 µl) at the same coordinates of both hemispheres, as previously described in detail.[19] The h-AD seeds consisted in a mixture of two post-mortem human brain extracts from tissues of confirmed AD patients (frontal cortex area, Braak stage VI, Brodmann area 10). The injections resulted in two groups of 7 and 9 mice per group. The mice were sacrificed after a month delay from the injection of the h-AD brain extract. All mice gained weight during the experimental protocol course and no mouse death was recorded, showing no indication of severe toxicity (**Figure S20**).

Tissue processing, immunohistochemistry and Tau pathology quantification

THY-tau30 were deeply anesthetized and trans-cardially perfused with ice-cold 0.9% saline solution and subsequently with 4% PFA for 10 min. The brains were immediately removed, fixed overnight in 4% PFA, washed in PBS, placed in 20% sucrose for 16 h and frozen in isopentane until further use. Free-floating coronal sections (40 µm thickness) were obtained using a cryostat microtome.

Cryostat sections were next used for immunohistochemistry. Non-specific binding was blocked by using 'Mouse in Mouse' reagent (1:100 in PBS, Vector Laboratories). Brain slices were next incubated with the primary monoclonal antibody AT8 (1:500, Thermo MN1020) in PBS- 0.2% Triton X-100, 16h at 4°C. Labelling was amplified by incubation with an anti-mouse biotinylated IgG (1:400 in PBS-0.2% TritonTM X-100, Vector) followed by the application of the avidin-biotin-HRP complex (ABC kit, 1:400 in PBS, Vector) prior to addition of diaminobenzidine tetrahydrochloride (DAB, Vector) in Tris-HCl 0.1 mol/l, pH 7.6, containing H_2O_2 for visualization. Brain sections were mounted, air-dried, steadily dehydrated in ethanol (30%, 70%, 95%, 100%), cleared in toluene and cover-slipped with VectaMount (Vector Laboratories). Mounted brain sections were analyzed using stereology software (Mercator image analysis system; Explora Nova, La Rochelle, France). Threshold was established manually to present a minimum background and remained constant throughout the analysis. The region defined as quantification zone is from bregmas -2.06 to -2.92 (based on the Mouse Atlas, George Paxinos and Keith B.J. Franklin, Second Edition, Academic Press).

ImmunoHistoFluorescence

Brain sections from mice injected with the LVs VHH Z70 with a N-terminal fusion to mCherry were saturated in normal goat serum (1/100, Vector), then were incubated with the primary polyclonal antibodies anti-RFP targeting mCherry protein (1:1000, rabbit, Polyclonal, Rockland) 16h at 4°C in PBS-0.2% TritonTM X-100. For the double labelling, incubation was performed in the additional presence of Tau-specific antibody AT8 conjugated with biotin (1:500, Thermo). Labelling was detected using a secondary anti-rabbit antibody (1:500, Invitrogen) functionalized with Alexa 488 and streptavidin functionalized with Alexa 647 (1:500, invitrogen, visualized in pseudocolor red) for AT8. Section imaging was performed by microscopy using a slide scanner (Axioscan Z1-Zeiss) with a 20X objective.

Statistical analysis

Data are presented as the means ± s.e.m for *in vitro* aggregation assays (**Figure 4**) and reporter-cell seeding assays (**Figure 5**), and ± SD for in-cell solubility assays (**Figure 2c**) and for *in vivo* experiments (**Figure 6c**). Experiments were performed at least in triplicate and obtained from three independent experiments. An ordinary one-way non-parametric ANOVAs with a sidak's multiple comparison test has been applied to analyze puncta in mCherry positive cells (**Figure 2**). One-way non-parametric ANOVAs (Kruskal-Wallis) with Dunn's multiple comparison test and Mann-Whitney U-Test were used to analyze data for FRET experiments (**Figure 5**) and unpaired t-test after normality test for *in vivo* experiments (**Figure 6**). Statistical analyses were performed with GraphPad Prism 8.0.0.

ACKNOWLEDGEMENTS

We thank Dr Z. Lens and Dr M. Aumercier for their help on the T200 biacore measurements and Mrs M. Oosterlynck for technical support. We also thank M. Tardivel and A. Bongiovanni for their help on the Zeiss confocal microscope, from the Photonic Microscopy Core BioImaging Center (BiCeL) and N. Jouy for the cytometry experiments, from the Flow Core Facility (BiCel). We would like to thank Tatiana Isabet, Serena Sirigu and William Shepard for their valuable support during data collection at beamlines PX1 and PX2A at the SOLEIL synchrotron facility (Paris, France). The NMR facilities were funded by the Nord Region Council, CNRS, Institut Pasteur de Lille, European Union (FEDER), French Research Ministry and Univ. Lille. We acknowledge support

from TGE RMN THC (FR-3050, France). We acknowledge SOLEIL for the provision of synchrotron-radiation facilities. This study was supported by the LabEx (Laboratory of Excellence) DISTALZ (Development of Innovative Strategies for a Transdisciplinary approach to Alzheimer's disease ANR-11-LABX-01), by EU project AgedBrainSYSBIO (Grant Agreement N° 305299), by I-site ULNE (project TUNABLE) and by ANR (project ToNIC). Our laboratories are also supported by LiCEND (Lille Centre of Excellence in Neurodegenerative Disorders), Inserm, Métropole Européenne de Lille, Univ. Lille and FEDER.

CONFLICT OF INTEREST

A.A. and J-C. R. are employees of Hybrigenic services.

AUTHOR CONTRIBUTION STATEMENT

Conceptualization, J-C.R., L.B. and I.L.; Investigation, C.D., E.D., O.Z., R.C., A.A., S.B., J.M., S.E., A.L., F-X.C.; Formal Analysis, C.D., E.D. and M.C.; Visualization, C.D., E.D. and M.C.; Writing - Original Draft, C.D., E.D. and I.L.; Writing – Review and Editing, J-C.R., M.C., X.H. and L.B.; Funding Acquisition, I.L. and L.B.; Supervision E.D., X.H., M.C., I.L. and L.B.

REFERENCES

1. Hamers-Casterman, C., Atarhouch, T., Muyldermans, S., Robinson, G., Hamers, C., Songa, E.B., et al. (1993). Naturally occurring antibodies devoid of light chains. Nature *363*, 446–448.

2. Messer, A., and Butler, D.C. (2020). Optimizing intracellular antibodies (intrabodies/nanobodies) to treat neurodegenerative disorders. Neurobiol. Dis. *134*, 104619.

3. Goedert, M., and Spillantini, M.G. (2006). A century of Alzheimer's disease. Science *314*, 777–781.

4. Brion, J.P., Flament-Durand, J., and Dustin, P. (1986). Alzheimer's disease and tau proteins. Lancet *2*, 1098.

5. Grundke-Iqbal, I., Iqbal, K., Quinlan, M., Tung, Y.C., Zaidi, M.S., and Wisniewski, H.M. (1986). Microtubule-associated protein tau. A component of Alzheimer paired helical filaments. J Biol Chem *261*, 6084–9.

6. Clavaguera, F., Bolmont, T., Crowther, R.A., Abramowski, D., Frank, S., Probst, A., et al. (2009). Transmission and spreading of tauopathy in transgenic mouse brain. Nat Cell Biol *11*, 909–13.

7. Frost, B., Jacks, R.L., and Diamond, M.I. (2009). Propagation of tau misfolding from the outside to the inside of a cell. J. Biol. Chem. *284*, 12845–12852.

8. Mudher, A., Colin, M., Dujardin, S., Medina, M., Dewachter, I., Alavi Naini, S.M., et al. (2017). What is the evidence that tau pathology spreads through prion-like propagation? Acta Neuropathol. Commun. *5*, 99.

9. Cummings, J., Lee, G., Mortsdorf, T., Ritter, A., and Zhong, K. (2017). Alzheimer's disease drug development pipeline: 2017. Alzheimers Dement. Transl. Res. Clin. Interv. *3*, 367–384.

10. Nelson, P.T., Alafuzoff, I., Bigio, E.H., Bouras, C., Braak, H., Cairns, N.J., et al. (2012). Correlation of Alzheimer Disease Neuropathologic Changes With Cognitive Status: A Review of the Literature. J. Neuropathol. Exp. Neurol. *71*, 362–381.

11. Schwarz, A.J., Yu, P., Miller, B.B., Shcherbinin, S., Dickson, J., Navitsky, M., et al. (2016). Regional profiles of the candidate tau PET ligand 18F-AV-1451 recapitulate key features of Braak histopathological stages. Brain J. Neurol. *139*, 1539–1550.

12. Wilcock, G.K., and Esiri, M.M. (1982). Plaques, tangles and dementia. A quantitative study. J. Neurol. Sci. *56*, 343–356.

13. Bi, M., Ittner, A., Ke, Y.D., Götz, J., and Ittner, L.M. (2011). Tau-targeted immunization impedes progression of neurofibrillary histopathology in aged P301L tau transgenic mice. PloS One *6*, e26860.

14. Asuni, A.A., Boutajangout, A., Quartermain, D., and Sigurdsson, E.M. (2007). Immunotherapy targeting pathological tau conformers in a tangle mouse model reduces brain pathology with associated functional improvements. J. Neurosci. Off. J. Soc. Neurosci. *27*, 9115–9129.

15. Boutajangout, A., Quartermain, D., and Sigurdsson, E.M. (2010). Immunotherapy targeting pathological tau prevents cognitive decline in a new tangle mouse model. J. Neurosci. Off. J. Soc. Neurosci. *30*, 16559–16566.

16. Dai, C.-L., Tung, Y.C., Liu, F., Gong, C.-X., and Iqbal, K. (2017). Tau passive immunization inhibits not only tau but also Aβ pathology. Alzheimers Res. Ther. *9*, 1.

17. Chai, X., Wu, S., Murray, T.K., Kinley, R., Cella, C.V., Sims, H., et al. (2011). Passive immunization with anti-Tau antibodies in two transgenic models: reduction of Tau pathology and delay of disease progression. J. Biol. Chem. *286*, 34457–34467.

18. Yanamandra, K., Kfoury, N., Jiang, H., Mahan, T.E., Ma, S., Maloney, S.E., et al. (2013). Anti-tau antibodies that block tau aggregate seeding in vitro markedly decrease pathology and improve cognition in vivo. Neuron *80*, 402–414.

19. Albert, M., Mairet-Coello, G., Danis, C., Lieger, S., Caillierez, R., Carrier, S., et al. (2019). Prevention of tau seeding and propagation by immunotherapy with a central tau epitope antibody. Brain J. Neurol. *142*, 1736–1750.

20. Troquier, L., Caillierez, R., Burnouf, S., Fernandez-Gomez, F.J., Grosjean, M.-E., Zommer, N., et al. (2012). Targeting phospho-Ser422 by active Tau Immunotherapy in the THYTau22 mouse model: a suitable therapeutic approach. Curr. Alzheimer Res. *9*, 397–405.

21. Congdon, E.E., and Sigurdsson, E.M. (2018). Tau-targeting therapies for Alzheimer disease. Nat. Rev. Neurol.

22. Jadhav, S., Avila, J., Schöll, M., Kovacs, G.G., Kövari, E., Skrabana, R., et al. (2019). A walk through tau therapeutic strategies. Acta Neuropathol. Commun. *7*, 22.

23. Kfoury, N., Holmes, B.B., Jiang, H., Holtzman, D.M., and Diamond, M.I. (2012). Trans-cellular propagation of Tau aggregation by fibrillar species. J. Biol. Chem. *287*, 19440–19451.

24. Dujardin, S., Lécolle, K., Caillierez, R., Bégard, S., Zommer, N., Lachaud, C., et al. (2014). Neuron-to-neuron wild-type Tau protein transfer through a trans-synaptic mechanism: relevance to sporadic tauopathies. Acta Neuropathol. Commun. *2*, 14.

25. Colin, M., Dujardin, S., Schraen-Maschke, S., Meno-Tetang, G., Duyckaerts, C., Courade, J.-P., et al. (2020). From the prion-like propagation hypothesis to therapeutic strategies of anti-tau immunotherapy. Acta Neuropathol. (Berl.) *139*, 3–25.

26. Clavaguera, F., Grueninger, F., and Tolnay, M. (2014). Intercellular transfer of tau aggregates and spreading of tau pathology: Implications for therapeutic strategies. Neuropharmacology *76 Pt A*, 9–15.

27. Dujardin, S., Bégard, S., Caillierez, R., Lachaud, C., Delattre, L., Carrier, S., et al. (2014). Ectosomes: a new mechanism for non-exosomal secretion of tau protein. PloS One *9*, e100760.

28. Leroux, E., Perbet, R., Caillierez, R., Richetin, K., Lieger, S., Espourteille, J., et al. (2021). Extracellular vesicles: Major actors of heterogeneity in tau spreading among human tauopathies. Mol. Ther. J. Am. Soc. Gene Ther., S1525-0016(21)00475–5.

29. Tardivel, M., Bégard, S., Bousset, L., Dujardin, S., Coens, A., Melki, R., et al. (2016). Tunneling nanotube (TNT)-mediated neuron-to neuron transfer of pathological Tau protein assemblies. Acta Neuropathol. Commun. *4*, 117.

30. Pain, C., Dumont, J., and Dumoulin, M. (2015). Camelid single-domain antibody fragments: Uses and prospects to investigate protein misfolding and aggregation, and to treat diseases associated with these phenomena. Biochimie *111*, 82–106.

31. Herce, H.D., Schumacher, D., Schneider, A.F.L., Ludwig, A.K., Mann, F.A., Fillies, M., et al. (2017). Cell-permeable nanobodies for targeted immunolabelling and antigen manipulation in living cells. Nat. Chem. *9*, 762–771.

32. Li, T., Bourgeois, J.-P., Celli, S., Glacial, F., Le Sourd, A.-M., Mecheri, S., et al. (2016). Cell-penetrating anti-GFAP VHH and corresponding fluorescent fusion protein VHH-GFP spontaneously cross the blood-brain barrier and specifically recognize astrocytes: application to brain imaging. FASEB J. Off. Publ. Fed. Am. Soc. Exp. Biol. *26*, 3969–3979.

33. Gormal, R.S., Padmanabhan, P., Kasula, R., Bademosi, A.T., Coakley, S., Giacomotto, J., et al. (2020). Modular transient nanoclustering of activated β2-adrenergic receptors revealed by single-molecule tracking of conformation-specific nanobodies. Proc. Natl. Acad. Sci. U. S. A. *117*, 30476–30487.

34. Li, T., Vandesquille, M., Koukouli, F., Dudeffant, C., Youssef, I., Lenormand, P., et al. (2016). Camelid single-domain antibodies: A versatile tool for in vivo imaging of extracellular and intracellular brain targets. J. Control. Release Off. J. Control. Release Soc. *243*, 1–10.

35. Vitale, F., Giliberto, L., Ruiz, S., Steslow, K., Marambaud, P., and d'Abramo, C. (2018). Anti-tau conformational scFv MC1 antibody efficiently reduces pathological tau species in adult JNPL3 mice. Acta Neuropathol. Commun. *6*, 82.

36. Goodwin, M.S., Sinyavskaya, O., Burg, F., O'Neal, V., Ceballos-Diaz, C., Cruz, P.E., et al. (2020). Anti-tau scFvs Targeted to the Cytoplasm or Secretory Pathway Variably Modify Pathology and Neurodegenerative Phenotypes. Mol. Ther. J. Am. Soc. Gene Ther.

37. von Bergen, M., Friedhoff, P., Biernat, J., Heberle, J., Mandelkow, E.M., and Mandelkow, E. (2000). Assembly of tau protein into Alzheimer paired helical filaments depends on a local sequence motif ((306)VQIVYK(311)) forming beta structure. Proc. Natl. Acad. Sci. U. S. A. *97*, 5129–5134.

38. Moutel, S., Bery, N., Bernard, V., Keller, L., Lemesre, E., de Marco, A., et al. (2016). NaLi-H1: A universal synthetic library of humanized nanobodies providing highly functional antibodies and intrabodies. eLife *5*.

39. Dupré, E., Danis, C., Arrial, A., Hanoulle, X., Homa, M., Cantrelle, F.-X., et al. (2019). Single Domain Antibody Fragments as New Tools for the Detection of Neuronal Tau Protein in Cells and in Mice Studies. ACS Chem. Neurosci. *10*, 3997–4006.

40. Dingus, J., Tang, J.C.Y., and Cepko, C. (2021). A general approach for stabilizing nanobodies for intracellular expression.

41. Vielemeyer, O., Nizak, C., Jimenez, A.J., Echard, A., Goud, B., Camonis, J., et al. (2010). Characterization of single chain antibody targets through yeast two hybrid. BMC Biotechnol. *10*, 59.

42. Zhang, Y., Chang, C., Gehling, D.J., Hemmati-Brivanlou, A., and Derynck, R. (2001). Regulation of Smad degradation and activity by Smurf2, an E3 ubiquitin ligase. Proc. Natl. Acad. Sci. U. S. A. *98*, 974–979.

43. Holmes, B.B., Furman, J.L., Mahan, T.E., Yamasaki, T.R., Mirbaha, H., Eades, W.C., et al. (2014). Proteopathic tau seeding predicts tauopathy in vivo. Proc. Natl. Acad. Sci. U. S. A. *111*, E4376-4385.

44. Vandermeeren, M., Borgers, M., Van Kolen, K., Theunis, C., Vasconcelos, B., Bottelbergs, A., et al. (2018). Anti-Tau Monoclonal Antibodies Derived from Soluble and Filamentous Tau Show Diverse Functional Properties in vitro and in vivo. J. Alzheimers Dis. JAD *65*, 265–281.

45. Malia, T.J., Teplyakov, A., Ernst, R., Wu, S.-J., Lacy, E.R., Liu, X., et al. (2016). Epitope mapping and structural basis for the recognition of phosphorylated tau by the anti-tau antibody AT8. Proteins *84*, 427–434.

46. Gallardo, G., Wong, C.H., Ricardez, S.M., Mann, C.N., Lin, K.H., Leyns, C.E.G., et al. (2019). Targeting tauopathy with engineered tau-degrading intrabodies. Mol. Neurodegener. *14*, 38.

47. Nobuhara, C.K., DeVos, S.L., Commins, C., Wegmann, S., Moore, B.D., Roe, A.D., et al. (2017). Tau Antibody-Targeting Pathological Species Block Neuronal Uptake and Interneuron Propagation of Tau in Vitro. Am. J. Pathol.

48. Spencer, B., Brüschweiler, S., Sealey-Cardona, M., Rockenstein, E., Adame, A., Florio, J., et al. (2018). Selective targeting of 3 repeat Tau with brain penetrating single chain antibodies for the treatment of neurodegenerative disorders. Acta Neuropathol. (Berl.) *136*, 69–87.

49. Chen, H.-H., Liu, P., Auger, P., Lee, S.-H., Adolfsson, O., Rey-Bellet, L., et al. (2018). Calpain-mediated tau fragmentation is altered in Alzheimer's disease progression. Sci. Rep. *8*, 16725.

50. Dam, T., Boxer, A.L., Golbe, L.I., Höglinger, G.U., Morris, H.R., Litvan, I., et al. (2021). Safety and efficacy of anti-tau monoclonal antibody gosuranemab in progressive supranuclear palsy: a phase 2, randomized, placebo-controlled trial. Nat. Med. *27*, 1451–1457.

51. Höglinger, G.U., Litvan, I., Mendonca, N., Wang, D., Zheng, H., Rendenbach-Mueller, B., et al. (2021). Safety and efficacy of tilavonemab in progressive supranuclear palsy: a phase 2, randomised, placebo-controlled trial. Lancet Neurol. *20*, 182–192.

52. Jabbari, E., and Duff, K.E. (2021). Tau-targeting antibody therapies: too late, wrong epitope or wrong target? Nat. Med. *27*, 1341–1342.

53. Courade, J.-P., Angers, R., Mairet-Coello, G., Pacico, N., Tyson, K., Lightwood, D., et al. (2018). Epitope determines efficacy of therapeutic anti-Tau antibodies in a functional assay with human Alzheimer Tau. Acta Neuropathol. (Berl.) *136*, 729–745.

54. Roberts, M., Sevastou, I., Imaizumi, Y., Mistry, K., Talma, S., Dey, M., et al. (2020). Pre-clinical characterisation of E2814, a high-affinity antibody targeting the microtubule-binding repeat domain of tau for passive immunotherapy in Alzheimer's disease. Acta Neuropathol. Commun. *8*, 13.

55. Fitzpatrick, A.W.P., Falcon, B., He, S., Murzin, A.G., Murshudov, G., Garringer, H.J., et al. (2017). Cryo-EM structures of tau filaments from Alzheimer's disease. Nature.

56. Arakhamia, T., Lee, C.E., Carlomagno, Y., Duong, D.M., Kundinger, S.R., Wang, K., et al. (2020). Posttranslational Modifications Mediate the Structural Diversity of Tauopathy Strains. Cell *180*, 633-644.e12.

57. Falcon, B., Zhang, W., Murzin, A.G., Murshudov, G., Garringer, H.J., Vidal, R., et al. (2018). Structures of filaments from Pick's disease reveal a novel tau protein fold. Nature *561*, 137–140.

58. Falcon, B., Zivanov, J., Zhang, W., Murzin, A.G., Garringer, H.J., Vidal, R., et al. (2019). Novel tau filament fold in chronic traumatic encephalopathy encloses hydrophobic molecules. Nature *568*, 420–423.

59. Sawaya, M.R., Sambashivan, S., Nelson, R., Ivanova, M.I., Sievers, S.A., Apostol, M.I., et al. (2007). Atomic structures of amyloid cross-beta spines reveal varied steric zippers. Nature *447*, 453–457.

60. Seidler, P.M., Boyer, D.R., Rodriguez, J.A., Sawaya, M.R., Cascio, D., Murray, K., et al. (2018). Structure-based inhibitors of tau aggregation. Nat. Chem. *10*, 170–176.

61. Mirbaha, H., Chen, D., Morazova, O.A., Ruff, K.M., Sharma, A.M., Liu, X., et al. (2018). Inert and seed-competent tau monomers suggest structural origins of aggregation. eLife *7*.

62. Moreira, G.G., Cantrelle, F.-X., Quezada, A., Carvalho, F.S., Cristóvão, J.S., Sengupta, U., et al. (2021). Dynamic interactions and Ca2+-binding modulate the holdase-type chaperone activity of S100B preventing tau aggregation and seeding. Nat. Commun. *12*, 6292.

63. Mok, S.-A., Condello, C., Freilich, R., Gillies, A., Arhar, T., Oroz, J., et al. (2018). Mapping interactions with the chaperone network reveals factors that protect against tau aggregation. Nat. Struct. Mol. Biol. *25*, 384–393.

64. Shi, Y., Zhang, W., Yang, Y., Murzin, A.G., Falcon, B., Kotecha, A., et al. (2021). Structure-based classification of tauopathies. Nature *598*, 359–363.

65. Carlomagno, Y., Manne, S., DeTure, M., Prudencio, M., Zhang, Y.-J., Hanna Al-Shaikh, R., et al. (2021). The AD tau core spontaneously self-assembles and recruits full-length tau to filaments. Cell Rep. *34*, 108843.

66. Zhang, W., Falcon, B., Murzin, A.G., Fan, J., Crowther, R.A., Goedert, M., et al. (2019). Heparin-induced tau filaments are polymorphic and differ from those in Alzheimer's and Pick's diseases. eLife *8*, e43584.

67. Dutt, T., Shaw, R.J., Stubbs, M.J., Yong, J., Bailiff, B., Cranfield, T., et al. (2020). Real-World Evidence of Caplacizumab Use in the Management of Acute TTP. Blood.

68. Matz, J., and Chames, P. (2012). Phage display and selections on purified antigens. Methods Mol. Biol. Clifton NJ *907*, 213–224.

69. Danis, C., Despres, C., Bessa, L.M., Malki, I., Merzougui, H., Huvent, I., et al. (2016). Nuclear Magnetic Resonance Spectroscopy for the Identification of Multiple Phosphorylations of Intrinsically Disordered Proteins. J. Vis. Exp. JoVE.

70. Luna-Vargas, M.P.A., Christodoulou, E., Alfieri, A., van Dijk, W.J., Stadnik, M., Hibbert, R.G., et al. (2011). Enabling high-throughput ligation-independent cloning and protein expression for the family of ubiquitin specific proteases. J. Struct. Biol. *175*, 113–119.

71. Smet, C., Leroy, A., Sillen, A., Wieruszeski, J.M., Landrieu, I., and Lippens, G. (2004). Accepting its random coil nature allows a partial NMR assignment of the neuronal Tau protein. Chembiochem *5*, 1639–46.

72. Lippens, G., Wieruszeski, J.M., Leroy, A., Smet, C., Sillen, A., Buee, L., et al. (2004). Proline-directed random-coil chemical shift values as a tool for the NMR assignment of the tau phosphorylation sites. Chembiochem *5*, 73–8.

73. Cadwell, R.C., and Joyce, G.F. (1992). Randomization of genes by PCR mutagenesis. PCR Methods Appl. *2*, 28–33.

74. Bartel P.L, and Sternglanz R (1993). Cellular interactions in development: A practical approach. In Cellular interactions in development: A practical approach Practical approach series., Hartley D.A, ed., pp. 153–179.

75. Vojtek, A.B., and Hollenberg, S.M. (1995). Ras-Raf interaction: two-hybrid analysis. Methods Enzymol. *255*, 331–342.

76. Fromont-Racine, M., Rain, J.C., and Legrain, P. (1997). Toward a functional analysis of the yeast genome through exhaustive two-hybrid screens. Nat. Genet. *16*, 277–282.

77. Karlsson, R., Katsamba, P.S., Nordin, H., Pol, E., and Myszka, D.G. (2006). Analyzing a kinetic titration series using affinity biosensors. Anal. Biochem. *349*, 136–147.

78. Vagin, A., and Teplyakov, A. (2010). Molecular replacement with MOLREP. Acta Crystallogr. D Biol. Crystallogr. *66*, 22–25.

79. Murshudov, G.N., Skubák, P., Lebedev, A.A., Pannu, N.S., Steiner, R.A., Nicholls, R.A., et al. (2011). REFMAC5 for the refinement of macromolecular crystal structures. Acta Crystallogr. D Biol. Crystallogr. *67*, 355–367.

80. Emsley, P., Lohkamp, B., Scott, W.G., and Cowtan, K. (2010). Features and development of Coot. Acta Crystallogr. D Biol. Crystallogr. *66*, 486–501.

81. Banning, C., Votteler, J., Hoffmann, D., Koppensteiner, H., Warmer, M., Reimer, R., et al. (2010). A flow cytometry-based FRET assay to identify and analyse protein-protein interactions in living cells. PloS One *5*, e9344.

82. Schindowski, K., Bretteville, A., Leroy, K., Bégard, S., Brion, J.-P., Hamdane, M., et al. (2006). Alzheimer's disease-like tau neuropathology leads to memory deficits and loss of functional synapses in a novel mutated tau transgenic mouse without any motor deficits. Am. J. Pathol. *169*, 599–616.

83. Leroy, K., Bretteville, A., Schindowski, K., Gilissen, E., Authelet, M., De Decker, R., et al. (2007). Early axonopathy preceding neurofibrillary tangles in mutant tau transgenic mice. Am. J. Pathol. *171*, 976–992.

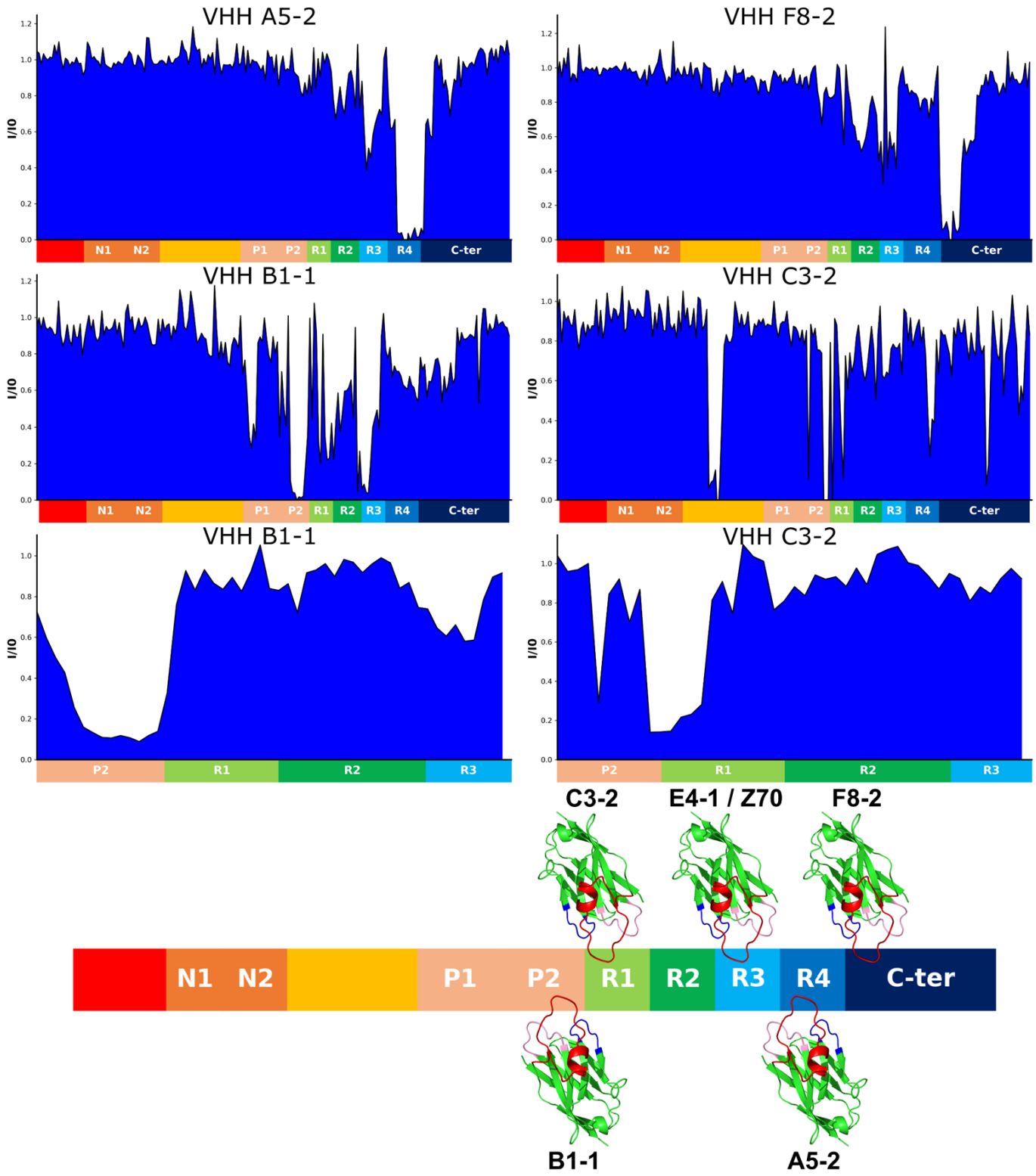

Figure S1 : Identification of synthetic VHHs directed against Tau microtubule-binding domain (MTBD) using 2D (two-dimensional) HSQC NMR experiment of Tau2N4R and Tau [208-324]. Intensity ratios I/I0 of corresponding resonances in the 2D spectra of Tau or Tau [208-324] with equimolar quantity ofVHH (I) or free in solution (I0) for residues along the Tau or Tau [208-324] sequences. Binding regions are illustrated along the Tau sequence with VHH images (from PDB 1MEL). CDR3 loop region is colored red.

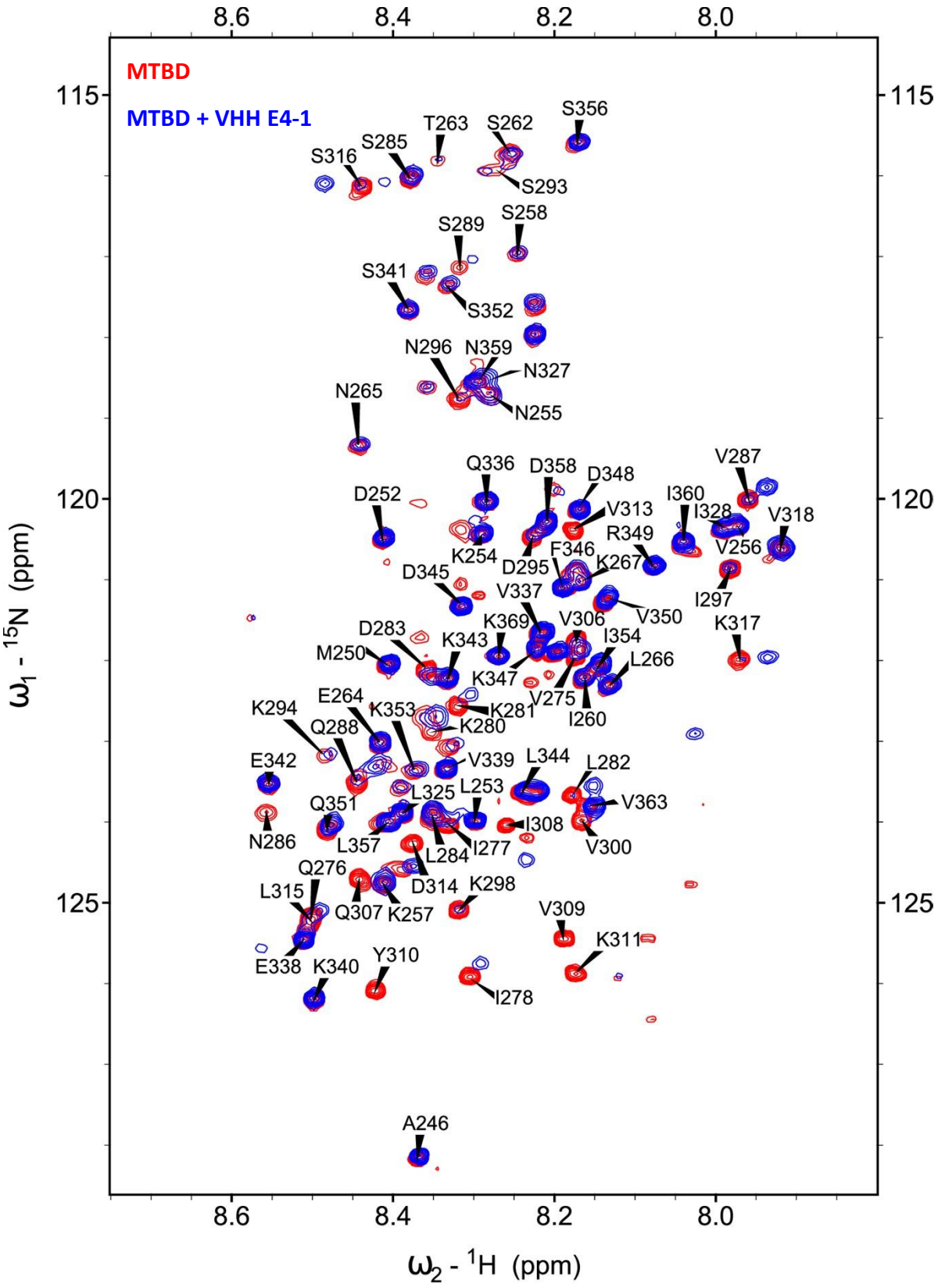

Figure S2 : Identification of VHH E4-1 binding region using 2D HSQC NMR experiment of Tau MTBD. Overlay of ^{1}H, ^{15}N, HSQC 2D spectra of ^{15}N-labelled Tau MTBD alone (red) or mixed with non- labelled VHH E4-1 spectra (blue). See enlarged regions of the spectra in **Figure S3**.

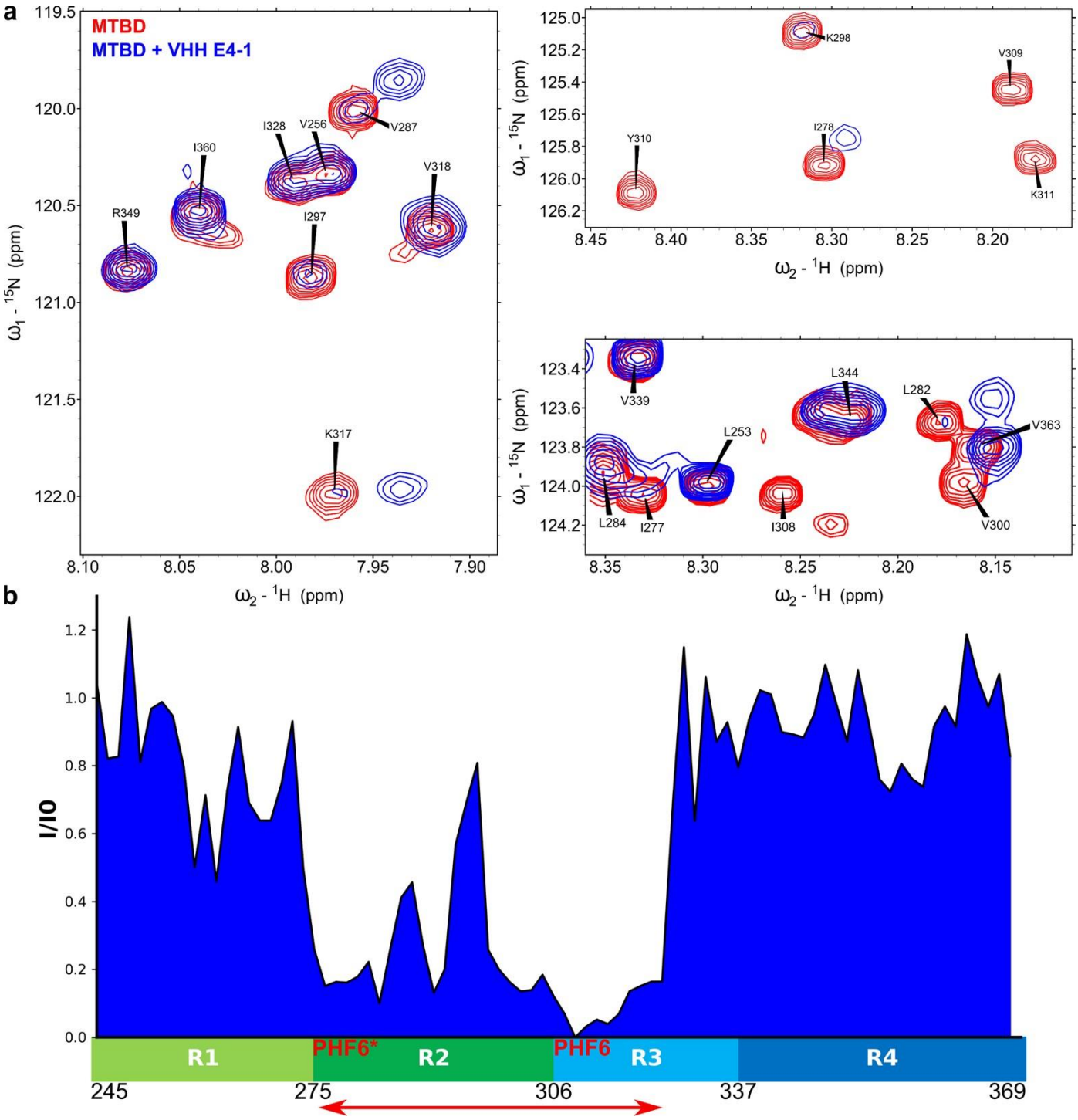

Figure S3 : Identification of VHH E4-1 epitope using 2D HSQC NMR experiment of Tau MTBD. **a :** Overlays of ^{1}H, ^{15}N, HSQC of 2D spectrum enlargements of ^{15}N-labelled Tau MTBD alone (red) or mixed with non-labelled VHH E4-1 (superimposed in blue). See full spectrum in **Figure S2. b :** Intensity ratios I/I0 of corresponding resonances in the 2D spectra of Tau MTBD with equimolar quantity of VHH E4-1 (I) or free in solution (I0) for residues along the Tau MTBD sequence. The red double-arrow indicates the region containing the corresponding major broadened resonances, which was mapped mostly on the R2-R3 repeats. Localization of the PHF6* and PHF6 peptide sequences is indicated.

a

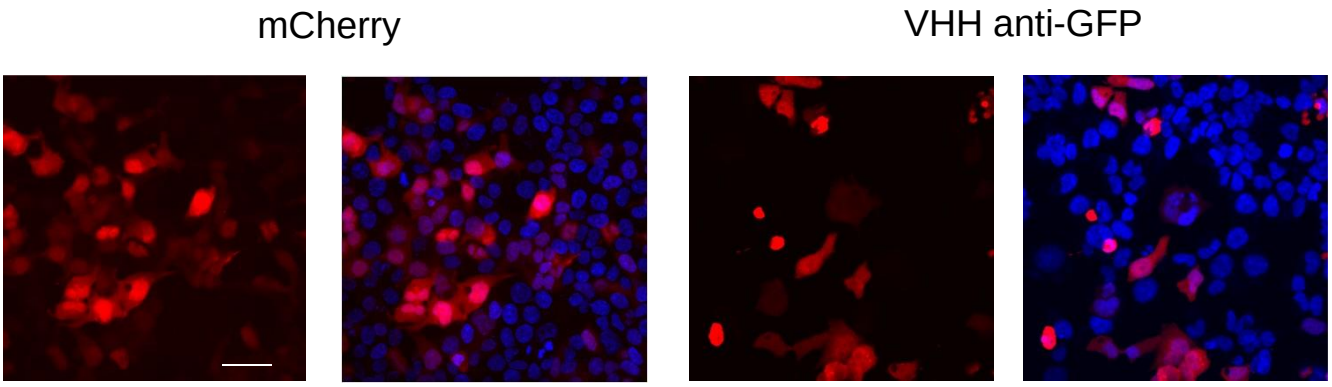

Figure S4 : VHH-70 is soluble inside cells - HEK293 cells were transfected with plasmid encoding either mCherry, mCherry-VHH E4.1 (**Figure 2c**), mCherry-VHH Z70 (**Figure 2d**) or mCherry-VHH anti-GFP. 48h later, cells were fixed and immunostained using a primary antibodyagainst mCherry tag and visualized in red. Nuclei are vizualized in blue. The scale bar isindicated on the figure. See percentage of cells with puncta in **Figure 2e**.

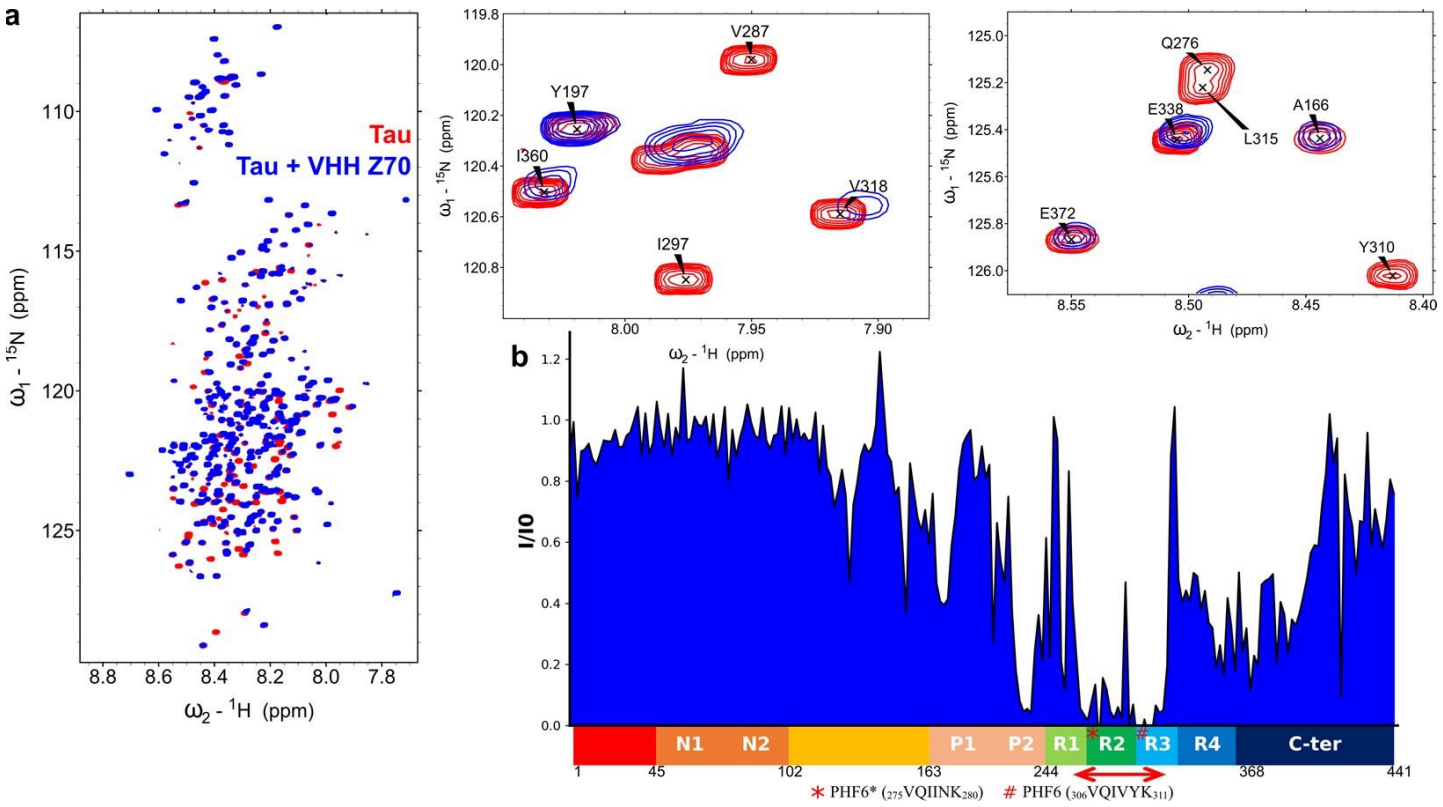

Figure S5 : Identification of VHH Z70 binding region using 2D HSQC NMR experiment of Tau2N4R. a : Overlays of ^{1}H, ^{15}N, HSQC full spectrum and enlargements of ^{15}N-labelled Tau, alone (red) or mixed with non-labelled VHH Z70 (in blue). Spectra enlargements show broadened resonances corresponding to residues implicated in the interaction **b :** Intensities ratio I/I0 of corresponding resonances in the 2D spectra of Tau with equimolar quantity of VHH Z70 (I) or free in solution (I0) for residues along the Tau sequence. The red double-arrow indicates the region containing the corresponding major broadened resonances, which was mapped mostly on the R2-R3 repeats. Localization of the PHF6* and PHF6 peptide sequences is indicated.

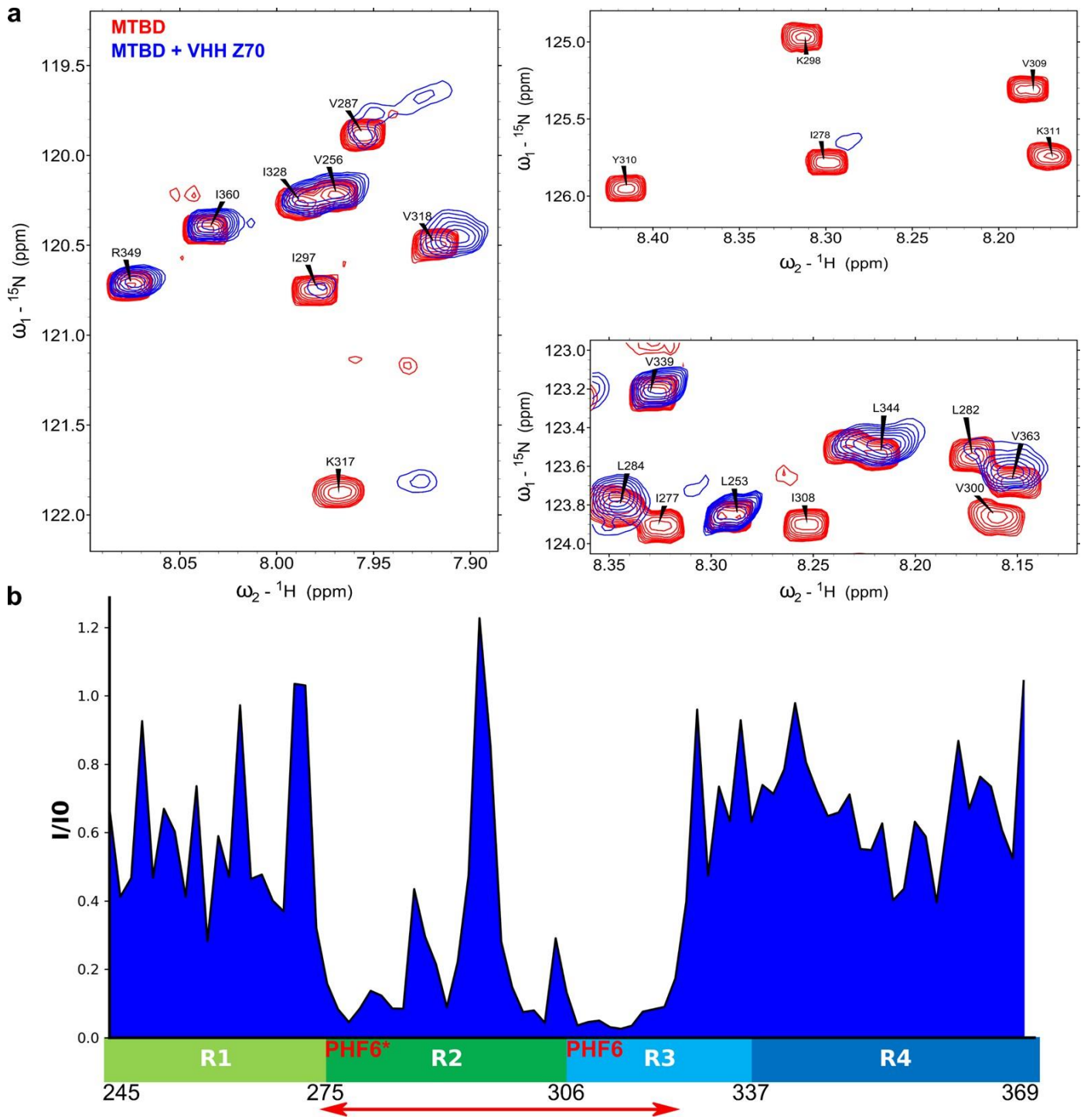

Figure S6 : Identification of VHH Z70 binding region using 2D HSQC NMR experiment of Tau MTBD. a : Overlays of ^{1}H, ^{15}N, HSQC enlargements of ^{15}N-labelled Tau MTBD alone (red) or mixed with non-labelled VHH Z70 (blue). **b :** Intensity ratios I/I0 of corresponding resonances in the 2D spectra of Tau MTBD with equimolar quantity of VHH Z70 (I) or free in solution (I0) for residues along the Tau MTBD sequence. The red double-arrow indicates the region containing the corresponding major broadened resonances, which was mapped mostly on the R2-R3 repeats. Localization of the PHF6* and PHF6 peptide sequences is indicated.

VHH	kon (1/M.s)	koff (1/s)	KD (nM)
E4-1	4982	0.0017	345
Z70	18100	0.0026	147

Tau peptide	sequence	kon (1/M.s)	koff (1/s)	KD (nM)
Tau[273-318]	$_{273}$GKVQIINKKLDLSNVQSKCGSKDNIKHVPGGGSVQIVYKPVDLSKV$_{318}$	106158	0.00214	20
K18	Tau[245-368]	23523	0.00343	146
K18 PHF6x2	Tau[245-368] with [274-282] mutated as SVQIVYKPV	29426	0.00099	34
K18 PHF6*x2	Tau[245-368] with [301-309] mutated as KVQIINKKL	16534	0.00659	398

Figure S7 : Thermokinetic parameters of the interaction of VHH Z70 and VHH E4-1 with Tau, Tau MTBD and the PHF6/PHF6* sequences. Tables corresponding to k_{on}, k_{off} and resulting Kd obtained from SPR experiments with biotinylated Tau (*upper table*) or VHH-Z70 biotinylated on a C-terminal Cys residue (*lower table*) immobilized on the chips. Sequence of the Tau[273-318] peptide (containing both PHF6* and PHF6 sequences) is included (*lower table*). See also **Figure S10.**

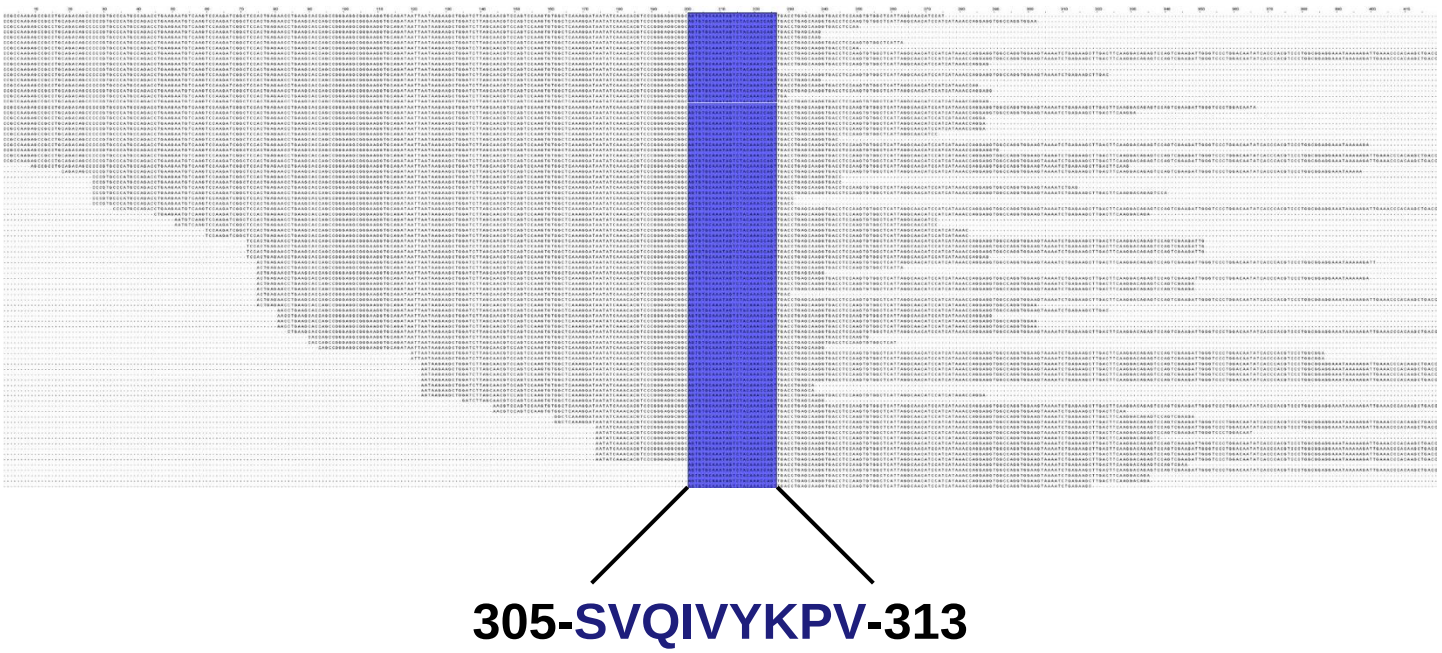

Figure S8 : Identification of the minimal epitope recognized by VHH Z70 using Tau fragment library and yeast two hybrid. Sequence alignment of the 90 Tau fragments corresponding to the 90 positive colonies picked on selective growth conditions and thus binding VHH Z70. The minimal common sequence is highlighted. Sequences are not meant to be read.

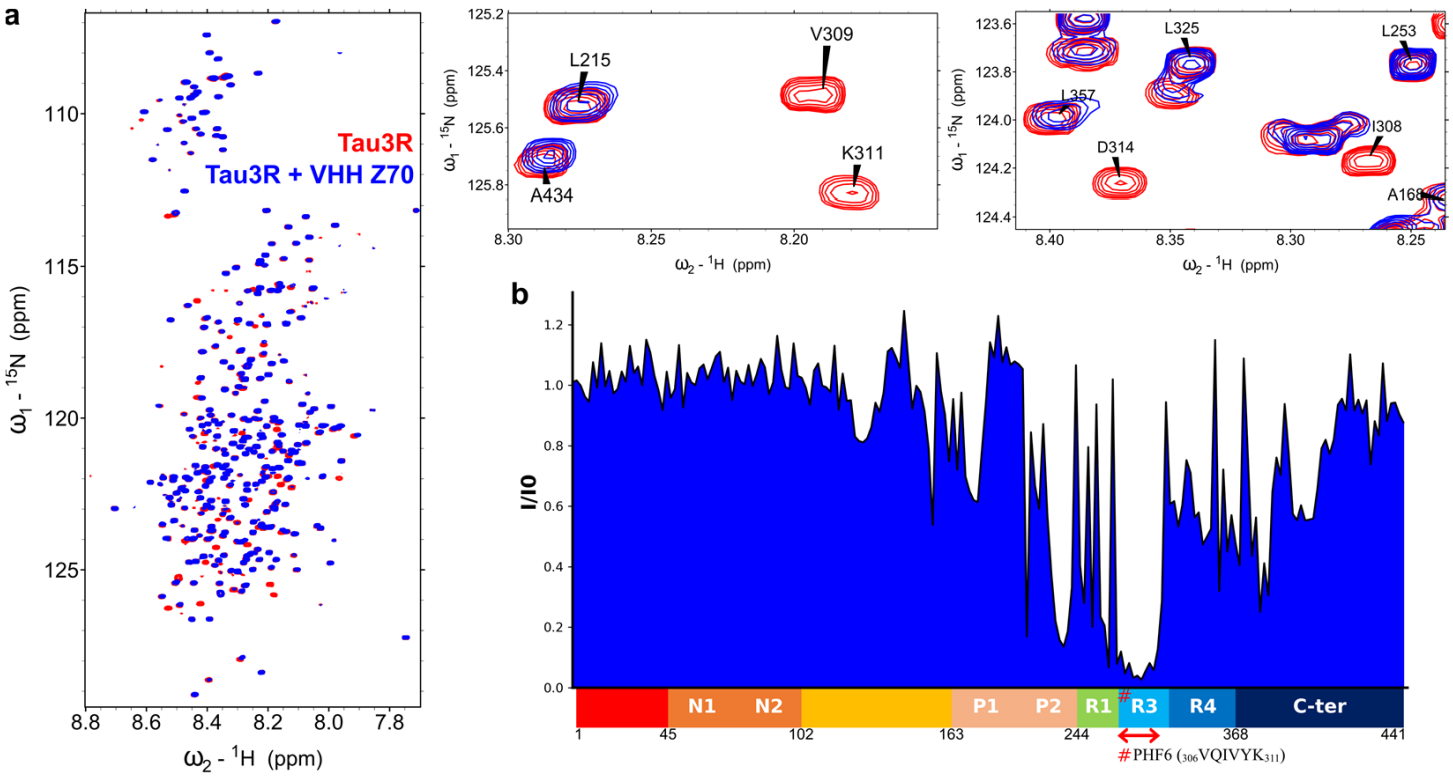

Figure S9 : Identification of VHH Z70 epitope using 2D HSQC NMR experiment of Tau2N3R. a : Overlays of ^{1}H, ^{15}N, full spectrum and enlargements of ^{15}N-labelled Tau 2N3R alone (red) or mixed with non-labelled VHH Z70 (blue). Spectra enlargements show broadened resonances corresponding to residues implicated in the interaction. **b :** Intensities ratio I/I0 of corresponding resonances in the 2D spectra of Tau 2N3R with equimolar quantity of VHH (I) or free in solution (I0) for residues along the Tau 2N3R sequence. Tau 2N3R lacks the R2 repeats. Tau 2N3R residue numbering corresponds to the Tau 2N4R sequence, for clarity. The red double-arrow indicates the region containing the corresponding major broadened resonances, which was mapped mostly on the PHF6 motif, showing PHF6 is sufficient for VHH Z70-Tau binding. Localization of the PHF6 peptide sequence is indicated.

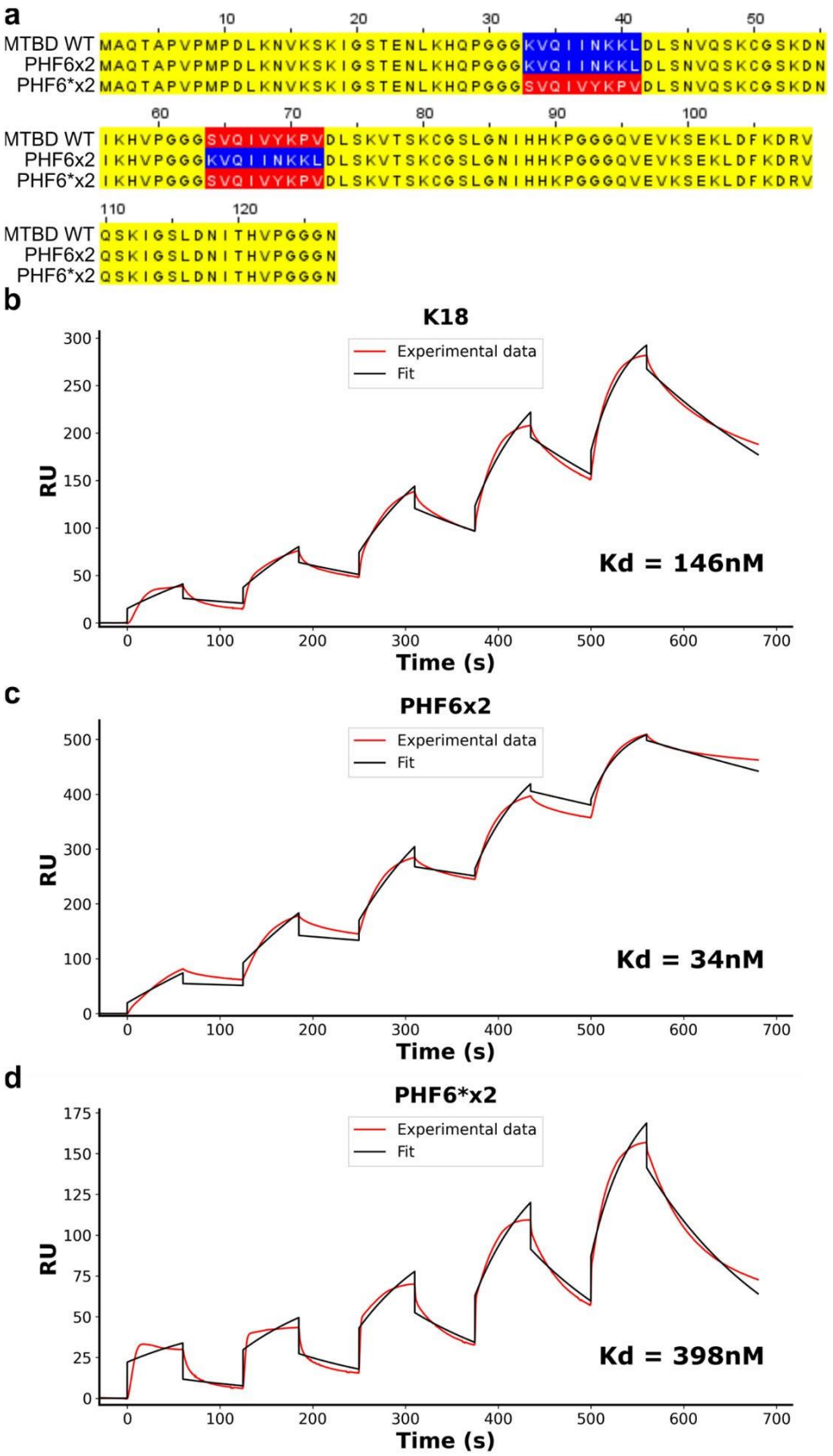

Figure S10 : The PHF6 peptide sequence is the main binding site for VHH Z70

a : Sequence alignment of Tau MTBD and chimeric MTBD sequences. PHF6 peptide is highlighted in blue, PHF6* in red. **b-d :** Sensorgrams (reference subtracted data) of single cycle kinetics analysis performed on immobilized biotinylated VHH Z70, with five injections of **b :** MTBD or K18 or **c :** chimeric MTBD with two PHF6/PHF6x2 or **d :** chimeric MTBD with two PHF6*/ PHF6*x2, at 0.125 µM, 0.25 µM, 0.5 µM, 1 µM, and 2 µM (n=1). Dissociation equilibrium constant Kd were calculated from the ratio of off-rate and on-rate kinetic constants koff/kon (**Figure S7**). Black lines correspond to the fitted curves, red lines to the measurements.

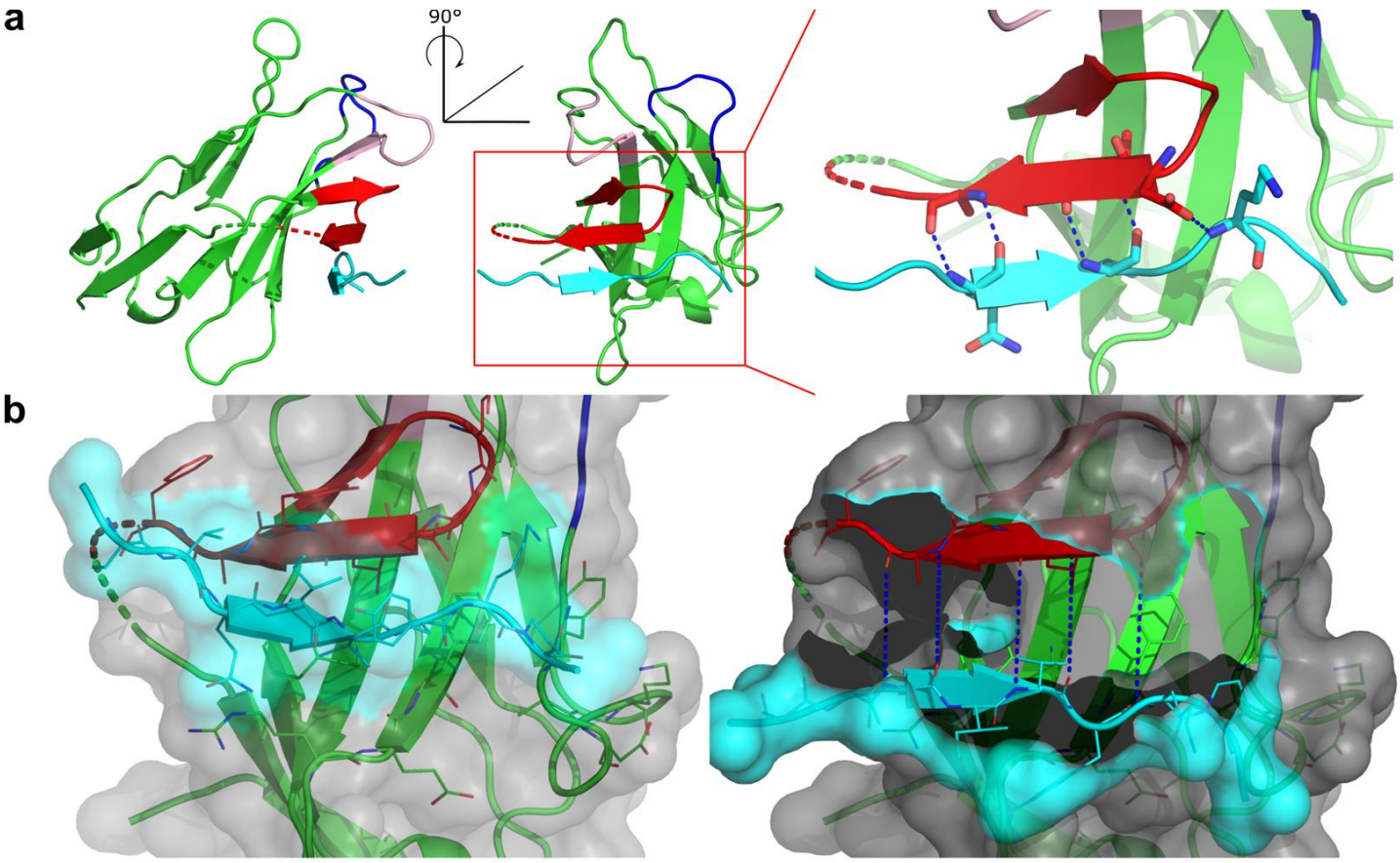

c

VHH residue	Atom	Tau residue	Atom	Distance (Å)
Asp 106	OD1	Lys 311	N	2.91
Leu 107	N	Vas 309	O	2.89
Leu 107	O	Val 309	N	2.80
Ala 109	N	Gln 307	0	2.77
Ala 109	O	Gln 307	N	2.88

Figure S11 : Crystal structure of the PHF6 peptide sequence bound to VHH Z70

a : Cartoon representation of VHH Z70 in complex with Tau[301-312] peptide. The two views correspond to a 90° rotation around the *y* axis. Framework regions of the VHH are represented in green and the PHF6 Tau peptide in cyan. VHH CDR1 is represented in pink, CDR2 in dark blue and CDR3 in red. The region boxed in red is enlarged. Dashed blue lines correspond to intermolecular H-bonds as detail in **c.** Red/green dashed cartoon line is undefined in the structure. See supplemental video. **b :** Cartoon and transparent surface representation. Color code as in **a.** Buried residues are represented as lines. Right panel is a tearing through the interface. Intermolecular H-bonds are represented as blue dashes and the residues involved in theinteraction are represented as sticks. **c :** Table of the intermolecular H-bonds

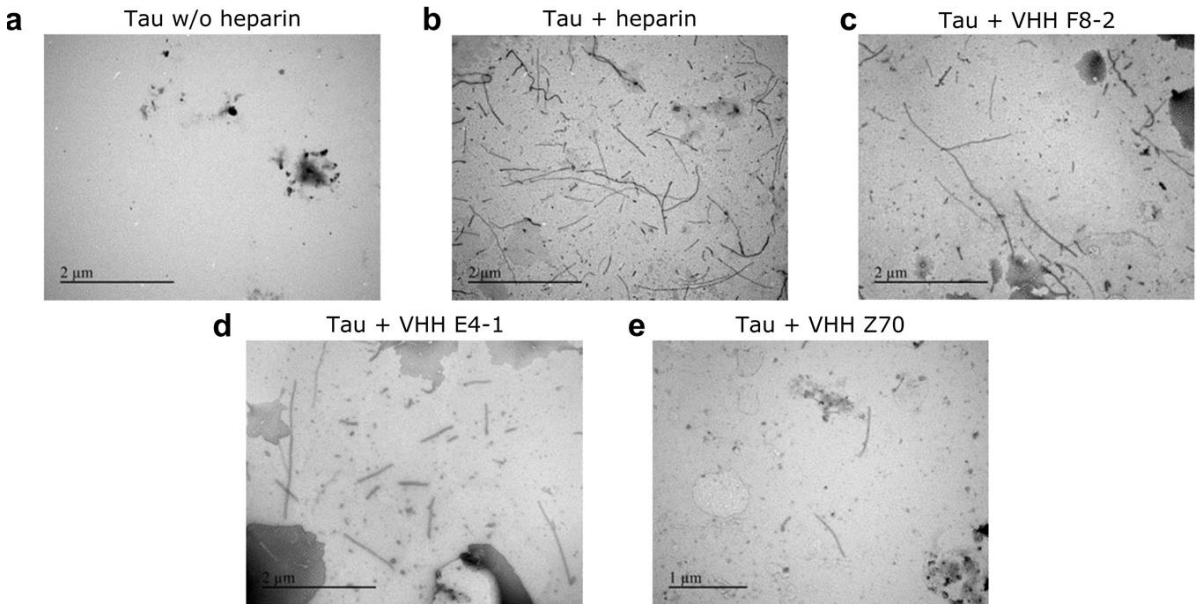

Figure S12 VHH E4-1 and VHH Z70 inhibit *in vitro* Tau aggregation Transmission electron microscopy images at the end point of the aggregation assays (**Figure 4**) **a :** in the absence of heparin or **b :** in the presence of heparin and **c-e** in the presence of heparin and the additional presence of **c :** VHH F8-2 **d:** VHH E4-1 **e :** VHH Z70 (for Tau/VHH molar ratio of 1 : 1) (n=2).

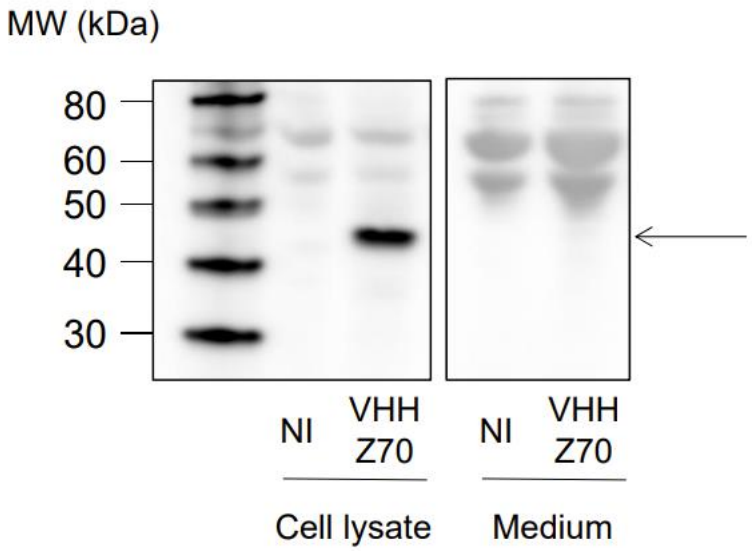

Figure S13 : Intracellular expression of VHH-Z70: HEK293 cells were infected with LVs encoding VHH-Z70 N-terminally fused to mCherry or non infected (NI). Forty-eight hours later, the cell lysate and the medium were recovered and analysed by western-blotting. VHH 70 expression (black arrow) was revealed thanks to the mCherry tag using primary antibody against mCherry.

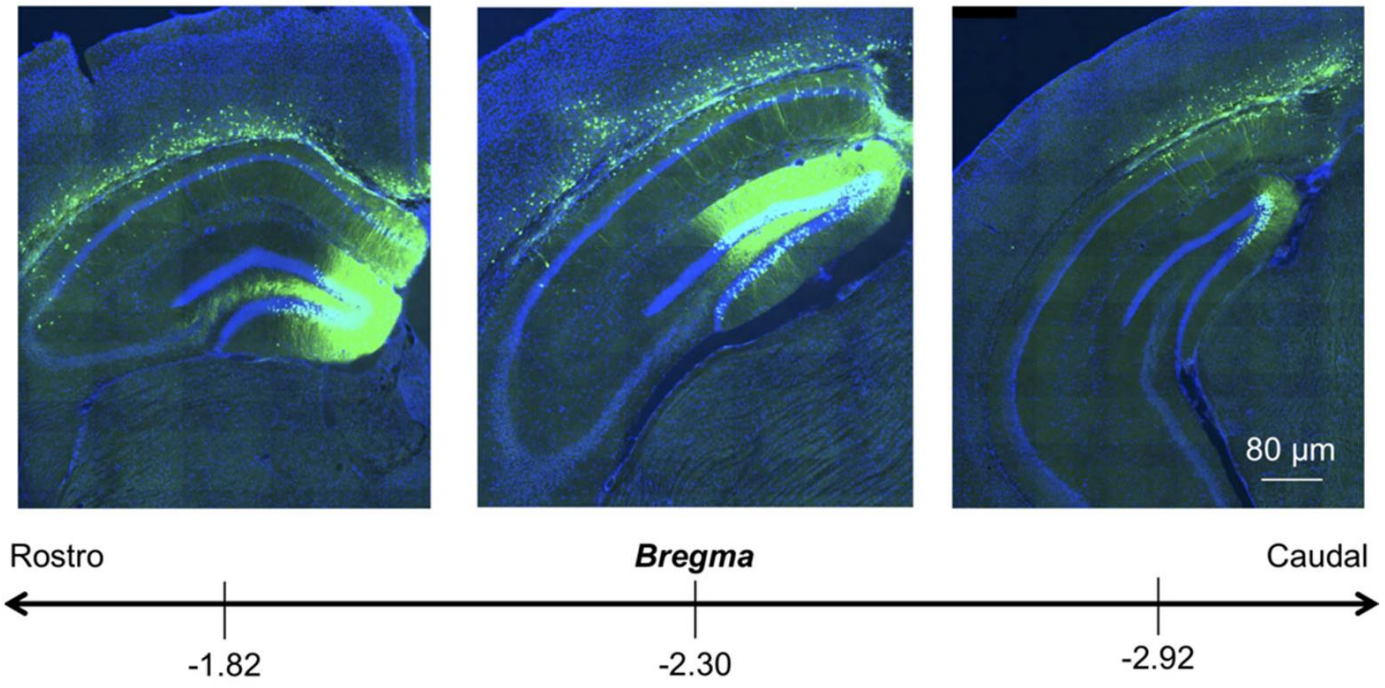

Figure S14 : VHH Z70 expression in the hippocampus. One month-old THY-tau30 mice were treated with bilateral intracranial injections of LVs encoding VHH Z70. Two weeks later mice received stereotaxic injection of AD brain lysate. Mice were sacrificed 4 weeks later and the whole brains were processed for immunohistochemical analyses. VHH Z70 was detected using a primary antibody against mCherry tag (visualised in green). VHH Z70-immunoreactivity is detected in all regions covering the bregma where Tau pathology has been quantified.

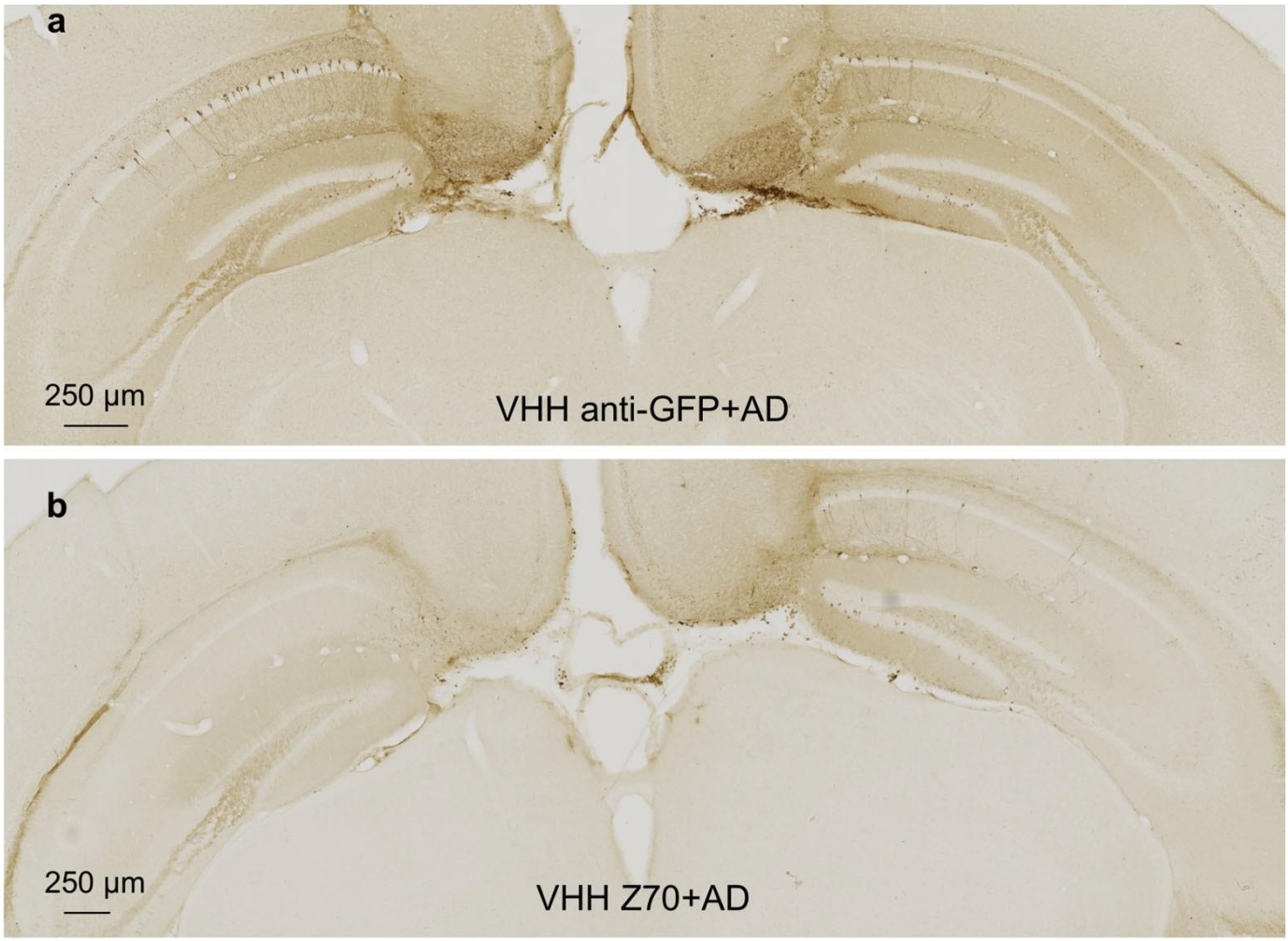

Figure S15 : VHH Z70 reduces human Tau seeding induced by extracellular human pathological Tau species: One month-old THY-tau30 mice were treated with bilateral injections of LVs **a :**encoding VHH-anti GFP or **b :** VHH Z70. Two weeks later mice received stereotaxic injection of AD brain lysate. Mice were sacrificed 4 weeks later and the whole brains were processed for immunohistochemical analysis using AT8. Sections from the hippocampus (injection site) are shown. Scale bars are indicated on the figure.

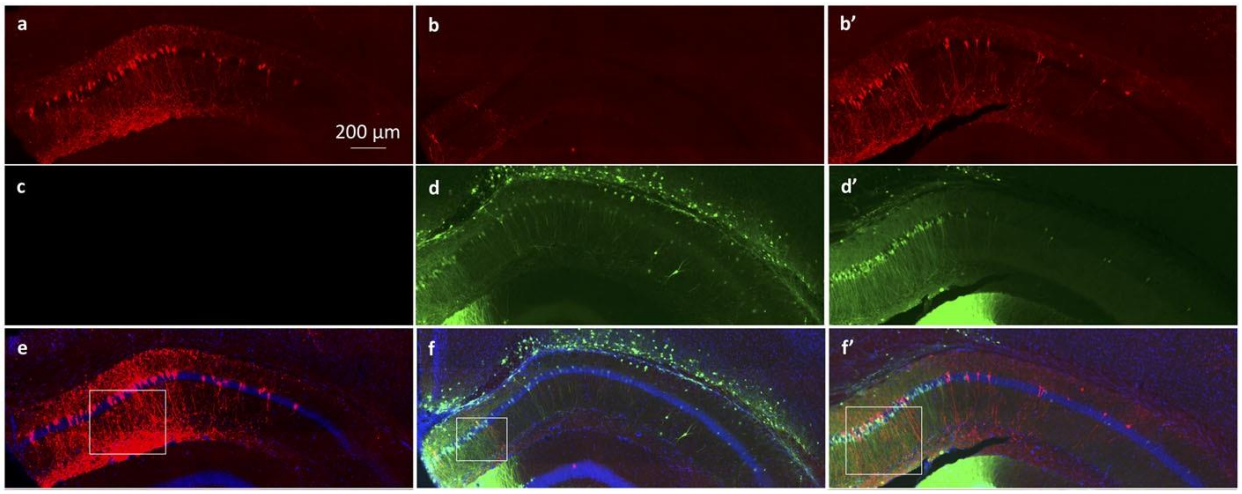

Figure S16 : No tau lesion in VHH 70-positive neurons- One month-old Tg30tau mice were treated with bilateral intracranial injections of LVs encoding GFP-specific VHH (a-c-e, one mouse) or VHH Z70 (b-d-f and b'-d'-f', two different mice). Two weeks later mice received stereotaxic injection of AD brain lysate. Mice were sacrificed 4 weeks later and the whole brains wereprocessed for AT8 (red) and mcherry (green) immunoreactivities (VHH Z70 was detected using a primary antibody against mCherry fusion domain). Nuclei are vizualized in blue. Enlargements (white rectangles) of e, f, f' are shown in **Figure 6d**. The scale bar is indicated on the figure.

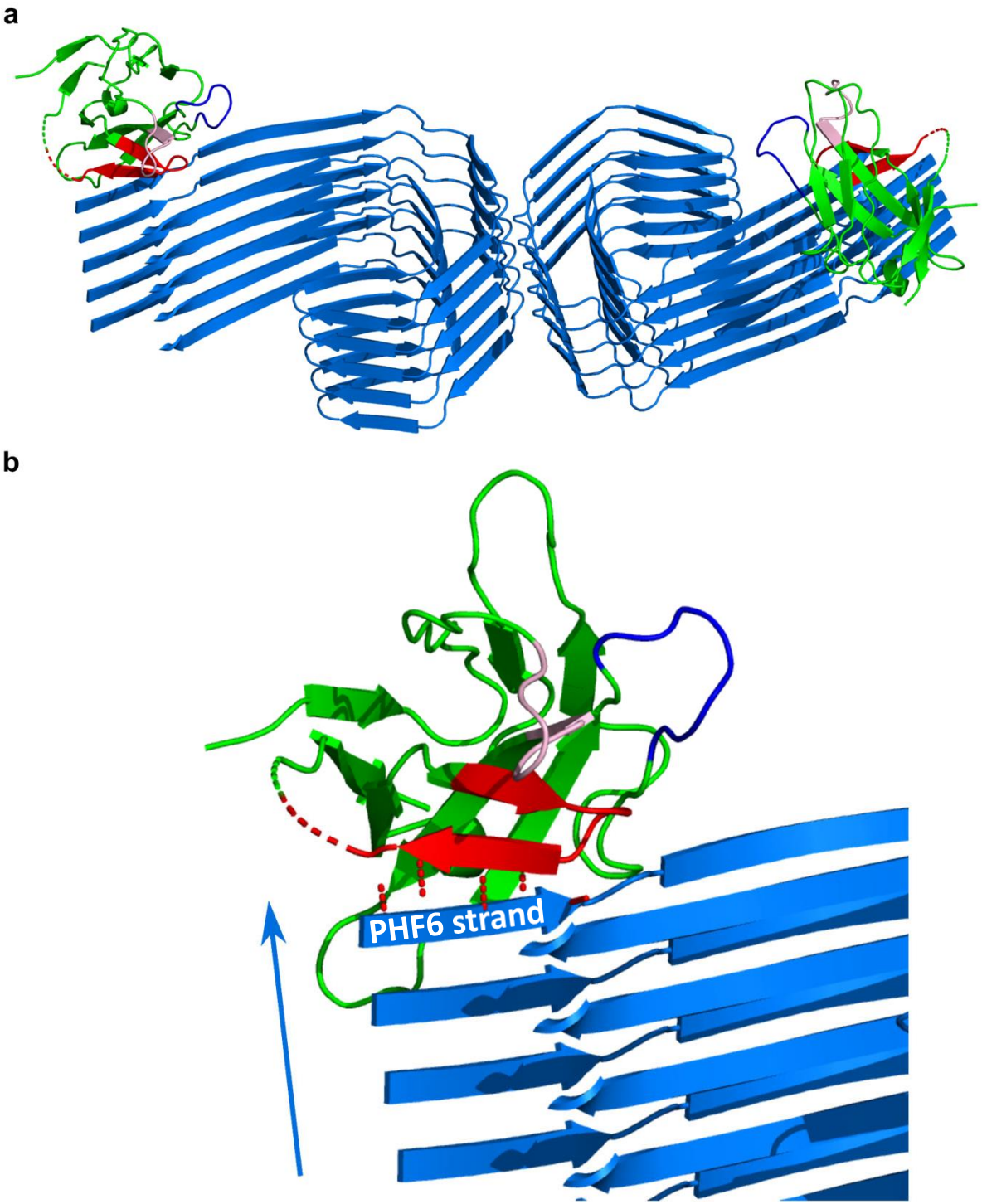

Figure S17 : Structure-based representation of VHH Z70 interaction with AD Tau fiber

a-b : Structure of VHH Z70 (in green) was solved in this study. Cryo-EM structure of Tau fiber (in blue) was obtained from pdb 5o3l. Color code of the loops as in **Figure S11**. Dashed cartoon line at CDR3 / FR4 junction illustrates the unresolved segment due to high flexibility. Structures were positioned by hand using superimposition of the PHF6 ß-strand respectively in complex with VHH Z70 and within the fiber (with Pymol). **b** : Enlargement of the red-boxed zone of **a**. Intermolecular H-bonds are illustrated by dashed red lines. The fiber elongation axis is illustrated by an arrow. The only accessible PHF6 strand at the fiber extremity is annotated.

This representation of the complex shows the complementation of the fiber ß-sheet by the VHH Z70 ß-hairpin in the CDR3 upon interaction with the PHF6 ß-strand within the fiber. This complex representation supports the hypothesis that the interaction is sterically only feasible at the free extremity of the fiber or oligomer of Tau. Such interaction would be expected to disrupt the seeding and fiber elongation.

3390

5pTCTGCACAATATTTCAAGCTATACCAAGCATACAATCAACTCCAAGCTAGAACCATGGCGGAAGTGCAGCTGCAGGCTC

3880

3pTCTTCTTTTTTGGAGGCTCGGGAATTAATTCCGCTTTATCCATCTTTGCGGCGGCCGCGCTACTCACAGTTACCTG

6690

5pCAGGGCAATAAAGTCGAACT,

6972

5pGACCTACAGGAAAGAGTTACTC

10829

5pCTATTCGATGATGAAGATACCCCACCAAACCCAAAAAAAGAGATCCTAGAACTAGACACTCTTTCCCTACACGACGCTCTTCC

10830

5pCCGGGCCTCTAGACACTAGCTACTCGAGGGGCCCCAGTGGCCCTATCTATGCGGCCGCTCAGACTGGAGTTCAGACGTGTGCTC

Figure S18 Oligonucleotide sequences (Material and Methods)

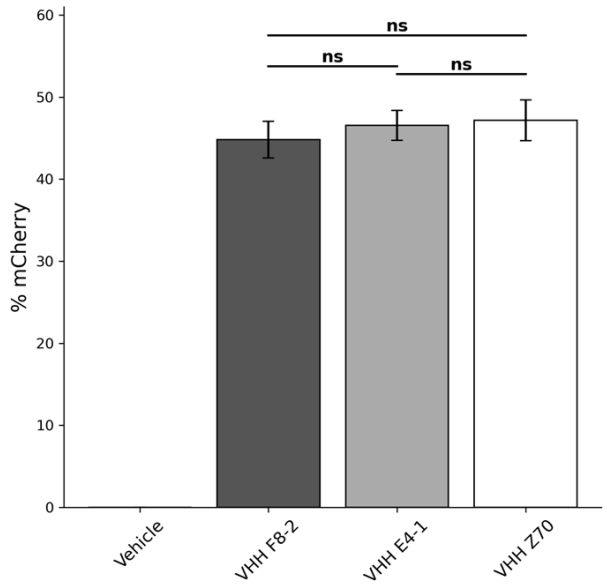

Figure S19 : VHH expression in the biosensor seeding reporter cells. HEK293 Tau RD P301S cells were transfected with plasmids encoding the different mCherry-VHH. mCherry fluorescence was evaluated by flow cytometry showing that transfection efficiency is equivalent : 44.8 % (± 2.2%) for VHH-F8-2, 46.6 % (± 1.8%) for VHH VE4-1 and 47.2 % (± 2;5%) for VHH Z70.

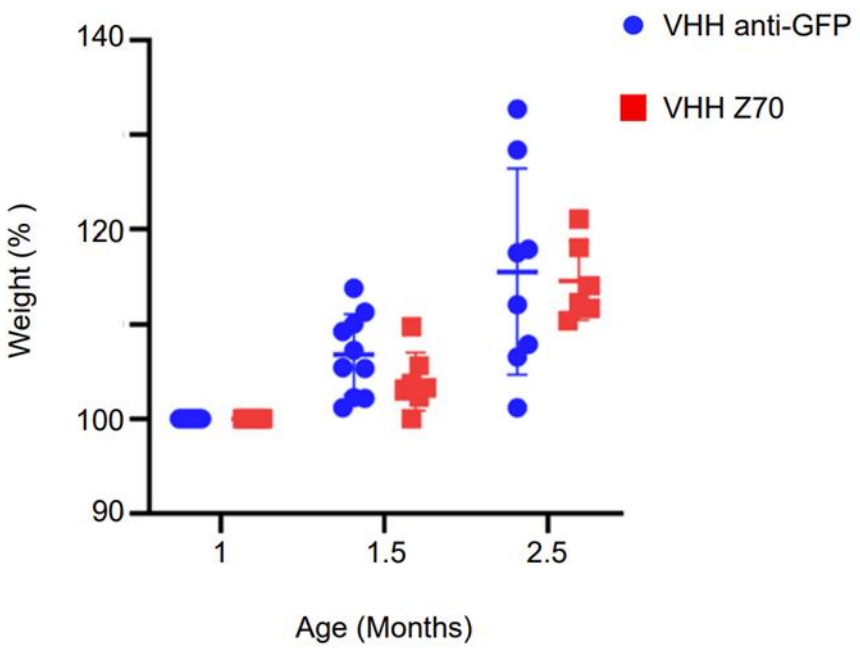

Figure S20 : No VHH toxicity in vivo- *Mice were weighted three times: 1 Month : before injection of LVs, 1.5 Month : before injection of human brain lysate and 2.5 Month : at sacrifice. Weights were normalized to the first weighting (100%). VHH 70 and VHH anti-GFP correspond to mice injected with one of these VHHs and AD human brain lysate.*

Role of Tau as a microtubule associated protein: structural and functional aspects

Pascale Barbier[1], Orgeta Zejneli[2,3], Marlene Marthino[4], Alessia Lasorsa[2], Valérie Belle[4], Caroline Smet-Nocca[2], Philipp O Tsvetkov[1], François Devred[1*], Isabelle Landrieu[2*]

[1]Aix Marseille Univ, Centre National de La Recherche Scientifique (CNRS), Inst Neurophysiopathol (INP), Fac Pharm, Marseille, France

[2]Univ Lille, Centre National de La Recherche Scientifique (CNRS), UMR8576, UGSF, Unité de glycobiologie structurale et fonctionnelle, 59000 Lille, France

[3]Univ Lille, Inserm, CHU-Lille, UMRS1172, JPArc, Jean-Pierre Aubert Research Centre, 59000 Lille, France

[4]Aix Marseille Univ, CNRS, UMR 7281, BIP, Bioénergétique et Ingénierie des Protéines, Marseille, France

Correspondence : isabelle.landrieu@univ-lille.fr; francois.devred@univ-amu.fr

Keywords

Post-translational modifications, biophysical methods, Alzheimer's disease, intrinsically disordered proteins, neurodegenerative diseases

Abstract

Microtubules (MTs) play a fundamental role in many vital processes such as cell division and neuronal activity. They are key structural and functional elements in axons, supporting neurite differentiation and growth, as well as transport along the axons by the motor proteins, which use MTs as support tracks. Tau is a stabilizing MT associated protein, whose functions are mainly regulated by phosphorylation. A disruption of the MT network, which might be caused by Tau loss of function, is observed in a group of related diseases called tauopathies, which includes Alzheimer's disease (AD). Tau is found hyperphosphorylated in AD, which might account for its loss of MT stabilizing capacity. Since destabilization of MTs after dissociation of Tau could contribute to toxicity in neurodegenerative diseases, a molecular understanding of this interaction and its regulation, is essential.

Introduction

Tau is a microtubule-associated protein (MAP) (Weingarten et al., 1975; Witman et al., 1976) that is abundant in the axons of neurons where it stabilizes microtubule (MT) bundles (Binder et al., 1985; Black et al., 1996). Together with other destabilizing MAPs, such as stathmin, Tau plays a central role in MT dynamics by regulating assembly, dynamic behaviour and spatial organization of MTs. Tau and other MAPs binding to MTs are tightly regulated by a number of factors, including post translational modifications (PTMs), ensuring the appropriate dynamics of the system (Lindwall and Cole, 1984; Mandelkow et al., 1995; Ramkumar et al., 2018). However, the exact mechanism of assembly and stabilization of MTs by Tau remains challenging to characterize due to the inherent dynamics of the system and the disordered nature of Tau. The number of approaches that have been conducted so far to gain knowledge on this particular interaction is striking (Devred et al., 2010; Di Maio et al., 2014; Nouar et al., 2013; Tsvetkov et al., 2019).

Tau is probably the most studied MAP because of its implication in a group of neurodegenerative diseases called tauopathies, associated with Tau aggregation into intraneuronal deposits (Brion et al., 1986), such as frontotemporal dementia (FTD), Alzheimer's disease (AD) and progressive supranuclear palsy.

Tau binding to MTs, as well as its propensity to aggregate, are affected by Tau mutations and by Tau PTMs, in particular its hyper-phosphorylation (Alonso et al., 1994; LeBoeuf et al., 2008). These pathologically modified Tau molecules perturb MT function and axonal transport, contributing to neurodegeneration. Indeed, a reduction of MT density and fast axonal transport are observed in transgenic AD mouse models that exhibit hyperphosphorylated Tau inclusions in neurons (Cash et al., 2003). Furthermore, Tau mutations carried by FTD patients cause MT-mediated deformation of the nucleus, which in turn results in perturbation of the nucleocytoplasmic transport (Paonessa et al., 2019). In addition, mislocalized Tau in neurons of Tau-overexpressing transgenic mouse brain and of human AD brain directly interacts with the nucleoporins of the nuclear pore complex. This interaction

disrupts the nuclear pore functions of nucleocytoplamic transport and might contribute to Tau-related neurotoxicity (Eftekharzadeh et al., 2018).

Efforts for clinical intervention in the AD field have so far focused mainly on blocking the formation of extracellular amyloid β deposits, another type of aggregates observed in brains of AD patients (Cummings et al., 2017). However, in the last several years, there has been an increase in studies aimed at therapeutic targeting of Tau. An improved understanding of Tau functions could lead to the development of new strategies for therapeutic interventions (Jadhav et al., 2019; Mudher et al., 2017). This emphasizes the need to understand the finer details of structural and functional aspects of Tau/MTs interaction.

Tubulin and MTs

MTs are hollow cylinders composed of parallel protofilaments of α and β tubulin subunits (α/β tubulin heterodimer, here named tubulin) assembled head-to-tail, and forming a pseudo helical lattice (Amos and Schlieper, 2005) (**Figure 1**). During MT formation, tubulins self-assemble in their guanosine 5' triphosphate (GTP)-bound state to form a sheet that closes into a 25-nm outside diameter tube (Chrétien et al., 1995). Whereas the MT core or lattice is constituted of guanosine 5' diphosphate (GDP)-tubulin, a GTP cap forms at MT ends because of the delay between assembly and GTP hydrolysis at the tubulin inter-dimer interface (Baas et al., 2016; Bowne-Anderson et al., 2015; Caplow and Shanks, 1990; Carlier et al., 1989). This cap has been proposed to stabilize growing MTs since its loss induces MT depolymerization, with characteristic curled protofilaments at MT ends (Chrétien et al., 1995). MTs constantly undergo phases of assembly and disassembly in a process called "dynamic instability" (Mitchison and Kirschner, 1984). Due to this intrinsic dynamics of the system, MTs have been difficult to study from a structural point of view. During the past decades, numerous molecular models were used to simulate the mechanism of MT formation resulting in a more nuanced model than the original GTP-cap one, which now accounts for the diverse regulatory activities of MAPs. In this model named "coupled-random models", GTP hydrolysis occurs with a constant rate for any tubulin in the MT lattice, except for the dimers at the very tip (Bowne-Anderson et al., 2015). GDP-tubulin does not assemble into MTs, but forms double rings (Howard and Timasheff, 1986). It was thus originally considered that GTP would allosterically induce a straight conformation of tubulin capable of MT assembly, and that GDP would induce a curved conformation favouring disassembly (Melki et al., 1989). It is now generally accepted that GTP-tubulin in solution is curved similarly to GDP-tubulin, based on the MT models derived from electron microscopy (EM) data, up to about 3.5 Å resolution (Zhang et al., 2015b) and from X-ray crystallography up to 2 Å resolution (Nawrotek et al., 2011; Pecqueur et al., 2012) together with biochemical evidences (Barbier et al., 2010). Tubulin only straightens upon incorporation into MTs (Alushin et al., 2014). In addition to the GDP/GTP dual nature

of tubulin, PTMs of tubulin, such as tyrosination and acetylation, modulate MT stability (Baas et al., 2016). In neurons, two MT regions are distinguished (**Figure 1**): a labile MT region mostly composed of tyrosinated and deacetylated GTP-tubulin, and a stable MT region (or lattice) mostly consisting of assembled detyrosinated and acetylated GDP-tubulin (Baas et al., 2016). These findings together with other recent studies of tubulin modifications - including phosphorylation, polyglycylation, deglutamylation and polyglutamylation - highlight the importance of these PTMs in regulating the different functions of MTs, generating a "tubulin code" (Gadadhar et al., 2017). Indeed, a defect of the deglutamylase CCP1, the enzyme responsible of tubulin deglutamylation, causes infantile-onset neurodegeneration (Shashi et al., 2018), while an excessive polyglutamylation of tubulin reduces the efficiency of neuronal transport in cultured hippocampal neurons (Magiera et al., 2018). Moreover, a defect of acetylated tubulin is linked to abnormal axonal transport in several neurodegenerative diseases (Dompierre et al., 2007; Godena et al., 2014; Guo et al., 2017). Taken together, these studies suggest that enzymes responsible for tubulin PTMs could be promising therapeutic targets.

Tau protein

There are two major MAPs present in cells from the central nervous system, MAP2 and Tau. The expression of one or the other isoform is regulated during development, and their localizations differ. Tau is mainly found in the axonal compartment while MAP2 is expressed specifically in cell bodies and dendrites (Melková et al., 2019). Both proteins exist as alternatively spliced isoforms, with some high-molecular weight isoforms for MAP2 (MAP2a and MAP2b). There are six isoforms of Tau protein present in the central nervous system (ranging from 352 to 441 amino acid residues), resulting from mRNA alternative splicing of a single gene (Goedert et al., 1989; Himmler et al., 1989). Tau is divided in functional domains (numbering according to the longest isoform, **Figure 2**): an N-terminal projection domain Tau(1-165), a proline-rich region Tau(166-242) or PRR, a MT binding region Tau(243-367) or MTBR and a C-terminal domain Tau(368-441). The MTBR consists of four partially repeated sequences R1(243-273), R2(274-304), R3(305-335), and R4(336-367) (**Figure 2**). The isoforms differ by the

presence, or not, of one/two insert(s) in the N-terminal domain (N1 and/or N2 presence or not), and 3 or 4 repeat sequences in the MTBR (R2 presence or not). Even though Tau is an intrinsically disordered protein (IDP), it has a tendency to form local secondary structures, in particular β-strands in the MTBR and polyproline II helices in the PRR (Mukrasch et al., 2009; Sibille et al., 2012). It has been proposed that Tau N- and C-terminal domains fold back on the central PRR and MTBR domains due to contacts between the N and C-termini of the protein (Jeganathan et al., 2006; Mukrasch et al., 2009). This model was initially built using distance measurements based on Förster Resonance Energy Transfer (FRET) detection between pairs of fluorophores attached to Tau (Jeganathan et al., 2006). Moreover, measurements of paramagnetic relaxation enhancement (PRE) by nuclear magnetic resonance spectroscopy (NMR) using paramagnetic centres attached at different positions along the Tau sequence, confirmed proximities of the N-and C-terminal domains with the central region of Tau (Mukrasch et al., 2009). Several co-factors were reported to enhance Tau structuration including ions such as Zinc (Roman et al., 2019), potentially regulating Tau functions.

MAP function of Tau

MT dynamics is regulated by proteins that stabilize or destabilize them (van der Vaart et al., 2009). The main role of Tau, one of the stabilizing MAPs, is to protect MTs against depolymerization by decreasing the dissociation of tubulin at both MT ends, resulting in an increased growth rate and decreased catastrophe frequency (Murphy et al., 1977; Trinczek et al., 1995). *In vitro*, Tau induces MT formation at 37°C and tubulin rings at 20°C under experimental conditions with no self-assembly of tubulin alone, suggesting that Tau is a MT inducer in addition to being a MT stabilizer (Devred et al., 2004; Kutter et al., 2016; Weingarten et al., 1975).

Tau was proposed to bind preferentially to the GDP-tubulin from the lattice, in detriment of the GTP-tubulin from the plus-end cap, in agreement with a stabilizing role of Tau (Duan et al., 2017). However, monitoring of Tau binding to MTs by FRET has shown Tau decoration on MT tips, as well as on the lattice (Breuzard et al., 2013). Furthermore, the capacity of Tau to induce *in vitro* MT formation is lost

when GDP-tubulin is used (Devred et al., 2004). In agreement, Tau depletion in rat cortical neurons results in the loss of MT mass in the axon, predominantly from the labile domain containing tyrosinated tubulin, rather than the stable domain of MTs (Qiang et al., 2018). Green fluorescent protein (GFP)-tagged Tau was indeed observed to be more abundant on the labile domain of the MTs, or GTP-tubulin cap. Based on these observations obtained by quantitative immunofluorescence, the authors propose that Tau is not strictly a MT stabilizer, but rather allows the MTs to conserve long labile domains (Baas and Qiang, 2019; Qiang et al., 2018). However a more likely explanation is that Tau is necessary to induce tubulin polymerization in the labile region.

Similarly to many other IDPs, Tau can undergo phase-transition under *in-vitro* conditions of molecular crowding, resulting in the formation of Tau liquid droplets similar to non-membrane compartments (Hernández-Vega et al., 2017). These Tau-rich drops have the capacity to concentrate tubulin ten times or higher than the surrounding solution. Nucleation of MTs is observed inside the Tau drops, and MT bundle formation results in the elongation of the drops. This bundle formation could not be reproduced by mimicking the high concentration effect, in the absence of drops. This nucleation environment could support stabilization and provide sufficient plasticity for the formation of the long axonal MT bundles. Although it is not yet known whether this phenomenon is of physiological relevance, GFP-Tau droplets have been observed in transfected neurons (Wegmann et al., 2018).

Structural aspects of Tau MTBR interaction with MTs

Tau structure when bound to MTs has been the object of numerous investigations, leading to several models of Tau/MTs complex. *In vitro,* single-molecule FRET experiments showed that Tau bound to soluble tubulin adopts an open conformation (Melo et al., 2016), losing the global fold observed for Tau in solution (Jeganathan et al., 2006; Mukrasch et al., 2009; Schwalbe et al., 2014). However, FRET experiments in cell, using a Tau protein labelled at its N and C-termini with fluorophores (Di Primio et al., 2017) show that labelled-Tau bound to MTs displays a global folding, with the N- and C-termini in close proximity, as described for the “paperclip conformation” of free Tau in *in vitro* conditions

(Jeganathan et al., 2006). This global fold is lost for unbound Tau, detached from the MTs. This discrepancy might be due to the fact that the cytoplasmic environment is much more complex than can be reproduced in *in vitro* experiments, and Tau might thus bind numerous other cellular partners that could influence its conformation (Di Primio et al., 2017).

Globally, tubulin-bound Tau retains its intrinsically disordered character, and forms a fuzzy complex with tubulin, which might be the reason why Tau binding mode accommodates more than one tubulin (Tompa and Fuxreiter, 2008; Martinho et al., 2018). In agreement, a combination of metal shadowing and cryo-electron microscopy (cryo-EM) revealed that Tau is randomly distributed on the MT surface (Santarella et al., 2004). FRET and fluorescence recovery after photo-bleaching in live cells similarly concluded to the distribution of the Tau/MTs interaction along the MTs, characterized by Tau diffusion coupled to binding phases (Breuzard et al., 2013). In-line with these observations, Tau was shown to diffuse along the MTs, bi-directionally and independently from active transport, in a manner described as kiss-and-hop interactions (Hinrichs et al., 2012). These interactions, observed by single molecule tracking in neurons, might explain why Tau does not seem to interfere with motor protein-mediated axonal transport along the MTs (Janning et al., 2014).

Early studies by peptide mapping allowed the first characterization of the interaction as an array of weakly interacting sites, defining the MTBR as the MT binding core, which contains the four highly homologous repeats R1-R4 (Butner and Kirschner, 1991; Goode et al., 2000). Recently, despite the challenges related to the dynamic and fuzzy nature of Tau/MTs interaction described above, the combination of cryo-EM at near-atomic resolution and Rosetta modelling generated models of the interaction. This breakthrough study highlights crucial residues of Tau MTBR directly mediating the interaction and confirms the longitudinal mode of Tau binding on MTs (Kellogg et al., 2018). The complex used in the study consists of dynamic MTs without stabilizing agents other than Tau. Tau is found along the protofilaments, following the H11-H12 helices that form a ridge at the MT surface and that are close to the point of attachment of the C-terminal tails of tubulin (**Figure 3**). The observed density spans Tau residues 242 to 367, covering the MTBR, and is centred on the α-tubulin subunit

while contacts with β-tubulin are detected on both sides. To obtain further details, artificial four-R1 and four-R2 constructs were used and showed that each repeat of the protein adopts an extended conformation that spans both intra- and inter-dimer interfaces, centred on α-tubulin and connecting three tubulin monomers.

A direct interaction of Tau peptides corresponding to residues 245–253 (in R1), 269–284 (in R2), and 300–313 (in R3) is proposed based on the attenuation of Tau NMR signal upon addition of paclitaxel-stabilized MTs (Kadavath et al., 2015b). The described bound-motif in the R2 repeat closely matches the bound-stretch found in the EM structure of four-R2 Tau repeats, but not the bound motif in the R1, for which the peptide 253-266 is rather proposed as the attachment point for R1 repeat (Kellogg et al., 2018). Additionally, the structure of the bound peptide Tau(267–312) (a peptide overlapping R2-R3 repeats) was probed using transfer-NOEs NMR signals. Based on the NOE contacts, which detect spatial proximities, a family of converging conformers were calculated for residues 269–284 (R2) and 300–310 (R3). Both peptides fold into a hairpin-like structure, formed by the conserved PGGG motifs, upon binding to MTs (Kadavath et al., 2015b). However, it should be noted that the electron density in the EM structure models cannot accommodate this hairpin (Kellogg et al., 2018). The hexapeptides 275-VQIINK-280 in R2 (PHF6* or paired helical filament hexapeptide) and 306-VQIVYK-311 in R3 (PHF6) (**Figure 2**) form an extended structure (Kadavath et al., 2015b), in agreement with the EM observation of an extended conformation for R2 (Kellogg et al., 2018). Both the EM and NMR models are incompatible with previous biochemical results, based on combined fluorescence correlation spectroscopy and acrylodan fluorescence screening, suggesting α-helical conformation of the bound-Tau repeats (Li et al., 2015).

The majority of structural data were obtained from the binding of Tau on MTs stabilized by exogenous agents such as Taxol, which facilitates the study by decreasing the dynamics of the system. Still a number of studies shows differences between Tau binding to Taxol pre-stabilized MTs, or to Tau-induced MTs, formed using Tau as inducer. Kinetics analysis of Tau binding to Taxol-stabilized MTs in comparison with Tau-induced MTs suggests the existence of two different binding sites of Tau to

tubulin (Makrides et al., 2004), one overlapping the Taxol binding site localized on β-tubulin in the inner surface of MTs, as previously suggested (Kar et al., 2003).

Site-directed spin labelling combined with electron-paramagnetic resonance spectroscopy (EPR) was used to compare Tau binding mode to Taxol-stabilized MTs and to tubulin when Tau is used as the sole inducer of the polymerization (Martinho et al., 2018). In these experiments, thiol disulfide exchanges between Tau and tubulin or Taxol-stabilized MTs was observed by EPR measurements of paramagnetic labels linked by disulfide bridges to Tau two natural cysteines, or to single-cysteine Tau mutants. Differences in the kinetics of the label release were observed between preformed MTs and Tau-induced MTs, explained by the accessibility of cysteines of tubulin and MTs deduced from available structural data. Localization of the two putative binding sites of Tau on tubulin was proposed (**Figure 4**). The first one in proximity of Cys347 of α-tubulin subunit could interact with Cys291 of Tau in R2. The second one, located at the interface between two protofilaments, in proximity of Cys131 of β-tubulin subunit, could interact with Cys322 of Tau in R3. The first site is in agreement with models proposing that the R2-R3 would encompass the interface between tubulin (Kadavath et al., 2015a; Kellogg et al., 2018). Both sites are less accessible in Taxol-stabilized MTs, which might explain the much slower release of the disulphide-linked Tau label involved in interaction with the Taxol-stabilized MTs.

Role of the regulatory regions outside of Tau MTBR

A number of studies addressed the role of the regulatory regions outside the MTBR. The N-terminal projection domain of Tau modulates the formation of MT bundles (Chen et al., 1992; Rosenberg et al., 2008). This domain, described as a polyelectrolyte polymer brush, is proposed based on atomic force microscopy to exert a repulsive force (Mukhopadhyay and Hoh, 2001). In another model, the electrostatic zipper model, Tau is proposed to organize MT spacing by dimerization of the projection domain and the PRR on adjacent MTs (Rosenberg et al., 2008). Both models might be valid but probably depend on the ionic strength of the solution (Donhauser et al., 2017). The N-terminal domain of Tau

remains disordered and highly flexible upon tubulin binding, as seen by both NMR (Kadavath et al., 2015a) and smFRET studies (Melo et al., 2016).

Repeats in the MTBR are required for MT binding and assembly. However, as an isolated fragment, the MTBR is not as efficient in tubulin polymerization and in MT binding as full-length Tau. The regions directly flanking the MTBR, in the PRR and in the C-terminal region, are needed to enhance the binding (**Figure 2**). Several models have been proposed to describe the roles of MTBR and flanking regions. In the first one, termed the "jaws" model (Gustke et al., 1994; Preuss et al., 1997; Trinczek et al., 1995), the PRR, MTBR, and C-terminal extension domains bind very weakly, if at all, to MTs, and the binding is enhanced when two consecutive domains are associated in a single construct. A NMR study has determined the residues in the PRR and in the downstream repeats that constitute the "jaws" (Mukrasch et al., 2007). The second model proposes that the initial binding of Tau to MTs is mediated by a MTs-binding core within the MTBR, whereas the flanking regions are regulatory (Goode et al., 2000).

The interaction between full-length Tau and Taxol-stabilized MTs allowed mapping of the binding region on the Tau protein at the residue level (Sillen et al., 2007). In particular, both the MTBR and the flanking regions, namely the PRR and 10 amino acid residues located at the C-terminal end of the MTBR, were found to interact with the MTs. In both the PRR and the MTBR, contribution of basic residues is important for Tau interaction with MTs (Goode et al., 1997; Kadavath et al., 2015b). Additionally, Tau proteolysis products interacting with tubulin were identified by using a complex named T_2R composed of two tubulins stabilized by the stathmin-like domain (SLD) of RB3 (Fauquant et al., 2011; Gigant et al., 2000). While the isolated fragments from the PRR and MTBR bind weakly to MTs, the Tau(208-324) construct, named TauF4, generated by combining two adjacent fragments included in the PRR and in the MTBR, binds strongly to MTs and stimulates MT assembly very efficiently (Fauquant et al., 2011). The MTBR included in TauF4 (R1, R2 and the N-terminal part of R3) mostly corresponds to the MT binding core initially proposed by Feinstein and co-workers (Goode et al., 2000).

PRE experiments performed by introducing four cysteine mutations on the SLD, located along the protein in proximity of the interface of every tubulin subunit, indicated that TauF4 binds asymmetrically to the two tubulins, with the PRR preferentially located closer to the β tubulin subunits (intra-dimer interface). When bound to a single tubulin stabilized by an engineered SLD protein (TR'), a part of the R1 repeat of TauF4 adopts a turn-like conformation, which remains flexible, and thus not in direct contact with α-tubulin surface (Gigant et al., 2014). The turn-like structure is centred on the 260-IGSTENL-266 sequence (**Figure 5**). This peptide becomes immobilized in the T2R complex, as can be now explained by its position in the EM structure at the inter-dimer interface (Kellogg et al., 2018). The turn-like structure present with a single tubulin is not detected by smFRET (Melo et al., 2016), which is proposed to result from the different conditions of the experiments (large excess of tubulin for the smFRET or excess of Tau for the NMR experiments). TauF4 fragment was further shown to bind, at least, at the inter-dimer interface as demonstrated by the competition between vinblastine binding and TauF4 for tubulin interaction (Kadavath et al., 2015a). Results of this study are in agreement with the stoichiometry of one Tau for two tubulin suggested by others (Gigant et al., 2014)

Finally, the interaction between soluble tubulin and the flanking region downstream of the four Tau repeats was investigated by NMR. This region has sequence homology with the repeats and is often referred to as R' (**Figure 2**). By using saturation transfer difference (STD) NMR spectroscopy, two residue stretches centred on F378 and Y394 were identified in interaction with MTs (Kadavath et al., 2018).

Impact of Tau phosphorylation on its interaction with MTs

Tau-induced neurodegeneration is correlated with the appearance of Tau hyperphosphorylation, Tau aggregation into Paired Helical Filaments and/or the loss of Tau/MT binding (Hernández and Avila, 2007). Overall, phosphorylations are reported to decrease the affinity of Tau for the MTs, ensuring the dynamics of the system in healthy neurons (Lindwall and Cole, 1984; Mandelkow et al., 1995). Specific phosphorylations such as phosphorylations of S214 (by PKA kinase) or of S262/356 (by MARK kinase)

have been described to strongly decrease the affinity of Tau for MTs (Biernat et al., 1993; Schneider et al., 1999; Scott et al., 1993; Sengupta et al., 1998). S262 makes hydrogen bonds with α-tubulin E434, thus explaining why phosphorylation of S262 residue strongly decreases MT binding (Kellogg et al., 2018). Since phosphorylation of S262 of the isolated R1 repeat peptide does not affect its affinity for MTs, it is likely that the consequences of S262 phosphorylation on Tau binding to tubulin are due to intramolecular rearrangements of the Tau protein (Devred et al., 2002). Interestingly, phosphorylation of S214 of Tau does not significantly affect the MT assembly capacity, despite the decreased affinity (Sillen et al., 2007). Phosphorylation of S214 could also have an indirect role *in vivo*, as this specific phosphorylation might play a role in the observed competition between MTs and the 14-3-3 proteins for Tau binding (Hashiguchi et al., 2000). Indeed, 14-3-3 protein binding to Tau is favored when S214 is phosphorylated (Tugaeva et al., 2017), which seems to result in neurite degeneration in neuronal cell cultures (Joo et al., 2015). The 14-3-3 protein family interacts mainly with phosphorylated protein partners and is especially abundant in brain tissue (Boston et al., 1982). 14-3-3 proteins have been implicated in a variety of human diseases, including neurodegenerative diseases. Indeed, 14-3-3 proteins are abundant in the intraneuronal deposits of aggregated Tau (Layfield et al., 1996; Qureshi et al., 2013; Umahara et al., 2004).

When Tau is phosphorylated by the CDK2/CycA3 kinase *in vitro*, phosphorylations at S202/T205 and T231/S235 sites are identified by NMR. Even though these phosphorylations do not significantly affect Tau binding to MTs (Amniai et al., 2009), Tau loses its capacity to assemble tubulin into MTs when at least three out of four positions are phosphorylated. This data shows that a decreased capacity of Tau to assemble tubulin into MTs, such as observed for the CDK-phosphorylated Tau, cannot be explained solely by a decreased affinity for MT surface. Additional experiments, using the shortest Tau isoform (Tau 0N3R) with T231E and S235E mutations as pseudophosphorylations, confirmed that E231/E235 do not abolish by themselves the interaction of Tau with the MTs (Schwalbe et al., 2015). However, NMR signals corresponding to residues in the PRR were less attenuated upon addition of MTs to the mutated Tau 0N3R rather than to the wild-type Tau (Schwalbe et al., 2015). This indicates that the

pseudophosphorylated Tau 0N3R was locally less tightly bound to the MTs. In addition, based on the models of the Tau(225-246) peptide phosphorylated on T231 and S235, issued from comprehensive calculations from NMR parameters (distances measurements and H-N orientations), the distances between the phosphate and the nitrogen in the directly preceding basic groups (R230 or K234 respectively) is less than 4.5Å, a distance compatible with the formation of a salt-bridge. The salt bridge proposed to link phosphorylated T231 and R230 side-chains of Tau could compete with a salt bridge formation with the MTs , participating in the effect of the phosphorylation of T231 (Schwalbe et al., 2015).

Finally, Pin1 peptidyl prolyl cis/trans isomerase was proposed to restore the capacity of CDK-phosphorylated Tau to bind to the MTs and restore MT assembly (Lu et al., 1999). However, this model was recently challenged as Pin1 does not promote *in vitro* formation of phosphorylated Tau-induced MTs (Kutter et al., 2016).

For repeat R', the impact of phosphorylation on the binding affinity was assessed by means of STD NMR. Both phosphorylated Y394 and S396 were proved to weaken the interaction between Tau and MTs. However, by measuring residue-specific Kd values by STD, phosphorylation on S396 had a more pronounced effect than phosphorylation on Y394, despite the fact that they are only one residue apart (Kadavath et al., 2018).

Thus, Tau phosphorylation can have an effect on MT binding and assembly through several molecular mechanisms, including electrostatic perturbations, alteration/destabilisation of Tau regions bound to the MTs, a disruption of hydrogen-bonds or salt-bridges and changes in structural parameters.

Impact of Tau acetylation on its interaction with MTs

Another Tau PTM reported to contribute to Tau pathology is lysine acetylation (Min et al., 2010, 2015); indeed, acetylated Tau is proposed as a marker of AD (Irwin et al., 2012, 2013). In this case, Lys residues are modified by addition of an acetyl group on the NH_3 moiety of their side chains, neutralizing their positive charges and modifying their steric characteristics. Consequently, acetylation affects Tau

binding to MTs and impairs MT assembly (Cohen et al., 2011). Mass spectrometry (MS) analysis revealed that 14 Lys residues, mainly located in the MTBR, were acetylated in Tau samples purified from healthy mice (Morris et al., 2015). Analysis of acetylation sites obtained by *in vitro* acetylation with recombinant p300 acetyl-transferase, by both MS and NMR (Kamah et al., 2014), identified as many as 23 modified-Lys residues. An acetylation mimicking mutation K274Q inhibits Tau tubulin polymerization ability and stimulates Tau aggregation *in vitro* (Rane et al., 2019). Interestingly, acetylation of K280 was detected in brain tissues from patients affected with AD and not in healthy brain tissues (Cohen et al., 2011). Similarly, Tau acetylation at K174 is reported as an early change in AD brain and in transgenic mice expressing Tau with the P301S mutation (PS19 transgenic mice) (Min et al., 2015).

In addition, cross-talks between acetylation and phosphorylation modifications of Tau interplay in their regulatory role of MT dynamics (Carlomagno et al., 2017). Acetylation of K321 prevents the phosphorylation of S324, the latter being reported to inhibit Tau function of tubulin polymerization in *in vitro* assays (Carlomagno et al., 2017). Interestingly, this phosphorylation is one of the few modifications of Tau (among 63 modifications) specifically present in a human amyloid precursor protein transgenic AD mouse model when compared to a wild type mouse (Morris et al., 2015). Furthermore, phosphorylation of S324 is detected in post-mortem tissues of AD patients, but not in the control sample ones (Carlomagno et al., 2017). Pseudo-phosphorylated mutants S324D and S324E have a diminished capacity to polymerize MTs from tubulin in *in vitro* assays. Similarly, acetylation of K259/K353 prevents phosphorylation of S356/S262 by the MARK kinase. Modulation of Tau acetylation could be a new strategy to inhibit Tau-mediated neurodegeneration. Indeed, studies in mice suggest that this is a valid disease-modifying target. Increasing acetylation of Tau by deleting SIRT1 deacetylase in a TauP301S transgenic mouse model aggravates synapse loss, while SIRT1 overexpression limits Tau pathology propagation (Min et al., 2018). In the PS19 FTD transgenic mouse model, inhibition of p300 acetyltransferase activity lowers total Tau and K174-acetylated Tau levels. P300 inhibition prevents hippocampal atrophy and rescues memory deficits (Min et al., 2015). However, the complexity of

regulation of Tau function by PTMs has to be kept in mind. Acetylation can have both a direct inhibitory effect on Tau function and an indirect activation effect, by preventing phosphorylation in the KXGS motifs of the MTBR.

Impact of Tau FTD mutations on its interaction with MTs

Tau protein is encoded by the *MAPT* gene located on chromosome 17. Pathogenic variants in this gene cause several related neurodegenerative diseases characterized by the presence of hyperphosphorylated Tau aggregates in neurons (D'Souza et al., 1999; Wilhelmsen et al., 1994). Animal models with these mutations, such as P301L, have been extensively studied and are considered AD models (Lee et al., 2005). The FTD mutations of *MAPT* gene alter Tau biochemical properties and/or the ratio of Tau isoforms (4R/3R ratio). Change in the isoform ratio has an indirect impact on MT assembly and the dynamics of the MT networks, because the 3R Tau is known to have a lower capacity of MT stabilization and tubulin polymerization than the 4R Tau (Panda et al., 2003; Scott et al., 1991). The influence on Tau PTMs of the FTD mutations represents another indirect effect on Tau/MT interaction. The R406W Tau mutation is for example consistently reported to diminish Tau phosphorylation (Dayanandan et al., 1999; Delobel et al., 2002; Matsumura et al., 1999). However, almost all the FTD mutations also directly affect the ability of Tau to bind MTs and to promote tubulin assembly (Hasegawa et al., 1998; Hong et al., 1998). Tau with P301L, V337M or R406W mutations has a reduced binding to MTs and a decrease efficiency to initiate tubulin assembly. For P301L Tau, the initiation rate is decreased but the tubulin polymerization reaches the same extent in *in vitro* assays. Surprisingly, R406W Tau is reported to be the most affected, despite the fact that the mutation is not near the MTBR (Hong et al., 1998). This suggests that an alternative conformation might be involved. Later studies confirm the initial finding that FTD mutations affect the ability of Tau to bind MTs and to promote tubulin assembly in *in vitro* assays. However, there is no agreement on the extent of the specific effect of each of these mutations (Barghorn et al., 2000; Combs and Gamblin, 2012; DeTure et al., 2000). The effect of R5L, P301L, and R406W mutations of Tau differ in regard to their impact on

Tau MT stabilizing capacity, not only based on their localization in Tau sequence, but also depending on the number of N-terminal inserts (0, 1 or 2 N isoforms), in the three considered 4R-Tau isoforms (Mutreja et al., 2019). In particular, the R5L mutation has a reduced ability to polymerize tubulin, with lower tubulin polymerization extent, lower rate, and longer lag time specifically for the 0N 4R Tau isoform, compared to the 1N and 2N that are behaving as the wild-type Tau (Mutreja et al., 2019). For the P301L mutation, the Tau-dependent defect in MTs seems to diminish with removal of each N-terminal insert. This might be due to a differential effect of conformational changes induced by the mutations on the global hairpin-like conformation of Tau, which brings the N-terminal region close to the MTBR (Jeganathan et al., 2006). The impact of the FTD mutations on the MT stabilization capacity of Tau has been confirmed in intact cell context, with variable effect depending on the mutation (Delobel et al., 2002). Mammalian cells expressing Tau P301L show proportionally less Tau bound to MTs (Di Primio et al., 2017; Nagiec et al., 2001) . However, a strong consensus on the impact of the FTD mutations in cellular context is not yet reached, as in neuroblastoma and CHO cells transfected with GFP-tagged Tau DNA constructs, the co-localization with MTs and generation of MT bundles was shown to be identical for both mutants and wild type Tau (DeTure et al., 2000). The site-dependent and isoform-dependent effect of the Tau mutations on MT stabilization was reproduced in COS cells transfected with 3R or 4R Tau isoforms (Sahara et al., 2000). For example, the V337M mutation has significant effect when introduced in 3R Tau, but not in 4R Tau, showing disruption of MT networks and diminished co-localization of Tau and tubulin. This isoform specific effect of some of the mutations might explain part of the discrepancies reported on the impact of the FTD mutations of Tau on its MAP functions.

Perspectives

One of the proposed strategies in seeking AD treatment consists in compensating the loss of MT-stabilizing Tau function (Ballatore et al., 2011; Brunden et al., 2009; Cash et al., 2003; Das and Ghosh, 2019). One path to this goal is to harness the therapeutic potential of MT-stabilizing agents, classically

used in cancer therapies. This strategy to treat tauopathies was validated *in vivo* using Paclitaxel treatment of AD mouse models (Cash et al., 2003; Zhang et al., 2005) and cell models (Brunden et al., 2011). Recently, Monacelli et al provided an updated survey on the potential of repurposing cancer agents for AD (Monacelli et al., 2017). Besides its implication in neurodegenerative disease, Tau is also involved in regulatory mechanisms linked to cancer development. For example, Tau was shown to regulate the MT-dependent migration of cancer cells (Breuzard et al., 2019). Finally, similarly to stathmin, Tau level of expression modulates clinical MT-targeting agent efficiencies, such as taxanes or vincaalcaloids. (Li et al., 2013; Lin et al., 2018; Malesinski et al., 2015; Rouzier et al., 2005; Smoter et al., 2013).

MT stabilizing peptides is another option chosen to restore MT stability (Mondal et al., 2018; Quraishe et al., 2016). Such a peptide, the PS3 octapeptide, was designed from the taxol-binding pocket of β-tubulin (Mondal et al., 2018). The advantage of this peptide strategy is the moderate peptide affinity for MTs that preserves the MT dynamic capacity, crucial for synaptic plasticity and memory. Consequently, PS3 stimulates MT polymerization and increases expression of acetylated tubulin in PC12 neuron cell cultures, but has much less toxic effects than taxol. Other neuroprotective peptides have MT stabilizing function thanks to their ability for interactions with MT end-binding proteins, which protect MT from depolymerization (Oz et al., 2014). The NAP/SAL peptides, which interact with EB1 through a SIP motif, prevent and reverse MT breakdown and axonal transport deficits in a drosophila model of tauopathy (Quraishe et al., 2013, 2016).

Finally, MTs could be stabilized not by mimicking MAP function, but by modulating MT PTMs, which have a crucial role in MT dynamics. Levels of total α-tubulin are reduced by approximately 65 % in the AD-patient brains compared to age-matched control brains but the relative ratio of acetylated tubulin is increase by approximately 31 % compared to controls (Zhang et al., 2015a). This suggests a compensatory mechanism to counteract MT reduction due to loss of Tau stabilization because this modification characterizes stable MTs with slow dynamics (Kull and Sloboda, 2014; Szyk et al., 2014).

Inhibition of histone deacetylase 6 (HDAC6), the major tubulin deacetylase, is thus an alternative strategy to compensate for Tau MAP function. Indeed, in transgenic mouse models of AD, inhibition of HDAC6 improves memory (Govindarajan et al., 2013; Kilgore et al., 2010; Selenica et al., 2014). Similarly, in *drosophila*, HDAC6 null mutation rescues MT defects through increased tubulin acetylation (Xiong et al., 2013).

Overall, Tau implication in neurodegenerative diseases, and other diseases where MTs play an important role, clearly shows the interest of the Tau/MTs interaction as a potential target for intervention (Das and Ghosh, 2019; Pachima et al., 2016). Many advances have been made in the understanding of Tau functions as a MAP, and in the structural aspects of the Tau/MTs interaction. On this basis, the importance of regulatory factors of the interaction, from PTMs to other endogenous cofactors such as Zinc (Fichou et al., 2019), can now be addressed. This will hopefully lead to new strategies targeting disease where MTs, and consequently Tau, are involved.

Acknowledgements

Il, CS-N, AL and GZ acknowledge support by the LabEx (Laboratory of Excellence) DISTALZ (Development of Innovative Strategies for a Transdisciplinary approach to Alzheimer's disease), LiCEND (Lille excellence centre for neurodegenerative disease) and the project TUNABLE from the I-site ULNE (Lille University).

Author contributions: the content of the manuscript was drafted and edited by all authors

Abbreviations: AD Alzheimer's Disease; EM Electron Microscopy; EPR Electron Paramagnetic Resonance spectroscopy; FRET Förster Resonance Energy Transfer; FTD Fronto-Temporal Dementia; GFP Green Fluorescent Protein; HSQC Heteronuclear Single Quantum Correlation; IDP Intrinsically Disordered Protein; MAP Microtubule Associated Protein; MS Mass Spectrometry; MT MicroTubule; NOE Nuclear Overhauser Effect; NMR Nuclear Magnetic Resonance spectroscopy; PHF6 Paired Helical Filament hexapeptide; PRE Paramagnetic Relaxation Enhancement; PTMs Post-Translational Modifications; SLD Stathmin-Like Domain; STD Saturation Transfer Difference

References

Alonso, A. C., Zaidi, T., Grundke-Iqbal, I., and Iqbal, K. (1994). Role of abnormally phosphorylated tau in the breakdown of microtubules in Alzheimer disease. *Proc Natl Acad Sci U A* 91, 5562–6.

Alushin, G. M., Lander, G. C., Kellogg, E. H., Zhang, R., Baker, D., and Nogales, E. (2014). High-resolution microtubule structures reveal the structural transitions in αβ-tubulin upon GTP hydrolysis. *Cell* 157, 1117–1129. doi:10.1016/j.cell.2014.03.053.

Amniai, L., Barbier, P., Sillen, A., Wieruszeski, J.-M., Peyrot, V., Lippens, G., et al. (2009). Alzheimer disease specific phosphoepitopes of Tau interfere with assembly of tubulin but not binding to microtubules. *FASEB J* 23, 1146–52. doi:doi: 10.1096/fj.08-121590.

Amos, L. A., and Schlieper, D. (2005). Microtubules and maps. *Adv Protein Chem* 71, 257–98. doi:S0065-3233(04)71007-4 [pii] 10.1016/S0065-3233(04)71007-4.

Baas, P. W., and Qiang, L. (2019). Tau: It's Not What You Think. *Trends Cell Biol.* 29, 452–461. doi:10.1016/j.tcb.2019.02.007.

Baas, P. W., Rao, A. N., Matamoros, A. J., and Leo, L. (2016). Stability properties of neuronal microtubules. *Cytoskelet. Hoboken NJ* 73, 442–460. doi:10.1002/cm.21286.

Ballatore, C., Brunden, K. R., Trojanowski, J. Q., Lee, V. M., Smith, A. B., and Huryn, D. M. (2011). Modulation of protein-protein interactions as a therapeutic strategy for the treatment of neurodegenerative tauopathies. *Curr Top Med Chem* 11, 317–30. doi:BSP/CTMC/E-Pub/-00023-11-4 [pii].

Barbier, P., Dorleans, A., Devred, F., Sanz, L., Allegro, D., Alfonso, C., et al. (2010). Stathmin and interfacial microtubule inhibitors recognize a naturally curved conformation of tubulin dimers. *J Biol Chem* 285, 31672–81. doi:10.1074/jbc.M110.141929 M110.141929 [pii].

Barghorn, S., Zheng-Fischhofer, Q., Ackmann, M., Biernat, J., von Bergen, M., Mandelkow, E. M., et al. (2000). Structure, microtubule interactions, and paired helical filament aggregation by tau mutants of frontotemporal dementias. *Biochemistry* 39, 11714–21.

Biernat, J., Gustke, N., Drewes, G., Mandelkow, E. M., and Mandelkow, E. (1993). Phosphorylation of Ser262 strongly reduces binding of tau to microtubules: distinction between PHF-like immunoreactivity and microtubule binding. *Neuron* 11, 153–63. doi:0896-6273(93)90279-Z [pii].

Binder, L. I., Frankfurter, A., and Rebhun, L. I. (1985). The distribution of tau in the mammalian central nervous system. *J Cell Biol* 101, 1371–8.

Black, M. M., Slaughter, T., Moshiach, S., Obrocka, M., and Fischer, I. (1996). Tau is enriched on dynamic microtubules in the distal region of growing axons. *J Neurosci* 16, 3601–19.

Boston, P. F., Jackson, P., and Thompson, R. J. (1982). Human 14-3-3 protein: radioimmunoassay, tissue distribution, and cerebrospinal fluid levels in patients with neurological disorders. *J Neurochem* 38, 1475–82.

Bowne-Anderson, H., Hibbel, A., and Howard, J. (2015). Regulation of Microtubule Growth and Catastrophe: Unifying Theory and Experiment. *Trends Cell Biol.* 25, 769–779. doi:10.1016/j.tcb.2015.08.009.

Breuzard, G., Hubert, P., Nouar, R., De Bessa, T., Devred, F., Barbier, P., et al. (2013). Molecular mechanisms of Tau binding to microtubules and its role in microtubule dynamics in live cells. *J. Cell Sci.* 126, 2810–2819. doi:10.1242/jcs.120832.

Breuzard, G., Pagano, A., Bastonero, S., Malesinski, S., Parat, F., Barbier, P., et al. (2019). Tau regulates the microtubule-dependent migration of glioblastoma cells via the Rho-ROCK signaling pathway. *J. Cell Sci.* 132, jcs222851. doi:10.1242/jcs.222851.

Brion, J. P., Flament-Durand, J., and Dustin, P. (1986). Alzheimer's disease and tau proteins. *Lancet* 2, 1098. doi:S0140-6736(86)90495-2 [pii].

Brunden, K. R., Trojanowski, J. Q., and Lee, V. M. (2009). Advances in tau-focused drug discovery for Alzheimer's disease and related tauopathies. *Nat Rev Drug Discov* 8, 783–93. doi:10.1038/nrd2959.

Brunden, K. R., Yao, Y., Potuzak, J. S., Ferrer, N. I., Ballatore, C., James, M. J., et al. (2011). The characterization of microtubule-stabilizing drugs as possible therapeutic agents for Alzheimer's disease and related tauopathies. *Pharmacol Res* 63, 341–51. doi:10.1016/j.phrs.2010.12.002.

Butner, K. A., and Kirschner, M. W. (1991). Tau protein binds to microtubules through a flexible array of distributed weak sites. *J Cell Biol* 115, 717–30.

Caplow, M., and Shanks, J. (1990). Mechanism of the microtubule GTPase reaction. *J. Biol. Chem.* 265, 8935–8941.

Carlier, M. F., Didry, D., Simon, C., and Pantaloni, D. (1989). Mechanism of GTP hydrolysis in tubulin polymerization: characterization of the kinetic intermediate microtubule-GDP-Pi using phosphate analogues. *Biochemistry* 28, 1783–1791.

Carlomagno, Y., Chung, D.-E. C., Yue, M., Castanedes-Casey, M., Madden, B. J., Dunmore, J., et al. (2017). An acetylation-phosphorylation switch that regulates tau aggregation propensity and function. *J. Biol. Chem.* 292, 15277–15286. doi:10.1074/jbc.M117.794602.

Cash, A. D., Aliev, G., Siedlak, S. L., Nunomura, A., Fujioka, H., Zhu, X., et al. (2003). Microtubule reduction in Alzheimer's disease and aging is independent of tau filament formation. *Am J Pathol* 162, 1623–7. doi:S0002-9440(10)64296-4 [pii].

Chen, J., Kanai, Y., Cowan, N. J., and Hirokawa, N. (1992). Projection domains of MAP2 and tau determine spacings between microtubules in dendrites and axons. *Nature* 360, 674–7. doi:10.1038/360674a0.

Chrétien, D., Fuller, S. D., and Karsenti, E. (1995). Structure of growing microtubule ends: two-dimensional sheets close into tubes at variable rates. *J. Cell Biol.* 129, 1311–1328.

Cohen, T. J., Guo, J. L., Hurtado, D. E., Kwong, L. K., Mills, I. P., Trojanowski, J. Q., et al. (2011). The acetylation of tau inhibits its function and promotes pathological tau aggregation. *Nat Commun* 2, 252. doi:10.1038/ncomms1255.

Combs, B., and Gamblin, T. C. (2012). FTDP-17 tau mutations induce distinct effects on aggregation and microtubule interactions. *Biochemistry* 51, 8597–8607. doi:10.1021/bi3010818.

Cummings, J., Lee, G., Mortsdorf, T., Ritter, A., and Zhong, K. (2017). Alzheimer's disease drug development pipeline: 2017. *Alzheimers Dement. N. Y. N* 3, 367–384. doi:10.1016/j.trci.2017.05.002.

Das, G., and Ghosh, S. (2019). Why Microtubules Should Be Considered as One of the Supplementary Targets for Designing Neurotherapeutics. *ACS Chem. Neurosci.* 10, 1118–1120. doi:10.1021/acschemneuro.9b00002.

Dayanandan, R., Van Slegtenhorst, M., Mack, T. G., Ko, L., Yen, S. H., Leroy, K., et al. (1999). Mutations in tau reduce its microtubule binding properties in intact cells and affect its phosphorylation. *FEBS Lett.* 446, 228–232.

Delobel, P., Flament, S., Hamdane, M., Jakes, R., Rousseau, A., Delacourte, A., et al. (2002). Functional characterization of FTDP-17 tau gene mutations through their effects on Xenopus oocyte maturation. *J. Biol. Chem.* 277, 9199–9205. doi:10.1074/jbc.M107716200.

DeTure, M., Ko, L. W., Yen, S., Nacharaju, P., Easson, C., Lewis, J., et al. (2000). Missense tau mutations identified in FTDP-17 have a small effect on tau-microtubule interactions. *Brain Res.* 853, 5–14. doi:10.1016/s0006-8993(99)02124-1.

Devred, F., Barbier, P., Douillard, S., Monasterio, O., Andreu, J. M., and Peyrot, V. (2004). Tau induces ring and microtubule formation from alphabeta-tubulin dimers under nonassembly conditions. *Biochemistry* 43, 10520–31.

Devred, F., Barbier, P., Lafitte, D., Landrieu, I., Lippens, G., and Peyrot, V. (2010). Microtubule and MAPs: thermodynamics of complex formation by AUC, ITC, fluorescence, and NMR. *Methods Cell Biol* 95, 449–80. doi:10.1016/S0091-679X(10)95023-1.

Devred, F., Douillard, S., Briand, C., and Peyrot, V. (2002). First tau repeat domain binding to growing and taxol-stabilized microtubules, and serine 262 residue phosphorylation. *FEBS Lett.* 523, 247–251.

Di Maio, I. L., Barbier, P., Allegro, D., Brault, C., and Peyrot, V. (2014). Quantitative analysis of tau-microtubule interaction using FRET. *Int J Mol Sci* 15, 14697–714. doi:10.3390/ijms150814697 ijms150814697 [pii].

Di Primio, C., Quercioli, V., Siano, G., Rovere, M., Kovacech, B., Novak, M., et al. (2017). The Distance between N and C Termini of Tau and of FTDP-17 Mutants Is Modulated by Microtubule Interactions in Living Cells. *Front. Mol. Neurosci.* 10, 210. doi:10.3389/fnmol.2017.00210.

Dompierre, J. P., Godin, J. D., Charrin, B. C., Cordelières, F. P., King, S. J., Humbert, S., et al. (2007). Histone deacetylase 6 inhibition compensates for the transport deficit in Huntington's disease by increasing tubulin acetylation. *J. Neurosci. Off. J. Soc. Neurosci.* 27, 3571–3583. doi:10.1523/JNEUROSCI.0037-07.2007.

Donhauser, Z. J., Saunders, J. T., D'Urso, D. S., and Garrett, T. A. (2017). Dimerization and Long-Range Repulsion Established by Both Termini of the Microtubule-Associated Protein Tau. *Biochemistry* 56, 5900–5909. doi:10.1021/acs.biochem.7b00653.

D'Souza, I., Poorkaj, P., Hong, M., Nochlin, D., Lee, V. M., Bird, T. D., et al. (1999). Missense and silent tau gene mutations cause frontotemporal dementia with parkinsonism-chromosome 17 type, by affecting multiple alternative RNA splicing regulatory elements. *Proc. Natl. Acad. Sci. U. S. A.* 96, 5598–5603. doi:10.1073/pnas.96.10.5598.

Duan, A. R., Jonasson, E. M., Alberico, E. O., Li, C., Scripture, J. P., Miller, R. A., et al. (2017). Interactions between Tau and Different Conformations of Tubulin: Implications for Tau Function and Mechanism. *J. Mol. Biol.* 429, 1424–1438. doi:10.1016/j.jmb.2017.03.018.

Eftekharzadeh, B., Daigle, J. G., Kapinos, L. E., Coyne, A., Schiantarelli, J., Carlomagno, Y., et al. (2018). Tau Protein Disrupts Nucleocytoplasmic Transport in Alzheimer's Disease. *Neuron* 99, 925-940.e7. doi:10.1016/j.neuron.2018.07.039.

Fauquant, C., Redeker, V., Landrieu, I., Wieruszeski, J. M., Verdegem, D., Laprevote, O., et al. (2011). Systematic identification of tubulin-interacting fragments of the microtubule-associated protein Tau leads to a highly efficient promoter of microtubule assembly. *J Biol Chem* 286, 33358–68. doi:10.1074/jbc.M111.223545.

Fichou, Y., Al-Hilaly, Y. K., Devred, F., Smet-Nocca, C., Tsvetkov, P. O., Verelst, J., et al. (2019). The elusive tau molecular structures: can we translate the recent breakthroughs into new targets for intervention? *Acta Neuropathol. Commun.* 7, 31. doi:10.1186/s40478-019-0682-x.

Gadadhar, S., Bodakuntla, S., Natarajan, K., and Janke, C. (2017). The tubulin code at a glance. *J. Cell Sci.* 130, 1347–1353. doi:10.1242/jcs.199471.

Gigant, B., Curmi, P. A., Martin-Barbey, C., Charbaut, E., Lachkar, S., Lebeau, L., et al. (2000). The 4 A X-ray structure of a tubulin:stathmin-like domain complex. *Cell* 102, 809–16. doi:S0092-8674(00)00069-6 [pii].

Gigant, B., Landrieu, I., Fauquant, C., Barbier, P., Huvent, I., Wieruszeski, J.-M., et al. (2014). Mechanism of Tau-promoted microtubule assembly as probed by NMR spectroscopy. *J. Am. Chem. Soc.* 136, 12615–12623. doi:10.1021/ja504864m.

Godena, V. K., Brookes-Hocking, N., Moller, A., Shaw, G., Oswald, M., Sancho, R. M., et al. (2014). Increasing microtubule acetylation rescues axonal transport and locomotor deficits caused by LRRK2 Roc-COR domain mutations. *Nat. Commun.* 5, 5245. doi:10.1038/ncomms6245.

Goedert, M., Spillantini, M. G., Jakes, R., Rutherford, D., and Crowther, R. A. (1989). Multiple isoforms of human microtubule-associated protein tau: sequences and localization in neurofibrillary tangles of Alzheimer's disease. *Neuron* 3, 519–26. doi:0896-6273(89)90210-9 [pii].

Goode, B. L., Chau, M., Denis, P. E., and Feinstein, S. C. (2000). Structural and functional differences between 3-repeat and 4-repeat tau isoforms. Implications for normal tau function and the onset of neurodegenetative disease. *J Biol Chem* 275, 38182–9. doi:10.1074/jbc.M007489200.

Goode, B. L., Denis, P. E., Panda, D., Radeke, M. J., Miller, H. P., Wilson, L., et al. (1997). Functional interactions between the proline-rich and repeat regions of tau enhance microtubule binding and assembly. *Mol Biol Cell* 8, 353–65.

Govindarajan, N., Rao, P., Burkhardt, S., Sananbenesi, F., Schlüter, O. M., Bradke, F., et al. (2013). Reducing HDAC6 ameliorates cognitive deficits in a mouse model for Alzheimer's disease. *EMBO Mol. Med.* 5, 52–63. doi:10.1002/emmm.201201923.

Guo, W., Naujock, M., Fumagalli, L., Vandoorne, T., Baatsen, P., Boon, R., et al. (2017). HDAC6 inhibition reverses axonal transport defects in motor neurons derived from FUS-ALS patients. *Nat. Commun.* 8, 861. doi:10.1038/s41467-017-00911-y.

Gustke, N., Trinczek, B., Biernat, J., Mandelkow, E. M., and Mandelkow, E. (1994). Domains of tau protein and interactions with microtubules. *Biochemistry* 33, 9511–22.

Hasegawa, M., Smith, M. J., and Goedert, M. (1998). Tau proteins with FTDP-17 mutations have a reduced ability to promote microtubule assembly. *FEBS Lett.* 437, 207–210.

Hashiguchi, M., Sobue, K., and Paudel, H. K. (2000). 14-3-3zeta is an effector of tau protein phosphorylation. *J Biol Chem* 275, 25247–54. doi:10.1074/jbc.M003738200.

Hernández, F., and Avila, J. (2007). Tauopathies. *Cell. Mol. Life Sci. CMLS* 64, 2219–2233. doi:10.1007/s00018-007-7220-x.

Hernández-Vega, A., Braun, M., Scharrel, L., Jahnel, M., Wegmann, S., Hyman, B. T., et al. (2017). Local Nucleation of Microtubule Bundles through Tubulin Concentration into a Condensed Tau Phase. *Cell Rep.* 20, 2304–2312. doi:10.1016/j.celrep.2017.08.042.

Himmler, A., Drechsel, D., Kirschner, M. W., and Martin, D. W., Jr. (1989). Tau consists of a set of proteins with repeated C-terminal microtubule-binding domains and variable N-terminal domains. *Mol Cell Biol* 9, 1381–8.

Hinrichs, M. H., Jalal, A., Brenner, B., Mandelkow, E., Kumar, S., and Scholz, T. (2012). Tau protein diffuses along the microtubule lattice. *J. Biol. Chem.* 287, 38559–38568. doi:10.1074/jbc.M112.369785.

Hong, M., Zhukareva, V., Vogelsberg-Ragaglia, V., Wszolek, Z., Reed, L., Miller, B. I., et al. (1998). Mutation-specific functional impairments in distinct tau isoforms of hereditary FTDP-17. *Science* 282, 1914–7.

Howard, W. D., and Timasheff, S. N. (1986). GDP state of tubulin: stabilization of double rings. *Biochemistry* 25, 8292–8300.

Irwin, D. J., Cohen, T. J., Grossman, M., Arnold, S. E., McCarty-Wood, E., Van Deerlin, V. M., et al. (2013). Acetylated tau neuropathology in sporadic and hereditary tauopathies. *Am. J. Pathol.* 183, 344–351. doi:10.1016/j.ajpath.2013.04.025.

Irwin, D. J., Cohen, T. J., Grossman, M., Arnold, S. E., Xie, S. X., Lee, V. M., et al. (2012). Acetylated tau, a novel pathological signature in Alzheimer's disease and other tauopathies. *Brain* 135, 807–18. doi:10.1093/brain/aws013.

Jadhav, S., Avila, J., Schöll, M., Kovacs, G. G., Kövari, E., Skrabana, R., et al. (2019). A walk through tau therapeutic strategies. *Acta Neuropathol. Commun.* 7, 22. doi:10.1186/s40478-019-0664-z.

Janning, D., Igaev, M., Sündermann, F., Brühmann, J., Beutel, O., Heinisch, J. J., et al. (2014). Single-molecule tracking of tau reveals fast kiss-and-hop interaction with microtubules in living neurons. *Mol. Biol. Cell* 25, 3541–3551. doi:10.1091/mbc.E14-06-1099.

Jeganathan, S., von Bergen, M., Brutlach, H., Steinhoff, H. J., and Mandelkow, E. (2006). Global hairpin folding of tau in solution. *Biochemistry* 45, 2283–93. doi:10.1021/bi0521543.

Joo, Y., Schumacher, B., Landrieu, I., Bartel, M., Smet-Nocca, C., Jang, A., et al. (2015). Involvement of 14-3-3 in tubulin instability and impaired axon development is mediated by Tau. *FASEB J. Off. Publ. Fed. Am. Soc. Exp. Biol.* 29, 4133–4144. doi:10.1096/fj.14-265009.

Kadavath, H., Cabrales Fontela, Y., Jaremko, M., Jaremko, Ł., Overkamp, K., Biernat, J., et al. (2018). The Binding Mode of a Tau Peptide with Tubulin. *Angew. Chem. Int. Ed Engl.* 57, 3246–3250. doi:10.1002/anie.201712089.

Kadavath, H., Hofele, R. V., Biernat, J., Kumar, S., Tepper, K., Urlaub, H., et al. (2015a). Tau stabilizes microtubules by binding at the interface between tubulin heterodimers. *Proc. Natl. Acad. Sci. U. S. A.* 112, 7501–7506. doi:10.1073/pnas.1504081112.

Kadavath, H., Jaremko, M., Jaremko, Ł., Biernat, J., Mandelkow, E., and Zweckstetter, M. (2015b). Folding of the Tau Protein on Microtubules. *Angew. Chem. Int. Ed Engl.* 54, 10347–10351. doi:10.1002/anie.201501714.

Kamah, A., Huvent, I., Cantrelle, F.-X., Qi, H., Lippens, G., Landrieu, I., et al. (2014). Nuclear magnetic resonance analysis of the acetylation pattern of the neuronal Tau protein. *Biochemistry* 53, 3020–3032. doi:10.1021/bi500006v.

Kar, S., Fan, J., Smith, M. J., Goedert, M., and Amos, L. A. (2003). Repeat motifs of tau bind to the insides of microtubules in the absence of taxol. *Embo J* 22, 70–7.

Kellogg, E. H., Hejab, N. M. A., Poepsel, S., Downing, K. H., DiMaio, F., and Nogales, E. (2018). Near-atomic model of microtubule-tau interactions. *Science* 360, 1242–1246. doi:10.1126/science.aat1780.

Kilgore, M., Miller, C. A., Fass, D. M., Hennig, K. M., Haggarty, S. J., Sweatt, J. D., et al. (2010). Inhibitors of class 1 histone deacetylases reverse contextual memory deficits in a mouse model of Alzheimer's disease. *Neuropsychopharmacol. Off. Publ. Am. Coll. Neuropsychopharmacol.* 35, 870–880. doi:10.1038/npp.2009.197.

Kull, F. J., and Sloboda, R. D. (2014). A slow dance for microtubule acetylation. *Cell* 157, 1255–1256. doi:10.1016/j.cell.2014.05.021.

Kutter, S., Eichner, T., Deaconescu, A. M., and Kern, D. (2016). Regulation of Microtubule Assembly by Tau and not by Pin1. *J. Mol. Biol.* 428, 1742–1759. doi:10.1016/j.jmb.2016.03.010.

Layfield, R., Fergusson, J., Aitken, A., Lowe, J., Landon, M., and Mayer, R. J. (1996). Neurofibrillary tangles of Alzheimer's disease brains contain 14-3-3 proteins. *Neurosci Lett* 209, 57–60. doi:0304394096125982 [pii].

LeBoeuf, A. C., Levy, S. F., Gaylord, M., Bhattacharya, A., Singh, A. K., Jordan, M. A., et al. (2008). FTDP-17 mutations in Tau alter the regulation of microtubule dynamics: an "alternative core" model for normal and pathological Tau action. *J. Biol. Chem.* 283, 36406–36415. doi:10.1074/jbc.M803519200.

Lee, V. M.-Y., Kenyon, T. K., and Trojanowski, J. Q. (2005). Transgenic animal models of tauopathies. *Biochim. Biophys. Acta* 1739, 251–259. doi:10.1016/j.bbadis.2004.06.014.

Li, X.-H., Culver, J. A., and Rhoades, E. (2015). Tau Binds to Multiple Tubulin Dimers with Helical Structure. *J. Am. Chem. Soc.* 137, 9218–9221. doi:10.1021/jacs.5b04561.

Li, Z.-H., Xiong, Q.-Y., Tu, J.-H., Gong, Y., Qiu, W., Zhang, H.-Q., et al. (2013). Tau proteins expressions in advanced breast cancer and its significance in taxane-containing neoadjuvant chemotherapy. *Med. Oncol. Northwood Lond. Engl.* 30, 591. doi:10.1007/s12032-013-0591-y.

Lin, H., Zheng, L., Li, S., Xie, B., Cui, B., Xia, A., et al. (2018). Cytotoxicity of Tanshinone IIA combined with Taxol on drug-resist breast cancer cells MCF-7 through inhibition of Tau. *Phytother. Res. PTR* 32, 667–671. doi:10.1002/ptr.6014.

Lindwall, G., and Cole, R. D. (1984). Phosphorylation affects the ability of tau protein to promote microtubule assembly. *J Biol Chem* 259, 5301–5.

Lu, P. J., Wulf, G., Zhou, X. Z., Davies, P., and Lu, K. P. (1999). The prolyl isomerase Pin1 restores the function of Alzheimer-associated phosphorylated tau protein. *Nature* 399, 784–8.

Magiera, M. M., Bodakuntla, S., Žiak, J., Lacomme, S., Marques Sousa, P., Leboucher, S., et al. (2018). Excessive tubulin polyglutamylation causes neurodegeneration and perturbs neuronal transport. *EMBO J.* 37, e100440. doi:10.15252/embj.2018100440.

Makrides, V., Massie, M. R., Feinstein, S. C., and Lew, J. (2004). Evidence for two distinct binding sites for tau on microtubules. *Proc Natl Acad Sci U A* 101, 6746–51.

Malesinski, S., Tsvetkov, P. O., Kruczynski, A., Peyrot, V., and Devred, F. (2015). Stathmin potentiates vinflunine and inhibits Paclitaxel activity. *PloS One* 10, e0128704. doi:10.1371/journal.pone.0128704.

Mandelkow, E. M., Biernat, J., Drewes, G., Gustke, N., Trinczek, B., and Mandelkow, E. (1995). Tau domains, phosphorylation, and interactions with microtubules. *Neurobiol Aging* 16, 355–62; discussion 362-3.

Martinho, M., Allegro, D., Huvent, I., Chabaud, C., Etienne, E., Kovacic, H., et al. (2018). Two Tau binding sites on tubulin revealed by thiol-disulfide exchanges. *Sci. Rep.* 8, 13846. doi:10.1038/s41598-018-32096-9.

Matsumura, N., Yamazaki, T., and Ihara, Y. (1999). Stable expression in Chinese hamster ovary cells of mutated tau genes causing frontotemporal dementia and parkinsonism linked to chromosome 17 (FTDP-17). *Am. J. Pathol.* 154, 1649–1656. doi:10.1016/S0002-9440(10)65420-X.

Melki, R., Carlier, M. F., Pantaloni, D., and Timasheff, S. N. (1989). Cold depolymerization of microtubules to double rings: geometric stabilization of assemblies. *Biochemistry* 28, 9143–9152.

Melková, K., Zapletal, V., Narasimhan, S., Jansen, S., Hritz, J., Škrabana, R., et al. (2019). Structure and Functions of Microtubule Associated Proteins Tau and MAP2c: Similarities and Differences. *Biomolecules* 9, E105. doi:10.3390/biom9030105.

Melo, A. M., Coraor, J., Alpha-Cobb, G., Elbaum-Garfinkle, S., Nath, A., and Rhoades, E. (2016). A functional role for intrinsic disorder in the tau-tubulin complex. *Proc. Natl. Acad. Sci. U. S. A.* 113, 14336–14341. doi:10.1073/pnas.1610137113.

Min, S. W., Cho, S. H., Zhou, Y., Schroeder, S., Haroutunian, V., Seeley, W. W., et al. (2010). Acetylation of tau inhibits its degradation and contributes to tauopathy. *Neuron* 67, 953–66. doi:10.1016/j.neuron.2010.08.044.

Min, S.-W., Chen, X., Tracy, T. E., Li, Y., Zhou, Y., Wang, C., et al. (2015). Critical role of acetylation in tau-mediated neurodegeneration and cognitive deficits. *Nat. Med.* 21, 1154–1162. doi:10.1038/nm.3951.

Min, S.-W., Sohn, P. D., Li, Y., Devidze, N., Johnson, J. R., Krogan, N. J., et al. (2018). SIRT1 Deacetylates Tau and Reduces Pathogenic Tau Spread in a Mouse Model of Tauopathy. *J. Neurosci. Off. J. Soc. Neurosci.* 38, 3680–3688. doi:10.1523/JNEUROSCI.2369-17.2018.

Mitchison, T., and Kirschner, M. (1984). Dynamic instability of microtubule growth. *Nature* 312, 237–42.

Monacelli, F., Cea, M., Borghi, R., Odetti, P., and Nencioni, A. (2017). Do Cancer Drugs Counteract Neurodegeneration? Repurposing for Alzheimer's Disease. *J. Alzheimers Dis. JAD* 55, 1295–1306. doi:10.3233/JAD-160840.

Mondal, P., Das, G., Khan, J., Pradhan, K., and Ghosh, S. (2018). Crafting of Neuroprotective Octapeptide from Taxol-Binding Pocket of β-Tubulin. *ACS Chem. Neurosci.* 9, 615–625. doi:10.1021/acschemneuro.7b00457.

Morris, M., Knudsen, G. M., Maeda, S., Trinidad, J. C., Ioanoviciu, A., Burlingame, A. L., et al. (2015). Tau post-translational modifications in wild-type and human amyloid precursor protein transgenic mice. *Nat Neurosci* 18, 1183–9. doi:10.1038/nn.4067 nn.4067 [pii].

Mudher, A., Brion, J.-P., Avila, J., Medina, M., and Buée, L. (2017). EuroTau: towing scientists to tau without tautology. *Acta Neuropathol. Commun.* 5, 90. doi:10.1186/s40478-017-0491-z.

Mukhopadhyay, R., and Hoh, J. H. (2001). AFM force measurements on microtubule-associated proteins: the projection domain exerts a long-range repulsive force. *FEBS Lett* 505, 374–8. doi:S0014-5793(01)02844-7 [pii].

Mukrasch, M. D., Bibow, S., Korukottu, J., Jeganathan, S., Biernat, J., Griesinger, C., et al. (2009). Structural polymorphism of 441-residue tau at single residue resolution. *PLoS Biol* 7, e34. doi:doi: 10.1371/journal.pbio.1000034.

Mukrasch, M. D., Markwick, P., Biernat, J., Bergen, M., Bernado, P., Griesinger, C., et al. (2007). Highly populated turn conformations in natively unfolded tau protein identified from residual dipolar couplings and molecular simulation. *J Am Chem Soc* 129, 5235–43.

Murphy, D. B., Johnson, K. A., and Borisy, G. G. (1977). Role of tubulin-associated proteins in microtubule nucleation and elongation. *J Mol Biol* 117, 33–52. doi:0022-2836(77)90021-3 [pii].

Mutreja, Y., Combs, B., and Gamblin, T. C. (2019). FTDP-17 Mutations Alter the Aggregation and Microtubule Stabilization Propensity of Tau in an Isoform-Specific Fashion. *Biochemistry* 58, 742–754. doi:10.1021/acs.biochem.8b01039.

Nagiec, E. W., Sampson, K. E., and Abraham, I. (2001). Mutated tau binds less avidly to microtubules than wildtype tau in living cells. *J. Neurosci. Res.* 63, 268–275. doi:10.1002/1097-4547(20010201)63:3<268::AID-JNR1020>3.0.CO;2-E.

Nawrotek, A., Knossow, M., and Gigant, B. (2011). The determinants that govern microtubule assembly from the atomic structure of GTP-tubulin. *J. Mol. Biol.* 412, 35–42. doi:10.1016/j.jmb.2011.07.029.

Nouar, R., Devred, F., Breuzard, G., and Peyrot, V. (2013). FRET and FRAP imaging: approaches to characterise tau and stathmin interactions with microtubules in cells. *Biol. Cell Auspices Eur. Cell Biol. Organ.* 105, 149–161. doi:10.1111/boc.201200060.

Oz, S., Kapitansky, O., Ivashco-Pachima, Y., Malishkevich, A., Giladi, E., Skalka, N., et al. (2014). The NAP motif of activity-dependent neuroprotective protein (ADNP) regulates dendritic spines through microtubule end binding proteins. *Mol. Psychiatry* 19, 1115–1124. doi:10.1038/mp.2014.97.

Pachima, Y. I., Zhou, L., Lei, P., and Gozes, I. (2016). Microtubule-Tau Interaction as a Therapeutic Target for Alzheimer's Disease. *J. Mol. Neurosci. MN* 58, 145–152. doi:10.1007/s12031-016-0715-x.

Panda, D., Samuel, J. C., Massie, M., Feinstein, S. C., and Wilson, L. (2003). Differential regulation of microtubule dynamics by three- and four-repeat tau: implications for the onset of neurodegenerative disease. *Proc. Natl. Acad. Sci. U. S. A.* 100, 9548–9553. doi:10.1073/pnas.1633508100.

Paonessa, F., Evans, L. D., Solanki, R., Larrieu, D., Wray, S., Hardy, J., et al. (2019). Microtubules Deform the Nuclear Membrane and Disrupt Nucleocytoplasmic Transport in Tau-Mediated Frontotemporal Dementia. *Cell Rep.* 26, 582-593.e5. doi:10.1016/j.celrep.2018.12.085.

Pecqueur, L., Duellberg, C., Dreier, B., Jiang, Q., Wang, C., Pluckthun, A., et al. (2012). A designed ankyrin repeat protein selected to bind to tubulin caps the microtubule plus end. *Proc. Natl. Acad. Sci.* 109, 12011–12016. doi:10.1073/pnas.1204129109.

Preuss, U., Biernat, J., Mandelkow, E. M., and Mandelkow, E. (1997). The "jaws" model of tau-microtubule interaction examined in CHO cells. *J Cell Sci* 110 (Pt 6), 789–800.

Qiang, L., Sun, X., Austin, T. O., Muralidharan, H., Jean, D. C., Liu, M., et al. (2018). Tau Does Not Stabilize Axonal Microtubules but Rather Enables Them to Have Long Labile Domains. *Curr. Biol. CB* 28, 2181-2189.e4. doi:10.1016/j.cub.2018.05.045.

Quraishe, S., Cowan, C. M., and Mudher, A. (2013). NAP (davunetide) rescues neuronal dysfunction in a Drosophila model of tauopathy. *Mol. Psychiatry* 18, 834–842. doi:10.1038/mp.2013.32.

Quraishe, S., Sealey, M., Cranfield, L., and Mudher, A. (2016). Microtubule stabilising peptides rescue tau phenotypes in-vivo. *Sci. Rep.* 6, 38224. doi:10.1038/srep38224.

Qureshi, H. Y., Li, T., MacDonald, R., Cho, C. M., Leclerc, N., and Paudel, H. K. (2013). Interaction of 14-3-3zeta with microtubule-associated protein tau within Alzheimer's disease neurofibrillary tangles. *Biochemistry* 52, 6445–55. doi:10.1021/bi400442d.

Ramkumar, A., Jong, B. Y., and Ori-McKenney, K. M. (2018). ReMAPping the microtubule landscape: How phosphorylation dictates the activities of microtubule-associated proteins. *Dev. Dyn. Off. Publ. Am. Assoc. Anat.* 247, 138–155. doi:10.1002/dvdy.24599.

Rane, J. S., Kumari, A., and Panda, D. (2019). An acetylation mimicking mutation, K274Q, in tau imparts neurotoxicity by enhancing tau aggregation and inhibiting tubulin polymerization. *Biochem. J.* 476, 1401–1417. doi:10.1042/BCJ20190042.

Roman, A. Y., Devred, F., Byrne, D., La Rocca, R., Ninkina, N. N., Peyrot, V., et al. (2019). Zinc Induces Temperature-Dependent Reversible Self-Assembly of Tau. *J. Mol. Biol.* 431, 687–695. doi:10.1016/j.jmb.2018.12.008.

Rosenberg, K. J., Ross, J. L., Feinstein, H. E., Feinstein, S. C., and Israelachvili, J. (2008). Complementary dimerization of microtubule-associated tau protein: Implications for microtubule bundling and tau-mediated pathogenesis. *Proc Natl Acad Sci U A* 105, 7445–50. doi:10.1073/pnas.0802036105.

Rouzier, R., Rajan, R., Wagner, P., Hess, K. R., Gold, D. L., Stec, J., et al. (2005). Microtubule-associated protein tau: a marker of paclitaxel sensitivity in breast cancer. *Proc. Natl. Acad. Sci. U. S. A.* 102, 8315–8320. doi:10.1073/pnas.0408974102.

Sahara, N., Tomiyama, T., and Mori, H. (2000). Missense point mutations of tau to segregate with FTDP-17 exhibit site-specific effects on microtubule structure in COS cells: a novel action of R406W mutation. *J. Neurosci. Res.* 60, 380–387. doi:10.1002/(SICI)1097-4547(20000501)60:3<380::AID-JNR13>3.0.CO;2-5.

Santarella, R. A., Skiniotis, G., Goldie, K. N., Tittmann, P., Gross, H., Mandelkow, E.-M., et al. (2004). Surface-decoration of microtubules by human tau. *J. Mol. Biol.* 339, 539–553. doi:10.1016/j.jmb.2004.04.008.

Schneider, A., Biernat, J., von Bergen, M., Mandelkow, E., and Mandelkow, E. M. (1999). Phosphorylation that detaches tau protein from microtubules (Ser262, Ser214) also protects it against aggregation into Alzheimer paired helical filaments. *Biochemistry* 38, 3549–58.

Schwalbe, M., Kadavath, H., Biernat, J., Ozenne, V., Blackledge, M., Mandelkow, E., et al. (2015). Structural Impact of Tau Phosphorylation at Threonine 231. *Structure* 23, 1448–1458. doi:10.1016/j.str.2015.06.002.

Schwalbe, M., Ozenne, V., Bibow, S., Jaremko, M., Jaremko, L., Gajda, M., et al. (2014). Predictive atomic resolution descriptions of intrinsically disordered hTau40 and alpha-synuclein in solution from NMR and small angle scattering. *Structure* 22, 238–49. doi:10.1016/j.str.2013.10.020.

Scott, C. W., Blowers, D. P., Barth, P. T., Lo, M. M., Salama, A. I., and Caputo, C. B. (1991). Differences in the abilities of human tau isoforms to promote microtubule assembly. *J. Neurosci. Res.* 30, 154–162. doi:10.1002/jnr.490300116.

Scott, C. W., Spreen, R. C., Herman, J. L., Chow, F. P., Davison, M. D., Young, J., et al. (1993). Phosphorylation of recombinant tau by cAMP-dependent protein kinase. Identification of phosphorylation sites and effect on microtubule assembly. *J Biol Chem* 268, 1166–73.

Selenica, M.-L., Benner, L., Housley, S. B., Manchec, B., Lee, D. C., Nash, K. R., et al. (2014). Histone deacetylase 6 inhibition improves memory and reduces total tau levels in a mouse model of tau deposition. *Alzheimers Res. Ther.* 6, 12. doi:10.1186/alzrt241.

Sengupta, A., Kabat, J., Novak, M., Wu, Q., Grundke-Iqbal, I., and Iqbal, K. (1998). Phosphorylation of tau at both Thr 231 and Ser 262 is required for maximal inhibition of its binding to microtubules. *Arch Biochem Biophys* 357, 299–309.

Shashi, V., Magiera, M. M., Klein, D., Zaki, M., Schoch, K., Rudnik-Schöneborn, S., et al. (2018). Loss of tubulin deglutamylase CCP1 causes infantile-onset neurodegeneration. *EMBO J.* 37, e100540. doi:10.15252/embj.2018100540.

Sibille, N., Huvent, I., Fauquant, C., Verdegem, D., Amniai, L., Leroy, A., et al. (2012). Structural characterization by nuclear magnetic resonance of the impact of phosphorylation in the proline-rich region of the disordered Tau protein. *Proteins* 80, 454–462. doi:10.1002/prot.23210.

Sillen, A., Barbier, P., Landrieu, I., Lefebvre, S., Wieruszeski, J. M., Leroy, A., et al. (2007). NMR investigation of the interaction between the neuronal protein tau and the microtubules. *Biochemistry* 46, 3055–64. doi:10.1021/bi061920i.

Smoter, M., Bodnar, L., Grala, B., Stec, R., Zieniuk, K., Kozlowski, W., et al. (2013). Tau protein as a potential predictive marker in epithelial ovarian cancer patients treated with paclitaxel/platinum first-line chemotherapy. *J. Exp. Clin. Cancer Res. CR* 32, 25. doi:10.1186/1756-9966-32-25.

Szyk, A., Deaconescu, A. M., Spector, J., Goodman, B., Valenstein, M. L., Ziolkowska, N. E., et al. (2014). Molecular basis for age-dependent microtubule acetylation by tubulin acetyltransferase. *Cell* 157, 1405–1415. doi:10.1016/j.cell.2014.03.061.

Tompa, P., and Fuxreiter, M. (2008). Fuzzy complexes: polymorphism and structural disorder in protein-protein interactions. *Trends Biochem. Sci.* 33, 2–8. doi:10.1016/j.tibs.2007.10.003.

Trinczek, B., Biernat, J., Baumann, K., Mandelkow, E. M., and Mandelkow, E. (1995). Domains of tau protein, differential phosphorylation, and dynamic instability of microtubules. *Mol Biol Cell* 6, 1887–902.

Tsvetkov, P. O., La Rocca, R., Malesinski, S., and Devred, F. (2019). Characterization of Microtubule-Associated Proteins (MAPs) and Tubulin Interactions by Isothermal Titration Calorimetry (ITC). *Methods Mol. Biol. Clifton NJ* 1964, 151–165. doi:10.1007/978-1-4939-9179-2_12.

Tugaeva, K. V., Tsvetkov, P. O., and Sluchanko, N. N. (2017). Bacterial co-expression of human Tau protein with protein kinase A and 14-3-3 for studies of 14-3-3/phospho-Tau interaction. *PloS One* 12, e0178933. doi:10.1371/journal.pone.0178933.

Umahara, T., Uchihara, T., Tsuchiya, K., Nakamura, A., Iwamoto, T., Ikeda, K., et al. (2004). 14-3-3 proteins and zeta isoform containing neurofibrillary tangles in patients with Alzheimer's disease. *Acta Neuropathol* 108, 279–86. doi:10.1007/s00401-004-0885-4.

van der Vaart, B., Akhmanova, A., and Straube, A. (2009). Regulation of microtubule dynamic instability. *Biochem. Soc. Trans.* 37, 1007–1013. doi:10.1042/BST0371007.

Wegmann, S., Eftekharzadeh, B., Tepper, K., Zoltowska, K. M., Bennett, R. E., Dujardin, S., et al. (2018). Tau protein liquid-liquid phase separation can initiate tau aggregation. *EMBO J.* 37, e98049. doi:10.15252/embj.201798049.

Weingarten, M. D., Lockwood, A. H., Hwo, S. Y., and Kirschner, M. W. (1975). A protein factor essential for microtubule assembly. *Proc. Natl. Acad. Sci. U A* 72, 1858–62.

Wilhelmsen, K. C., Lynch, T., Pavlou, E., Higgins, M., and Nygaard, T. G. (1994). Localization of disinhibition-dementia-parkinsonism-amyotrophy complex to 17q21-22. *Am. J. Hum. Genet.* 55, 1159–1165.

Witman, G. B., Cleveland, D. W., Weingarten, M. D., and Kirschner, M. W. (1976). Tubulin requires tau for growth onto microtubule initiating sites. *Proc. Natl. Acad. Sci. U. S. Am. A* 73, 4070–4.

Xiong, Y., Zhao, K., Wu, J., Xu, Z., Jin, S., and Zhang, Y. Q. (2013). HDAC6 mutations rescue human tau-induced microtubule defects in Drosophila. *Proc. Natl. Acad. Sci. U. S. A.* 110, 4604–4609. doi:10.1073/pnas.1207586110.

Zhang, B., Maiti, A., Shively, S., Lakhani, F., McDonald-Jones, G., Bruce, J., et al. (2005). Microtubule-binding drugs offset tau sequestration by stabilizing microtubules and reversing fast axonal transport deficits in a tauopathy model. *Proc. Natl. Acad. Sci. U. S. A.* 102, 227–231. doi:10.1073/pnas.0406361102.

Zhang, F., Su, B., Wang, C., Siedlak, S. L., Mondragon-Rodriguez, S., Lee, H.-G., et al. (2015a). Posttranslational modifications of α-tubulin in alzheimer disease. *Transl. Neurodegener.* 4, 9. doi:10.1186/s40035-015-0030-4.

Zhang, R., Alushin, G. M., Brown, A., and Nogales, E. (2015b). Mechanistic Origin of Microtubule Dynamic Instability and Its Modulation by EB Proteins. *Cell* 162, 849–859. doi:10.1016/j.cell.2015.07.012.

Figure legends

Figure 1: **Assembly of tubulins into microtubules** Models of a depolymerizing (*left*) and polymerized (*right*) MTs. The GTP cap or labile domain is composed mostly of tyrosinated GTP-tubulin. The stable domain is mostly composed of detyrosinated GDP-tubulin. β-tubulin subunits are represented as orange cubes in their GTP-bound states and green cubes in their GDP-bound states. α-tubulin subunits are represented as blue cubes. Red sticks planted on the cubes represent the C-terminal tail of α- and β-tubulin subunits. Tyrosination is represented by a red dot on the C-terminal tail. Two MT regions are distinguished: a labile MT region mostly composed of tyrosinated GTP-tubulins, including the GTP cap, and a stable MT region mostly consisting of assembled detyrosinated GDP-tubulins. MT depolymerisation is characterized by curled protofilaments at MT ends (*left*).

Figure 2: **Tau protein sequence** and **domain organisation** The sequence numbering is according to the longest Tau isoform (441 amino acid residues). **A.** amino acid sequence of the MTBR and flanking regions, P2 in the PRR and R' in the C-terminal domain **B**. General scheme of the full-length Tau protein and of TauF4 fragment. **A** and **B**: the MTBR region of Tau consists in four partially repeated sequences, R1 to R4, highlighted in dark and light brown. PHF6* and PHF6 hexapeptides, in R1 and R2 repeats respectively, are highlighted in green and the KXGS motifs in yellow. Phosphorylation sites mentioned in the text are indicated with a v sign, cysteine residues with a star sign and acetylation with a circle. Segments of R1 and R2 shown in Fig. 3 are indicated with dashed lines.

Figure 3: **EM models of Tau/MTs interaction** α-tubulin subunit is represented as a blue cube and β-tubulin subunit as a brown cube. H12 C-terminal helix is schematized, the C-terminal tail prolonges the H12 helix. Model based on cryo-EM coupled to Rosetta modelling: Contacts of the R1 repeat with the α-tubulin subunit, at the inter-dimer interface: S258 and S262 of R1 make hydrogen bonds with E434; K259 of R1 interacts with an acidic patch formed by E420, E423 and D424; I260 of R1 is in a hydrophobic pocket formed by residues I265, V435 and Y262; K267 of R1 is in contact with the acidic C-terminal tail. Additional contacts for the R2 repeat with β-tubulin subunit, at the intra-dimer interface: K274 of R2 interacts with an acidic patch formed by D427 and S423; K281 of R2 is in contact with the acidic C-terminal tail of β-tubulin subunit. The PHF6* peptide (highlighted green) is close to this tail and localize at the intra-dimer interface. Additional contacts for the R2 repeat with α-tubulin subunit: K294 and K298 are in contact with the acidic C-terminal tail of α-tubulin subunit. Finally, H299 of R2 is buried in a cleft formed by residues F395 and F399 of β-tubulin subunit.

Figure 4 EPR models of the interaction of Tau F4 with MTs C291 of Tau in R2 is proposed to interact with C347 of α-tubulin, and the C322 of Tau in R3 with C131 of β-subunit. Note that C322 could actually

interact either with the β-subunit of the same protofilament, or with the one of an adjacent protofilament (as depicted here).

Figure 5 NMR model of the interaction of TauF4 with SLD-stabilized **tubulins A.** In interaction with a single tubulin, the IGSTENL peptide of TauF4 is proposed to adopt a turn conformation and is not bound to tubulin. The PRR is mainly detected in proximity to the β-subunit. **B.** In interaction with two tubulins, the IGSTENL peptide of TauF4 would be straight and overlapping two consecutive α- and β- subunits.

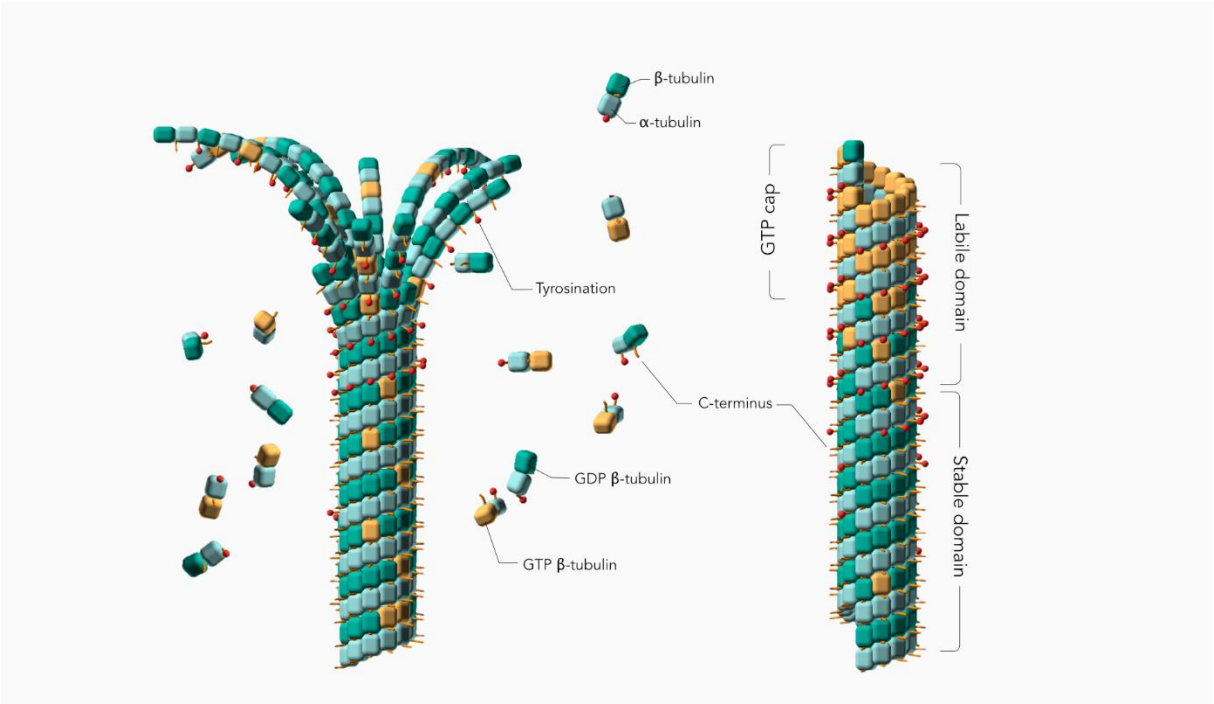

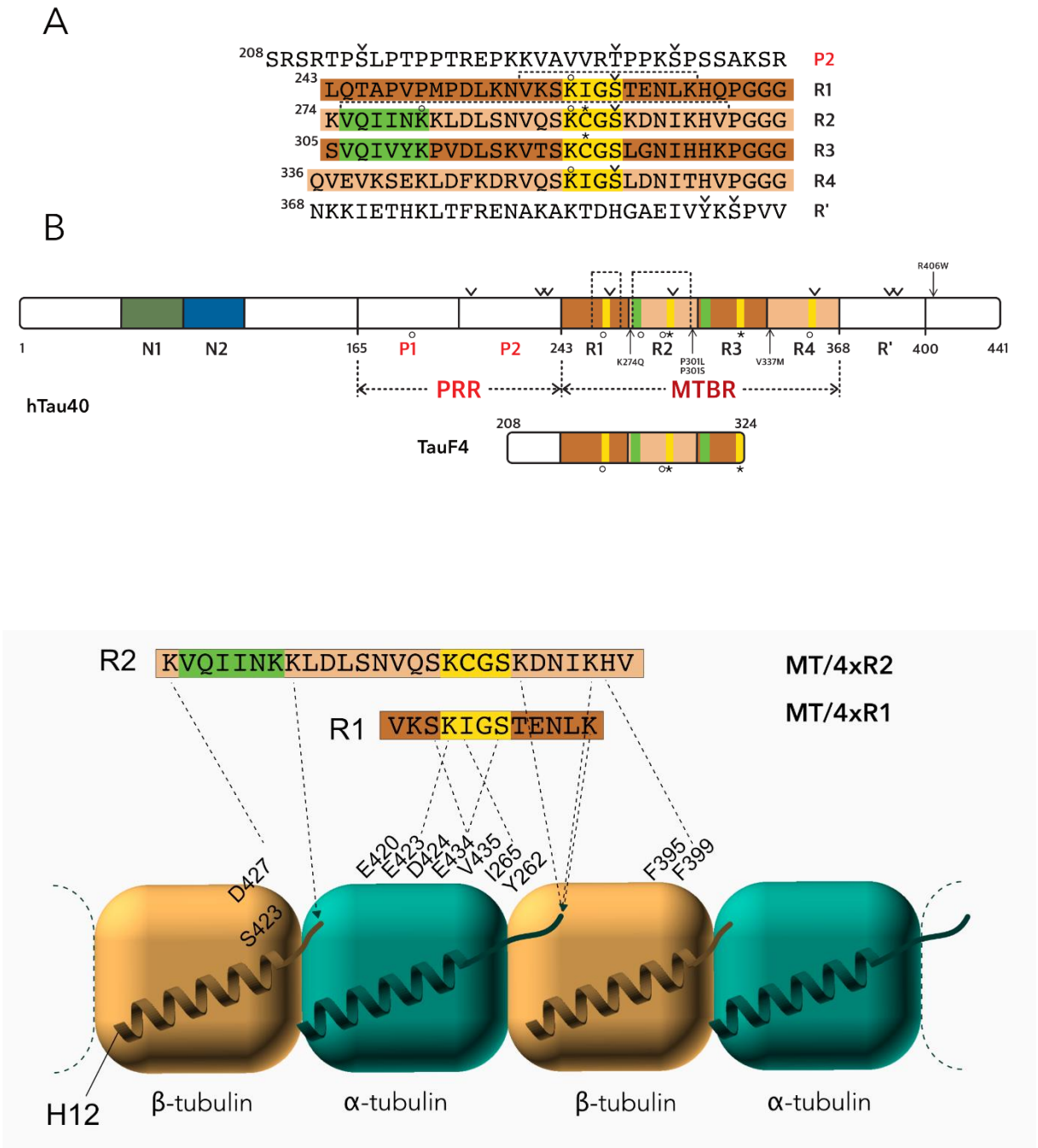
A
208 SRSRTPSLPTPPTREPKKVAVVRTPPKSPSSAKSR P2
243 LQTAPVPMPDLKNVKSKIGSTENLKHQPGGG R1
274 KVQIINKKLDLSNVQSKCGSKDNIKHVPGGG R2
305 SVQIVYKPVDLSKVTSKCGSLGNIHHKPGGG R3
336 QVEVKSEKLDFKDRVQSKIGSLDNITHVPGGG R4
368 NKKIETHKLTFRENAKAKTDHGAEIVYKSPVV R'
B
R406W
1
N1
N2
165
P1
P2
243
R1
K274Q
R2
P301L
P301S
R3
V337M
R4
368
R'
400
441
PRR
MTBR
hTau40
208
324
TauF4
R2 KVQIINKKLDLSNVQSKCGSKDNIKHV
R1 VKSKIGSTENLK
MT/4xR2
MT/4xR1
D427
S423
E420
E423
D424
E434
V435
I265
Y262
F395
F399
H12
β-tubulin
α-tubulin
β-tubulin
α-tubulin

IX. Congress Attendancies

Attendancies

1. **NMR a tool for biology:**

   Nuclear Magnetic Resonance as a powerful tool to identify the target epitopes of single domain antibodies for immunotherapeutic approaches in tauopathies **(Paris, January; 2019) – Poster**

   Orgeta Zejneli[1,2*,] Clément Danis[1,2*], Elian Dupré[1,2*], François-Xavier Cantrelle [1] , Morvane Colin [2] , Jean-Christophe Rain [3], Xavier Hanoulle [1] , Luc Buée[2] , Isabelle Landrieu [1] [1]Univ. Lille, CNRS UMR8576, F-59000 Lille, France [2]Univ. Lille, Inserm, CHU-Lille, UMRS1172, F-59000 Lille, France [3]Hybrigenic Services, Paris, France, *Equal contribution

2. **LiCEND summer school:**

   A VHH directed against tau as a novel therapeutic approach in tauopathies **(Lille, France; June 2019)- Flash Talk 3min + Poster**

   Orgeta Zejneli[1,2], Clément Danis[1,2], Elian Dupré[1], Alexis Arrial[3], Hamida Merzougui[2], Jean-Christophe Rain[3], Morvane Colin[1], Luc Buée[2], Isabelle Landrieu[2]
   [1]Univ. Lille, CNRS UMR8576, F-59000 Lille, France [2]Univ. Lille, Inserm, CHU-Lille, UMRS1172, F-59000 Lille, France [3]Hybrigenic Services, Paris, France

3. **New Frontiers in Structure Based Drug Discovery :**

   A VHH directed against tau as a novel therapeutic approach in tauopathies **(Florence, Italy; September 2019) – Oral presentation 15min + Poster**

   Orgeta Zejneli[1,2], Clément Danis[1,2], Elian Dupré[1], Alexis Arrial[3], Hamida Merzougui [2] , Jean-Christophe Rain[3], Morvane Colin[1], Luc Buée[2], Isabelle Landrieu[2]
   [1]Univ. Lille, CNRS UMR8576, F-59000 Lille, France 2Univ. Lille, Inserm, CHU-Lille, UMRS1172, F-59000 Lille, France 3Hybrigenic Services, Paris, France, *Equal contribution

4. **Journée André Verbert 2020 - Colloque des doctorants :**

   A VHH directed against tau as a novel therapeutic approach in tauopathies? (**November 2020)**

   Orgeta Zejneli[1,2], Clément Danis[1,2], Elian Dupré[1] , Alexis Arrial[3] , Hamida Merzougui[2], Jean-Christophe Rain[3],Morvane Colin[1], Isabelle Landrieu[2], Luc Buée[2]
   [1]Univ. Lille, CNRS UMR8576, F-59000 Lille, France [2]Univ. Lille, Inserm, CHU-Lille, UMRS1172, F-59000 Lille, France [3]Hybrigenic Services, Paris, France

5. **American Association International Conference (AAIC):**

   A VHH directed against tau as a novel therapeutic approach in tauopathies? **(November 2020, web-conference, Poster)**

   Orgeta Zejneli [1, 2], Clément Danis[1, 2], Elian Dupré[2], Raphaelle Caillierez[1], Justine Mortelecque[2], Arrial A[3], Rain JC[3], Morvane Colin[1], Isabelle Landrieu[2], Luc Buee[1]
   [1]Univ. Lille, Inserm, CHU Lille, U1172 - LilNCog - Lille Neuroscience & Cognition [2].CNRS ERL9002 Integrative Structural Biology F-59000 Lille, France. [3.] Hybrigenics Service, Hybribody, France

6. **ADPD:**

   A VHH directed against tau as a novel therapeutic approach in tauopathies? **(March 2021, web-conference)- Oral Presentation, 15min**

   Orgeta Zejneli [1, 2], Clément Danis[1, 2], Elian Dupré[2], Raphaelle Caillierez[1], Severine Begard[1], Justine Mortelecque[2], Arrial A[3], Rain JC[3], Morvane Colin[1], Isabelle Landrieu[2], Luc Buee[1]
   [1]Univ. Lille, Inserm, CHU Lille, U1172 - LilNCog - Lille Neuroscience & Cognition [2].CNRS ERL9002 Integrative Structural Biology F-59000 Lille, France. 3. Hybrigenics Service, Hybribody, France

7. **NeuroFrance 2021:**

   A VHH directed against tau as a novel therapeutic approach in tauopathies? **(May 2021, web-conference)- Oral Presentation, 3min**